Thermo- and chemosensitive properties of Transient Receptor Potential Ankyrin 1 ion channels

Moparthi, Lavanya

2016

Document Version:
Publisher's PDF, also known as Version of record

Thermo- and chemosensitive properties of Transient Receptor Potential Ankyrin 1 ion channels

BIOCHEMISTRY AND STRUCTURAL BIOLOGY | LUND UNIVERSITY
LAVANYA MOPARTHI | DOCTORAL THESIS

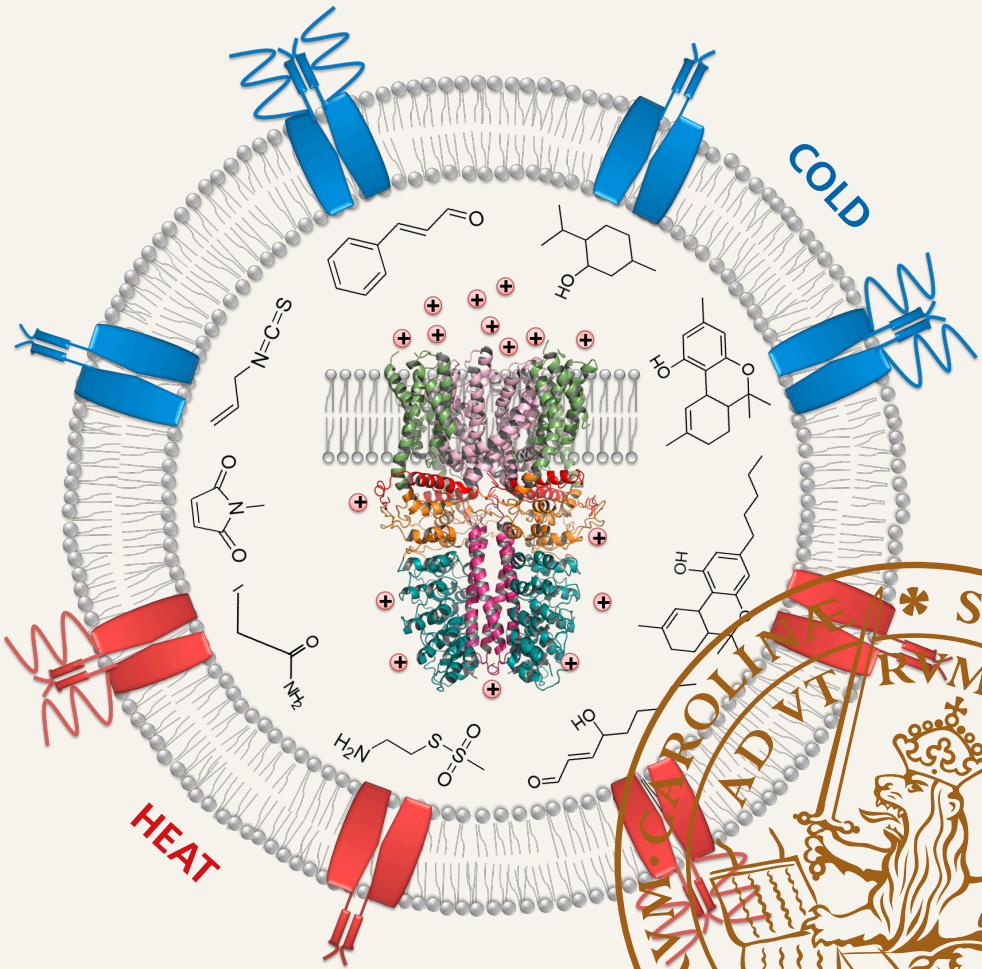

Thermo- and chemosensitive properties of Transient Receptor Potential Ankyrin 1 ion channels

Lavanya Moparthi

LUND
UNIVERSITY

DOCTORAL DISSERTATION

by due permission of the Faculty of Science, Lund University, Sweden.
To be publicly defended on Friday April 8th 2016 at 9.30 a.m. in Lecture hall C at the Centre of Chemistry and Chemical Engineering, Naturvetarvägen 14, Lund.

Faculty opponent

Dr. Félix Viana de la Iglesia

Universidad Miguel Hernández-CSIC,
Instituto de Neurociencias, Alicante, Spain.

Organization	Document name
LUND UNIVERSITY Department of Biochemistry and Structural Biology Center for Molecular Protein Science	DOCTORAL DISSERTATION
	Date of issue 15-03-2016
Author(s) Lavanya Moparthi	Sponsoring organization

Title and subtitle

Thermo- and chemosensitive properties of Transient Receptor Potential Ankyrin 1 ion channels

Abstract

The ability to sense and accommodate to an ever-changing environment is crucial for the survival of living organisms. Transient Receptor Potential (TRP) ion channels comprise a large superfamily of cation conducting membrane proteins that function as molecular sensors in diverse sensory processes including perception of light, taste, smell, sound, touch and temperature. The TRP Ankyrin 1 (TRPA1) ion channel is a unique member of the mammalian TRP superfamily, containing a large N-terminal ankyrin repeat domain (ARD) which constitutes half of the entire protein. TRPA1 responds to a variety of unrelated noxious stimuli such as chemicals, temperature and mechanical stress. It seems convincing that TRPA1 acts as a noxious chemical sensor and also plays a role in the detection of warm temperatures in non-mammalian species. The role of mammalian TRPA1 as a cold sensor is, however, controversial. The mammalian TRPA1 has been implicated in acute and inflammatory pain conditions and has been proposed as an important target for analgesics. If TRPA1 ion channels are intrinsically chemo-, thermo- and mechanosensitive proteins, regardless of species, remains to be shown.

The overall of aim of this thesis was to investigate possible inherent thermo- and chemosensitive properties of human TRPA1 (hTRPA1) and the malaria mosquito *Anopheles gambiae* TRPA1 (AgTRPA1), and the role of the N-terminal ARD, containing suggested key temperature elements as well as cysteines targeted by thiol reactive oxidants and electrophiles known to activate TRPA1. Difficulties to express and purify large amounts of proteins have hampered structural and functional studies of TRPs but were here overcome by heterologous expression in the yeast *Pichia pastoris*. Single-channel electrophysiological recordings of purified hTRPA1 reconstituted into artificial lipid bilayers indicated that cold- and chemosensitivity are inherent channel properties recognized by structures outside the N-terminal ARD. Surprisingly, hTRPA1 is also intrinsically sensitive to warm temperatures, and thus displays U-shaped thermosensitivity. Notably, redox state and ligands showed modulatory effects on the mammalian TRPA1 thermosensitivity. The purified AgTRPA1 was activated by heat and the electrophile allyl isothiocyanate (a major pungent ingredient in wasabi and mustard) independently of the N-terminal ARD. The TRPA1 proteins displayed fluorescence quenching upon exposure to temperature and ligands, suggesting that conformational changes occur in a membrane-independent manner and thus that TRPA1 is an intrinsic chemo- and thermosensitive protein. Mass spectrometry was used to map hTRPA1 binding sites of the frequently used electrophilic TRPA1 activator N-methyl maleimide. Our results indicate that thermal and chemical sensitivities of mammalian and non-mammalian TRPA1 are intrinsic channel properties and that the N-terminal ARD is not key but plays a modulatory role in TRPA1 chemo- and thermosensation. Our findings provide a better understanding of the function of hTRPA1, which can help to develop novel treatments for pain and illnesses/symptoms caused by sensory hypersensitivity.

Key words: TRP ion channels, TRPA1, ankyrin repeat domain, thermosensation, chemosensation, cold sensor, electrophiles, non-electrophiles, planar lipid bilayers, patch-clamp, fluorescence spectroscopy, mass spectrometry.

Classification system and/or index terms (if any)

Supplementary bibliographical information — Language: English

ISSN and key title — ISBN: 978-91-7422-432-0

Recipient's notes — Number of pages: 196 — Price

Security classification

Signature Lavanya Moparthi Date 02/03/2016

Thermo- and chemosensitive properties of Transient Receptor Potential Ankyrin 1 ion channels

Lavanya Moparthi

Doctoral dissertation

LUND
UNIVERSITY

Faculty of Science
Department of Biochemistry and Structural Biology
2016

Supervisors:

Prof. Urban Johanson,
Dept. of Biochemistry and Structural Biology, Lund University

Prof. Peter Zygmunt
Clinical Chemistry and Pharmacology, Dept. of Laboratory Medicine, Lund University

Front cover: Single-particle cryo-EM structure of human TRPA1 (PDB ID: 3J9P) shown in the center of the picture. Schematic drawing of a membrane (grey) containing TRPA1 proteins in blue and red are representing cold and heat sensitivity, respectively.

Graphic design by Lavanya Moparthi with help from Dr. Vamsi K Moparthi.

Faculty of Science
Department of Biochemistry and Structural Biology
Center of Molecular Protein Science, Lund, Sweden

ISBN 978-91-7422-432-0

Printed in Sweden by Media-Tryck, Lund University
Lund 2016

Dedicated to my lovely son Vishwak

Table of contents

Popular science summary

All living things have the ability to detect and respond to changes in the surrounding environment and most of us take sensations caused by changes in light, sound, taste, temperature, and touch for granted. However, the process of detection and transmission of the signal generated to the brain is quite complex and some aspects not known. This thesis explores the sensors that detect the various changes and initiate this chain of events. In particular, one type of sensor named Transient Receptor Potential Ankyrin 1 (TRPA1) is studied.

This sensor can detect a variety of unrelated dangerous conditions, such as toxic chemicals from nature or industry, chemicals produced in damaged tissue, harmful temperatures and mechanical stimuli, which lead to perception of pain and avoidance behaviour. Among the chemicals that activate TRPA1 are the plant derived spicy compounds in mustard, wasabi, cinnamon, garlic, mint, pepper, and oregano that many of us appreciate if the amount is right. Hence, TRPA1 is also called the wasabi receptor. This receptor is also found in chicken, lizards, snakes, insects, and worms but not in plants, and it helps the animals in finding appropriate temperatures. In insects and the vampire bat, the temperature sensitivity of the wasabi receptor helps in identification of a warm-blooded host or prey for feeding. However, the function as a temperature sensor in mammals is controversial ever since it was first proposed as a sensor of painful cold.

In man, TRPA1 has been involved in several pathological conditions like pain, itch, and respiratory diseases and more, there by this receptor has been potential target for the novel drugs. Fortunately the principle of these sensors is simple, they work as a switch that when activated allows a current to pass the membrane of a nerve cell, generating an electrical signal which eventually transmits to the brain. In more detail, the switch is a protein based molecular machine that forms a gated channel in the membrane and only allow ions to pass when activated by a stimuli. The molecular mechanisms that allow temperature and all the diverse compounds to regulate the gate of the channel are not known. Only a small part of the wasabi receptor sits in the membrane, the bulk of the protein protrudes from the membrane into the cytosol. This protrusion is mainly folded by the first half of the protein that is named the N-terminal Ankyrin Repeat Domain (ARD). The

function of the first half of the protein is not clear but changes here have suggested an involvement in regulation of the gating of the channel both by temperature and by binding of chemicals.

The general aim of this thesis was to understand the functional role of TRPA1 as a sensor of temperature and chemicals. Genes from man and the malaria mosquito coding for TRPA1 and truncated versions lacking the first half, were used to transform a certain yeast, *Pichia pastoris*, into a protein production factory to achieve large amounts of these receptors. To examine the functionality of these extracted and purified proteins, a very sensitive technique was used measure currents passing through a single ion channel after activation by various means. In this purified and well-defined system, the human wasabi receptor responded to cold temperatures, even when lacking the first half of the protein. These results indicate that temperature sensation is intrinsic response of the channel and not dependent on intracellular molecules. Furthermore, the long N-terminal repeat structure is not needed for the activation by cold temperatures. Surprisingly, the human TRPA1 not only responded to cold but also to heat. We observed that the same isolated single ion channel can respond to both heat and cold and that these responses are modified by activators and the redox state of the channel. Similarly, we show that purified malaria mosquito TRPA1 is activated by heat and that this property is inherent to the channel and not dependent on the first half of the protein. Another technique, mass spectrometry was performed to identify binding sites of one key chemical activator and the results clearly show binding sites outside the N-terminal half of the human TRPA1.

In conclusion for the first time we show that thermo- and chemosensitivity of the human TRPA1 is an inherent property of the receptor, irrespective of the N-terminal ARD. It is my hope that this thesis provides a better understanding of the function of TRPA1 that can be used for the development of novel treatments for human pain as well as control of insects transmitting diseases such as malaria.

List of papers

This PhD thesis is based on the following papers, which will be referred in the text by their Roman numerals. The papers are appended at the end of the thesis.

Paper I

Human TRPA1 is intrinsically cold- and chemosensitive with and without its N-terminal ankyrin repeat domain
Moparthi L, Survery S, Kreir M, Simonsen C, Kjellbom P, Högestätt ED, Johanson U and Zygmunt PM (2014)
Proceedings of the National Academy of Sciences USA, 111 (47):16901–16906.

Paper II

Human TRPA1 is a heat sensor displaying intrinsic U-shaped thermosensitivity
Moparthi L, Kichko TI, Eberhardt M, Kjellbom P, Johanson U, Reeh PW, Leffler A, Filipovic MR and Zygmunt PM
Submitted

Paper III

The N-terminal ankyrin repeat domain is not required for activation of purified mosquito TRPA1 by heat or mustard oil
Survery S, Moparthi L, Kjellbom P, Högestätt ED, Zygmunt PM and Johanson U
Submitted

Paper IV

Agonist-induced conformational switch of the human TRPA1 ion channel detected by mass spectrometry
Moparthi L, Kjellström S, Högestätt ED, Kjellbom P, Filipovic MR, Zygmunt PM and Johanson U
Manuscript

My contribution to the papers

Paper I - I participated in designing the study. I purified human TRPA1 proteins and I performed most of the electrophysiological experiments and data analysis. I performed CD experiments. I participated in writing of the paper.

Paper II - I participated in designing the study. I purified hTRPA1 protein, and performed and analysed all electrophysiological experiments on planar bilayers. I participated in drafting of the manuscript.

Paper III - I was involved in planning of electrophysiological experiments. I performed and analysed all electrophysiological experiments. I took part in drafting of related parts of the manuscript.

Paper IV - I took a major role in designing the study. I purified hTRPA1 proteins and prepared samples for the mass spectrometry experiments. I performed data analysis. I drafted the manuscript together with all co-authors.

Abbreviations

AITC	allyl isothiocyanate
AR	ankyrin repeat
ARD	ankyrin repeat domain
ATP	adenosine triphosphate
CA	cinnamaldehyde
CD	circular dichroism
CGRP	calcitonin gene-related peptide
CO_2	carbon dioxide
DRG	dorsal root ganglion
DTT	dithiothreitol
FEPS	familial episodic pain syndrome
GUV	giant unilamellar vesicles
HEK	human embryonic kidney
H_2O_2	hydrogen peroxide
4-HNE	4-hydroxynonenal
H_2S	hydrogen sulphide
MTSEA	2-aminoethyl methanethiosulfonate ethylammonium
NO	nitric oxide
NMM	N-methyl maleimide
O_2	oxygen
PKC	protein kinase C
PIP_2	phosphatidylinositol 4,5-bisphosphate
PDZ	Post synaptic density protein (PSD95), Drosophila disc large tumour suppressor (Dlg1) and Zonula occludens-protein (zo-1)
PLC	phospholipase C
P_o	open probability
PPi	inorganic pyrophosphate
PPPi	inorganic tripolyphosphate
TCEP	tris(2-carboxyethyl)phosphine
TG	trigeminal ganglion
TRP	transient receptor potential
TRPA	transient receptor potential ankyrin
TRPC	transient receptor potential canonical
TRPM	transient receptor potential melastatin
TRPML	transient receptor potential mucolipin
TRPN	transient receptor potential NOMPC

TRPP	transient receptor potential polycystin
TRPV	transient receptor potential vanilloid

Chapter 1
Introduction

1.1 Somatosensation and nociception

The ability to sense and respond on environmental cues is very important for the survival of an organism. In animals, this ability relies on the sensory nervous system, which receives and processes various signals from the surroundings of the organism. Aristotle was the first to define the five senses, which allow humans monitor their external milieu; these are vision, hearing, smell, taste, and touch. In addition to our capacity to sense external environment, we have senses that are able to perceive changes within the body, like proprioception (the sense of body position) (Damann, Voets et al. 2008). Somatosensation is a collection of several sensory submodalities that besides proprioception, also include mechanosensation, thermosensation, and nociception (Julius 2013).

Nociception is the process of transmitting painful stimuli, detected by nociceptors and converted to electrical signals in the form of action potential, which can propagate to the spinal cord, thalamus, and cerebral cortex, to sense pain (Fig. 1.1). Nociceptors are specialized peripheral sensory neurons that are capable to detect various harmful stimuli such as noxious mechanical, thermal and chemical stimuli (Dubin and Patapoutian 2010). Nociceptors are divided into two major classes. The first class contains myelinated medium-diameter afferent fibres (Aδ), which mediate acute well-localized pain (sharp pricking pain). The second class contains unmyelinated small-diameter slow conducting fibres, called C-fibres, which mediate slow pain (dull aching, poorly localized). Another group of rapidly conducting myelinated fibres (Aβ) that detect the innocuous stimuli from the skin, joints and muscle, do not contribute to pain. Like myelinated afferents, the majority of C-fibre nociceptors are polymodal and respond to thermal, mechanical, and noxious chemical stimuli (Julius and Basbaum 2001, Basbaum, Bautista et al. 2009). Some nociceptors that are not responding to stimuli under normal conditions are called silent or sleeping nociceptors and are only sensitized in tissue injury (Schmidt, Schmelz et al. 1995). The cell bodies of nociceptors are mainly located in the trigeminal ganglia (TG) and dorsal root ganglia (DRG), which innervate head and body respectively. The nociceptive neurons are

pseudounipolar with an axon projecting to the periphery with free nerve endings innervating e.g., the skin where it detects the sensory stimuli, and a central axon that transmits the signal to the brain via the spinal cord (Dubin and Patapoutian 2010). Nociceptors release a variety of endogenous chemical compounds (neurotransmitters) at peripheral and central synapses thereby maintaining efferent and afferent sensory neuronal signalling, respectively (Fig. 1.1). Key neurotransmitters involved in nociceptive signalling are glutamate and calcitonin gene-related peptide (CGRP) and substance P (Dubin and Patapoutian 2010). The temperature detecting nociceptors are divided into unimodal (only responding to temperature) and polymodal (also responding to pressure and chemicals) (Dhaka, Viswanath et al. 2006). The specialized proteins that detect and translate the noxious stimuli into a pain response are called nocisensors and this has been proposed to be the function of certain ion channels such as Transient Receptor Potential (TRP) ion channels (Dubin and Patapoutian 2010).

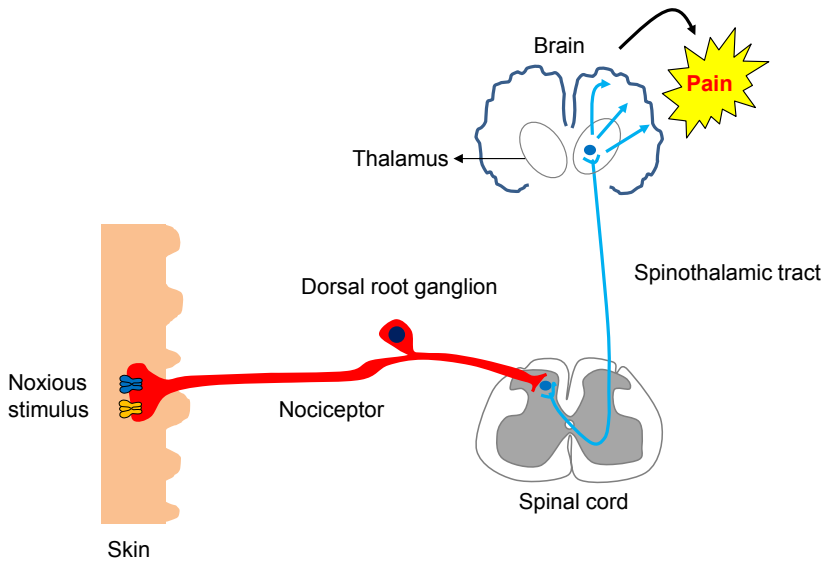

Figure 1.1 Schematic diagram of the nociceptive pathway. The detection of noxious stimuli by nocisensors such as TRPA1 (blue) and TRPV1 (orange) at primary afferent nerve endings innervating peripheral tissues and organs such as the skin, leads to generation and propagation of an action potential, which via the spinal cord transmits a signal to thalamus through the spinothalamic tract and then further to the primary sensory cortex, where it results in perception of pain. The release of sensory neurotransmitters locally in the periphery contributes to inflammatory responses and regulation of tissue blood flow (Zygmunt and Högestätt 2014).

1.2 Ion channels and their sensory function

All living cells are delimited by plasma membranes, which act as barriers between the extracellular environment and the cytoplasm. Ion channels are integral membrane proteins that act as gatekeepers to control and allow only selected ions to pass from one side of the membrane to the other side, since the lipid membrane as such is impermeable to charged particles. At rest, the charges are usually not in balance over the membrane (the membrane is more negatively charged on the inside than the outside) and this is the basis for the resting potential over the membrane. This electrochemical gradient can be used in cell signalling by ion channels that possess special gating properties and different selectivity to ions, to depolarize the membrane to generate an action potential that is propagated along the neuronal membrane. The gating mechanism is a process of conformational changes in the protein that leads to opening or closing of the ion channel. The gating process can be triggered by different stimuli like voltage (in voltage-gated ion channels), ligands (in ligand-gated ion channels), and intracellular messengers (in second messenger-operated channels).

Ion channels are involved in different functions in the sensory system, such as transduction of detected chemical and physical stimuli into electrical signals and transmission to the central nervous system. Some of the ion channel families involved in sensory processes are the ENaC/ASIC/degenerin superfamily, the purinergic (P2X) receptor family, the two-pore-domain K^+ channel family (TREK-1) and the TRP ion channel superfamily (Voets and Nilius 2003). For example, ion channels participate in the process of thermosensation, in that TRP ion channels (TRPV1, TRPM8, and TRPA1) perceive changes in temperature and cause an influx of cations, which leads to depolarization of the cell membrane. Furthermore, the voltage-gated sodium and potassium channels respond to this membrane depolarization and contribute to the propagation of the action potential along the neuron. The two-pore domain K^+ channels (TREK-1, TREK-2, and TRAAK), are responsible for maintaining the membrane potential at rest by efflux of K^+ ions (Bagriantsev and Gracheva 2014).

1.3 TRP superfamily

All members in the TRP ion channel superfamily share common features such as having six transmembrane segments, permeability to cations, and some degree of sequence similarity. However, these proteins show diversity in activation mechanisms, selectivity of cations and physiological functions (Julius and

Basbaum 2001, Clapham 2003, Montell 2005, Pedersen, Owsianik et al. 2005). TRP ion channels play roles in the perception of external stimuli, which contributes to vision, smell, taste, hearing, and touch as well as nociception. TRP ion channels are often considered as multiple signal integrators, since sensitivity to one stimulus is modulated by others (Montell 2005, Venkatachalam and Montell 2007).

1.3.1 History and classification

In 1969, Cosens and Manning identified a *Drosophila* mutant that showed a transient response to bright light rather than a sustained response and hence named it *trp,* transient receptor potential (Cosens and Manning 1969). Twenty years later, the *trp* gene was cloned and recognized to encode an integral membrane protein (Montell and Rubin 1989) which was subsequently characterized as a Ca^{2+} permeable cation channel (Hardie and Minke 1992). The mammalian TRP homologues were first identified in 1995 (Petersen, Berridge et al. 1995, Wes, Chevesich et al. 1995, Birnbaumer, Zhu et al. 1996, Zhu, Jiang et al. 1996, Zitt, Zobel et al. 1996). Today, more than 100 TRP ion channels have been identified in various organisms, including yeast, worms, insects, fish, snakes, chicken and mammals (Nilius and Owsianik 2011). The expression of *trp* genes have been shown in all cell types and TRPs have been detected in all membranes except the nuclear and mitochondrial membranes (Nilius and Owsianik 2011).

Members of the TRP superfamily are grouped into seven subfamilies on the basis of their amino acid sequence similarity: TRPC (Canonical or Classical), TRPV (Vanilloid), TRPM (Melastatin), TRPA (Ankyrin), TRPP (Polycystin), TRPML (Mucolipin) and TRPN (*no mechanoreceptor potential C* gene; nompC). The TRPN subfamily does not contain any mammalian member (Montell 2005) (Fig 1.2). The seven subfamilies further fall into two groups based on sequence and topological differences. Group 1 TRPs consist of five subfamilies, which show the strongest sequence similarity with the *Drosophila* TRP, and they are TRPC, TRPV, TRPM, TRPA, and TRPN. The two remaining subfamilies, TRPP and TRPML, form group 2 since they are more distantly related to the group 1 TRPs. Proteins from the group 2 subfamilies share sequence similarity over transmembrane segments and contain a large extracellular loop that separates the first two transmembrane segments (Montell 2005, Venkatachalam and Montell 2007).

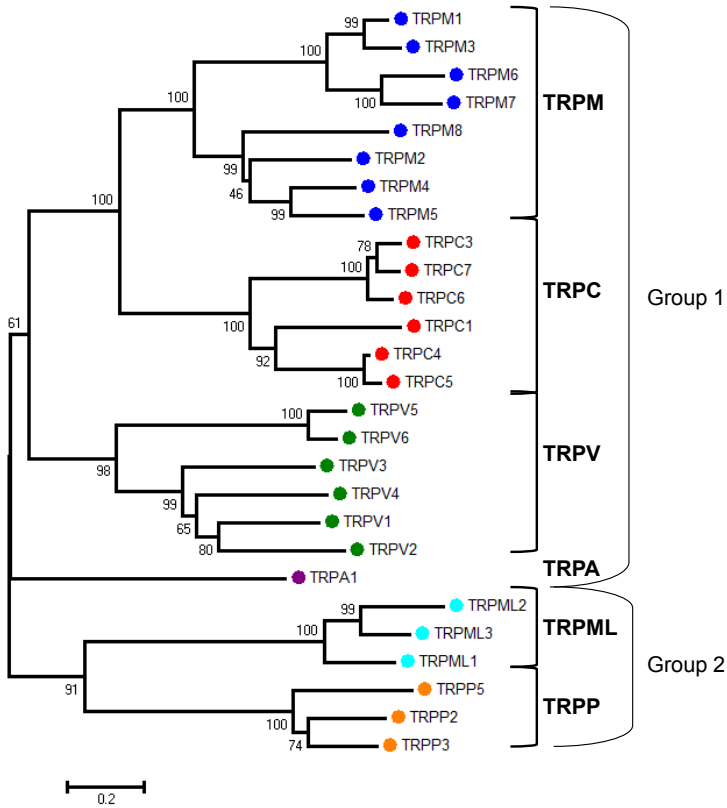

Figure 1.2 Phylogenetic tree of the human TRP ion channel family. Members of the mammalian TRP superfamily are grouped into six subfamilies: TRPM, TRPC, TRPV, TRPA, TRPML and TRPP, which are highlighted by dotted blue, red, green, purple, cyan and orange colours respectively. The phylogenetic tree was constructed with the Neighbor Joining method and bootstrap values of 100 replicates are shown.

The total number of TRP ion channels present in each species varies. For example there are 17 in fruit fly (*Drosophila melanogaster*), 17 in worm (*Caenorhabditis elegans)*, 27 in Zebrafish (*Danio rerio*), 27 in sea squirt (*Ciona intestinalis*) 28 in mouse (*Mus musculus*) and 27 in human (*Homo sapiens*) (Nilius and Owsianik 2011). In mammals, there are in general seven members in the TRPC subfamily (TRPC1-C7), six members in the TRPV subfamily (TRPV1-V6), eight members in the TRPM subfamily (TRPM1-M8), only one member in the TRPA subfamily (TRPA1), three members present in the TRPML (TRPML1-ML3) and TRPP (TRPP2, TRPP3, and TRPP5) subfamilies (Montell 2005, Nilius and Owsianik 2011). However, in humans the TRPC family contain only six members, since TRPC2 has become a pseudogene (Fig. 1.2) (Montell 2005, Nilius and Owsianik

2011). Overall the TRP family does not have much sequence similarity, since only 35% sequence similarity has been shown between subfamilies, even within same species (Nilius and Owsianik 2011).

1.3.2 Structural features

1.3.2.1 Transmembrane domain

A shown in Fig. 1.3, a shared feature among all members of the TRP superfamily is the transmembrane domain, containing six transmembrane α-helices (S1-S6) in each subunit, which in turn are arranged as a functional tetramer holding a common central pore (Clapham 2003). Because of resemblances in topology and quaternary structure to the voltage-gated potassium channel (Kv1.2), the architecture of TRPs was assumed to be similar and more specific predictions were made based on the high-resolution structure of Kv1.2 (Clapham 2003, Wu, Sweet et al. 2010). According to this, each subunit of a TRP ion channel was expected to be divided into two domains such as a ligand- or voltage-sensing domain (S1-S4) and a central pore-forming domain (S5 and S6). The pore-forming domain from each subunit come together and forms a common ion permeation pathway (Clapham 2003, Wu, Sweet et al. 2010). The highly flexible linker (S4-S5 linker) connects the S1-S4 domain with the pore-forming domain in each subunit. The linker also interacts with the C-terminal end of the sixth transmembrane segment. Based on identified ligand-binding sites in the S1-S4 domain of TRP channels, this region was proposed to be involved in the ligand-dependent channel gating mechanism (e.g. capsaicin binding in TRPV1) (Jordt and Julius 2002, Gavva, Klionsky et al. 2004). Most of the TRP ion channels are believed to form homotetramers, but there are certain exceptions, which appear to form heteromers (Latorre, Zaelzer et al. 2009, Cheng, Sun et al. 2010, Fischer, Balasuriya et al. 2014). Recent medium resolution structural models of TRPV1 and TRPA1 from electron micrographs have confirmed the expected architecture and tetrameric assembly of TRP ion channels (Liao, Cao et al. 2013, Paulsen, Armache et al. 2015).

1.3.2.2 Ion permeation pathway

The loop region between the fifth and sixth transmembrane segments re-enters into the membrane and forms a lining of the ion pore (Voets and Nilius 2003, Owsianik, D'Hoedt et al. 2006). In general all TRP channels are considered as non-selective cation channels (with $P_{Ca}/P_{Na} \leq 10$), but there is a large variation in

permeation of ions (Clapham 2003, Venkatachalam and Montell 2007). Particularly members of the TRPM family show large variation in selectivity, from highly permeable to Ca^{2+} and Mg^{2+} ions (TRPM6 and M7) to only permeable to monovalent cations (TRPM4 and M5), but impermeable to Ca^{2+} ions (Launay, Fleig et al. 2002). Both TRPV5 and TRPV6 are highly Ca^{2+}-selective with P_{Ca}/P_{Na} > 100 (Venkatachalam and Montell 2007). The rest of the TRP channels in the superfamily are relatively non-selective to mono- and divalent cations. The TRPV1, TRPML1and TRPP3 are highly permeable to H^+ ions (Nilius 2007). Some TRP ion channels, TRPA1, TRPM8 and TRPV1-TRPV4, also permeate large molecular weight compounds such as membrane impermeable fluorescent dyes and local anaesthetics (Ferreira and Faria 2016).

1.3.2.3 Intracellular domains

Based on their common topology, both N- and C-terminal regions in each TRP subunit are located intracellularly. Apart from this feature, there are no collectively shared similarities in the intracellular domains of the TRP family (Clapham 2003, Gaudet 2008) (Fig. 1.3). However, among the seven TRP subfamilies, prominent ankyrin repeats (AR) were identified in the N-termini of TRPC, TRPV, TRPN and TRPA members (Gaudet 2008). In general, the AR is a 33-residue motif that is involved in protein-protein interactions and acts as a flexible region that connects to the cytoskeleton elements. The function of TRP ion channel ARs is not clear, but some studies reported an involvement in the tetramerization of the channel (Gaudet 2008). Ankyrin repeats in TRPA1 and TRPN were proposed to be involved in mechanotransduction (Owsianik, D'Hoedt et al. 2006). The number of ARs varies between subfamilies of the TRP superfamily, like 3 to 4 in TRPCs, 6 in TRPVs, 14 to 17 in TRPAs and ~29 in TRPN (Gaudet 2008, Nilius and Owsianik 2011). Members of the TRPM family also have a large intracellular N-terminal domain, but it is composed by four subdomains called TRPM homology regions and unrelated to AR. The function of this domain is unknown (Clapham 2003).

Some TRP members contain a conserved 23-25 amino acid stretch in the proximal part of the C-terminal directly after sixth transmembrane helix, called the TRP domain. The highly conserved region with the amino acid sequence of "EWKFAR" in the TRP domain, was named as the 'TRP box' (Montell 2005). The TRP box is highly conserved in the TRPC family and less conserved in TRPVs and TRPMs, and absent in the other subfamilies. It has been suggested that the TRP box form a binding site for PIP_2 (Owsianik, D'Hoedt et al. 2006).

Some TRP channel members, TRPC, TRPM and TRPV, are suggested to contain coiled-coil domains either in the N-terminus or in the C-terminus, which would contribute in the tetrameric assembly (Montell 2005). As mentioned above, some TRPs may form heteromers. Specifically, TRPP2 is thought to interact with TRPP1 through their coiled-coil domains, forming a functional polycystin complex (Pedersen, Owsianik et al. 2005).

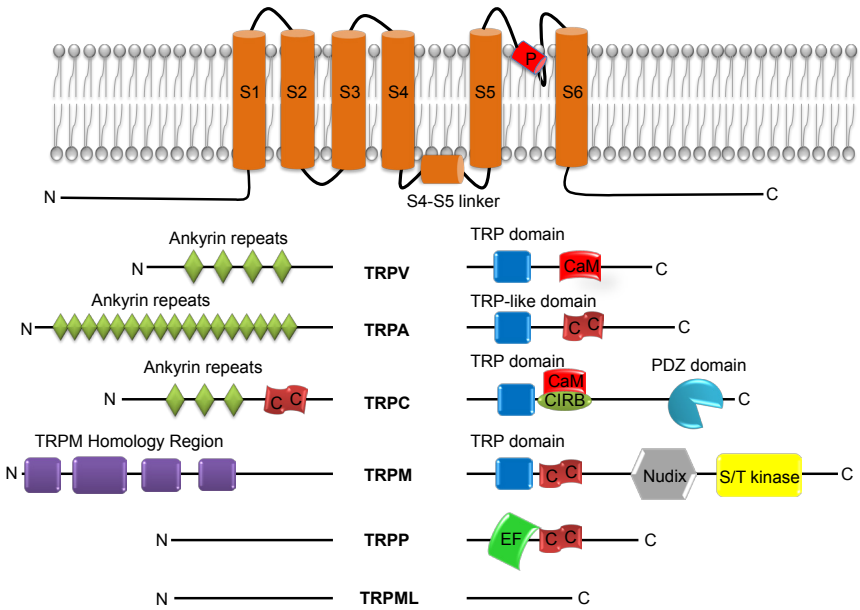

Figure 1.3 Schematic overview of domain organization in TRP ion channels. All TRP family members share a common topology, consisting of six membrane spanning α-helices (S1-S6), a short pore helix (P) and intracellularly located N- and C-termini. The N- and C-termini of these subfamilies show large variation in length and structural domains. Ankyrin repeats are present in the TRPV, TRPA and TRPC subfamilies. The TRPM homology region, NUDIX hydrolase domain, and S/T kinase – serine/threonine kinase domains are found specifically in the TRPM subfamily. In contrast, the TRP domain is present in the TRPC, TRPV, TRPM subfamilies and an analogous structure has also been identified in TRPA1. The PDZ domain is restricted to the TRPC family. CC indicates a coiled-coil domain; CaM – calmodulin; CIRB – putative calmodulin- and IP_3R-binding domain; EF – EF-hand Ca^{2+} binding domain.

Some TRP members are also called chanzymes since they are channels and contain C-terminal enzyme domains which are atypical for TRPs. TRPM2 contains a NUDIX hydrolase domain (NudT9-H) in its C-terminus that activates the channel through binding with β-nicotinamide adenine dinucleotide (NAD) or adenosine diphosphate ribose (ADP-ribose) (Perraud, Fleig et al. 2001, Jiang,

Gamper et al. 2011). Both TRPM6 and TRPM7 contain functional serine/threonine kinases within the C-terminal domain, which are involved in the regulation of channel activation (Nadler, Hermosura et al. 2001, Runnels, Yue et al. 2001). Members of the TRPC family, TRPC1, TRPC4 and TRPC5, contain a PDZ domain which may interact with scaffolding proteins in forming functional protein complexes (Pedersen, Owsianik et al. 2005). Calcium sensitivity of TRPM4 is regulated by PKC-dependent phosphorylation and binding of calmodulin (CaM) at the C-terminus of the channel (Nilius, Prenen et al. 2005), whereas TRPP2 contain an EF-hand type of Ca^{2+} binding motif without known function (Pedersen, Owsianik et al. 2005).

1.3.3 Functional roles

TRP ion channels are activated by diverse stimuli. For example, many TRP channels are activated by exogenous and endogenous ligands and some TRP channels are also activated by temperature and mechanical stress. Members in TRPC family share a common gating mechanism that depends on activation via phospholipase C (PLC), either directly through diacylglycerol, or indirectly by an unknown mechanism (Nilius 2007). A PLC-mediated mechanism involving 2-arachidonoylglycerol has also been shown in TRPV1 (Zygmunt, Ermund et al. 2013). The TRP ion channels are expressed in all cell types, both excitable and non-excitable cells (mast cells, T-lymphocytes, vascular endothelial cells, pancreatic acinar cells). Because of their ubiquitous expression, TRP ion channels may have important roles in a wide variety of cellular functions from sensory signalling to ion homeostasis (Nilius and Owsianik 2011).

1.3.3.1 Chemosensation

Several TRP ion channels are involved in chemosensation, of which some contribute to the perception of noxious chemical stimuli (e.g. TRPV1 and TRPA1) and some are involved in taste transduction (TRPM5) or signalling of pheromones (TRPC2) (Venkatachalam and Montell 2007). Many TRP ion channels are polymodal in nature, thus responding to several types of stimuli. For example, TRP ion channels are activated by either a chemical alone or together with temperature. Sometimes the chemical activation mimics a physical stimuli and this is termed chemesthesis (e.g. hot sensation from chilli pepper and feeling of cool from mint) (Vriens, Nilius et al. 2014). As listed in Table 1, chemical activators of some TRP ion channels are commonly used as pharmacological tools to understand the role of modality specific nociceptive signalling (Holzer 2011,

Gees, Owsianik et al. 2012, Almaraz, Manenschijn et al. 2014, Zygmunt and Högestätt 2014).

Table 1 TRP ion channels in chemosensation

TRP ion channel	Chemical activators
TRPV1	Capsaicin (chilli), resiniferatoxin (cactus), piperine (black pepper), camphor, 2-aminoethyl diphenylborinate (2-APB), anandamide, H^+
TRPV2	2-APB, probenecid
TRPV3	2-APB, camphor, eugenol, carvacrol, menthol
TRPV4	Arachidonic acid, anandamide and epoxyeicosatrienoic acid
TRPM1	Steroid pregnenolone sulphate
TRPM2	NAD and ADP-ribose, H_2O_2
TRPM3	Spingosines, pregnenolone sulphates
TRPM4 & M5	Ca^{2+}
TRPM6 & M7	2-APB
TRPM8	Menthol (mint), eucalyptol (eucalyptus), icillin.
TRPA1	Isothiocyanates (mustard, wasabi, horseradish), cinnamaldehyde (cinnamon), allicin and diallyl disulphide (garlic), Δ^9-tetrahydrocannabinol (cannabis), 4-hydroxynonenal, Ca^{2+}

1.3.3.2 Mechanosensation

There are several TRP ion channel members that have been reported to be involved in mechanosensation, ranging from hearing in fruit fly to pain in mammals. The TRP family member, OSM-9 was first identified as a mechanosensor in *C. elegans* (Colbert, Smith et al. 1997). Numerous studies on its mammalian homologue TRPV4, suggested that it acts as an osmosensor, but the activation mechanism is still unclear (Christensen and Corey 2007). TRPV2, TRPC3, TRPC6, TRPM4 and TRPM7 are suggested to be involved in mechanosensation in vascular smooth muscle, but the mechanism of activation is not known and neither if these channels sense pressure directly or depend on intracellular messengers or by increasing membrane insertion of these TRP proteins (Christensen and Corey 2007). Functional characterization of TRPM3 in a heterologous system demonstrated its activation by hypo-osmotic solutions (Grimm, Kraft et al. 2003). Corey *et al.*, proposed that TRPA1 plays a role as a mechanotransducer in the cochlear hair cells in vertebrates (Corey, Garcia-Anoveros et al. 2004). In addition, TRPP2/TRPP1 expressed in the primary cilia of kidney epithelial cells has been proposed to respond to fluid flow through the nephron (Nauli, Alenghat et al. 2003). Taken together, further studies are needed to understand the activation mechanism of TRP ion channels by mechanical stress.

1.3.3.3 Thermosensation

Temperature is one of the most important internal and environmental factors for survival of organisms (Digel, Kayser et al. 2008). The temperature affects all metabolic processes of a cell for example reaction rates of enzymes and chemicals, membrane fluidity, diffusion of solutes and conductivity of electrolytes (Islas 2014). Hence, a specific sensory transduction machinery with a molecular sensor is needed for organisms to avoid or adapt to temperature changes. The living organisms can use biomolecules as thermometers and thermostats (Digel, Kayser et al. 2008). In a living cell, all kinds of macromolecules (nucleic acids, lipids, and proteins) are involved in the sensing of temperatures (Digel, Kayser et al. 2008). In some organisms such as bacteria, conformational changes in RNA and DNA cause temperature-dependent gene regulation (Digel, Kayser et al. 2008). In some prokaryotic organisms and plants, changes in the lipid fluid state of the membrane together with regulatory proteins, sense the temperature and adjust biological processes (Islas 2014). Certain TRP ion channels in the afferent neurons of the somatosensory system have been proposed as detectors of thermal stimuli and convert it to an electrical signal, which is propagated to the central nervous system to evoke adequate responses including temperature sensation.

TRPs in thermosensation (ThermoTRPs)

The TRP ion channels that are associated with the detection of temperatures collectively span the whole physiological range of temperatures and are called thermoTRPs (Fig. 1.4). These thermoTRPs are involved in transduction of thermal stimuli into chemical and electrical signals in the sensory nervous system (Patapoutian, Peier et al. 2003). In general, the activation mechanism of many ion channels is modulated by temperature (Belmonte, Brock et al. 2009), but only a few postulated thermoTRPs have been shown to directly respond to temperature (Zakharian, Cao et al. 2010, Cao, Cordero-Morales et al. 2013). Each thermoTRP ion channel is thought to detect a distinctive temperature range (Patapoutian, Peier et al. 2003). The discovery of TRPV1 (Caterina, Schumacher et al. 1997) sparkled the search for other thermoTRPs and many subsequent studies have advanced the understanding of the molecular and cellular mechanism of thermosensation in organisms (Patapoutian, Peier et al. 2003, Vriens, Nilius et al. 2014). In general, humans perceive a skin temperature around 33°C as thermoneutral, and temperatures lower or higher than this temperature are perceived as cool, cold, warm and hot, respectively (Vriens, Nilius et al. 2014).

The temperature dependence is often quantified as a temperature coefficient (Q_{10}), which can be defined as the relative change in the rate of a reaction when the temperature changes 10°C. The Q_{10} can be calculated using the following equation:

$$Q_{10} = \left(\frac{R_2}{R_1}\right)^{\frac{10}{(T2-T1)}} \qquad \text{(eq.1)}$$

In the above equation, R_1 and R_2 are reaction rates at two different temperatures (T_1 and T_2). In principle, T_1 and T_2 can be any temperature and do not need to differ in 10°C. Most ion channels display Q_{10} values in between 1 and 3, and are therefore not considered as thermosensors (Vriens, Nilius et al. 2014). It has been proposed that for a TRP ion channel to be classified as a thermoTRP, it must show a Q_{10} value of ≥ 5 or ≤ 0.2 at relevant temperatures for heat activated and cold-activated ion channels, respectively (Voets 2012).

ThermoTRPs in warm and hot sensation

TRPV1 is the first cloned and best-studied thermoTRP among all TRP ion channels. It is a polymodal sensor as it also responds to chemicals such as the pungent compound capsaicin from chilli pepper (Caterina, Schumacher et al. 1997) and endogenous capsaicin like compounds such as anandamide and 2-arachidonoyl glycerol (Zygmunt, Petersson et al. 1999, Zygmunt, Ermund et al. 2013). TRPV1 is highly expressed in small-diameter Aδ and C-fibres and plays a role as a noxious heat sensor with a temperature threshold of ≥ 42°C (Caterina, Schumacher et al. 1997). Studies showed that TRPV1 is also involved in heat hyperalgesia associated with inflammation (Davis, Gray et al. 2000). Another thermoTRP, TRPV2, has a sequence identity of 50% to TRPV1 and is activated by noxious heat in a heterologous expression system with an activation threshold of ≥ 52°C (Caterina, Rosen et al. 1999). In contrast to these findings, studies on knockout mice concluded that TRPV2 is not noxious heat sensor *in vivo* (Park, Vastani et al. 2011). TRPV2 is highly expressed in a sub population of medium to large-diameter sensory neurons (Caterina, Rosen et al. 1999).

Two other thermoTRPs belonging to the TRPV subfamily are TRPV3 and TRPV4, both of which show 40-50% sequence similarity with TRPV1 and are involved in innocuous-warmth sensation (Patapoutian, Peier et al. 2003). In a heterologous system, TRPV3 is activated in a temperature range of 34°C - 38°C. TRPV4 was originally identified as an osmosensor, but can also be activated by warm temperatures in a slightly lower range of 27°C - 34°C (Patapoutian, Peier et

al. 2003). Interestingly, these TRPs are highly expressed in keratinocytes compared to sensory neurons (Peier, Reeve et al. 2002), and it has been proposed that sensing warm temperatures by these TRPs is causing the release of ATP or nitric oxide from keratinocytes and subsequent activation of sensory neurons (Vriens, Nilius et al. 2014). Interestingly, TRPV3 exhibits sensitization with repeated and prolonged exposure to temperature, whereas TRPV4 shows desensitization by the same treatment (Patapoutian, Peier et al. 2003).

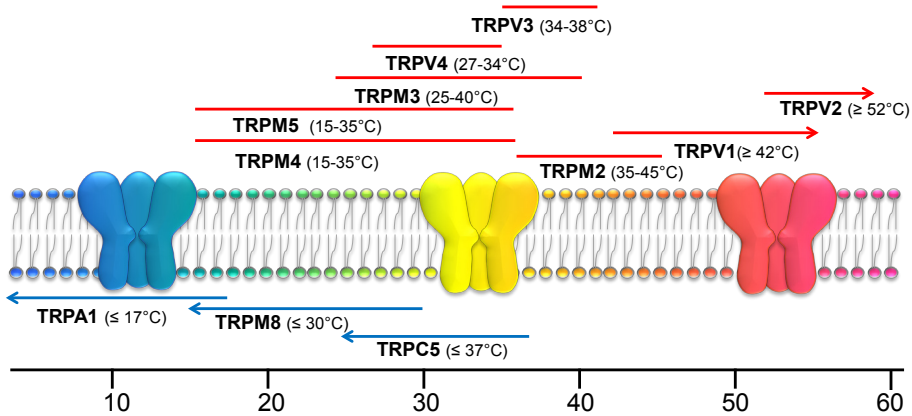

Figure 1.4 Schematic representations of thermoTRPs and their temperature activation thresholds. Together all thermoTRPs detect physiological temperatures from extreme cold (≤ 17°C) to extreme heat (≥ 52°C) (María Pertusa and Ramón Latorre 2012).

In the TRPM subfamily, TRPM2, TRPM3, TRPM4 and TRPM5 are activated by heat, but TRPM8 is activated by cold. Recently TRPM3 was identified as a noxious heat sensor and shown to be expressed in a large subset of small-diameter sensory neurons (Vriens, Owsianik et al. 2011). TRPM2, TRPM4, and TRPM5 are also activated by warm temperatures in the physiological range. TRPM2 channels are activated by warm temperatures > 35°C (Togashi, Hara et al. 2006), whereas both TRPM4 and TRPM5 are activated at temperatures > 15°C (Talavera, Yasumatsu et al. 2005). In contrast to other thermoTRPs, TRPM2, TRPM4, and TRPM5 are expressed in neither primary sensory neurons nor keratinocytes and their role in thermosensation has not yet been resolved. However, the temperature modulates the voltage sensitivity of TRPM4 and also has a modulatory effect on TRPM5 in the sensation of taste (Talavera, Yasumatsu et al. 2005).

ThermoTRPs in cool and cold sensation

The two best-studied cold-activated TRPs are TRPM8 and TRPA1. TRPM8 was first identified in prostate cancer cells and show highest expression in a small subpopulation of Aδ and C-fibres that originates from DRG and TG (Tsavaler, Shapero et al. 2001, Vriens, Nilius et al. 2014). TRPM8 is activated by innocuous cold temperatures with a temperature range from 15°C to 30°C (McKemy, Neuhausser et al. 2002, Peier, Moqrich et al. 2002). In contrast to TRPM8, TRPA1 the only mammalian member in TRPA subfamily is activated by noxious cold temperatures ≤ 17°C (Story, Peier et al. 2003). Structural and functional details of TRPA1 are described in chapters 2 and 3. Recently, it has been reported that TRPC5 in the TRPC subfamily is also activated by cooling temperatures, from 37°C to 25°C, and is expressed in primary sensory neurons (Zimmermann, Lennerz et al. 2011).

1.3.4 TRP ion channels and medical importance

As mentioned earlier, TRP channels carry out a wide variety of functions including, nociception, thermosensation, mechanosensation, redox signalling, thermoregulation, regulation of endosomal and lysosomal function and ion homeostasis. TRP ion channel family members (TRPV1-V4, TRPA1, TRPM2, TRPM3, TRPM8, TRPC1 and TRPC6) expressed in the peripheral nervous system are important for transduction of noxious stimuli that leads to the generation of pain sensation in mammals (Sousa-Valente, Andreou et al. 2014). TRPs are not merely mediating inflammatory pain, but additionally play a role in the process of chronic inflammatory diseases, like asthma and diabetes (Jordt and Ehrlich 2007, Dai 2015). Regular physiological functioning of TRP ion channels is crucial for the survival of an organism, whereas malfunction of TRP ion channels developed either by alternation of channel expression, sensitization, or desensitization of TRP ion channels leads to a wide range of diseases and symptoms such as heat, cold and mechanical hyperalgesia* and allodynia** in humans (Nilius 2007, Sousa-Valente, Andreou et al. 2014). An impaired TRP ion channel function by mutations is the cause for development of several genetic diseases, which are listed under channelopathies in Table 2 (Nilius and Owsianik 2011). The involvement of TRPs in various diseases has been extensively reviewed (Jordt and Ehrlich 2007, Nilius 2007, Nilius and Owsianik 2011).

* Hyperalgesia is an increased sensitivity to painful stimuli.

**Allodynia is characterized by non-harmful stimuli evoking a pain response.

Table 2 Channelopathies linked to (dysfunctional) TRP ion channels

Channel	Hereditary disease	Clinical manifestations	References
TRPC6	Focal segmental glomerulosclerosis(FSGS)	Proteinuria, nephritic syndrome and progressive loss of renal function.	(Winn, Conlon et al. 2005)
TRPV4	Spondylometaphyseal dysplasia, Kozlowski type	Abnormalities in the bone growth.	(Rock, Prenen et al. 2008, Deng, Klein et al. 2010, Landoure, Zdebik et al. 2010)
	Scapuloperoneal spinal muscular atrophy (SPSMA)	Progressive weakness of scapular and peroneal muscle, bone abnormalities	
	Charcot-Marie-Tooth disease type 2C (CMT2C)	Progressive weakness of distal limbs, vocal cords, diaphragm and impaired hearing as well as vision.	
TRPM1	Autosomal recessive congenital stationary night blindness (CSNB)	Non progressive impaired night vision.	(van Genderen, Bijveld et al. 2009)
TRPM4	Autosomal dominant progressive familial heart block type 1(PFHB1)	Heart block	(Kruse, Schulze-Bahr et al. 2009)
TRPM6	Autosomal recessive hypomagnesemia associated with secondary hypocalcaemia	Low serum levels of Mg^{2+} and Ca^{2+}. Symptoms are seizures and muscle spasms in infancy.	(Walder, Landau et al. 2002)
TRPML1	Autosomal recessive neurodegenerative lysosomal storage disorder (mucolipidosis type IV)	Mental retardation and retinal degeneration.	(Bach 2005)
TRPP2	Autosomal dominant polycystic kidney disease (PKD)	Progressive enlargement of renal cysts leads to renal failure.	(Grantham 1993)
TRPA1	Familial episodic pain syndrome (FEPS)	Episodes of upper body pain, and triggered by cold, fasting and physical stress.	(Kremeyer, Lopera et al. 2010)

Because of their involvement in many diseases, disease-related conditions, pain and inflammation, it is very important to understand the molecular mechanism of these channels to facilitate the development of specific novel analgesics and anti-inflammatory agents.

Chapter 2
Structural features of TRPA1

The focus of this thesis is on TRPA1 as a polymodal sensory receptor. TRPA1 was first identified and cloned from cultured human fibroblasts without a known function and it was originally named according to the predicted structural domains as ANKTM1 (Ankyrin-like with transmembrane domains protein-1). The corresponding gene, *trpa1*, contains 27 exons and is located on human chromosome 8 (8q13) (Jaquemar, Schenker et al. 1999, Zygmunt and Högestätt 2014). Later Story *et al.*, identified ANKTM1 (now TRPA1) expression in a subpopulation of nociceptive sensory neurons, where it is co-expressed with TRPV1 but not with TRPM8, and proposed it to be a noxious cold sensor (Story, Peier et al. 2003). Independently, TRPA1 was identified as an ionotropic cannabinoid receptor and a chemosensor of mustard oil containing electrophilic compounds (Jordt, Bautista et al. 2004). In the sensory nervous system, TRPA1 is expressed in primary afferent nociceptors that originate from trigeminal, nodose, and dorsal root ganglia (DRG). In addition, TRPA1 is also found in the central nervous system and non-neuronal cells like epithelial cells, hair cells, mast cells, fibroblasts, odontoblast, β-cells of Langerhans islets (Zygmunt and Högestätt 2014). Several orthologues of TRPA1 have been identified in both mammalian and non-mammalian species (Nilius, Appendino et al. 2012). The number of TRPA1 homologues varies between species e.g. one in mammals, four in fruit fly, two in zebrafish, and two in *C. elegans* (Nilius, Appendino et al. 2012).

To understand the molecular mechanism of TRP proteins, we need to know their structural details at the atomic level. In TRP research, one great hurdle has been to determine the structure at such a high resolution, due to the demands and limitations of X-ray crystallography and NMR techniques. For crystallographers it is crucial to have large amounts of stable and pure proteins to be able to grow crystals, which is usually very difficult to obtain for membrane proteins. Although crystals are not needed for NMR spectroscopy, proteins belonging to the TRP family are too large in size to be resolved by this technique. Furthermore, having multiple large flexible domains in each subunit exhibiting a pool of different conformations also hamper structural studies like, crystallization and single-particle electron microscopy (EM) (Gaudet 2008). Considering the difficulties to resolve the complete TRP ion channel structure, researchers have instead solved

the structures of individual soluble intracellular domains that can be expressed and purified alone, like the ankyrin repeat domain (ARD) from TRPV, the coiled-coil domain from TRPM and the α-kinase domain from TRPM7 channels (Gaudet 2008).

The aim of this chapter is to describe the structural features of TRPA1. Cvetkov *et al.*, reported the first resolved EM structure of full-length TRPA1 (mouse) although only at the very low resolution of 16 Å (Cvetkov, Huynh et al. 2011). Using recent technological advances in the field of single-particle electron cryo-microscopy (cryo-EM), Paulsen *et al.*, resolved the structure of human TRPA1 (hTRPA1) in the presence of agonist (AITC) and antagonists (HC-030031 and A-967076) at a resolution of ~4 Å (Paulsen, Armache et al. 2015). The same research group also resolved the rat TRPV1 structure with a resolution of ≤ 4 Å (Liao, Cao et al. 2013). Very recently this technique also allowed determination of the structure of rabbit TRPV2 at a nominal resolution of ~4 Å (Zubcevic, Herzik et al. 2016).

2.1 General structural features

The human *trpa1* gene encodes 1,119 amino acids protein with a molecular weight of 127.4 kDa. As for other TRP ion channels, TRPA1 forms a functional homotetrameric complex with one central pore. Each subunit in the tetramer contains six membrane spanning α-helical segments (S1-S6). Human TRPA1 contains large (80% of the channel mass) intracellular N- and C-terminal domains. The C-terminal has a central tetrameric parallel coiled-coil domain just below the ion pore that is covered with a part of the N-terminal ARD (Fig. 2.1A) (Paulsen, Armache et al. 2015). The following sections of this chapter describe in detail the TRPA1 structural domains (Fig. 2.2).

2.2 Ankyrin repeat domain

Among the TRP subfamilies, only TRPC, TRPV, TRPA, and TRPN contain ankyrin repeat motifs in their N-terminal domain (Gaudet 2008). Of these TRPA1 stands out with its very long ARD, predicted to contain 14-17 ankyrin repeats (Story, Peier et al. 2003, Gaudet 2008). The ankyrin repeat (AR) is a 33-amino acids sequence motif that forming an anti-parallel helix-loop-helix and followed by β-hairpin loop. This is one of the most evolutionary conserved motifs (Sedgwick and Smerdon 1999). The inner α-helix is slightly shorter than the outer α-helix and forms a distinctive curved structure with outer convex and inner

concave surface (Herbert, Squire et al. 2015). A stretch of three or more ARs form structural domains in many different types of proteins (Gaudet 2008). The overall shape looks like a cupped hand where helices form as hand and loops form as fingers. Generally, ARs are involved in protein-protein interactions and ligand binding (Hellmich and Gaudet 2014).

The structure of the hTRPA1 was resolved only for the proximal part of the N-terminus (12-16 AR) (Fig. 2.2A). The rest of the N-terminus appeared as a weak density map in all electron micrographs. Predictions show that the density consists of 11 ARs that form a curved shaped structure under rest of the protein (Paulsen, Armache et al. 2015). Based on the appearance of two separate densities in the N-terminal region it was suggested that the ARD forms a broken domain with a relatively flexible distal part (Brewster and Gaudet 2015). Even though the ARD typically is a region for protein/ligand interaction, no such sites of interaction were identified (Brewster and Gaudet 2015). Studies have proposed that the N-terminal ARD plays a role in mechanosensation (Nagata, Duggan et al. 2005, Sotomayor, Corey et al. 2005) and thermosensation (Cordero-Morales, Gracheva et al. 2011). Because of incomplete structural information of the ARD, it is still unclear how it regulates the channel gating.

2.2.1 Calcium (Ca^{2+}) binding

It has been shown that Ca^{2+} is not only permeating through the pore, but is also strongly regulating TRPA1 activity (Nilius, Prenen et al. 2011). Two mechanisms for Ca^{2+} regulation of TRP ion channels have been suggested, one of the mechanisms is via binding of Ca^{2+}-calmodulin (CaM) to the C-terminus of TRPV1 and the other mechanism is by binding of Ca^{2+} to a paired EF-hand motif in the C-terminus of TRPP channel (Fig. 1.3) (Hellmich and Gaudet 2014). However, structural details of Ca^{2+} regulation in TRPA1 ion channels are not known yet. Some studies suggested that Ca^{2+} is binding to a putative EF-hand domain in the TRPA1 N-terminus between 11^{th} and 12^{th} ARD (Doerner, Gisselmann et al. 2007, Zurborg, Yurgionas et al. 2007). Chimeric studies reported that AR 7 - 11 and/or AR 11 - 14 of hTRPA1 are prerequisites for Ca^{2+} regulation (Cordero-Morales, Gracheva et al. 2011). In addition, mutational studies reported the involvement of a C-terminal acidic cluster (Glu1077, Asp1080 - Asp1082) in TRPA1 Ca^{2+}-mediated regulation (Sura, Zima et al. 2012). Since we are lacking the structural details of the distal part of C- and N-terminal region of TRPA1, the regulatory mechanism of Ca^{2+} remains to be uncovered. However, the proximity of proposed N-terminal and C-terminal

regions for Ca^{2+} binding indicates that they can possibly form a common binding/regulatory site.

2.3 Pre-S1 region

Pre-S1 region connects the N-terminal ARD to the first transmembrane segment of the hTRPA1. This region is composed of a pre-S1 helix and a linker region. The linker region contains two helix-turn-helix motifs that are separated with anti-parallel β-sheets. The proposed critical amino acids for electrophilic binding and activation are located in the first helix-turn-helix (Cys621), in the first putative β-sheet (Cys641), in the loop connecting β-strand to second helix-turn-helix (Cys665), and in the pre-S1 helix (Lys710) (Fig**.** 2.2C) (Paulsen, Armache et al. 2015). The close proximity of these cysteines could form disulphide bonds and could be involved in the activation and desensitization of TRPA1 by electrophiles (Cvetkov, Huynh et al. 2011).

2.4 Transmembrane domain

Each subunit of TRPA1 contains six membrane-spanning α-helices (S1-S6), of which the first four (S1-S4) helices form one subdomain and is followed by a linker connecting S4 and S5 of the pore region. The S4-S5 linker is lined almost parallel to the membrane. The ion-conducting pore is formed by the S5 and S6 transmembrane helices from each subunit. Like TRPV1, TRPA1 displays swapping of domains, where the S1-S4 subdomain of one subunit is interacting with S5-S6 of the neighbouring subunit (Fig. 2.1B) (Cao, Liao et al. 2013, Liao, Cao et al. 2013, Paulsen, Armache et al. 2015). Although TRP ion channels share a common transmembrane architecture with the voltage-gated potassium channels, they do not have the characteristic positively charged amino acids in the fourth transmembrane segment, which is in line with TRP ion channels being less sensitive to voltage (Nilius, Talavera et al. 2005, Wu, Sweet et al. 2010). Nevertheless, several basic residues in the C-terminal domain were identified to have a role in voltage-dependent gating of hTRPA1 (Samad, Sura et al. 2011). Interestingly, the extracellular loop between S1 and S2 contains two putative N-glycosylation sites but its functional role is not known yet.

The agonist treated structure of the hTRPA1 ion-conducting pore displays two major constrictions. Although, the pore structure of TRPA1 is similar to TRPV1 there are still some differences such as, the outer vestibule of the TRPA1 is steeper and formed by two pore helices, the upper gate is formed by one residue (Asp915)

and lower gate formed by two hydrophobic residues (Ile957 and Val961). The latter form the narrowest constriction that blocks the passage of rehydrated cations. In contrast, the outer vestibule of the TRPV1 is wider and contains one single pore helix, the upper gate is formed by two residues (Gly643, Met644) and lower gate is formed by a single residue (Ile679) (Paulsen, Armache et al. 2015). It has been proposed that inner pore forming residues controls the gating of the TRPA1 ion channel (Benedikt, Samad et al. 2009). The functional role of the second pore helix and its conservation in TRPA1 orthologues remains to be clarified. Importantly, the TRPA1 structure also revealed a binding pocket for the antagonist A-967076, which is formed by residues in S5, S6, and the first pore helix (Paulsen, Armache et al. 2015).

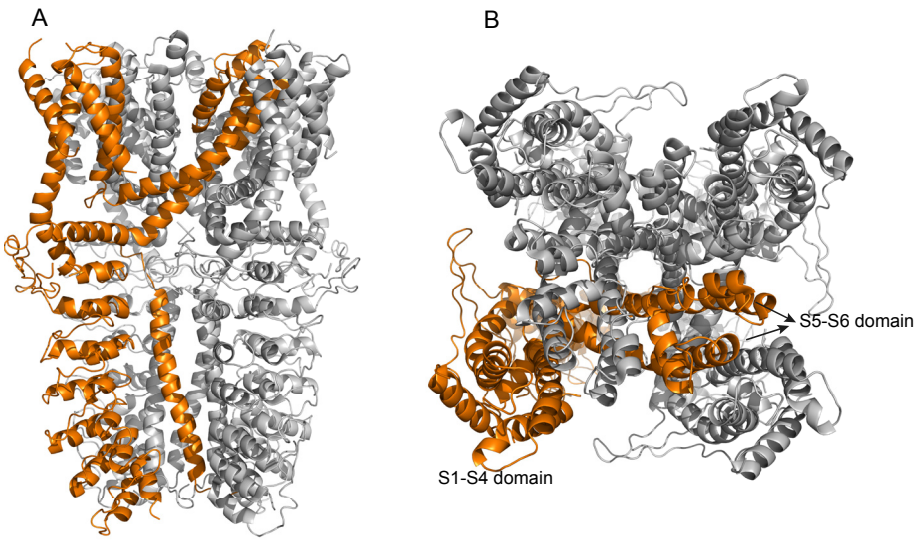

Figure 2.1 Single particle cryo-EM structure of human TRPA1 (PDB ID: 3J9P): A. Cartoon representation of TRPA1 showing a side view of the tetrameric assembly with the transmembrane domain at the top. A single subunit is highlighted in orange colour. **B.** Cartoon diagram of TRPA1 in top view (extracellular side), showing domain swapping of the S5-S6 region of one subunit with the S1-S4 subdomain of another subunit. The S5-S6 subdomain, including the two short pore helices, from each of the four subunits together form a central ion pore.

2.5 TRP-like domain

Like many other TRP ion channels, TRPA1 does not have the canonical TRP motif sequence (EWKFAR), found in e.g. TRPV1. However, the structure revealed that it contains an analogous α-helix structure in the C-terminal right after sixth transmembrane segment, hence called the TRP-like domain. The TRP-

like domain interacts with N-terminal pre-S1 region and S4-S5 linker through hydrophobic interactions between α-helices and its subsequent extension also contributes in the formation of a putative three-stranded β-sheet. All interactions together form an "allosteric nexus" (Fig. 2.2). The placement of cysteines within the allosteric nexus allows us to speculate that interaction of electrophiles to these cysteines leads to channel gating through transmission of conformational rearrangements to the TRP-like domain. Unfortunately, the insufficient resolution and the reversible nature of the agonist modifications hinder any information from this structure regarding interaction with e.g. the electrophile AITC (see section 3.1.1 below) (Paulsen, Armache et al. 2015).

2.6 Coiled-coil domain

Coiled-coils are identified in a large number of structurally and functionally divergent proteins. They are involved in protein-protein interactions and protein oligomerization. Coiled-coil domains contain two or more α-helices, which form supercoils by winding around each other. The helices can be arranged in parallel or in an antiparallel manner and also either homo- or heteromeric in nature. The classical coiled-coil structure contains a seven residue (heptad) repeat where the residues are named from 'a' to 'g'. Typically, positions 'a' and 'd' residues are hydrophobic in nature and project towards the core of the supercoil causing tight helix-helix interactions. Positions 'e' and 'g' residues are hydrophilic in nature and are located outside of the coiled-coil, thereby allowing inter helical interactions. Rest of the positions, b, c and f, are less involved in the assembly of coiled-coils (Hellmich and Gaudet 2014).

Coiled-coil domains have been identified in either the N- or C-terminal part of TRP family proteins such as TRPM (X-ray structure of TRPM7 (Fujiwara and Minor 2008)), TRPP (X-ray structure TRPP2 and TRPP3 (Yu, Ulbrich et al. 2009, Molland, Paul et al. 2012, Yu, Ulbrich et al. 2012)), yeast TRP (Ihara, Hamamoto et al. 2013) and TRPC (Lepage, Lussier et al. 2009). TRPA1 was not predicted to contain a coiled-coil structure, however, structural studies revealed that a tetrameric assembly of a coiled-coil in hTRPA1 is positioned in the centre of the cytosolic domain. The coiled-coil subunit interactions of TRPA1 occur in similar way as described above for a classical coiled-coil. Unlike the classic coiled-coil heptad, two glutamines are positioned in place of hydrophobic residues at 'a' and 'd' . The positioning of these polar residues could permit destabilization (Gln1047) or stabilization (Gln1061) of the TRPA1 ion channel. The destabilization of the channel can be neutralized by inter helical interaction

through inositol hexakisphosphate, which is located at the interface between ARD and coiled-coil domain (Paulsen, Armache et al. 2015). The removal of these phosphates from the channel by e.g. Ca^{2+} could lead to inactivation, hence the inositol hexakisphosphate proposed as a "molecular kill switch" in the process of channel inactivation (Brewster and Gaudet 2015). This process can explain the requirement of polyphosphates for the stable activity of TRPA1 (Kim and Cavanaugh 2007).

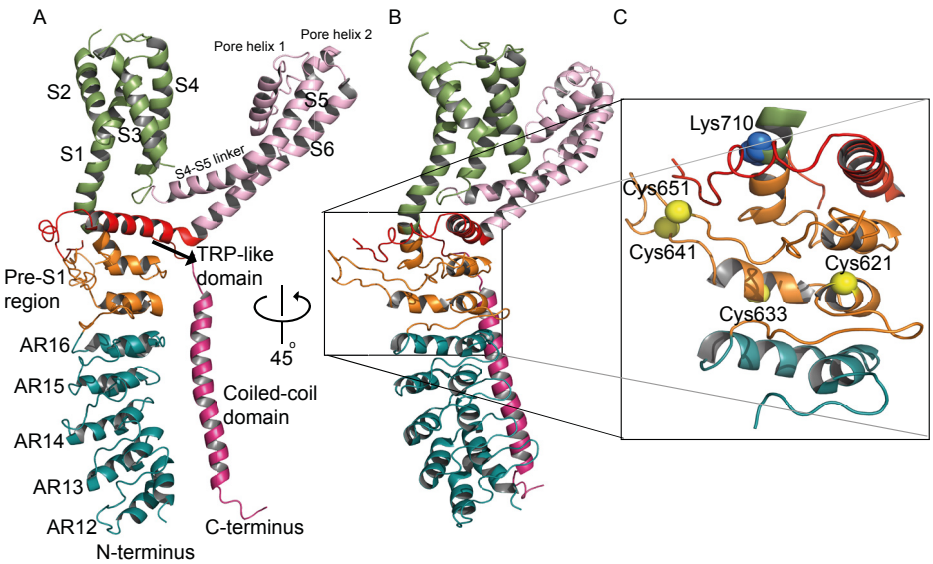

Figure 2.2 Single subunit of human TRPA1 contains different structural domains (PDB ID: 3J9P). A. Individual structural domains are presented in different colours, such as ARs are in deep teal, pre-S1 region is in orange, S1-S4 domain is in green, S4-S5 linker, S5-S6 and pore helix are in light pink, TRP-like domain is in red, coiled-coil domain is in warm pink. **B.** Single subunit in "A" rotated in 45° to clearly visualize the linker region. **C.** Close-up view of the nexus region with highlighted cysteines and lysine are important for the binding of electrophilic compounds.

Chapter 3
Role of TRPA1 in chemo- and thermosensation

The ubiquitous expression of TRPA1 suggests that it plays a role in diverse functions from somatosensation to cellular homeostasis and is involved in causing many pathological conditions, involving pain, inflammation, itch, migraine and cardiovascular diseases. Remarkably, TRPA1 responds to different types of stimuli such as chemicals, temperatures, and mechanical force that elicit pain sensation. TRPA1 is a non-selective cation channel with a relatively high conductance. The single-channel conductance of TRPA1 at various experimental conditions and in different species varies between 40 and 180 pS (Zygmunt and Högestätt 2014).
In this chapter, the functional role of TRPA1 in chemo- and thermosensation is discussed.

3.1 TRPA1 as a chemosensor

As a chemosensor, TRPA1 was originally identified as a detector of thiol-reactive electrophiles and oxidants and non-electrophilic compounds as well as indirectly activated by G protein-coupled receptor binding pro-inflammatory agents and Ca^{2+} (Bandell, Story et al. 2004, Jordt, Bautista et al. 2004, Bautista, Movahed et al. 2005, Macpherson, Geierstanger et al. 2005). The electrophile-sensitivity of TRPA1 has been conserved for ~500 million years, since TRPA1 in vertebrates and invertebrates originates from a common ancestor, which contains key molecular prerequisites for the electrophilic detection (Kang, Pulver et al. 2010). Today, TRPA1 has been shown to be activated by more than 100 compounds including environmental, plant-derived and endogenous activators (Zygmunt and Högestätt 2014). Some of these compounds are suggested to interact directly with TRPA1, whereas others activate TRPA1 indirectly through a receptor-operated mechanism. However, only few TRPA1 activators have been shown to bind directly to TRPA1 (Hinman, Chuang et al. 2006, Macpherson, Dubin et al. 2007, Wang, Cvetkov et al. 2012) and thus for many electrophilic and non-electrophilic compounds it remains to be shown that TRPA1 is indeed an intrinsic chemosensor.

3.1.1 Covalent interaction

Cysteine is the most highly reactive residue among the 20 amino acids, since it has a free thiol (-SH) group. Cysteines play an important role in the function of proteins and formation of tertiary as well as quaternary structures. These structures are stabilized by cysteines, forming intermolecular and intramolecular disulphide bonds (S-S) in the protein. Cysteines are also found to be involved in various modifications of proteins. These include oxidation reactions with reactive oxygen species (ROS), either reversibly or irreversibly, and interactions with nitric oxide (NO) causing nitrosylation. Furthermore, sulfhydration reactions occur when cysteines interact with hydrogen sulphide (H_2S), and in addition, cysteines interact with electrophiles resulting in alkylation (Giron, Dayon et al. 2011, Filipovic 2015).

Activation of TRPA1 by covalent interaction is one of the most well-characterized and studied mechanisms. TRPA1 can be activated by a large number of a wide variety of structurally different exogenous and endogenous compounds (Zygmunt and Högestätt 2014). These are ranging from natural pungent compounds such as allyl isothiocyanate (AITC; wasabi, horseradish and mustard) (Jordt, Bautista et al. 2004), cinnamaldehyde (CA; cinnamon) (Bandell, Story et al. 2004), allicin and dialyl disulphide (garlic, onion) (Bautista, Movahed et al. 2005), to non-natural/environmental irritants such as formalin, hypochlorite, acrolein from smoke and tear gas, and industrial isothiocyanates (Bautista, Pellegrino et al. 2013). Although, one strong commonality among these compounds is their electrophilic nature preferably interacting with free thiol groups, their activation of TRPA1 is also determined by their structural features including steric hindrance (Fig. 3.1) (Bessac, Sivula et al. 2009, Gijsen, Berthelot et al. 2010, Sadofsky, Boa et al. 2011, Ibarra and Blair 2013). Thus, there are a number of factors involved in the modification of the cysteine side chains in native proteins by thiol reactive compounds and oxidants, such as chemical microenvironment (thiol ionization promoted by close proximity to positive charged amino acids that affects the p*K*a value of cysteine) (Lutolf, Tirelli et al. 2001) and steric hindrance (Paulsen and Carroll 2013). Altogether, this can explain fine-tuning of TRPA1 by activators also can be used to achieve pain relief (Zygmunt and Högestätt 2014).

In general, cysteine, lysine, and histidine residues are known to be targets for electrophilic attack. It has been suggested that conserved cysteines (Cys621, Cys641 and Cys665 (Hinman, Chuang et al. 2006) in the hTRPA1 and Cys415, Cys422 and Cys622 in the mouse TRPA1 are critical for the electrophilic

activation by reversible covalent modification (Macpherson, Dubin et al. 2007). These cysteines are located in the linker region between N-terminal ARD and transmembrane domain in hTRPA1 (Fig. 2.2C). Wang *et al.,* have shown that these critical cysteines are involved in the formation of disulphide bonds and this network could play a role in electrophilic activation and desensitization of TRPA1. These bonds include Cys193-Cys666, Cys463-Cys666, Cys609-Cys622 and Cys622-Cys666 in mouse TRPA1 (Wang, Cvetkov et al. 2012). Along with these critical residues, lysine 710 in hTRPA1 is also involved in irreversible covalent modification to some extent (Hinman, Chuang et al. 2006). Even though, many electrophiles target three critical cysteines (Cys621, Cys641 and Cys665) for the activation of TRPA1, there are some exceptions such as *p*-benzoquinone, isovelleral and polygodial compounds, which activate TRPA1 that are lacking these critical cysteines (Escalera, von Hehn et al. 2008, Ibarra and Blair 2013). This indicates that cysteines outside the N-terminal region are also involved in electrophilic activation. It has been shown that 14 cysteines react with iodoacetamide (IA) and 30 cysteines react with N-methylmaleimide (NMM) (Macpherson, Dubin et al. 2007, Wang, Cvetkov et al. 2012). However, how many of these interactions that can lead to channel activation remains to be studied. The location of these critical cysteines in the nexus region (Fig. 2.2C) and its involvement in formation of disulphide bonds indicate that these cysteines could possibly maintain a conformation that favours the TRPA1 ion channel to respond to certain electrophiles. This may explain why critical cysteine mutations abolish the channel activity, possibly indirectly by "physiological antagonism".

In addition to exogenous stimuli, endogenous inflammatory mediators are also interacting with TRPA1 cysteines by covalent modifications. Prostaglandins (PGs) are important inflammatory mediators which are produced after tissue injury, among them the cyclopentenone PG 15-deoxy-Δ12,14-prostaglandin J2 (15d-PGJ_2) is a highly reactive product of the cyclooxygenase pathway (Zygmunt and Högestätt 2014). In addition to 15d-PGJ_2, tissue injury produces a range of highly reactive inflammatory mediators: ATP, protons, NO, H_2O_2, bradykinin, cytokines, and lipid peroxidation products, 4-hydroxynonenal (4-HNE). 15d-PGJ_2 and 4-HNE contain α, β-unsaturated carbonyl moieties like CA, which can covalently interact with thiol groups in cysteines via a Michael addition reaction (Takahashi, Mizuno et al. 2008). NO and H_2S is also known to interact with free thiols via nitrosylation (Filipovic 2015). Likewise, H_2O_2 is also known to interact with cysteines via oxidation to form either cysteine sulfenic acid or disulphide bonds (Poole, Karplus et al. 2004, Filipovic 2015). Site-directed mutagenesis and pharmacological assays identified that the activation of TRPA1 by these

inflammatory mediators occur via covalent modification of N-terminal cysteines, but the preference of critical cysteines varied depending on the inflammatory mediator (Takahashi, Mizuno et al. 2008). 15d-PGJ_2 modifies the Cys421 and Cys621, which leads to activation of hTRPA1. Cysteine 421 in TRPA1 is proposed to be a common site for covalent modifications by oxidants. In addition to Cys421, Cys641 and Cys665 are also involved in the activation of TRPA1 by H_2O_2 and NO (Takahashi, Mizuno et al. 2008). This activity was reversed by dithiothreitol (DTT) but DTT had no effect on activation by 15d-PGJ_2 and 4-HNE, which supports that the latter are forming Michael adducts (Takahashi, Mizuno et al. 2008).

In contrast to the above mentioned inflammatory mediators, bradykinin, ATP and monoamines activate TRPA1 indirectly via the PLC pathway (Bandell, Story et al. 2004, Jordt, Bautista et al. 2004). Bradykinin is produced at tissue injury, ischemia, and inflammation and binds to bradykinin receptors (BK2 receptors) which are coupled with PLC and co-expressed with TRPA1 in sensory neurons.

Near ultra violet light (UVA) also activates TRPA1 indirectly, by generation of ROS from the tissue damage and this explains the involvement of TRPA1 in pain sensation during photodynamic therapy (Hill and Schaefer 2009).
TRPA1 is also acts as an oxygen (O_2) sensor and displayed a U-shaped sensitivity to O_2 by responding directly to hyperoxia and indirectly to hypoxia. Oxidation of reactive cysteines and hydroxylation of prolines are involved in the mechanisms of TRPA1 activation by hyperoxia and hypoxia, respectively (Takahashi, Kuwaki et al. 2011). Cys633 and Cys856 were identified as major targets for sensing increased levels of O_2 (Takahashi, Kuwaki et al. 2011). The free thiol group of these cysteines were first oxidized under hyperoxia resulting in conversion to sulfenic acids and later converted to relatively stable disulphide bonds (Takahashi, Kuwaki et al. 2011). Regarding hydroxylation of prolines, Pro394 in the N-terminus of hTRPA1 has been identified as a regulatory switch for the activation or inactivation of the channel at different levels of oxygen conditions like normoxia and hypoxia (Takahashi, Kuwaki et al. 2011). Thus, TRPA1 may be an important redox sensor controlling peripheral blood flow via CGRP containing sensory neurons (Zygmunt 2011).

TRPA1 is also indirectly activated by CO_2 through the increase of intracellular protons. CO_2 perfused through the membrane forms carbonic acid, which leads to intracellular acidosis (Wang, Chang et al. 2010). Due to its sensitivity to cellular acidosis, TRPA1 also works as a sensor for other weak acids and the extent of

TRPA1 activation is proportional to the amount of intracellular acidification (Wang, Chang et al. 2011). The activation mechanism of weak acids is distinct from the mechanism of reactive compounds, which target N-terminal critical cysteines (Wang, Chang et al. 2011). TRPA1 also works as a sensor for extracellular acidosis in sensory neurons, which explains its involvement in proton-evoked pain and inflammation. The S5 and S6 transmembrane domains and Val942 and Ser943 were identified as important regions for activation of hTRPA1 by protons, but not the N-terminal critical cysteines (de la Roche, Eberhardt et al. 2013). In addition to acidosis, TRPA1 is also activated by intracellular alkalization and the activation mechanism is suggested to work in similar way as covalent activation since Cys422 and Cys622 in mouse TRPA1 were identified as key residues for the activation by alkalization (Fujita, Uchida et al. 2008). Importantly, there are species-specific differences that must be considered when developing hTRPA1 therapeutic screening assays of TRPA1 analgesics (Zygmunt and Högestätt 2014).

TRPA1 can also be directly activated by metal ions such as zinc, copper and cadmium. Overexposure to these metal ions causes pain and inflammation and eventually leads to death. It has been known that zinc binding is mediated predominantly by interaction with side chains of cysteines and histidines in proteins (FALCHUK 1993). Hu *et al.*, have shown that zinc activates TRPA1 after influx of zinc ions through the TRPA1 ion channel via a novel mechanism by binding to intracellular specific cysteines and histidines (Hu, Bandell et al. 2009). N-terminal Cys641, C-terminal His983 and Cys1021 were identified as important sites for the zinc-mediated activation. Cadmium also exhibits a similar activation effect as zinc on TRPA1, which suggests there is a common mechanism for the metal toxicity (Hu, Bandell et al. 2009). Andersson *et al.*, also suggested that TRPA1 act as an intracellular zinc sensor (Andersson, Gentry et al. 2009).

3.1.2 Non-covalent interaction

As mentioned earlier, TRPA1 also senses many non-electrophilic plant-derived and synthetic chemicals. Their interactions with TRPA1 are probably taking place in a classical lock and key receptor-ligand binding manner, rather than by covalent interactions. These compounds include Δ^9-tetrahydrocannabinol (Δ^9-THC) (Jordt, Bautista et al. 2004), menthol and its analogues (Karashima, Damann et al. 2007), nicotine (Talavera, Gees et al. 2009), clotrimazole (Meseguer, Karashima et al. 2008), dihydropyridines (Fajardo, Meseguer et al. 2008), carvacrol, oleocanthol, lidocaine (Leffler, Lattrell et al. 2011) and eudesmol (Ohara, Fukuda

et al. 2015). The mechanism(s) by which non-electrophilic compounds activate TRPA1 is less characterized.

However, there are some hints from chimeric and mutagenesis studies suggesting that critical amino acids for menthol binding are Ser873 and Thr874 of the fifth transmembrane segment of hTRPA1 (Xiao, Dubin et al. 2008). Three amino acid residues, namely Ser813, Tyr840 and Ser873 in the 3rd, 4th and 5th transmembrane segments of hTRPA1 respectively, were identified as a key sites for the eudesmol (β-eudesmol) activation (Ohara, Fukuda et al. 2015). Based on these studies, it is more likely that non-electrophilic compounds are interacting with amino acid hydroxyl side chain and form hydroxyl-bonding (Ohara, Fukuda et al. 2015). It remains to be known whether all non-electrophilic compounds share a common binding site and what their activation mechanism and physiological role is. Many of these compounds show a bimodal effect on channel activity that can possibly be of interest for developing TRPA1 desensitizing compounds (Nilius, Prenen et al. 2011, Zygmunt and Högestätt 2014).

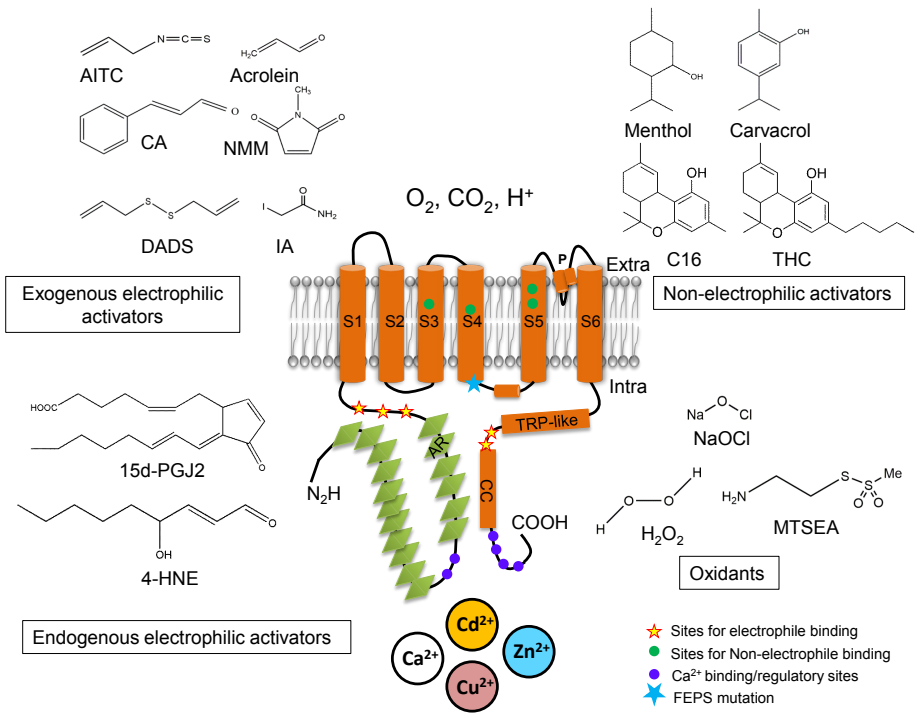

Figure 3.1 Schematic representation of TRPA1 and key determinants for the electrophilic, non-electrophilic and Ca^{2+} binding/activation/regulation. Chemical structures of the TRPA1 activators grouped according to their properties and mode of action.

3.1.3 Modulation of TRPA1 ion channel activity

Calcium is an important endogenous modulator that plays a dual role in activation/potentiation and inactivation/desensitization of TRPA1 (Jordt, Bautista et al. 2004). Studies have shown that Ca^{2+} causes potentiation of agonist activity and direct activation on TRPA1 by binding to the putative EF-hand domain (Doerner, Gisselmann et al. 2007, Zurborg, Yurgionas et al. 2007) (section 2.2.1). In addition, Ca^{2+} causes inactivation of TRPA1 ion channel activity (Wang, Chang et al. 2008). Early studies reported that extracellular calcium employs activation and inactivation of the TRPA1 (Nagata, Duggan et al. 2005). Wang *et al*. clarified that the potentiation of TRPA1 by extracellular Ca^{2+} occurred by Ca^{2+} through the pore and demonstrated that intracellular Ca^{2+} is enough to exert both potentiation and inactivation of the TRPA1 ion channels (Wang, Chang et al. 2008). The activation and desensitization mechanisms of TRPA1 were also demonstrated to be cysteine-dependent, but cysteines involved in the desensitization differed from critical cysteines involved in electrophile activation (Ibarra and Blair 2013).

Polyphosphates (PPi and PPPi) have been proposed to act as stabilizing factors for TRPA1 activation triggered by electrophilic compounds (Kim and Cavanaugh 2007), whereas addition of phosphatidylinositol-(4,5)-bisphosphate (PIP_2) reduces the activation of TRPA1 caused by electrophiles (Kim, Cavanaugh et al. 2008). However, another study reported a positive modulation of TRPA1 activation by PIP_2 (Karashima, Prenen et al. 2008). Taken together, further studies are needed to clarify how TRPA1 is modulated by intracellular factors.

3.2 TRPA1 as a thermosensor

The role of TRPA1 in mammals as a thermosensor besides its function as a chemosensor is highly controversial, and furthermore opposite thermal sensitivities has been reported for some TRPA1 orthologues (Fig. 3.3).

3.2.1 Activation of TRPA1 by cold

The TRPA1 ion channel was first characterized as a noxious cold sensor in mice, with an activation threshold of ≤ 17°C (Story, Peier et al. 2003). However, the role of TRPA1 as a cold sensor is still under debate. Some researchers failed to show the cold activation of TRPA1 in heterologous expression systems (Jordt, Bautista et al. 2004) and suggested that observed cold activation is due to cold-induced Ca^{2+} influx rather than a direct effect (Zurborg, Yurgionas et al. 2007).

However, the single-channel recordings of mouse TRPA1 expressed in HEK293 cells, using excised patches under Ca^{2+}-free condition, showed that the channel open probability is increasing exponentially with lowering temperatures, which suggests that cold activation is a direct effect on channel gating (Sawada, Hosokawa et al. 2007). Another group confirmed cold activation of TRPA1 (Karashima, Talavera et al. 2009), but found the effect was smaller in the absence of extracellular Ca^{2+}. This suggests the cold activation is intrinsic to the channel and that Ca^{2+} modulates the TRPA1 cold sensitivity (Karashima, Talavera et al. 2009). Kremeyer *et al.*, have confirmed the activation of hTRPA1 by cold in a heterologous expression system and shown that the FEPS hTRPA1 mutant displays increased activity upon cold stimuli (Kremeyer, Lopera et al. 2010). However, there is also discrepancy among the results generated by *in vivo* studies on TRPA1 as a cold sensor, in which two research groups developed and characterized knockout mice independently. Kwan *et al.* found that TRPA1 knockout mice dramatically decreased their behavioural responses in a sex-dependent manner, when exposed to a cold plate (0°C) and acetone application (Kwan, Allchorne et al. 2006). In contrast, Bautista *et al.*, reported no difference in response to cold plate and acetone application between wild type and knockout mice and concluded that TRPA1 is not involved in painful cold sensation (Bautista, Jordt et al. 2006). On the other hand, Obata *et al.*, have shown that cold hyperalgesia developed by nerve growth factor (NGF) induced an increased TRPA1 expression in DRG neurons through a p38 mitogen-activated protein kinase (MAPK) pathway (Obata, Katsura et al. 2005). Del Camino *et al.* showed that TRPA1 currents produced by the agonists AITC and 4-HNE were increased upon cooling from 25°C to 10°C and suggested that TRPA1 plays a major role in cold hypersensitivity in the presence of ROS and inflammatory mediators (del Camino, Murphy et al. 2010). In contrast to this study, Karashima *et al.* identified that cooling decreases the agonist evoked TRPA1 currents. These apparent contradictions may be caused by differences in cooling rate and presence of extracellular Ca^{2+} (Karashima, Talavera et al. 2009, del Camino, Murphy et al. 2010). The sensitivity of TRPA1 to cold has been suggested to differ between different neurons within the same animal species (Fajardo, Meseguer et al. 2008). This raises the possibility that mammalian TRPA1 cold responsiveness is modulated by the intracellular environment.

In conclusion, some studies advocate that mammalian TRPA1 act as a cold sensor at temperatures ≤ 17°C and others that TRPA1 is not involved in cold activation. These differences in reported results have been attributed the experimental conditions like duration of expression, reagents used in transfection, recording

solution, basal holding temperatures, cooling application and sensitivity of the technique (Sawada, Hosokawa et al. 2007).

Unlike TRPV1, TRPA1 has not been shown to play a role in thermoregulation. The influence of TRPA1 on thermoregulation has been examined by the use of genetic knockout mice and by TRPA1-specific antagonists, with no differences observed in core body temperature (Bautista, Siemens et al. 2007, Chen, Joshi et al. 2011).

3.2.2 Activation of TRPA1 by heat

It has been shown that TRPA1 orthologues play a role in the heat sensitivity of sub-mammalian species. Some studies have proposed the involvement of mammalian TRPA1 in agonist-induced heat hyperalgesia (Bandell, Story et al. 2004, Bautista, Jordt et al. 2006, Albin, Carstens et al. 2008, Sawyer, Carstens et al. 2009, Tsagareli, Tsiklauri et al. 2010). Furthermore, based on single fibre recordings and measurement of CGRP release combined with behavioural studies, Hoffmann e*t al*. demonstrated a contribution of TRPA1 in heat sensation (Hoffmann, Kistner et al. 2013). It was concluded that TRPA1 determines the heat threshold in naïve animals. Common for all studies is that the effect of TRPA1 is most likely indirect and dependent on TRPV1. In contrast to these studies, Wang *et al*., have shown that activation of heterologously expressed human and rat TRPA1 by electrophilic and non-electrophilic compounds were strongly inhibited by warm temperatures (39°C), most likely by enhancing the desensitization of TRPA1 (Wang, Lee et al. 2012).

3.2.3 Mechanistic insights into temperature activation

The molecular mechanism of temperature activation of TRPA1 is not very well known. There are three proposed mechanisms for the temperature activation of TRP ion channels. First, temperature activation is based on changes in enthalpy and entropy. These changes must be large for cold-and heat-activated channels, but with opposite signs (Brauchi, Orio et al. 2004, Voets, Droogmans et al. 2004). Second, large molar changes in heat capacity (ΔC_p) between open and closed states of the channel cause channel activity. The molecular mechanism predicted from this hypothesis is an exposure of a large number (approx. 20 amino acids per subunit) of non-polar residues to the polar molecules of water which leads to an increase in heat capacity upon channel opening (Clapham and Miller 2011). These residues need not to be localized in a specific region of TRPA1 instead they

can be dispersed throughout the whole protein. The temperature activation is predicted to be bidirectional, i.e., displaying a U-shaped relation between the equilibrium constant and temperature postulating that all hot sensing ion channels can also be activated by cold. A U-shaped temperature sensitivity of TRPA1 ion channels has not been possible to verify experimentally so far (Clapham and Miller 2011). However, Chowdhury *et al.*, have supported this hypothesis experimentally by engineering of the shaker K^+ ion channel and its heat capacity responsiveness by systematic substitution of residues in the voltage sensing domain (VSD), where those residues are exposed to water upon channel opening, and leading to sensitization of shaker channel both by heat and cold (Chowdhury, Jarecki et al. 2014). Third, temperature activation is based on allosteric coupling of the temperature sensor to the channel gate (Salazar, Moldenhauer et al. 2011, Voets 2012, Jara-Oseguera and Islas 2013). This proposed mechanism have been put forward to explain the cold-hypersensitivity of TRPA1, where different sensors are located in different structural domains of TRPA1 that are allosterically coupled with each other and to channel gating (Salazar, Moldenhauer et al. 2011).

In summary, there is no clear experimental evidence clarifying the mechanism for the temperature activation of TRP ion channels and the fundamental question, concerning the nature of the temperature sensing structure in TRPA1 ion channels, remains unanswered. Importantly, there is no experimental evidence to support that native thermoTRPs are both cold- and heat-activated.

3.2.4 Searching for regions involved in temperature sensitivity

Numerous studies have attempted to pinpoint the molecular temperature sensing structure in the channel. Based on chimeric studies between human and rattlesnake TRPA, it has been concluded that the regions for thermal and chemical sensitivity are located in two separate modules in the ARD (Cordero-Morales, Gracheva et al. 2011). The chimera with substitution of AR 3-8 and AR 10-15 with corresponding rattle snake ARs confer heat sensitivity to hTRPA1 (Fig. 3.2, ovals 4 and 5). These findings suggest that the ARD is involved in detection and modulation of the TRPA1 function (Cordero-Morales, Gracheva et al. 2011). The alternative splice variants of drosophila and mosquito TRPA1 differ in their distal N-terminal regions that appear to dictate their sensitivity to temperatures (Fig. 3.2, oval 1) (Kang, Panzano et al. 2012). A stretch of 37 amino acids between the last AR and the first transmembrane segment has also been identified as a key determinant for the temperature sensitivity of drosophila TRPA1 (dTRPA1) (Zhong, Bellemer et al. 2012). In addition, the genetic variant E179K positioned

in the fourth AR of hTRPA1 causes a paradoxical heat sensation in patients (Fig. 3.2, circle 2) (May, Baastrup et al. 2012). In contrast, the single amino acid, Gly878, on the fifth transmembrane segment has been identified as a critical site for cold activation of rodent TRPA1 (Fig. 3.2, circle 7) (Chen, Kang et al. 2013). Furthermore, a chimera with human N- and C-termini and the *Drosophila* transmembrane region retained the sensitivity to heat characteristic of dTRPA1 (Wang, Schupp et al. 2013). Point mutations in this chimera, in S6 (L1105A+I1106Q) and the pore helix (R1073K), introducing corresponding human residues, abolished the heat activation of dTRPA1 (Fig. 3.2, circles 8 and 9) (Wang, Schupp et al. 2013). Recently, an unbiased random mutagenesis screen identified three mutations in the sixth AR (S250L, M258L and D261G) based on their ability to convert the cold-activated mouse TRPA1 into a heat-activated channel without affecting the chemical activation (Fig. 3.2, circle 3) (Jabba, Goyal et al. 2014). Altogether, this suggests that multiple regions are involved in the temperature regulation of TRPA1.

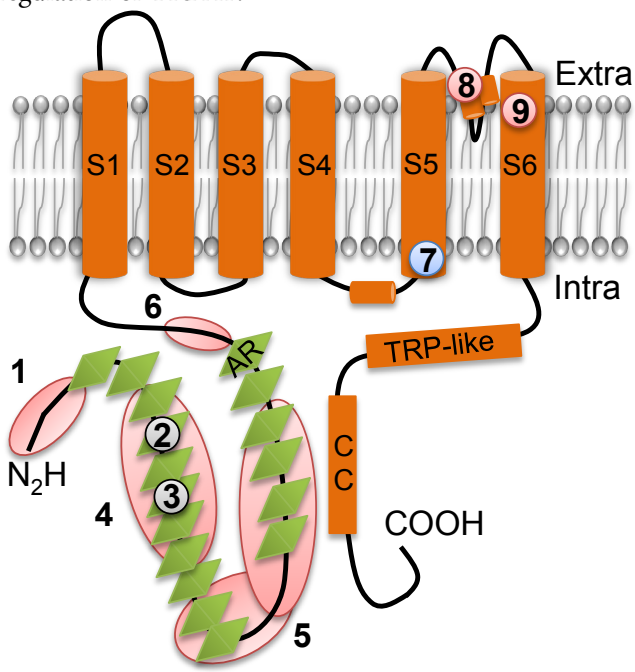

Figure 3.2 Schematic overview of TRPA1 thermosensitive regions. Ovals and circles represent regions and individual amino acid residues, respectively, that are proposed to play a role in thermosensitivity. (1) Insect pre-ARD, (4) rattle snake three to eight ARs, (5) rattle snake 10-15 ARs, (6) 37 amino acids post-ARD (2) E179K, human TRPA1 (3) S250L, M258L and D261G, mouse TRPA1 (7) Gly878, rodent TRPA1 (8) Arg1073, drosophila TRPA1 and (9) Leu1105, Ile1106 in drosophila TRPA1.

3.3 TRPA1: Species differences

TRPA1 orthologues exhibit profound species-specific difference in their sensitivity to temperature. TRPA1s also display some species-specific differences in their chemical sensitivity even though there is an overall conservation of this feature in all TRPA1 orthologues. The chemical sensitivity of TRPA1 plays a major physiological role in mammals, whereas in lower beings such as insects, chicken and snakes the sensitivity to electrophiles is reduced in order to intensify the temperature response. Although human and rodent TRPA1 exhibits ~80% sequence similarity at amino acid level there are clear species differences in their function (Zygmunt and Högestätt 2014, Laursen, Anderson et al. 2015).

Although, there are different views on mammalian TRPA1 as a noxious cold sensor, there is a consensus on the role of some TRPA1 orthologues as heat sensors. Reasons behind opposite results regarding TRPA1 as cold sensor might be a variation in experimental conditions, in addition to regional differences within the same species (Fajardo, Meseguer et al. 2008, Karashima, Talavera et al. 2009). To clarify this issue, a research group employed experiments on different TRPA1 orthologues under identical conditions (Chen, Kang et al. 2013). Experiments for the cold activation were performed in parallel between mouse, rat, rhesus monkey and human TRPA1. The results from the Ca^{2+} assay, and whole-cell as well as single-channel recordings reported that only mouse and rat TRPA1s were activated by cold, but not rhesus monkey and human TRPA1s, both of which were classified as thermoneutral. These findings corroborated that mammalian TRPA1 definitely exhibit species-specific differences (Chen, Kang et al. 2013).

Like mammalian TRPA1s, insect TRPA1s are polymodal sensors that can detect both temperature and chemicals (Kang, Pulver et al. 2010). The temperature threshold for heat activation of heterologously expressed dTRPA1 is around 27°C to 29°C (Viswanath, Story et al. 2003, Kang, Panzano et al. 2012). The physiological role of TRPA1 ion channels in insects can be avoidance to noxious chemicals and temperature. For some insects that require blood for their reproduction, TRPA1 helps in finding a warm-blooded host (Laursen, Anderson et al. 2015). In order to differentiate between the detection of electrophiles and heat, some insects have evolved different splice isoforms of TRPA1. Such isoforms are TRPA1 (A) and (B) with different N-terminal regions and as a consequence divergent temperature sensitivities but similar sensitivity to electrophilic compounds. The dTRPA1 (A) isoform is expressed in proboscis, and is less temperature sensitive (Q_{10} of ~9). In contrast, the dTRPA1 (B) isoform is mainly

expressed in the head, and is more sensitive to temperature than the TRPA1 (A) (Q_{10} of ~116). Similar isoform organization and differential temperature sensitivity is also found in the malaria mosquito, *Anopheles gambiae,* where Q_{10} is ~4 for TRPA1 (A) and ~200 for TRPA1 (B) (Kang, Panzano et al. 2012).

It is known that honeybees can detect and maintain the hive temperature between 32°C and 36°C, which is important for the development their off springs. In contrast to other insects, a true TRPA1 orthologue does not exist in honeybees. Kohno *et al*. identified a honeybee hymenoptera-specific TRPA (AmHsTRPA), which shows sensitivity to noxious chemicals and warm temperatures. The AmHsTRPA activation threshold of 34°C may help in monitoring and maintaining the hive temperature (Kohno, Sokabe et al. 2010). *Caenorhabditis elegans* TRPA1 (ceTRPA1) also acts as a polymodal sensor, and mainly functions as a mechanosensor. In comparison with other TRPA1s, ceTRPA1 is insensitive to electrophiles, since it does not have the conserved cysteines, which are critical for the electrophilic sensitivity (Kindt, Viswanath et al. 2007). A recent study proposed that ceTRPA1 can act as a cold sensor and detects the decrease in environmental temperature to prolong its life span (Xiao, Zhang et al. 2013).

The zebrafish (*Danio rerio*) contains two TRPA1 paralogues namely, TRPA1a and TRPA1b. Both are sensitive to electrophiles, but not to temperature (Prober, Zimmerman et al. 2008). TRPA1 orthologues from non-pit bearing snakes (*Elaphe obsolete lindheimeri*), frogs (*Xenopus tropicalis*) and lizards *(Anolis Carolinensis)* are sensitive to chemicals and noxious heat, with thresholds for activation around 40°C, 34°C and 37°C, respectively (Gracheva, Ingolia et al. 2010, Saito, Nakatsuka et al. 2012, Kurganov, Zhou et al. 2014). In these organisms, TRPA1 helps to find a comfortable temperature and to avoid heat. In contrast, TRPA1 in pit-bearing snakes (boas, pythons and rattlesnakes) plays a key role in detection of infrared radiation monitored to localize the prey. In these snakes, the TRPA1 expression is localized to trigeminal neurons that innervate the pit rather than the neurons innervating the body. It has been proposed that the TRPA1s in these snakes have gained enhanced thermal sensitivity on the expense of chemosensitivity (Gracheva, Ingolia et al. 2010). TRPA1 from the non-mammalian homeotherm chicken (*Gallus gallus domesticus*) is also activated by both electrophiles and heat with a temperature threshold of ~39.4°C (Saito, Banzawa et al. 2014).

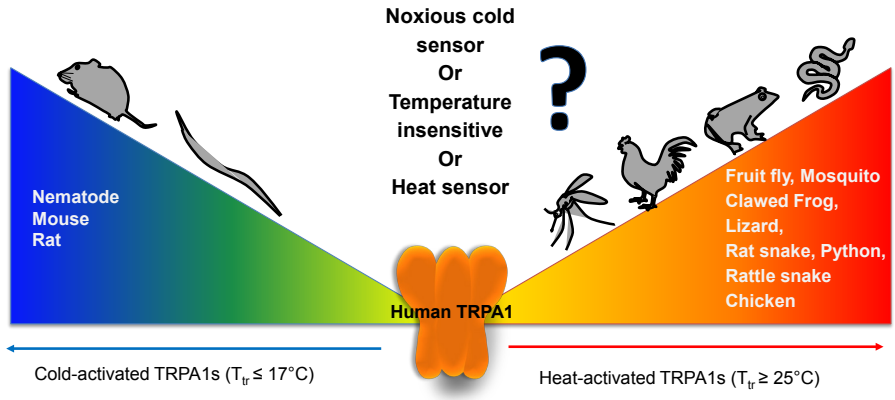

Figure 3.3 TRPA1 orthologues displaying opposite temperature sensitivity. Rat, mouse and nematode TRPA1s detect cold temperatures, whereas insect, frog, snake, chicken TRPA1s detect warm temperatures. Whether the human TRPA1 is a temperature sensor or not, has been much debated.

Chapter 4
Present investigation

4.1 Aim of the study

To develop novel treatments for TRPA1 related diseases/symptoms and repellents for the control of vector-borne diseases, it is crucial to understand the molecular mechanism of these channels. In this study, the focus is on thermo- and chemo-sensitive properties of hTRPA1 and the malaria mosquito, *Anopheles gambiae* TRPA1 isoform A (AgTRPA1) ion channels, and the role of their peculiar long N-terminal ARDs.

4.2 Methodology

To study the role of the N-terminal ARD of TRPA1, constructs lacking the N-terminal ARD were designed and compared with the full-length TRPA1 channel in functional studies. Whole-cell patch clamp was performed to study TRPA1 thermo-sensitive properties in a cellular environment. The patch-clamp technique on planar lipid bilayers allowed a detailed functional characterization at a single-channel level avoiding the complexity that is present in a cellular system. Circular dichroism was performed to verify the folding of the purified proteins. Fluorescence spectroscopy was used to assess the agonist and temperature-induced conformational changes of TRPA1 proteins in membrane-independent manner. Tandem mass spectrometry was used to identify the binding sites in hTRPA1 for the electrophilic TRPA1 activator NMM.

4.2.1 Protein expression and purification

To express constructs of human TRPA1 proteins, the eukaryotic expression system of *Pichia pastoris* was used, which allows proper folding and post-translational modifications of the expressed proteins. The cDNA coding for human TRPA1 (hTRPA1) and a N-terminal truncated construct (Δ1–688 hTRPA1) was sub-cloned from the pFROG3 plasmid (kindly provided by Sven-Eric Jordt, Duke University, Durham, NC) (Jordt, Bautista et al. 2004) into modified *P. pastoris* expression vector pPICZB that containing N-terminal deca-histidine tag

(generously provided by Andreas Kirscht, Lund University, Lund, Sweden). The wild type Pichia X-33 cells were transformed linearized constructs. In order to get high expression clones, high gene copy number clones were selected with the Zeocin resistance marker (Norden, Agemark et al. 2011). Selected high expression clones were cultured by a 3-L bench-top fermenter (Fig. 4.1). The cells were lysed mechanically with a Bead Beater using cold glass beads (0.5 mm; BioSpec Products). The cell lysate underwent differential centrifugation to collect the membranes, initially with a low-speed centrifugation to remove cell debris and unbroken cells and then a high-speed centrifugation to collect the membranes. The cell membranes were washed with a urea solution to remove peripheral membrane proteins (Karlsson, Fotiadis et al. 2003). To find a suitable detergent, which makes the protein soluble and stable, a detergent screen was performed. As a result, the fos-cholin group of detergents were identified, since they gave a better solubility than others. The fos-cholin-14 detergent was chosen and used for the solubilization and purification. The solubilized proteins were subjected to Ni-NTA affinity purification to get pure proteins. The purified proteins were later either desalted or further purified by size-exclusion chromatography. A similar approach had been used for the purification of AgTRPA1 proteins with few differences (see paper III).

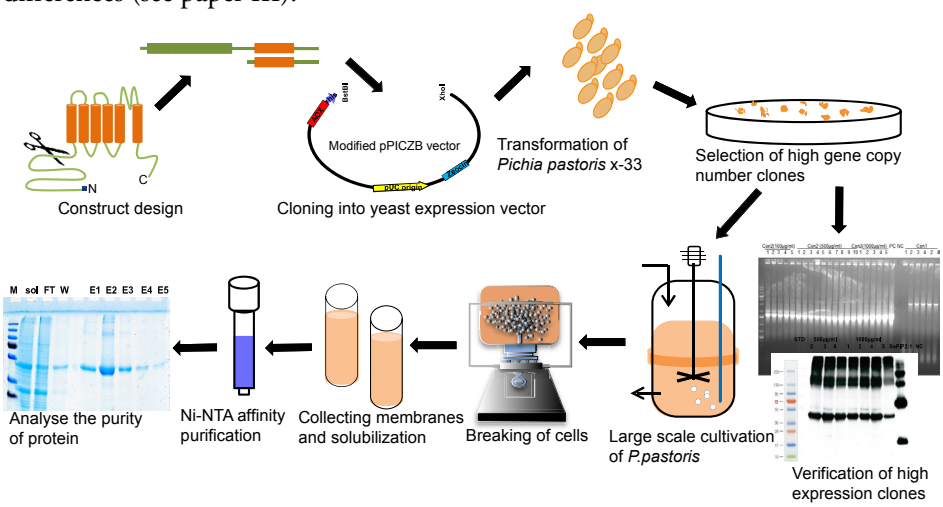

Figure 4.1 Schematic overview of the steps in expression and purification of TRPA1 proteins. For protein expression, the designed constructs were first cloned into an expression vector and then transformed into *P. pastoris*. In subsequent steps, high gene copy number clones were selected, high expression clones were identified and finally cultivated in large scale. For purification of proteins, after breaking of cells, membranes were harvested by differential ultracentrifugation, from which solubilized proteins were isolated with suitable detergents and further purified by Ni-NTA purification method. The purity of the obtained proteins were analysed by SDS-PAGE.

4.2.2 Liposomes

Liposomes were first produced by Alec D. Bangham in 1961 (Bangham and Horne 1964). It was found that mixing of phospholipids with an aqueous solution causes immediate formation of spherical shaped closed structures due to the amphipathic nature of the molecules. The lipids are arranged into bilayers that are called lamellae. In general, different types of liposomes differ in size, ranging from 30 nm to several micrometres. Liposomes can be classified into two groups like unilamellar and multilamellar, based on the number of bilayers they possess. Unilamellar vesicles are further classified according to size, into small unilamellar vesicles (SUV, radii of 30 to 100 nm), large unilamellar vesicles (LUV, with radii of 100 nm and above), and giant unilamellar vesicles (GUV radii of 1μm and above).

4.2.2.1 Giant unilamellar vesicles

For the functional characterization of TRP ion channels, we used giant unilamellar vesicles (GUVs) as artificial model membranes for reconstitution of the purified protein. The GUVs were prepared by the electroformation method that has been well described before (Dimitrov 1986, Estes and Mayer 2005, Kreir, Farre et al. 2008). The mechanism of electroformation is based on the electroosmotic effect, membrane elasticity and the hydration of lipid membranes, which depends on the applied alternating current (AC) and voltage of the electric field (Dimitrov 1986). The lipids were dissolved in an organic solvent and then spread on the conductive side of one of the electrodes. The electrodes consist of two transparent Indium Tin Oxide (ITO) coated glass slides (Fig. 4.2). After total evaporation of the solvent, lipids can form a thin film in which they are assembled in a lamellar phase. An O-ring of rubber was placed on the top of the dried lipid film and a non-ionic intracellular solution, usually a sorbitol, was added to the lipid film inside the O-ring without agitation. Then, the second ITO-slide was placed on the top of the O-ring. The whole process of electroformation was controlled by the Vesicle Prep Pro setup (Nanion Technologies, Munich, Germany) and all parameters (amplitude, frequency, main time, rise time and fall time) programmed by the Vesicle Control software (Nanion Technologies, Munich, Germany). The size of the formed liposomes can vary from 1 to 100 μm in a single preparation. The size of GUVs needed to make a seal on NPC-1 chip (for planar patch clamp) is 5-25 μm. GUVs can be used directly to make planar lipid bilayers for later insertion of proteins, but can and also be incubated with

proteins to form proteoliposomes which can be further used to make planar lipid bilayers.

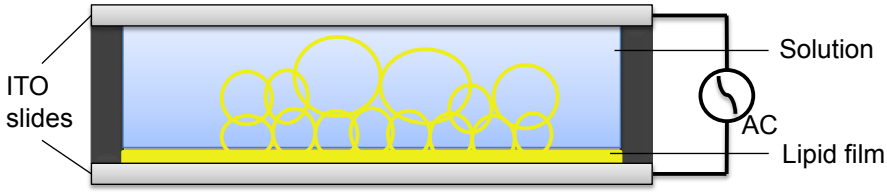

Figure 4.2 Schematic representation of the GUVs formation by the electroformation method. The dehydrated lipid film rehydrated with non-ionic solution under an alternating electrical field leads to the formation of GUVs.

4.2.3 Patch-clamp technique

The patch-clamp technique was developed by Erwin Neher and Bert Sakmann in 1976 and has made it possible to study ion channels in detail (Neher and Sakmann 1976). The principle of this technique is an electrical isolation of a small part of the membrane (the patch) in order to record small currents that are passing through the membrane. Electrical isolation of the membrane patch and reduction of current noise of the recording can be achieved by obtaining a high resistance seal between membrane and pipette. A high resistance seal is crucial in order to study small single-channel currents of a few pico-amperes. There are different configurations of the patch-clamp technique such as whole-cell, cell-attached, inside-out, outside-out that allow studies of either macroscopic currents or single-channel currents (Molleman 2003). In this thesis, both macroscopic and single-channel currents have been studied by using the whole-cell configuration measuring currents flowing through TRPA1 when expressed in HEK293 cells and purified TRPA1 inserted into artificial lipid bilayers.

4.2.3.1 Planar patch-clamp recording

The advances in patch-clamp techniques developed into automated patch- clamp setups. One of these is the Port-a-Patch, a planar patch-clamp system, in which borosilicate glass chips with a very small aperture are used in place of the glass micropipettes employed in the conventional patch-clamping (Fertig, Blick et al. 2002). All planar lipid bilayer single-channel recordings were done using the Port-a-Patch planar patch-clamp system (Fig. 4.3). Planar lipid bilayers were formed with GUVs (section 4.2.2.1).

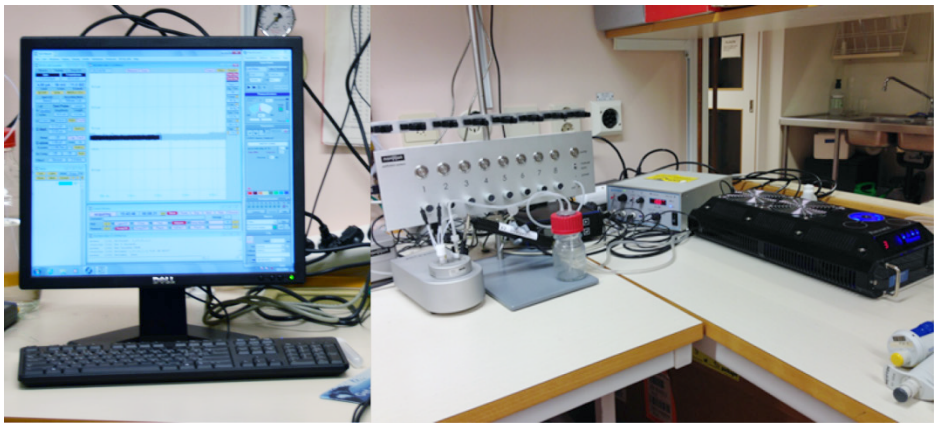

Figure 4.3 Photos showing the control interface in the software (left) and a miniaturized patch-clamp setup (Port-a-Patch, Nanion Technologies), which is connected with a SC-20 dual in-line solution heater/cooler that is controlled by the CL-100 liquid cooling system (Warner Instruments; right).

For the formation of a planar lipid bilayer, 5 µl of the GUVs or proteoliposomes solution was pipetted onto the patch clamp chip. For bilayer experiments, the micro structured chip containing an aperture with 3.5-5 MΩ resistance was used. The GUVs were positioned onto the aperture in the chip by application of a slight negative pressure (–10 to –40 mbars). Once the GUVs touch the glass surface of the chip, they burst and form a planar lipid bilayer with a seal resistance of 10 to 100 GΩ (Fig. 4.4). Signals were acquired with an EPC 10 amplifier and the data acquisition software Patch Master (both from HEKA, Lambrecht, and Germany) at a sampling rate of 50 kHz. The recorded data were digitally filtered at 3 kHz.

The planar lipid bilayer patch-clamp configuration was used to study the functional properties of purified TRPA1 proteins (Papers I, II and III), whereas whole-cell patch-clamp was used to study the functional properties of hTRPA1 expressed in HEK293t cells (Paper III).

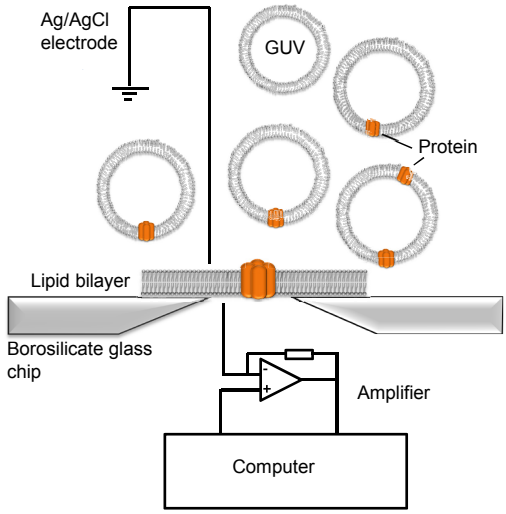

Figure 4.4 Schematic representation of the planar patch-clamp technique and the formation of planar bilayers. The application of GUVs or GUVs containing reconstituted proteins, on a planar glass chip causes them to burst and form planar lipid bilayers.

Analysis of single-channel patch-clamp recordings

The single-channel recording provides information about current amplitudes, channel openings and their open and closed times. The ion channel mainly fluctuates between an open and a closed conductive state, but sometimes a channel can also exhibit sub-conductance states. The ion channel transition from one state to another is depending on the stimulus that causes channel activation or inactivation. These changes occur randomly in a time period-stochastic process and represent conformational changes of the channel. In the analysis of single-channel recoding, parameters that includes single-channel conductance (G_s) and open probability (P_o) were measured. Single-channel data were filtered using low-pass Gaussian filter to reduce high frequency noises before analysis.

The information regarding single-channel conductance and ion specificity can be obtained from the current amplitude of the studied ion channel. Conductance of the ion channel is determined by Ohm's law (I=gV). In this equation I is the current that is passing through the membrane, g is the conductance of the membrane and V is the applied voltage over the membrane. The current amplitudes were obtained from the point-amplitude histograms, which show the distribution of amplitudes of the current based on all data points at all currents levels in the recording. The amplitude of the channel provides clues about

permeation properties of the ion channel. To simplify the analysis, we only considered recordings of single ion channels and excluded recordings with more than one channel, or sub-conductance states.

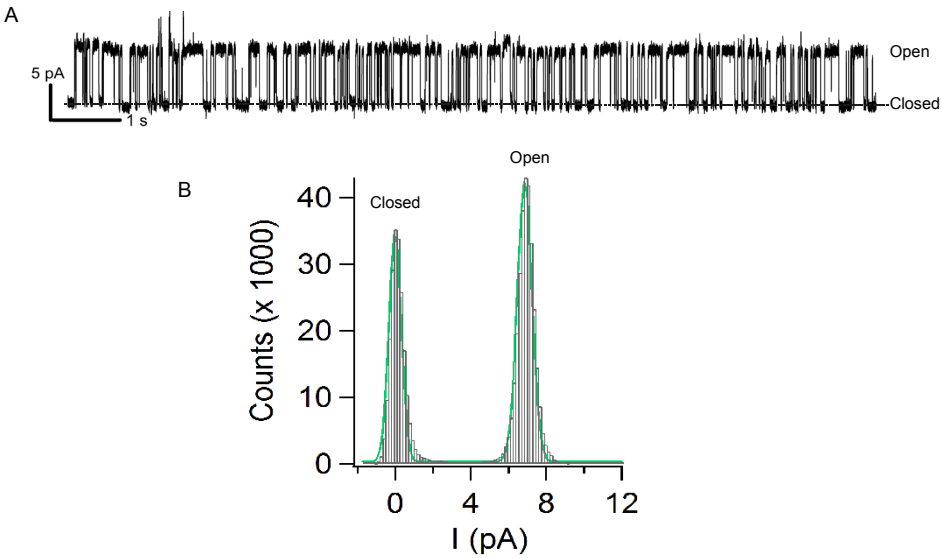

Figure 4.5 A. Single channel recording of the Δ1-688 hTRPA1 ion channel activated by 500 µM menthol at a membrane potential of +60 mV in a symmetrical K^+ solution. When the channel opens a current is displayed in outward direction. **B**. The represenative point-amplitude histogram in which the number of data points on the y-axis are plotted against the current amplitudes on the x-axis. Plotting of the current amplitude of the data points distributed into groups according to current levels displayed one closed and one open channel level. The data were fitted (green line) with a Gaussian distribution. The mean current amplitude of the channel is 6.86 ± 0.40 pA corresponding to a single channel conductance of 114 ± 7 pS.

Another important parameter in single-channel analysis is the open probability (P_o), which can be defined as the probability of a channel being open in a fraction of time. This can provide information about the channel activity, which can alternate between open and closed states of various durations (dwell times). To measure dwell times, each transition has to be identified as an event, which can be done automatically by using selected threshold criteria. All counted open and closed dwell times are plotted in a separate dwell time histogram for each state, using a constant bin width. An exponential fit is then used to get mean dwell open and closed times, which can be used to calculate the open probability.

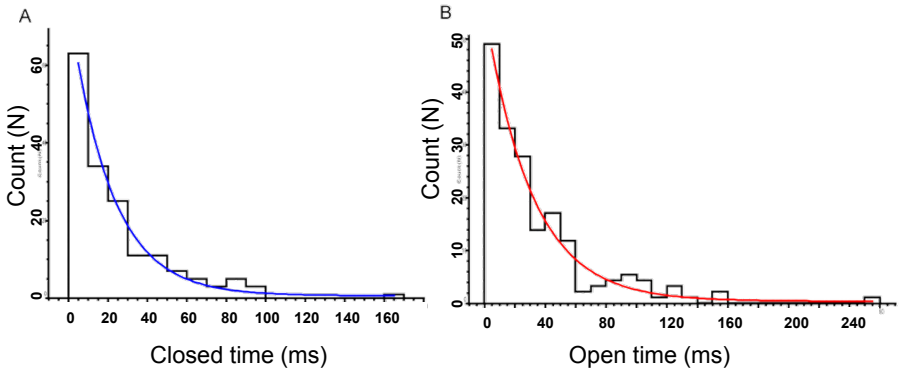

Figure 4.6 The representative closed dwell time histogram (A) and open dwell time histogram (B) for the single channel recording in Fig. 4.5 A. The mean open dwell time (30.7 ms) and closed dwell time (20.9 ms), were obtained from exponential fits of the dwell time histograms. Based on this, the calculated open probability (P_o) of hTRPA1 when activated by menthol is 0.59.

4.2.4 Mass spectrometry

Mass spectrometry is a device that measures the mass-to-charge ratio (*m/z*) of charged molecules. The instrument mainly consists of three parts: An ion source that give charges to molecules, a mass analyser that measures the mass-to-charge ratio of the charged molecules and a detector that documents the number of ions at each *m/z* ratio (Aebersold and Mann 2003). There are two primary types of ionization methods are used for proteins, named as matrix-assisted laser desorption ionization (MALDI) and electrospray ionization (ESI). There are four types of mass analysers that include time of flight (TOF), ion trap, quadrupole and Fourier transform ion cyclotron (FT-MS). MALDI usually coupled with TOF and ESI with ion traps and triple quadruple analysers. Mass spectrometry can be used in many ways in protein research that include identification and characterization of proteins, protein interactions, protein profiling and determining post-translational modifications (Aebersold and Mann 2003). Mass spectrometry was used to map binding sites for the TRPA1 activator NMM at hTRPA1 and quantify the relative labelling efficiency (Paper IV). Samples were prepared according to an in-gel digestion protocol (Shevchenko, Tomas et al. 2006).

4.2.5 Circular dichroism

Circular dichroism is a spectroscopic technique, which is based on the ability of chromophores (amino acids in the protein) to absorb left- and right-handed circularly polarized light differentially (Kelly, Jess et al. 2005). To determine the secondary structural elements in a protein, the far-UV range (190-250 nm) can be used in CD spectra. The resulting spectrum represents a combination of different secondary structural elements in a protein. Hence, this technique can be used to determine the secondary structure, the folding properties and the conformational changes of proteins relating to temperature, pH, ligand binding and mutations etc. The composition of secondary structure can be estimated from the CD data by using various algorithms such as SELCON3, CONTIN, and CDSSTR (Greenfield 2006). The CD technique was employed to evaluate the effect of N-terminal deletion on the folding of TRPA1 proteins (Paper I) as well as for studies of temperature stability and related conformational changes of AgTRPA1 proteins (Paper III).

4.2.6 Fluorescence spectroscopy

Fluorescence spectroscopy is a technique that measures the fluorescence from a fluorophore (Lakowicz 2002). Fluorophores can be either intrinsic or extrinsic. A few amino acids in proteins display fluorescence these are phenylalanine (Phe), tyrosine (Tyr) and tryptophan (Trp). Only Trp and Tyr are used to study proteins, since these two give good fluorescence signals, and both are excited at 280 nm. However, in contrast to Tyr, Trp selectively excite at 295 nm and the emission maximum of Trp is highly sensitive to the local environment. The intrinsic properties of these residues make tracking of changes in protein folding or conformation possible. In the native state of soluble globular proteins, these residues are buried in a hydrophobic environment, where they have a high quantum yield and high fluorescence intensity. At exposure to hydrophilic surfaces, their quantum yield decreases which causes low fluorescence intensity.
Fluorescence spectroscopy was used to study chemical- and temperature-induced conformational changes of TRPA1 proteins in a membrane- independent manner (Papers II and III).

Chapter 5
Results and general discussion

5.1 Purification of TRPA1 proteins (Papers I-IV)

The methylotrophic *P. pastoris* expression system was implemented to express hTRPA1 and its orthologue AgTRPA1 (A), with and without their ankyrin repeat domains (ARD). Higher expression levels were observed for the N-terminal ARD deleted proteins compared to the full-length TRPA1 proteins. The fos-cholin group of detergents were identified as effective in extraction of TRPA1 proteins from the *Pichia* membranes. Fos-cholin-14 and fos-cholin-12 were used for both solubilisation and further purification of the hTRPA1 and AgTRPA1 proteins, respectively. Proteins were purified by nickel affinity chromatography using an N-terminal deca-histidine tag on both hTRPA1 and Δ1-688 hTRPA1, and C-terminal hexa-histidine tag on AgTRPA1 and Δ1-776 AgTRA1. After nickel affinity purification, proteins were further purified either by desalting or size-exclusion chromatography. As a result, the N-terminal ARD deleted proteins gave a high yield and purity like, Δ1-688 hTRPA1 which yielded 3 mg/10 g cells with 95% purity after a one-step purification and Δ1-776 AgTRA1 tetramers which yielded 1.3 mg/20 g of cells after a two-step purification. In comparison, full-length proteins were obtained at a lower yield and purity such as 0.3 mg/10 g cells for hTRPA1 after one-step purification and 0.7 mg/20 g cells for AgTRPA1 after two-step purification. Circular dichroism (CD) was employed to evaluate the effect of N-terminal deletion on folding of the TRPA1 proteins. Far-UV CD spectra of Δ1-688 hTRPA1 exhibit the characteristics of a mainly α-helical structure. In case of AgTRPA1 and Δ1-776 AgTRA1, Synchrotron Radiation Circular Dichroism (SRCD) spectroscopy was performed, and for both proteins the characteristic spectra of α-helical structures were recorded.

Conclusions: Purification of TRPA1 proteins
• Δ1-688 hTRPA1, hTRPA1, Δ1-776 AgTRPA1 and AgTRPA1 are successfully expressed and purified using *P. pastoris.* • N-terminal ARD deleted proteins, Δ1-688 hTRPA1 and Δ1-776 AgTRA1, were obtained at higher yield and purity than full-length TRPA1 proteins. • CD data and size-exclusion chromatography suggest that the isolated solubilized proteins were properly folded also without the large N-terminal ARD.

5.2 Thermosensitive properties of TRPA1 (Papers I, II and III)

The ability to sense the environmental temperature, to avoid noxious temperatures and to find a comfortable temperature is very important for the survival of all animals. The thermoTRPs have been shown to be molecular sensors for the perception of temperature. Thus, it is of fundamental importance to study the thermosensitive properties of the TRPs. Especially since the molecular mechanism of temperature sensitivity of these channels is still abstractive. In the case of hTRPA1, its role in thermosensation is still under debate. To understand the functionality of both hTRPA1 and AgTRPA1, we addressed the following questions:

1. Is hTRPA1 itself activated by cold?
2. Is hTRPA1 itself activated by warm temperatures?
3. Is the thermosensitivity of hTRPA1 modulated by its redox status and ligands?
4. Is the heat sensitivity of AgTRPA1 an inherent channel property?
5. Is the N-terminal ARD required for thermosensation?

To understand the thermosensitive properties of the TRPA1 ion channels, we primarily employed electrophysiological experiments on planar lipid bilayers (single-channel recordings), in which purified TRPA1 ion channels were reconstituted. Hereby any influences of an intracellular milieu and Ca^{2+} were avoided, which is important as some studies reported that cold activation of mammalian TRPA1 is dependent on the intracellular Ca^{2+} and modifications like phosphorylation by kinases. A symmetrical K^+ solution was perfused on purified TRPA1 in the lipid bilayer at different test temperatures ranging from 10°C to 40°C. In addition, whole-cell patch-clamp studies of hTRPA1 expressed in mammalian cells (HEK293t) were performed, and intrinsic tryptophan fluorescence spectroscopy was employed to monitor conformational changes of TRPA1.

5.2.1 TRPA1 as a cold sensor

The single-channel recordings of hTRPA1 in planar lipid bilayers show occasional activity at room temperature and further cooling causes an increase in channel activity. The TRPA1 ion channel activity was expressed as the single-channel open probability (P_o), which was increased to 0.69 when lowering the temperature from

22°C to 10°C. The temperature dependence of the channel was quantified as a temperature coefficient (Q_{10}), which was extrapolated from the Arrhenius plot (ln P_o vs 1/T (K)) (Fig. 5.1A). A Q_{10} value of 0.025 was obtained using P_o values between 20°C and 10°C for hTRPA1, which is in agreement with the data reported for heterologously expressed mouse TRPA1 (Karashima, Talavera et al. 2009). Lipid bilayers without hTRPA1 protein did not respond on the lowering of temperatures. Although we used purified protein to measure the channel activity, we further confirmed that the cold response is taking place through hTRPA1 by the specific TRPA1 channel antagonist HC-030031, which abolished the cold activation. Cold-induced hTRPA1 channel activity was reversible in a temperature-dependent manner and regained by removal of antagonist. Repeated exposure of the same hTRPA1 ion channel to cold displayed a decrease in channel conductance by 49% ± 10%, which suggests channel desensitization in a Ca^{2+}-independent manner. AgTRPA1 (A) has been reported as a heat sensor with a temperature threshold of 32°C (Kang, Panzano et al. 2012). For a comparison, we exposed AgTRPA1 to cooling (15°C) to see if it also responds to cold. However, we did not observe any activity by cooling, further supporting that the cold-evoked currents were generated specifically by hTRPA1.

TRPA1 has been grouped with the redox-sensitive TRPs, having high oxidation sensitivity with threshold redox potential of approximately -3400 mV (Mori, Takahashi et al. 2016). Hence, we tested whether alteration in cellular redox state, which usually is a balance between the levels of intracellular antioxidants and redox reactive species, could modulate the temperature sensitivity of hTRPA1 or not. As a first step, the oxidation state of the purified hTRPA1 used in functional studies was analysed with a modified biotin-switch assay. The findings from this assay infer that hTRPA1 was partially oxidized and that it could be further oxidized with H_2O_2 or reduced with the reducing agent DTT. The activity of the TRPA1 in planar lipid bilayers evoked by cold (15°C) was inhibited by reducing agents (DTT and TCEP) and augmented by H_2O_2. In line with these findings, H_2O_2 pre-treated HEK293t cells expressing hTRPA1 triggered cold-evoked currents. Similarly, the electrophilic TRPA1 activators AITC and acrolein sensitized the hTRPA1 to cold. Interestingly, the non-electrophilic TRPA1 activator carvacrol also triggered cold responsiveness of hTRPA1, but only after heat exposure.

To test whether the temperature-induced activity is an inherent property of hTRPA1 or indirectly caused by changing fluidity of the membrane, we measured intrinsic tryptophan (Trp) fluorescence to detect any membrane-independent

conformational changes by cold. Tryptophan fluorescence studies suggest that the cold activation of hTRPA1 is indeed an intrinsic property of the protein. The quenching of the Trp florescence in hTRPA1 by cooling was abolished by DTT and enhanced by H_2O_2.

Taken together, hTRPA1 is an intrinsic cold-sensitive nocisensor dependent on the redox state and ligands, which would fit with the observed TRPA1-dependent cold hyperalgesia associated with certain chronic pain conditions and chemotherapy (Zygmunt and Högestätt 2014). The results may also explain the opposing findings on TRPA1 as a cold sensor obtained in different experimental setups and species (Zygmunt and Högestätt 2014). The sensitivity to cold is an intrinsic property of TRPA1 that may also be modulated by intracellular messengers such as Ca^{2+} (Zurborg, Yurgionas et al. 2007, Karashima, Talavera et al. 2009).

5.2.2 TRPA1 as a heat sensor

It has already been shown that TRPA1 of non-mammalian species is activated by heat when expressed in cellular test systems (section 3.2.5). In this study, we tested whether the insect AgTRPA1 is indeed an inherent temperature-sensitive ion channel. The single-channel recordings of AgTRPA1 on planar lipid bilayers did not display any activity at room temperature, however an increase in temperature caused slight activation at 25°C and intense activation at 30°C and above. The Q_{10} value of 28 for the AgTRPA1 was calculated using P_o values at 25°C and 30°C with a simplified equation (chapter 1 eq.1). Based on this, the heat activation threshold for AgTRPA1 was estimated to ~25°C. The lipid bilayers without AgTRPA1 did not show any activity when exposed to the same temperatures. Similar to cold activation of hTRPA1, heat activation of AgTRPA1 was also temperature-dependent and reversible. We further investigated temperature-induced conformational changes of AgTRPA1 by intrinsic Trp fluorescence spectroscopy in the temperature range 25 to 48°C. The fluorescence quenching observed at this temperature range confirmed that the conformation of AgTRPA1 is intrinsically heat-sensitive.

ThermoTRPs have been predicted to respond to both heat and cold temperatures (section 3.2.3), but experimental evidence is lacking to support this view. In this thesis, recordings of hTRPA1 in planar lipid bilayers showed an increased single-channel P_o by raising the temperature from room temperature to 35°C. Further increasing the temperature to 40°C caused a decrease in P_o, which could be

explained by channel desensitization. Temperature dependence was quantified in similar way as for the cold activation using the Arrhenius plot (25°C to 35°C) that resulted in a Q_{10} value of 6 (Fig. 5.1C), which is close to the Q_{10} value 7.5 of the heterologously expressed heat sensor TRPM3 (Vriens, Owsianik et al. 2011). The single-channel conductance (G_s) did not change with increasing temperatures, which would be expected if the pore permeation of ions were intact. The control experiments on lipid bilayers without protein did not show any activity with increasing temperatures and furthermore the selective TRPA1 antagonist HC-030031 as well as TRP channel pore blocker, ruthenium red inhibited the heat activation of hTRPA1. Thus, we provide for the first time evidence of thermoTRPs being intrinsically U-shaped thermosensitive (Fig. 5.1B).

The effect of changes in redox state and ligands on the heat sensitivity of hTRPA1 was further examined in electrophysiological experiments using purified and heterologously expressed hTRPA1. The heat activation of hTRPA1 in planar lipid bilayers was inhibited by the reducing agent TCEP. In contrast to its effect on cold activation, H_2O_2 decreased the single-channel activity of hTRPA1 generated by heat (30°C). This argues that hTRPA1 needs to be in a partially oxidized state to respond to not only cold but also heat. These results also suggest that different thermo-sensing properties (cold and heat) of hTRPA1 are due to different conformational states of the protein. Quenching of the intrinsic Trp fluorescence with increasing temperatures up to 40°C strengthens the notion that heat activation is an intrinsic property of the channel. A relatively reduced quenching of Trp fluorescence was observed both in the DTT and the H_2O_2 treated hTRPA1.

In HEK293t cells, in contrast to cold, heat itself evoked hTRPA1 currents, which were abolished by the selective TRPA1 antagonist HC-030031. A similar desensitization effect at 40°C as reported for the isolated protein was also observed. Compared to carvacrol and acrolein, heat-evoked hTRPA1 currents did not increase in the presence of H_2O_2, indicating that hTRPA1 heat sensitivity is regulated by the redox state. To further confirm the contribution of mammalian TRPA1 in heat sensation, heat responses were examined in mouse trachea using CGRP release as a read-out. This data reported robust TRPA1-dependent CGRP release under ROS treatment at 36°C. Further increasing the temperature to 40°C caused a decline of CGRP release, which is in agreement with the reduced hTRPA1 activity observed in single-channel recordings on planar lipid bilayers and whole-cell patch-clamp recordings.

As, TRPA1 is co-expressed with the noxious heat sensors TRPV1 and TRPM3 in peripheral sensory neurons and there is a lack of complete elimination of heat responses in TRPM3 knockout mice by TRPV1 inhibition (Vriens, Nilius et al. 2014), it is possible that TRPA1 itself contributes to heat sensation in mammals. Indeed, it has been shown that TRPA1 is involved in heat responses in mice (Bandell, Story et al. 2004, Hoffmann, Kistner et al. 2013), but in those studies it was not clear whether TRPA1 directly responded to heat or if it was indirectly activated via TRPV1 as has been suggested previously (Bautista, Jordt et al. 2006). Here we show, for the first time that hTRPA1 is indeed directly sensitive to heat. However, the physiological relevance of the hTRPA1 heat activation and desensitization remains to be studied. Similar to hTRPA1, the intrinsic capability for heat activation is also preserved in AgTRPA1. Based on our findings and those of others (Zakharian, Cao et al. 2010, Cao, Cordero-Morales et al. 2013, Uchida, Demirkhanyan et al. 2015), it is proposed that the temperature sensor is an intrinsic property of thermoTRPs.

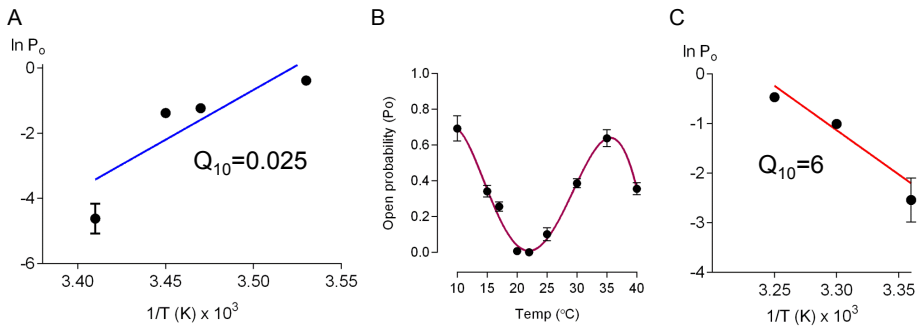

Figure 5.1 Temperature dependence of hTRPA1. **A**. Arrhenius plot with ln P_o versus inverse temperatures in Kelvin (temperature range between 10°C and 20°C). **B**. P_o values plotted against temperatures (°C) display U-shaped thermosensitivity of hTRPA1 (activated by both cold and warm temperatures). **C**. Arrhenius plot with ln P_o versus inverse temperatures in Kelvins (temperature range between 25°C and 35°C). Q10 values ≤ 0.2 and ≥ 5 indicates that hTRPA1 is both a cold and heat-sensitive ion channel (Voets 2012).

5.2.3 The role of the N-terminal ARD of TRPA1

The TRPA1 proteins contain a peculiar long N-terminal ARD. Several studies suggested that the ARD dictates the sensitivity to temperatures in mammalian and non-mammalian species (section 3.2.4 and Fig. 3.2). To understand the role of ARD, we made a construct, Δ1-688 hTRPA1 that is lacking the ARD. This truncated protein also responded to cold in a similar way as hTRPA1, although

the temperature dependence was steeper (Q_{10} = 0.018) than observed for hTRPA1. The channel activity was blocked with the TRPA1 selective antagonist HC-030031, which suggests that antagonist-binding sites are located outside the N-terminal region. Likewise, AgTRPA1 with deleted ARD, Δ1-776 AgTRA1, also responded to heat with a temperature threshold around 30°C. These findings indicate that the N-terminal ARD is not needed for the temperature activation of TRPA1, but perhaps plays a regulatory role on channel gating because the shift in temperature thresholds seemed different with and without the N-terminal ARD with regard to hTRPA1 cold and AgTRPA1 heat sensitivity.

Conclusions: Thermosensitive properties of TRPA1
• The purified hTRPA1 is intrinsically cold- and heat-sensitive, i.e. displays U-shaped thermosensitivity. • Both redox status and ligands have a modulatory role on the thermosensitivity of mammalian TRPA1. • The purified AgTRPA1 is an inherent heat-sensitive non-mammalian TRPA1. • The N-terminal ARD of hTRPA1 and AgTRPA1 is not needed for sensing temperature, but modulates this sensory modality.

5.3 Chemosensitive properties of TRPA1 (Papers I, III and IV)

Chemosensitivity is the most studied property of TRPA1 (section 3.1). As already mentioned, TRPA1 is a unique promiscuous chemosensor activated by more than 100 chemical compounds, but our understanding at a molecular level of how all these compounds interact with and fine-tune TRPA1 activity is far from complete (Zygmunt and Högestätt 2014). Here, we have explored inherent chemosensitive properties of TRPA1 with and without its N-terminal ARD using single-channel lipid bilayer recordings and tandem mass spectrometry.

In functional studies, we tested a few key compounds that are commonly used for characterization of the TRPA1. These include the electrophilic activators: AITC, CA and N-methylmaleimide (NMM) and the non-electrophilic activators: Δ^9-THC, C16 and menthol. The activation of hTRPA1 by these compounds was tested at both positive (+60 mV) and negative (-60 mV) test potentials to disclose any obvious voltage dependence. As anticipated, the above electrophilic compounds activated TRPA1 in the absence of an intracellular environment. However, in contrast to the literature, where it is proposed that pre-transmembrane N-terminal cysteines are critical for the electrophilic activation (section 3.1.1), Δ1-688 hTRPA1 lacking these cysteines was also activated by the

above mentioned electrophilic compounds. Lipid bilayers alone did not show any activity upon application of agonists in the absence of protein. The agonist-induced activity of both hTRPA1 and Δ1-688 hTRPA1 was abolished with the TRPA1 selective antagonist HC-030031, but re-appeared after the complete wash-out of the antagonist. This confirmed the observed activity was mediated by hTRPA1.

The mechanism behind TRPA1 activation by non-electrophilic compounds and their TRPA1 binding sites are less understood. It has been reported that the *Drosophila melanogaster* TRPA1 (dTRPA1) is not activated by menthol, since it is lacking sites for menthol binding on the fifth transmembrane segment (Xiao, Dubin et al. 2008). Therefore, we used a chimera between TRPA1 from drosophila and human TRPA1 (dTM5-hTRPA1) to examine the binding sites for cannabinoids on TRPA1. As the cannabinoid TRPA1 agonist, C16 activated the menthol insensitive chimera (dTM5-hTRPA1), this indicates that non-electrophilic compounds exhibit different binding sites. In line with this, analysis of G_s and P_o for single-channel activity revealed that C16 and menthol activate hTRPA1 in different ways.

To evaluate any voltage-dependent modulatory role of the N-terminal ARD on hTRPA1 responsiveness to electrophilic and non-electrophilic compounds, TRPA1 properties (G_s and P_o) were collected at positive (+60 mV) and negative (-60 mV) test potentials and analysed by calculating the rectification index (+60 mV/-60 mV). This approach together with a more detailed investigation using menthol, activating both hTRPA1 and its N-terminal truncated ARD variant at different voltage steps between -100 to +100 mV, consolidated that the N-terminal ARD domain regulates channel activity in a voltage-dependant manner.

It has been suggested that, TRPA1 displays a species-specific response to electrophiles (section 3.2.5). Although we did not compare the effect of AITC in a concentration-dependent manner between purified hTRPA1 and AgTRPA1, the responses of these TRPA1 ion channels when exposed to a supposed maximum effective concentration of AITC (100 μM), indicated obvious differences regarding channel behaviour. The G_s values were much lower for AgTRPA1 when compared to hTRPA1, and multiple open channel current levels were observed for hTRPA1 but not for AgTRPA1. Nevertheless, data suggest that electrophiles activate both hTRPA1 and AgTRPA1 directly and outside the N-terminal ARD region.

To further understand electrophilic activation of hTRPA1, the irreversible electrophilic TRPA1 activator NMM was used to map the binding sites and to monitor agonist-induced conformational changes of purified hTRPA1 proteins by mass spectrometry. To achieve this, labelling reactions were conducted incubating purified proteins individually with three different molar ratios of NMM in respect to the total cysteines of the hTRPA1 protein in a fixed time. As a result, NMM adducts were identified to most of the cysteines in the covered peptides of hTRPA1, which is in par with a previously reported mass spectrometry study on mouse TRPA1 (Wang, Cvetkov et al. 2012). The majority of the cysteines of hTRPA1 did not show a concentration-dependent increase of labelling at a ten-fold or hundred-fold increase of NMM, suggesting that these cysteines are either inaccessible in the structure or involved in disulphide bonds. In contrast to the saturation of the majority of the cysteines even at lower molar ratio of NMM, Cys308 and Cys540 show increased labelling at the equimolar ratio of NMM. Interestingly, Cys651 showed a significant decrease in labelling at the highest concentration of NMM, suggesting that NMM adducts at Cys308 and Cys540 cause conformational changes that make Cys651 less accessible and/or less reactive. Cys834 also shows decreased labelling with a higher molar ratio of NMM.

As mentioned earlier TRPA1 lacking the N-terminal ARD (Δ1-688 hTRPA1) is also activated by electrophilic compounds including NMM (Fig. 5.2C). In comparison with hTRPA1, Δ1-688 hTRPA1 contains only 9 of the 28 cysteines of hTRPA1 thus providing a simplified model system (Fig. 5.2A). NMM adducts were identified to all cysteines of Δ1-688 hTRPA1. In contrast to hTRPA1, there was little or no labelling at the lowest concentration of NMM, but an increased labelling at equimolar ratio of NMM was observed at all cysteines. Further, a ten-fold increase in concentration causes increased labelling at Cys727 concurrent with decreased labelling at Cys834, suggesting that similar conformational changes occur in the transmembrane region in both hTRPA1 and hTRPA1 lacking the N-terminal ARD. In addition to cysteines, NMM adducts were also observed to lysines of hTRPA1. In conclusion, here we provide new insights into the binding sites and conformational changes related to electrophilic activation mechanism of hTRPA1.

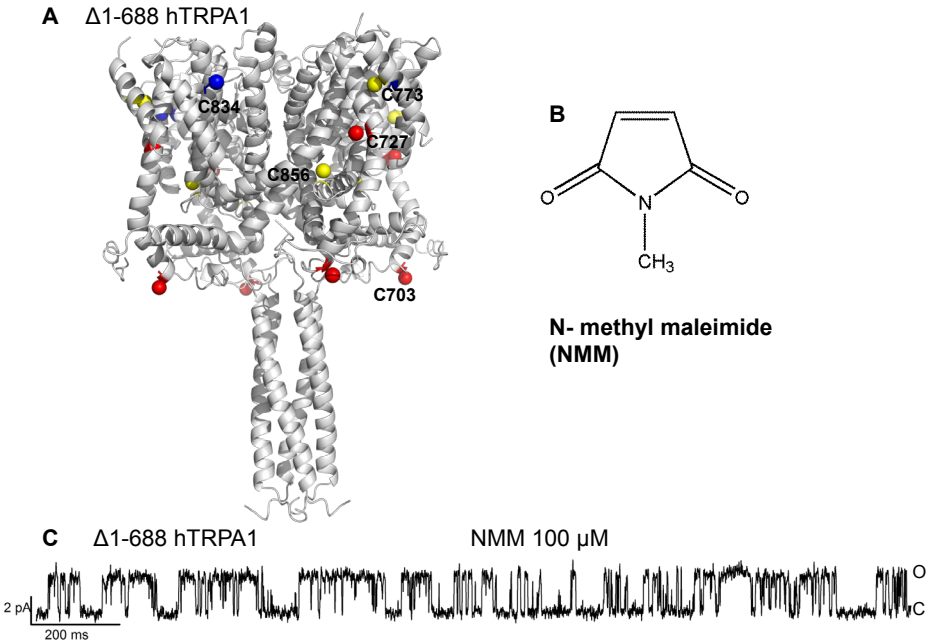

Figure 5.2 Electrophilic binding and activation of hTRPA1 lacking the N-terminal ARD (Δ1-688 hTRPA1). A. Structure of hTRPA1 with complete removal of N-terminal ARD, showing a side view of the tetrameric assembly with the transmembrane domain at the top **(PDB ID: 3J9P)**. Five of the nine cysteines in the monomer are resolved in the structure and sulphur atoms are displayed as spheres. The red and blue coloured spheres represent cysteines showing an increase and decrease in the N-methyl maleimide (NMM) labelling respectively at higher concentrations of NMM. **B.** Chemical structure of the TRPA1 electrophilic activator, NMM. **C.** Representative single-channel patch-clamp recording (at +60 mV) of Δ1-688 hTRPA1 activity in planar lipid bilayers when exposed to 100 μM NMM.

Conclusions: Chemosensitive properties of TRPA1
• Electrophiles and non-electrophiles activate hTRPA1 directly without need of intracellular factors. • Electrophilic and Non-electrophilic compounds (menthol and C16) activate hTRPA1 outside the N-terminal ARD. • The non-electrophilic compounds menthol and C16 interact with hTRPA1 at different sites. • The N-terminal ARD is not needed for hTRPA1 and AgTRPA1 chemosensation, but modulates hTRPA1 chemosensitivity in a voltage-dependent manner. • Both hTRPA1 and AgTRPA1 are polymodal sensors detecting chemicals in addition to temperature. • Cysteines outside the N-terminal region of hTRPA1 are involved in the detection and activation by the electrophile NMM.

5.4 Future perspectives

The finding of TRPA1 as a polymodal nocisensor has provided an excellent opportunity to study basic mechanisms behind chemo-, thermo- and mechanosensation at the molecular level. Many functional studies of TRPA1 (Zygmunt and Högestätt 2014), and the recently published near atomic resolution structure of hTRPA1, (Paulsen, Armache et al. 2015) have revealed new clues on how temperature and electrophilic as well as non-electrophilic compounds interact and activate hTRPA1. Further studies of channel function and high-resolution structures at different conformational states together with molecular dynamic simulations are needed to provide a deeper understanding of TRPA1 gating by temperature and ligands. Regarding temperature activation of TRPA1, important questions remain, such as how the channel at a molecular level can sense temperature, what is the identity of the thermosensor and is it restricted to a specific domain or scattered over the whole protein.

In this thesis, we show that hTRPA1 and AgTRPA1 are intrinsic thermosensitive proteins, but the physiological role of mammalian TRPA1 in warm sensation remains to be determined. Our findings indicate that although hTRPA1 is both cold- and heat-activated, the molecular mechanisms behind these thermosensitive properties may be different and need to be further investigated. It will also be of great interest to understand the exact molecular mechanism behind the redox regulation of the thermosensitivity of TRPA1.

The role of TRPA1 as a mechanosensor has been equally controversial as its role as a thermosensor. Whether or not TRPA1 is an inherent mechanosensitive protein and its N-terminal ARD has a key role in mechanosensation could be resolved by studies using purified TRPA1. Numerous studies have shown that TRPA1 channels are activated and regulated by Ca^{2+} (section 3.1.3). It has been proposed that Ca^{2+} binds to the 11^{th} AR and to acidic residues in the distal part of the C-terminal, but how Ca^{2+}-induced conformational changes are linked to channel gating is unknown.

Identifying binding sites for various non-electrophilic ligands and understanding how some activators evoke desensitization/inactivation of TRPA1 might help in developing novel analgesics/anti-inflammatory agents without detrimental side effects.

Acknowledgements

I would like to thank everyone who has helped and encouraged me at various stages of my graduate studies at the Department of Biochemistry and Structural Biology, Lund University. It is my pleasure to express gratitude to the following people.

First of all my supervisors, ***Prof. Urban Johanson***, I want to express my warmest gratitude to you for giving me the opportunity to do my graduate studies under your supervision. Thanks for motivating and giving opportunities to work in different projects. Thank you for giving me space to work as an independent researcher. I am so thankful to you for carefully reading my PhD thesis. ***Prof. Peter Zygmunt***, I would like to express my sincere gratitude to you for support and encouragement during my PhD studies. I enjoyed our scientific discussions and exchanging views on various topics of TRP field. Thank you for the given opportunities to attend scientific conferences and workshops in various parts of Europe and make me to visit and establish fruitful collaborations with renowned researchers in TRP field. I am so thankful to you for revising of my PhD thesis.

Prof. Edward Högestätt, thank you very much for your support. I enjoyed discussions with you about TRP channels. Thank you for teaching me statistical analysis of the data and taking such a special care. ***Prof. Per Kjellbom***, thank you so much for your support, encouragement and discussions in our group meetings.

Prof. Cecilia Hägerhäll, I would give a special thanks to you for your inspiring scientific ideas and support in my Master thesis in your group. You are truly inspirational and have positive influence on my life. I still remember your help at my initial days in Sweden. I am missing you a lot.

Dr. Mohamed Kreir, you are my patch clamp GURU. Thank you very much for introducing planar patch clamp and your patience on my endless questions regarding patch-clamp trouble shooting. Thanks for your very nice and fruitful collaboration to get our PNAS paper. ***Dr. Sven Kjellström*** thanks for introducing mass spectrometry technique to me and your suggestions on MS analysis, which clearly helped me to have better understanding of my results. Thanks for your fruitful collaboration. ***Dr. Milos Filipovic***, thanks for your wonderful collaboration and intriguing scientific discussions in my Erlangen visit. I truly enjoyed them a lot. Thanks for taking such care of me during entire trip and introducing me to modified biotin-switch assay technique. ***Dr. Andreas Leffler***, thank you very much for introducing whole-cell patch clamping and also for good collaboration. ***Prof. Peter Reeh***, thank you for valuable discussions about TRP channels in Erlangen research visit and for fruitful collaboration.

I would like to thank past and current group members for creating and keeping a good atmosphere in the lab. Thanks to ***Hanna, Kristina, Anders, Angelica, Aron, Michael*** *and* ***Eva,*** for your suggestions in group meetings. Thanks to ***Sabeen,*** for introducing the CD spectrometry and also for the collaboration. ***Andreas*** *and* ***Henry,*** thanks for helping in the beginning days of my PhD, especially in purification and crystallization. ***Yonathan,*** thanks for your nice discussions and suggestions on crystallization of hTRPA1. ***Johan,*** thank you very much for being such a nice colleague in Klinfarm and also for discussions about TRPA1 activation. We certainly had a lot of fun during lunchtime with spicy Indian food and making experiments with chilli ice cream (TRPV1 and TRPA1 activator). ***Charlotte*** thanks for being such a nice colleague in the lab and it has been pleasure working with you. Thanks for your suggestions and collaboration. ***Brita*** *and* ***Christina,*** thanks for your help in experiments and I enjoyed lunchtime meetings with you. It is my pleasure to thank ***Jonas, Hanna, Anna*** *and* ***Francesco*** for being great colleagues during teaching of the plant molecular biology course. ***Adine Karlsson****,* special thanks to you for all your support in practically and personally. Thank you for your nice talks during lunchtime. ***Gert Carlsson*** *and* ***Magnus Alsterfjord***, Thank you very much for technical support.

Kalyani, thanks for being such a nice friend in the department. ***Lande***, thank you for being a good friend and for great fun times we had. I am grateful to all my friends in Lund and Malmo for the great times during the parties and outings. I would like to thank all my friends in India for keeping our friendship alive even though we are so far apart.

My dear family, *father*, ***Venkata Rao*** and *mother*, ***Padmavathi***, *grandma*, ***Subbarathnamma***, *sister*, ***Prathiba*** and *brother*, ***Sreedhar***, thank you all for your support and affection. I never imagined that I came this far away from you. *Brother-in-law*, ***Satish****,* my dear brother thanks very much for your support and motivation during my PhD. It is so nice of you that you always treated me as your sister and thanks for collaboration that we shared in two projects. *Mother-in-law,* ***Radha****,* and *father-in-law*, ***Ramesh Babu***, you are my second mom and dad after my marriage. Thanks for taking such good care of me. I do not have any words to say about you and your support for raising my *son* ***Vishwak***. I know how much effort you put through to take care of him and supporting me to complete my PhD studies. I am very lucky to have a *mother-in-law* like you.

My lovely *son****, Vishwak,*** fisrt of all, I am so sorry that I am being away from you. It is very hard for me aswell, soon we will be in one place. I am really blessed and proud to have a son like you. I miss you lot. Thank you little dear for making my life very happy with your beautiful smile and your words. ***Vamsi,*** last but not least my dear *husband*. You are such a wonderful person, a good friend and very supportive, encouraged me throughout my PhD time. I cannot thank you in words; I just say, "*I love you"*.

Lavanya Moparthi
Lund, 01 March, 2016

References

Aebersold, R. and M. Mann (2003). "Mass spectrometry-based proteomics." Nature **422**(6928): 198-207.

Albin, K. C., M. I. Carstens*, et al.* (2008). "Modulation of oral heat and cold pain by irritant chemicals." Chem Senses **33**(1): 3-15.

Almaraz, L., J. A. Manenschijn*, et al.* (2014). "Trpm8." Handb Exp Pharmacol **222**: 547-579.

Andersson, D. A., C. Gentry*, et al.* (2009). "Clioquinol and pyrithione activate TRPA1 by increasing intracellular Zn2+." Proc Natl Acad Sci U S A **106**(20): 8374-8379.

Bach, G. (2005). "Mucolipin 1: endocytosis and cation channel--a review." Pflugers Arch **451**(1): 313-317.

Bagriantsev, S. N. and E. O. Gracheva (2014). "Molecular mechanisms of temperature adaptation." J Physiol.

Bandell, M., G. M. Story*, et al.* (2004). "Noxious Cold Ion Channel TRPA1 Is Activated by Pungent Compounds and Bradykinin." Neuron **41**(6): 849-857.

Bangham, A. D. and R. W. Horne (1964). "Negative Staining of Phospholipids and Their Structural Modification by Surface-Active Agents as Observed in the Electron Microscope." J Mol Biol **8**: 660-668.

Basbaum, A. I., D. M. Bautista*, et al.* (2009). "Cellular and molecular mechanisms of pain." Cell **139**(2): 267-284.

Bautista, D. M., S. E. Jordt*, et al.* (2006). "TRPA1 mediates the inflammatory actions of environmental irritants and proalgesic agents." Cell **124**(6): 1269-1282.

Bautista, D. M., P. Movahed*, et al.* (2005). "Pungent products from garlic activate the sensory ion channel TRPA1." Proc. Natl Acad. Sci. USA **102**: 12248-12252.

Bautista, D. M., M. Pellegrino*, et al.* (2013). "TRPA1: A gatekeeper for inflammation." Annu Rev Physiol **75**: 181-200.

Bautista, D. M., J. Siemens*, et al.* (2007). "The menthol receptor TRPM8 is the principal detector of environmental cold." Nature **448**(7150): 204-208.

Belmonte, C., J. A. Brock*, et al.* (2009). "Converting cold into pain." Exp Brain Res **196**(1): 13-30.

Benedikt, J., A. Samad*, et al.* (2009). "Essential role for the putative S6 inner pore region in the activation gating of the human TRPA1 channel." Biochim Biophys Acta **1793**(7): 1279-1288.

Bessac, B. F., M. Sivula*, et al.* (2009). "Transient receptor potential ankyrin 1 antagonists block the noxious effects of toxic industrial isocyanates and tear gases." FASEB J **23**(4): 1102-1114.

Birnbaumer, L., X. Zhu, *et al.* (1996). "On the molecular basis and regulation of cellular capacitative calcium entry: roles for Trp proteins." Proc Natl Acad Sci U S A **93**(26): 15195-15202.

Brauchi, S., P. Orio, *et al.* (2004). "Clues to understanding cold sensation: Thermodynamics and electrophysiological analysis of the cold receptor TRPM8." PNAS **101**(43): 15494-15499.

Brewster, M. S. and R. Gaudet (2015). "How the TRPA1 receptor transmits painful stimuli: Inner workings revealed by electron cryomicroscopy." Bioessays **37**(11): 1184-1192.

Cao, E., J. F. Cordero-Morales, *et al.* (2013). "TRPV1 channels are intrinsically heat sensitive and negatively regulated by phosphoinositide lipids." Neuron **77**(4): 667-679.

Cao, E., M. Liao, *et al.* (2013). "TRPV1 structures in distinct conformations reveal activation mechanisms." Nature **504**(7478): 113-118.

Caterina, M. J., T. A. Rosen, *et al.* (1999). "A capsaicin-receptor homologue with a high threshold for noxious heat." Nature **398**(6726): 436-441.

Caterina, M. J., M. A. Schumacher, *et al.* (1997). "The capsaicin receptor: a heat-activated ion channel in the pain pathway." Nature **389**(6653): 816-824.

Chen, J., S. K. Joshi, *et al.* (2011). "Selective blockade of TRPA1 channel attenuates pathological pain without altering noxious cold sensation or body temperature regulation." Pain **152**(5): 1165-1172.

Chen, J., D. Kang, *et al.* (2013). "Species differences and molecular determinant of TRPA1 cold sensitivity." Nat Commun **4**: 2501.

Cheng, W., C. Sun, *et al.* (2010). "Heteromerization of TRP channel subunits: extending functional diversity." Protein Cell **1**(9): 802-810.

Chowdhury, S., B. W. Jarecki, *et al.* (2014). "A molecular framework for temperature-dependent gating of ion channels." Cell **158**(5): 1148-1158.

Christensen, A. P. and D. P. Corey (2007). "TRP channels in mechanosensation: direct or indirect activation?" Nat Rev Neurosci **8**(7): 510-521.

Clapham, D. E. (2003). "TRP channels as cellular sensors." Nature **426**(6966): 517-524.

Clapham, D. E. and C. Miller (2011). "A thermodynamic framework for understanding temperature sensing by transient receptor potential (TRP) channels." Proc Natl Acad Sci U S A **108**(49): 19492-19497.

Colbert, H. A., T. L. Smith, *et al.* (1997). "OSM-9, a novel protein with structural similarity to channels, is required for olfaction, mechanosensation, and olfactory adaptation in Caenorhabditis elegans." J Neurosci **17**(21): 8259-8269.

Cordero-Morales, J. F., E. O. Gracheva, *et al.* (2011). "Cytoplasmic ankyrin repeats of transient receptor potential A1 (TRPA1) dictate sensitivity to thermal and chemical stimuli." Proc Natl Acad Sci U S A **108**(46): E1184-1191.

Corey, D., J. Garcia-Anoveros, *et al.* (2004). "TRPA1 is a candidate for the mechanosensitive transduction channel of vertebrate hair cells." Nature **432**(7018): 723-730.

Cosens, D. and A. Manning (1969). "Abnormal electroretinogram from a Drosophila mutant." Nature **224**(216): 285-287.

Cvetkov, T. L., K. W. Huynh, *et al.* (2011). "Molecular architecture and subunit organization of TRPA1 ion channel revealed by electron microscopy." J Biol Chem **286**(44): 38168-38176.

Dai, Y. (2015). "TRPs and pain." Semin Immunopathol.

Damann, N., T. Voets, *et al.* (2008). "TRPs in our senses." Curr Biol **18**(18): R880-889.

Davis, J. B., J. Gray, *et al.* (2000). "Vanilloid receptor-1 is essential for inflammatory thermal hyperalgesia." Nature **405**(6783): 183-187.

de la Roche, J., M. J. Eberhardt, *et al.* (2013). "The Molecular Basis for Species-specific Activation of Human TRPA1 Protein by Protons Involves Poorly Conserved Residues within Transmembrane Domains 5 and 6." J Biol Chem **288**(28): 20280-20292.

del Camino, D., S. Murphy, *et al.* (2010). "TRPA1 contributes to cold hypersensitivity." J Neurosci **30**(45): 15165-15174.

Deng, H. X., C. J. Klein, *et al.* (2010). "Scapuloperoneal spinal muscular atrophy and CMT2C are allelic disorders caused by alterations in TRPV4." Nat Genet **42**(2): 165-169.

Dhaka, A., V. Viswanath, *et al.* (2006). "TRP Ion Channels and Temperature Sensation." Annu Rev Neurosci.

Digel, I., P. Kayser, *et al.* (2008). "Molecular processes in biological thermosensation." J Biophys **2008**: 602870.

Dimitrov, M. I. A. a. D. S. (1986). "Liposome Electro formation." Faraday Discuss. Chem. SOC **81**: 303-311.

Doerner, J. F., G. Gisselmann, *et al.* (2007). "Transient receptor potential channel A1 is directly gated by calcium ions." J Biol Chem **282**(18): 13180-13189.

Dubin, A. E. and A. Patapoutian (2010). "Nociceptors: the sensors of the pain pathway." J Clin Invest **120**(11): 3760-3772.

Escalera, J., C. A. von Hehn, *et al.* (2008). "TRPA1 mediates the noxious effects of natural sesquiterpene deterrents." J Biol Chem **283**(35): 24136-24144.

Estes, D. J. and M. Mayer (2005). "Giant liposomes in physiological buffer using electroformation in a flow chamber." Biochim Biophys Acta **1712**(2): 152-160.

Fajardo, O., V. Meseguer, *et al.* (2008). "TRPA1 channels mediate cold temperature sensing in mammalian vagal sensory neurons: pharmacological and genetic evidence." J Neurosci **28**(31): 7863-7875.

Fajardo, O., V. Meseguer, *et al.* (2008). "TRPA1 channels: novel targets of 1,4-dihydropyridines." Channels (Austin) **2**(6): 429-438.

FALCHUK, B. L. V. A. K. H. (1993). "The Biochemical Basis of Zinc Physiology " Physiological Reviews **73**(1): 79-118.

Ferreira, L. G. and R. X. Faria (2016). "TRPing on the pore phenomenon: what do we know about transient receptor potential ion channel-related pore dilation up to now?" J Bioenerg Biomembr.

Fertig, N., R. H. Blick, *et al.* (2002). "Whole cell patch clamp recording performed on a planar glass chip." Biophys J **82**(6): 3056-3062.
Filipovic, M. R. (2015). "Persulfidation (S-sulfhydration) and H2S." Handb Exp Pharmacol **230**: 29-59.
Fischer, M. J., D. Balasuriya, *et al.* (2014). "Direct evidence for functional TRPV1/TRPA1 heteromers." Pflugers Arch **466**(12): 2229-2241.
Fujita, F., K. Uchida, *et al.* (2008). "Intracellular alkalization causes pain sensation through activation of TRPA1 in mice." J Clin Invest **118**(12): 4049-4057.
Fujiwara, Y. and D. L. Minor, Jr. (2008). "X-ray crystal structure of a TRPM assembly domain reveals an antiparallel four-stranded coiled-coil." J Mol Biol **383**(4): 854-870.
Gaudet, R. (2008). "A primer on ankyrin repeat function in TRP channels and beyond." Mol Biosyst **4**(5): 372-379.
Gaudet, R. (2008). "TRP channels entering the structural era." J Physiol **586**(Pt 15): 3565-3575.
Gavva, N. R., L. Klionsky, *et al.* (2004). "Molecular determinants of vanilloid sensitivity in TRPV1." J Biol Chem **279**(19): 20283-20295.
Gees, M., G. Owsianik, *et al.* (2012). "TRP channels." Compr Physiol **2**(1): 563-608.
Gijsen, H. J., D. Berthelot, *et al.* (2010). "Analogues of morphanthridine and the tear gas dibenz[b,f][1,4]oxazepine (CR) as extremely potent activators of the human transient receptor potential ankyrin 1 (TRPA1) channel." J Med Chem **53**(19): 7011-7020.
Giron, P., L. Dayon, *et al.* (2011). "Cysteine tagging for MS-based proteomics." Mass Spectrom Rev **30**(3): 366-395.
Gracheva, E. O., N. T. Ingolia, *et al.* (2010). "Molecular basis of infrared detection by snakes." Nature **464**(7291): 1006-1011.
Grantham, J. J. (1993). "Polycystic kidney disease: hereditary and acquired." Adv Intern Med **38**: 409-420.
Greenfield, N. J. (2006). "Using circular dichroism spectra to estimate protein secondary structure." Nat Protoc **1**(6): 2876-2890.
Grimm, C., R. Kraft, *et al.* (2003). "Molecular and functional characterization of the melastatin-related cation channel TRPM3." J Biol Chem **278**(24): 21493-21501.
Hardie, R. C. and B. Minke (1992). "The trp gene is essential for a light-activated Ca2+ channel in Drosophila photoreceptors." Neuron **8**(4): 643-651.
Hellmich, U. A. and R. Gaudet (2014). "Structural biology of TRP channels." Handb Exp Pharmacol **223**: 963-990.
Herbert, M. H., C. J. Squire, *et al.* (2015). "Poxviral ankyrin proteins." Viruses **7**(2): 709-738.
Hill, K. and M. Schaefer (2009). "Ultraviolet light and photosensitising agents activate TRPA1 via generation of oxidative stress." Cell Calcium **45**(2): 155-164.
Hinman, A., H. H. Chuang, *et al.* (2006). "TRP channel activation by reversible covalent modification." Proc Natl Acad Sci U S A **103**(51): 19564-19568.

Hoffmann, T., K. Kistner, *et al.* (2013). "TRPA1 and TRPV1 are differentially involved in heat nociception of mice." Eur J Pain **17**(10): 1472-1482.

Holzer, P. (2011). "Transient receptor potential (TRP) channels as drug targets for diseases of the digestive system." Pharmacol Ther **131**(1): 142-170.

Hu, H., M. Bandell, *et al.* (2009). "Zinc activates damage-sensing TRPA1 ion channels." Nat Chem Biol **5**(3): 183-190.

Ibarra, Y. and N. T. Blair (2013). "Benzoquinone reveals a cysteine-dependent desensitization mechanism of TRPA1." Mol Pharmacol **83**(5): 1120-1132.

Ihara, M., S. Hamamoto, *et al.* (2013). "Molecular bases of multimodal regulation of a fungal transient receptor potential (TRP) channel." J Biol Chem **288**(21): 15303-15317.

Islas, L. D. (2014). "Thermal effects and sensitivity of biological membranes." Curr Top Membr **74**: 1-17.

Jabba, S., R. Goyal, *et al.* (2014). "Directionality of Temperature Activation in Mouse TRPA1 Ion Channel Can Be Inverted by Single-Point Mutations in Ankyrin Repeat Six." Neuron **82**(5): 1017-1031.

Jaquemar, D., T. Schenker, *et al.* (1999). "An Ankyrin-like Protein with Transmembrane Domains Is Specifically Lost after Oncogenic Transformation of Human Fibroblasts." J. Biol. Chem. **274**(11): 7325-7333.

Jara-Oseguera, A. and L. D. Islas (2013). "The role of allosteric coupling on thermal activation of thermo-TRP channels." Biophys J **104**(10): 2160-2169.

Jiang, L. H., N. Gamper, *et al.* (2011). "Properties and therapeutic potential of transient receptor potential channels with putative roles in adversity: focus on TRPC5, TRPM2 and TRPA1." Curr Drug Targets **12**(5): 724-736.

Jordt, S. E., D. M. Bautista, *et al.* (2004). "Mustard oils and cannabinoids excite sensory nerve fibres through the TRP channel ANKTM1." Nature **427**(15): 260-265.

Jordt, S. E. and B. E. Ehrlich (2007). "TRP channels in disease." Subcell Biochem **45**: 253-271.

Jordt, S. E. and D. Julius (2002). "Molecular basis for species-specific sensitivity to "hot" chili peppers." Cell **108**(3): 421-430.

Julius, D. (2013). "TRP channels and pain." Annu Rev Cell Dev Biol **29**: 355-384.

Julius, D. and A. I. Basbaum (2001). "Molecular mechanisms of nociception." Nature **413**(6852): 203-210.

Kang, K., V. C. Panzano, *et al.* (2012). "Modulation of TRPA1 thermal sensitivity enables sensory discrimination in Drosophila." Nature **481**(7379): 76-80.

Kang, K., S. Pulver, *et al.* (2010). "Analysis of Drosophila TRPA1 reveals an ancient origin for human chemical nociception." Nature **464**: 597-600.

Karashima, Y., N. Damann, *et al.* (2007). "Bimodal action of menthol on the transient receptor potential channel TRPA1." J Neurosci **27**(37): 9874-9884.

Karashima, Y., J. Prenen, *et al.* (2008). "Modulation of the transient receptor potential channel TRPA1 by phosphatidylinositol 4,5-biphosphate manipulators." Pflugers Arch **457**(1): 77-89.

Karashima, Y., K. Talavera, *et al.* (2009). "TRPA1 acts as a cold sensor in vitro and in vivo." Proc Natl Acad Sci U S A **106**(4): 1273-1278.

Karlsson, M., D. Fotiadis, *et al.* (2003). "Reconstitution of water channel function of an aquaporin overexpressed and purified from Pichia pastoris." FEBS Lett **537**(1-3): 68-72.

Kelly, S. M., T. J. Jess, *et al.* (2005). "How to study proteins by circular dichroism." Biochim Biophys Acta **1751**(2): 119-139.

Kim, D. and E. J. Cavanaugh (2007). "Requirement of a soluble intracellular factor for activation of transient receptor potential A1 by pungent chemicals: role of inorganic polyphosphates." J Neurosci **27**(24): 6500-6509.

Kim, D., E. J. Cavanaugh, *et al.* (2008). "Inhibition of transient receptor potential A1 channel by phosphatidylinositol-4,5-bisphosphate." Am J Physiol Cell Physiol **295**(1): C92-99.

Kindt, K. S., V. Viswanath, *et al.* (2007). "Caenorhabditis elegans TRPA-1 functions in mechanosensation." Nat Neurosci **10**(5): 568-577.

Kohno, K., T. Sokabe, *et al.* (2010). "Honey bee thermal/chemical sensor, AmHsTRPA, reveals neofunctionalization and loss of transient receptor potential channel genes." J Neurosci **30**(37): 12219-12229.

Kreir, M., C. Farre, *et al.* (2008). "Rapid screening of membrane protein activity: electrophysiological analysis of OmpF reconstituted in proteoliposomes." Lab Chip **8**(4): 587-595.

Kremeyer, B., F. Lopera, *et al.* (2010). "A gain-of-function mutation in TRPA1 causes familial episodic pain syndrome." Neuron **66**(5): 671-680.

Kruse, M., E. Schulze-Bahr, *et al.* (2009). "Impaired endocytosis of the ion channel TRPM4 is associated with human progressive familial heart block type I." J Clin Invest **119**(9): 2737-2744.

Kurganov, E., Y. Zhou, *et al.* (2014). "Heat and AITC activate green anole TRPA1 in a membrane-delimited manner." Pflugers Arch **466**(10): 1873-1884.

Kwan, K. Y., A. J. Allchorne, *et al.* (2006). "TRPA1 contributes to cold, mechanical, and chemical nociception but is not essential for hair-cell transduction." Neuron **50**(2): 277-289.

Lakowicz, J. R. (2002). Topics in fluorescence spectroscopy. In: Protein fluorescence. J. R. Lakowicz, Kluwer Academic Publisher.

Landoure, G., A. A. Zdebik, *et al.* (2010). "Mutations in TRPV4 cause Charcot-Marie-Tooth disease type 2C." Nat Genet **42**(2): 170-174.

Latorre, R., C. Zaelzer, *et al.* (2009). "Structure-functional intimacies of transient receptor potential channels." Q Rev Biophys **42**(3): 201-246.

Launay, P., A. Fleig, *et al.* (2002). "TRPM4 is a Ca2+-activated nonselective cation channel mediating cell membrane depolarization." Cell **109**(3): 397-407.

Laursen, W. J., E. O. Anderson, *et al.* (2015). "Species-specific temperature sensitivity of TRPA1

" Temperature.

Leffler, A., A. Lattrell, *et al.* (2011). "Activation of TRPA1 by membrane permeable local anesthetics." Mol Pain **7**: 62.

Lepage, P. K., M. P. Lussier, *et al.* (2009). "The self-association of two N-terminal interaction domains plays an important role in the tetramerization of TRPC4." Cell Calcium **45**(3): 251-259.

Liao, M., E. Cao, *et al.* (2013). "Structure of the TRPV1 ion channel determined by electron cryo-microscopy." Nature **504**(7478): 107-112.

Lutolf, M. P., N. Tirelli, *et al.* (2001). "Systematic modulation of Michael-type reactivity of thiols through the use of charged amino acids." Bioconjug Chem **12**(6): 1051-1056.

Macpherson, L. J., A. E. Dubin, *et al.* (2007). "Noxious compounds activate TRPA1 ion channels through covalent modification of cysteines." Nature **445**(7127): 541-545.

Macpherson, L. J., B. H. Geierstanger, *et al.* (2005). "The pungency of garlic: activation of TRPA1 and TRPV1 in response to allicin." Curr Biol **15**(10): 929-934.

María Pertusa, H. M., Sebastián Brauchi, and R. M. a. P. O. Ramón Latorre (2012). Mutagenesis and

Temperature-Sensitive Little Machines. Mutagenesis. D. R. Mishra, InTech.

May, D., J. Baastrup, *et al.* (2012). "Differential expression and functionality of TRPA1 protein genetic variants in conditions of thermal stimulation." J Biol Chem **287**(32): 27087-27094.

McKemy, D., W. Neuhausser, *et al.* (2002). "Identification of a cold receptor reveals a general role for TRP channels in thermosensation." Nature **416**(6876): 52-58.

Meseguer, V., Y. Karashima, *et al.* (2008). "Transient receptor potential channels in sensory neurons are targets of the antimycotic agent clotrimazole." J Neurosci **28**(3): 576-586.

Molland, K. L., L. N. Paul, *et al.* (2012). "Crystal structure and characterization of coiled-coil domain of the transient receptor potential channel PKD2L1." Biochim Biophys Acta **1824**(3): 413-421.

Molleman, A. (2003). Patch clamping : an introductory guide to patch clamp electrophysiology : Areles Molleman. Chichester, J. Wiley.

Montell, C. (2005). "The TRP superfamily of cation channels." Sci STKE **2005**(272): re3.

Montell, C. and G. M. Rubin (1989). "Molecular characterization of the Drosophila trp locus: a putative integral membrane protein required for phototransduction." Neuron **2**(4): 1313-1323.

Mori, Y., N. Takahashi, *et al.* (2016). "Redox-sensitive transient receptor potential channels in oxygen sensing and adaptation." Pflugers Arch **468**(1): 85-97.

Nadler, M. J., M. C. Hermosura, *et al.* (2001). "LTRPC7 is a Mg.ATP-regulated divalent cation channel required for cell viability." Nature **411**(6837): 590-595.

Nagata, K., A. Duggan, *et al.* (2005). "Nociceptor and hair cell transducer properties of TRPA1, a channel for pain and hearing." J. Neurosci. **25**(16): 4052-4061.

Nauli, S. M., F. J. Alenghat, *et al.* (2003). "Polycystins 1 and 2 mediate mechanosensation in the primary cilium of kidney cells." Nat Genet **33**(2): 129-137.

Neher, E. and B. Sakmann (1976). "Single-channel currents recorded from membrane of denervated frog muscle fibres." Nature **260**(5554): 799-802.
Nilius, B. (2007). "TRP channels in disease." Biochim Biophys Acta.
Nilius, B., G. Appendino, *et al.* (2012). "The transient receptor potential channel TRPA1: from gene to pathophysiology." Pflugers Arch **464**(5): 425-458.
Nilius, B. and G. Owsianik (2011). "The transient receptor potential family of ion channels." Genome Biol **12**(3): 218.
Nilius, B., J. Prenen, *et al.* (2011). "Irritating channels: the case of TRPA1." J Physiol **589**(Pt 7): 1543-1549.
Nilius, B., J. Prenen, *et al.* (2005). "Regulation of the Ca2+ sensitivity of the nonselective cation channel TRPM4." J Biol Chem **280**(8): 6423-6433.
Nilius, B., K. Talavera, *et al.* (2005). "Gating of TRP channels: a voltage connection?" J Physiol **567**(Pt 1): 35-44.
Norden, K., M. Agemark, *et al.* (2011). "Increasing gene dosage greatly enhances recombinant expression of aquaporins in Pichia pastoris." BMC Biotechnol **11**: 47.
Obata, K., H. Katsura, *et al.* (2005). "TRPA1 induced in sensory neurons contributes to cold hyperalgesia after inflammation and nerve injury." J Clin Invest **115**(9): 2393-2401.
Ohara, K., T. Fukuda, *et al.* (2015). "Identification of significant amino acids in multiple transmembrane domains of human transient receptor potential ankyrin 1 (TRPA1) for activation by eudesmol, an oxygenized sesquiterpene in hop essential oil." J Biol Chem **290**(5): 3161-3171.
Owsianik, G., D. D'Hoedt, *et al.* (2006). "Structure-function relationship of the TRP channel superfamily." Rev Physiol Biochem Pharmacol **156**: 61-90.
Park, U., N. Vastani, *et al.* (2011). "TRP vanilloid 2 knock-out mice are susceptible to perinatal lethality but display normal thermal and mechanical nociception." J Neurosci **31**(32): 11425-11436.
Patapoutian, A., A. M. Peier, *et al.* (2003). "ThermoTRP channels and beyond: mechanisms of temperature sensation." Nat Rev Neurosci **4**(7): 529-539.
Paulsen, C. E., J. P. Armache, *et al.* (2015). "Structure of the TRPA1 ion channel suggests regulatory mechanisms." Nature **520**(7548): 511-517.
Paulsen, C. E. and K. S. Carroll (2013). "Cysteine-mediated redox signaling: chemistry, biology, and tools for discovery." Chem Rev **113**(7): 4633-4679.
Pedersen, S. F., G. Owsianik, *et al.* (2005). "TRP channels: an overview." Cell Calcium **38**(3-4): 233-252.
Peier, A. M., A. Moqrich, *et al.* (2002). "A TRP channel that senses cold stimuli and menthol." Cell **108**(5): 705-715.
Peier, A. M., A. J. Reeve, *et al.* (2002). "A heat-sensitive TRP channel expressed in keratinocytes." Science **296**(5575): 2046-2049.
Perraud, A. L., A. Fleig, *et al.* (2001). "ADP-ribose gating of the calcium-permeable LTRPC2 channel revealed by Nudix motif homology." Nature **411**(6837): 595-599.

Petersen, C. C., M. J. Berridge, *et al.* (1995). "Putative capacitative calcium entry channels: expression of Drosophila trp and evidence for the existence of vertebrate homologues." Biochem J **311 (Pt 1)**: 41-44.

Poole, L. B., P. A. Karplus, *et al.* (2004). "Protein sulfenic acids in redox signaling." Annu Rev Pharmacol Toxicol **44**: 325-347.

Prober, D. A., S. Zimmerman, *et al.* (2008). "Zebrafish TRPA1 channels are required for chemosensation but not for thermosensation or mechanosensory hair cell function." J Neurosci **28**(40): 10102-10110.

Rock, M. J., J. Prenen, *et al.* (2008). "Gain-of-function mutations in TRPV4 cause autosomal dominant brachyolmia." Nat Genet **40**(8): 999-1003.

Runnels, L. W., L. Yue, *et al.* (2001). "TRP-PLIK, a bifunctional protein with kinase and ion channel activities." Science **291**(5506): 1043-1047.

Sadofsky, L. R., A. N. Boa, *et al.* (2011). "TRPA1 is activated by direct addition of cysteine residues to the N-hydroxysuccinyl esters of acrylic and cinnamic acids." Pharmacol Res **63**(1): 30-36.

Saito, S., N. Banzawa, *et al.* (2014). "Heat and noxious chemical sensor, chicken TRPA1, as a target of bird repellents and identification of its structural determinants by multispecies functional comparison." Mol Biol Evol **31**(3): 708-722.

Saito, S., K. Nakatsuka, *et al.* (2012). "Analysis of transient receptor potential ankyrin 1 (TRPA1) in frogs and lizards illuminates both nociceptive heat and chemical sensitivities and coexpression with TRP vanilloid 1 (TRPV1) in ancestral vertebrates." J Biol Chem **287**(36): 30743-30754.

Salazar, M., H. Moldenhauer, *et al.* (2011). "Could an allosteric gating model explain the role of TRPA1 in cold hypersensitivity?" J Neurosci **31**(15): 5554-5556.

Samad, A., L. Sura, *et al.* (2011). "The C-terminal basic residues contribute to the chemical- and voltage-dependent activation of TRPA1." Biochem J **433**(1): 197-204.

Sawada, Y., H. Hosokawa, *et al.* (2007). "Cold sensitivity of recombinant TRPA1 channels." Brain Res **1160**: 39-46.

Sawyer, C. M., M. I. Carstens, *et al.* (2009). "Mustard oil enhances spinal neuronal responses to noxious heat but not cooling." Neurosci Lett **461**(3): 271-274.

Schmidt, R., M. Schmelz, *et al.* (1995). "Novel classes of responsive and unresponsive C nociceptors in human skin." J Neurosci **15**(1 Pt 1): 333-341.

Sedgwick, S. G. and S. J. Smerdon (1999). "The ankyrin repeat: a diversity of interactions on a common structural framework." Trends Biochem Sci **24**(8): 311-316.

Shevchenko, A., H. Tomas, *et al.* (2006). "In-gel digestion for mass spectrometric characterization of proteins and proteomes." Nat Protoc **1**(6): 2856-2860.

Sotomayor, M., D. P. Corey, *et al.* (2005). "In search of the hair-cell gating spring elastic properties of ankyrin and cadherin repeats." Structure **13**(4): 669-682.

Sousa-Valente, J., A. P. Andreou, *et al.* (2014). "Transient receptor potential ion channels in primary sensory neurons as targets for novel analgesics." Br J Pharmacol **171**(10): 2508-2527.

Story, G. M., A. M. Peier, *et al.* (2003). "ANKTM1, a TRP-like channel expressed in nociceptive neurons, is activated by cold temperatures." Cell **112**(6): 819-829.

Sura, L., V. Zima, *et al.* (2012). "C-terminal acidic cluster is involved in Ca2+-induced regulation of human transient receptor potential ankyrin 1 channel." J Biol Chem **287**(22): 18067-18077.

Takahashi, N., T. Kuwaki, *et al.* (2011). "TRPA1 underlies a sensing mechanism for O2." Nat Chem Biol **7**(10): 701-711.

Takahashi, N., Y. Mizuno, *et al.* (2008). "Molecular characterization of TRPA1 channel activation by cysteine-reactive inflammatory mediators." Channels (Austin) **2**(4): 287-298.

Talavera, K., M. Gees, *et al.* (2009). "Nicotine activates the chemosensory cation channel TRPA1." Nat Neurosci **12**(10): 1293-1299.

Talavera, K., K. Yasumatsu, *et al.* (2005). "Heat activation of TRPM5 underlies thermal sensitivity of sweet taste." Nature **438**(7070): 1022-1025.

Togashi, K., Y. Hara, *et al.* (2006). "TRPM2 activation by cyclic ADP-ribose at body temperature is involved in insulin secretion." EMBO J **25**(9): 1804-1815.

Tsagareli, M. G., N. Tsiklauri, *et al.* (2010). "Behavioral evidence of thermal hyperalgesia and mechanical allodynia induced by intradermal cinnamaldehyde in rats." Neurosci Lett **473**(3): 233-236.

Tsavaler, L., M. H. Shapero, *et al.* (2001). "Trp-p8, a novel prostate-specific gene, is up-regulated in prostate cancer and other malignancies and shares high homology with transient receptor potential calcium channel proteins." Cancer Res **61**(9): 3760-3769.

Uchida, K., L. Demirkhanyan, *et al.* (2015). "Stimulation-dependent gating of TRPM3 channel in planar lipid bilayers." FASEB J.

van Genderen, M. M., M. M. Bijveld, *et al.* (2009). "Mutations in TRPM1 are a common cause of complete congenital stationary night blindness." Am J Hum Genet **85**(5): 730-736.

Venkatachalam, K. and C. Montell (2007). "TRP channels." Annu Rev Biochem **76**: 387-417.

Viswanath, V., G. M. Story, *et al.* (2003). "Opposite thermosensor in fruitfly and mouse." Nature **423**(6942): 822-823.

Voets, T. (2012). "Quantifying and modeling the temperature-dependent gating of TRP channels." Rev Physiol Biochem Pharmacol **162**: 91-119.

Voets, T., G. Droogmans, *et al.* (2004). "The principle of temperature-dependent gating in cold- and heat-sensitive TRP channels." Nature **430**(7001): 748-754.

Voets, T. and B. Nilius (2003). "The pore of TRP channels: trivial or neglected?" Cell Calcium **33**(5-6): 299-302.

Voets, T. and B. Nilius (2003). "TRPs make sense." J Membr Biol **192**(1): 1-8.

Vriens, J., B. Nilius, *et al.* (2014). "Peripheral thermosensation in mammals." Nat Rev Neurosci **15**(9): 573-589.

Vriens, J., G. Owsianik, *et al.* (2011). "TRPM3 is a nociceptor channel involved in the detection of noxious heat." Neuron **70**(3): 482-494.

Walder, R. Y., D. Landau, *et al.* (2002). "Mutation of TRPM6 causes familial hypomagnesemia with secondary hypocalcemia." Nat Genet **31**(2): 171-174.

Wang, H., M. Schupp, *et al.* (2013). "Residues in the pore region of Drosophila transient receptor potential A1 dictate sensitivity to thermal stimuli." J Physiol **591**(Pt 1): 185-201.

Wang, L., T. L. Cvetkov, *et al.* (2012). "Identification of in vivo disulfide conformation of TRPA1 ion channel." J Biol Chem **287**(9): 6169-6176.

Wang, S., J. Lee, *et al.* (2012). "Warmth suppresses and desensitizes damage-sensing ion channel TRPA1." Mol Pain **8**: 22.

Wang, Y. Y., R. B. Chang, *et al.* (2011). "A TRPA1-dependent mechanism for the pungent sensation of weak acids." J Gen Physiol **137**(6): 493-505.

Wang, Y. Y., R. B. Chang, *et al.* (2010). "TRPA1 is a component of the nociceptive response to CO2." J Neurosci **30**(39): 12958-12963.

Wang, Y. Y., R. B. Chang, *et al.* (2008). "The nociceptor ion channel TRPA1 is potentiated and inactivated by permeating calcium ions." J Biol Chem **283**(47): 32691-32703.

Wes, P., J. Chevesich, *et al.* (1995). "TRPC1, a Human Homolog of a Drosophila Store-Operated Channel." PNAS **92**(21): 9652-9656.

Winn, M. P., P. J. Conlon, *et al.* (2005). "A mutation in the TRPC6 cation channel causes familial focal segmental glomerulosclerosis." Science **308**(5729): 1801-1804.

Wu, L. J., T. B. Sweet, *et al.* (2010). "International Union of Basic and Clinical Pharmacology. LXXVI. Current progress in the mammalian TRP ion channel family." Pharmacol Rev **62**(3): 381-404.

Xiao, B., A. E. Dubin, *et al.* (2008). "Identification of transmembrane domain 5 as a critical molecular determinant of menthol sensitivity in mammalian TRPA1 channels." J Neurosci **28**(39): 9640-9651.

Xiao, R., B. Zhang, *et al.* (2013). "A genetic program promotes C. elegans longevity at cold temperatures via a thermosensitive TRP channel." Cell **152**(4): 806-817.

Yu, Y., M. H. Ulbrich, *et al.* (2009). "Structural and molecular basis of the assembly of the TRPP2/PKD1 complex." Proc Natl Acad Sci U S A **106**(28): 11558-11563.

Yu, Y., M. H. Ulbrich, *et al.* (2012). "Molecular mechanism of the assembly of an acid-sensing receptor ion channel complex." Nat Commun **3**: 1252.

Zakharian, E., C. Cao, *et al.* (2010). "Gating of transient receptor potential melastatin 8 (TRPM8) channels activated by cold and chemical agonists in planar lipid bilayers." J Neurosci **30**(37): 12526-12534.

Zhong, L., A. Bellemer, *et al.* (2012). "Thermosensory and nonthermosensory isoforms of Drosophila melanogaster TRPA1 reveal heat-sensor domains of a thermoTRP Channel." Cell Rep **1**(1): 43-55.

Zhu, X., M. Jiang, *et al.* (1996). "trp, a novel mammalian gene family essential for agonist-activated capacitative Ca2+ entry." Cell **85**(5): 661-671.

Zimmermann, K., J. K. Lennerz, *et al.* (2011). "Transient receptor potential cation channel, subfamily C, member 5 (TRPC5) is a cold-transducer in the peripheral nervous system." Proc Natl Acad Sci U S A **108**(44): 18114-18119.

Zitt, C., A. Zobel*, et al.* (1996). "Cloning and functional expression of a human Ca2+-permeable cation channel activated by calcium store depletion." Neuron **16**(6): 1189-1196.

Zubcevic, L., M. A. Herzik, Jr.*, et al.* (2016). "Cryo-electron microscopy structure of the TRPV2 ion channel." Nat Struct Mol Biol **23**(2): 180-186.

Zurborg, S., B. Yurgionas*, et al.* (2007). "Direct activation of the ion channel TRPA1 by Ca^{2+}." Nat Neurosci **10**(3): 277-279.

Zygmunt, P. M. (2011). "Channels: A TR(i)P in the air." Nat Chem Biol **7**(10): 661-663.

Zygmunt, P. M., A. Ermund*, et al.* (2013). "Monoacylglycerols activate TRPV1 – a link between phospholipase C and TRPV1." PLoS One **8**(12): e81618.

Zygmunt, P. M. and E. D. Högestätt (2014). "Trpa1." Handb Exp Pharmacol **222**: 583-630.

Zygmunt, P. M., J. Petersson*, et al.* (1999). "Vanilloid receptors on sensory nerves mediate the vasodilator action of anandamide." Nature **400**(6743): 452-457.

Paper I

Human TRPA1 is intrinsically cold- and chemosensitive with and without its N-terminal ankyrin repeat domain

Lavanya Moparthi[a], Sabeen Survery[a], Mohamed Kreir[b,c], Charlotte Simonsen[d], Per Kjellbom[a], Edward D. Högestätt[d,1], Urban Johanson[a,1], and Peter M. Zygmunt[d]

[a]Department of Biochemistry and Structural Biology, Center for Molecular Protein Science, Lund University, SE-221 00 Lund, Sweden; [b]Nanion Technologies GmbH, D-80636 Munich, Germany; [c]Department of Biophysics, Jacobs University Bremen, D-27857 Bremen, Germany; and [d]Clinical Chemistry and Pharmacology, Department of Laboratory Medicine, Lund University, SE-221 85 Lund, Sweden

Edited* by Lutz Birnbaumer, National Institute of Environmental Health Sciences, Research Triangle Park, NC, and approved October 14, 2014 (received for review July 7, 2014)

We have purified and reconstituted human transient receptor potential (TRP) subtype A1 (hTRPA1) into lipid bilayers and recorded single-channel currents to understand its inherent thermo- and chemosensory properties as well as the role of the ankyrin repeat domain (ARD) of the N terminus in channel behavior. We report that hTRPA1 with and without its N-terminal ARD (Δ1–688 hTRPA1) is intrinsically cold-sensitive, and thus, cold-sensing properties of hTRPA1 reside outside the N-terminal ARD. We show activation of hTRPA1 by the thiol oxidant 2-((biotinoyl)amino)ethyl methanethiosulfonate (MTSEA-biotin) and that electrophilic compounds activate hTRPA1 in the presence and absence of the N-terminal ARD. The nonelectrophilic compounds menthol and the cannabinoid Δ^9-tetrahydrocannabiorcol (C16) directly activate hTRPA1 at different sites independent of the N-terminal ARD. The TRPA1 antagonist HC030031 inhibited cold and chemical activation of hTRPA1 and Δ1–688 hTRPA1, supporting a direct interaction with hTRPA1 outside the N-terminal ARD. These findings show that hTRPA1 is an intrinsically cold- and chemosensitive ion channel. Thus, second messengers, including Ca^{2+}, or accessory proteins are not needed for hTRPA1 responses to cold or chemical activators. We suggest that conformational changes outside the N-terminal ARD by cold, electrophiles, and nonelectrophiles are important in hTRPA1 channel gating and that targeting chemical interaction sites outside the N-terminal ARD provides possibilities to fine tune TRPA1-based drug therapies (e.g., for treatment of pain associated with cold hypersensitivity and cardiovascular disease).

cold sensing | irritants | pain | sensory neuron | TRP channels

A number of vertebrate and invertebrate transient receptor potential (TRP) ion channels have been implicated in temperature sensation (1–3), but only the rat menthol receptor TRP subtype M8 (TRPM8) and the rat capsaicin receptor TRP subtype V1 (TRPV1) have been shown to possess intrinsic thermosensitivity (4, 5). In 2003, Story et al. (6) proposed that the mouse TRPA1 is a noxious cold sensor. Story et al. (6) showed that TRPA1 was present in nociceptive primary sensory neurons and that CHO cells heterologously expressing the mouse TRPA1 displayed cold sensitivity. Most subsequent studies of cold responses in heterologous TRPA1 expression systems, isolated primary sensory neurons, and whole animals have provided evidence in support of mouse and rat TRPA1 being involved in noxious cold transduction (7). Interestingly, a familial episodic pain syndrome triggered by cold is caused by a gain-of-function mutation in the TRPA1 gene, indicating that TRPA1 may have a key role in human noxious cold sensation (8). Thus, human TRPA1 (hTRPA1) may be a relevant drug target for treatment of this condition and other pathological conditions, such as inflammation, nerve injury, and chemotherapy-induced neuropathy, that are characterized by TRPA1-dependent cold allodynia or hypersensitivity (7). However, in vitro studies of the expressed hTRPA1 have generated conflicting findings (8–15), and no study has provided evidence that mammalian TRPA1 channels are, indeed. intrinsically cold-sensitive proteins, which would require examination of the purified protein in a defined membrane environment.

Heterologous expression studies of chimeric or mutated TRPA1 channels have proposed that the N-terminal region plays an important role in thermal and chemical sensitivity of both mammalian and insect TRPA1 (14, 16–19). Initial studies indicated that mammalian TRPA1 is activated by cysteine-reactive electrophilic compounds and oxidants, such as diallyl disulfide in garlic (9, 10, 20, 21). Targeted gene mutations have identified cysteines present in the N terminus of TRPA1 as important for electrophilic and oxidative TRPA1 channel activation (22, 23). Because several of these cysteines are involved in protein disulfide formation (24–26), it is not unlikely that such mutations will have pronounced effects on the overall TRPA1 channel structure and function (7). Electrophilic compounds can also covalently bind to cysteines in the transmembrane segments and the C-terminal domain of mammalian TRPA1 (23, 26), and the electrophiles *p*-benzoquinone, isovelleral, and polygodial robustly activate the heterologously expressed triple mutant hTRPA1-3C (27, 28) that was initially used to identify certain N-terminal cysteine residues in hTRPA1 as key targets for electrophiles (22). However, it is yet to be shown that covalent binding sites outside the N-terminal

Significance

The ability of an organism to detect and avoid noxious temperatures is crucial for survival. It is, therefore, of great interest that several transient receptor potential (TRP) ion channels have been proposed as temperature sensors. However, to date, only the menthol receptor (TRP subtype M8) and the chili pepper receptor (TRP subtype V1) have been shown to be intrinsically temperature-sensitive proteins in mammals. In this study, we show that the purified wasabi receptor (TRP subtype A1) is a cold sensor. Thus, mammals have at least two cold sensors that, together, cover pleasant (TRP subtype M8) and unpleasant (TRP subtype A1) cold temperatures. Our findings add to the understanding of how the temperature sense is organized and its role in pain associated with cold hypersensitivity.

Author contributions: P.K., E.D.H., U.J., and P.M.Z. designed research; L.M., S.S., M.K., C.S., E.D.H., and P.M.Z. performed research; L.M., S.S., M.K., C.S., E.D.H., U.J., and P.M.Z. analyzed data; L.M., E.D.H., and P.M.Z. wrote the paper; L.M. performed and analyzed biochemistry and electrophysiology; S.S. performed and analyzed circular dichroism spectroscopy; M.K. performed and analyzed electrophysiology; C.S. designed, performed, and analyzed calcium imaging; P.K. directed the study; E.D.H. and P.M.Z. conceived, designed, and directed the study; and U.J. designed and directed the study.

Conflict of interest statement: M.K. is employed by Nanion Technologies GmbH.

*This Direct Submission article had a prearranged editor.

Freely available online through the PNAS open access option.

[1]To whom correspondence may be addressed. Email: edward.hogestatt@med.lu.se or urban.johanson@biochemistry.lu.se.

This article contains supporting information online at www.pnas.org/lookup/suppl/doi:10.1073/pnas.1412689111/-/DCSupplemental.

ankyrin repeat domain (ARD) contribute to the regulation of channel gating.

Another key feature of mammalian TRPA1 is the responsiveness to nonelectrophilic compounds with very different chemical structures, such as menthol and the cannabinoids Δ^9-tetrahydrocannabinol (Δ^9-THC) and Δ^9-tetrahydrocannabiorcol (C16) (7). However, if nonelectrophilic compounds activate TRPA1 directly and at the same site on TRPA1 is not known. The site of action of nonelectrophilic TRPA1 activators is important to clarify, because some TRPA1 activators are antinoiceptive (29, 30), and nontissue-damaging TRPA1 activators may be used clinically for pharmacological regulation of TRPA1 channel activity (29).

Here, we have purified and inserted hTRPA1 with and without its N-terminal ARD (Δ1–688 hTRPA1) into lipid bilayers for functional studies using patch-clamp electrophysiology to explore the inherent thermo- and chemosensitivity of hTRPA1. Because of the great potential of TRPA1 as a drug target for treatment of human pain and the existence of mammalian TRPA1 species differences (7), the human variant of TRPA1 was chosen for these studies. We addressed the role of the N-terminal ARD in cold and chemical sensitivity by deleting the N-terminal ARD, something that cannot be studied in cells heterologously expressing TRPA1, because the N-terminal ARD is needed for insertion of the ion channel into the plasma membrane (31). Our findings consolidate hTRPA1 as a multimodal nocisensor responding to cold and chemicals. It is suggested that conformational changes outside the N-terminal ARD by cold, electrophiles, and nonelectrophilic compounds are important in hTRPA1 channel gating. Targeting chemical interaction sites outside the N-terminal ARD may provide possibilities to fine tune TRPA1-based drug therapies [e.g., for treatment of pain associated with cold hypersensitivity (7) and cardiovascular disease (32)].

Results

Purification of Functional hTRPA1. To purify hTRPA1 and Δ1–688 hTRPA1, we used a *Pichia pastoris* expression system previously proven to be successful in the purification of other integral membrane proteins (33, 34). Initial screening of various detergents identified a series of fos-choline detergents as particularly effective for extraction of hTRPA1 and Δ1–688 hTRPA1 from *P. pastoris* cell membranes. Out of this screening, we chose fos-choline-14 for the purification and functional studies of the hTRPA1 channels. Intact hTRPA1 and Δ1–688 hTRPA1 with N-terminal decahistidine tags, which did not compromise the functionality of hTRPA1 when expressed in HEK293 cells (Fig. S1 *A–D*), were purified by Nickel affinity chromatography (Fig. 1); Δ1–688 hTRPA1 was obtained at a higher yield (3 mg/10 g cells) and purity than hTRPA1 (0.3 mg/10 g cells) using a one-step purification procedure. Based on Image Quant analysis, the purities of hTRPA1 and Δ1–688 hTRPA1 were estimated to be 50% and 95%, respectively.

In contrast to the heterologously expressed hTRPA1, there is no information on the functional properties and folding of Δ1–688 hTRPA1. Therefore, gel filtration and circular dichroism (CD) spectroscopy were implemented to evaluate the consequences of the removal of the N terminus on tetramerization and folding of the protein. As shown by the chromatogram, Δ1–688 hTRPA1 eluted mainly as a tetramer (Fig. 1*C*), and the far UV CD spectra showed that Δ1–688 hTRPA1 has the characteristics of a predominately α-helical structure with minima at 208 and 222 nm (Fig. 1*D*). The secondary structure composition was estimated by the Dicroweb software using CDSSTR, SELCON3, and CONTINLL algorithms, suggesting that Δ1–688 hTRPA1 contains 35–45% of α-helices, 15–20% of β-strands, 20–25% of turns, and 20–25% of unordered structure. The expected minima of α-helical content based on prediction of transmembrane domains (transmembrane hidden Markov models) and sequence alignment of Δ1–688 hTRPA1 with the potassium channel (Kv1.2) with

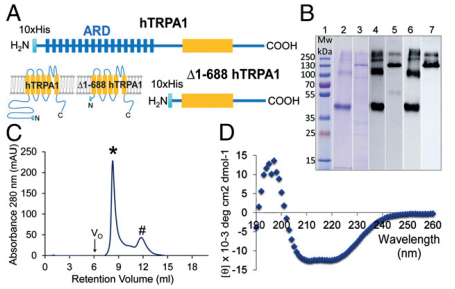

Fig. 1. Purification of hTRPA1 with and without the N-terminal ARD. (*A*) hTRPA1 was expressed either intact (1–1,119 aa) or without the ARD of the N terminus (Δ1–688 hTRPA1; 689–1,119 aa) with N-terminal decahistidine tags (10×His). (*B*) Affinity-purified hTRPA1 (lanes 3, 5, and 7) and Δ1–688 hTRPA1 (lanes 2, 4, and 6) visualized by Coomassie staining (lanes 2 and 3) and Western blotting (lanes 4–7) using either tetrahistidine antibody (lanes 4 and 5) or hTRPA1 antibody (lanes 6 and 7). The amounts of protein were 5 μg for Coomassie staining and 200 ng hTRPA1 and 40 ng Δ1–688 hTRPA1 for Western blotting. (*C*) As shown by the chromatogram, using a Superdex 200 size exclusion column, Δ1–688 hTRPA1 eluted mainly as a tetramer (*). V_o and # indicate void volume and monomer, respectively. (*D*) CD spectroscopy analysis disclosed typical characteristics of Δ1–688 hTRPA1 as a folded protein of high α-helical content. Mw, molecular mass.

known structure were 27% and 36%, respectively, which are in good agreement with the experimental data. Both the CD spectral data and the tetrameric oligomeric state of the purified protein suggest that it is correctly folded and functionally intact. In line with the general view that functional TRP channels are tetrameric protein complexes (2, 24), initial electrophysiological experiments measuring ramp currents (−100 to + 100 mV in 2 s) showed that hTRPA1 and Δ1–688 hTRPA1 reconstituted into planar lipid bilayers are functional proteins, because they responded to allyl isothiocyanate (AITC) and menthol, respectively, with single-channel currents at both negative and positive test potentials (Fig. S1*E*). Because AITC is supposed to activate TRPA1 by binding to the N terminus (22, 23), menthol was used to assess the functionality of Δ1–688 hTRPA1, because this nonelectrophilic compound presumably interacts with the S5 transmembrane domain (35).

Activation of hTRPA1 by Cold. TRPA1 activity was rarely observed at room temperature (22 °C), whereas cooling consistently activated hTRPA1 and Δ1–688 hTRPA1 at both positive and negative test potentials (Fig. 2, Figs. S2*B* and S3 *A* and *D*, and Table S1). Bilayers without proteins did not respond to cooling (Fig. S2*C*). Exposure to the TRPA1 blocker HC030031 inhibited cold-induced activation of hTRPA1 and Δ1–688 hTRPA1 by 71% and 76%, respectively (Fig. 2 *C* and *D*). Cooling from 22 °C to 10 °C dramatically increased single-channel open probability (P_o) (Fig. 2 *A*, *B*, and *E*). Our experimental setup did not allow us to obtain stable temperatures below 10 °C, which is why P_o values between 22 °C and 10 °C were used to calculate Q10 values of 0.025 and 0.018 from Arrhenius plots for hTRPA1 and Δ1–688 hTRPA1, respectively (Fig. 2*E*). A similar temperature dependence of the heterologously expressed mouse TRPA1 was observed in cell-attached and inside-out patches (36, 37) and with single-channel conductance (G_s) values at 10 °C, comparable with what we found for hTRPA1 (G_s = 50 ± 4 pS, n = 4). The G_s values at 10 °C differed between hTRPA1 and Δ1–688 hTRPA1 ($P < 0.05$, one-way ANOVA followed by Bonferroni's multiple comparison test) (Table S1). Notably, the cold-induced activity was reversible, and the G_s, but not P_o, decreased by 49% ± 10% (n = 3;

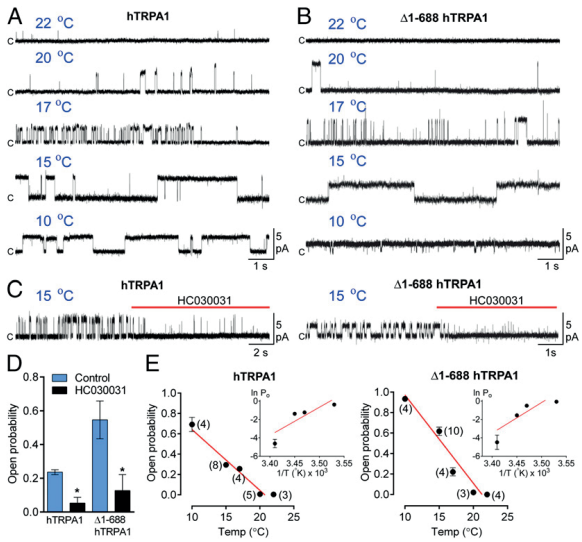

Fig. 2. The hTRPA1 is intrinsically cold-sensitive with and without the N-terminal ARD. Purified hTRPA1 and Δ1–688 hTRPA1 were inserted into planar lipid bilayers. (*A–C*) As shown by representative traces, cooling evoked substantial hTRPA1 and Δ1–688 hTRPA1 single-channel activity at a test potential of +60 mV (upward deflection shows open-channel state, and c shows closed-channel state). Amplitude histograms corresponding to each trace are shown in Fig. S2*A*. (*C*) Traces showing inhibition of cold responses of hTRPA1 and Δ1–688 hTRPA1 by the TRPA1 antagonist HC030031 (100 μM). (*D*) Graph with P_o values calculated from a time period of 1 min before and a time period of 1 min after treatment of hTRPA1 ($n = 3$) and Δ1–688 hTRPA1 ($n = 4$) with HC030031 at 15 °C. Complete inhibition was achieved after 1 min. Data are represented as means ± SEMs. $^*P < 0.05$ indicates statistically significant differences using the Student's paired *t* test. (*E*) Plots summarize the P_o at various temperatures (number of experiments within parentheses) for (*Left*) hTRPA1and (*Right*) Δ1–688 hTRPA1. *Insets* show Arrhenius plots of the same data, with P_o values as the natural logarithm (ln) and temperature (T) as reciprocal Kelvin. Single-channel currents were recorded with the patch-clamp technique in a symmetrical K^+ solution.

$P < 0.05$, one-sample *t* test) when hTRPA1 was repeatedly exposed to 15 °C (Fig. S3*A*). This decline in G_s may reflect an inherent calcium-independent change in pore size, but it should not affect our analysis of cold-induced responses, because the analysis was based only on a first exposure to the indicated temperatures.

Activation of hTRPA1 by Electrophiles in the Absence of the N-Terminal ARD. Having established that the N-terminal ARD of hTRPA1 is not required for activation by cold, we asked if electrophiles can activate hTRPA1 in the absence of its N-terminal ARD at room temperature. Single-channel currents were rarely observed at test potentials of −60 and +60 mV or in voltage ramp recordings from −100 to +100 mV in the absence of TRPA1 activators (Fig. 2 *A*, *B*, and *E*, and Figs. S1*E* and S3*A*). However, AITC, cinnamaldehyde (CA), and *N*-methylmaleimide (NMM) but not the vehicle (1% ethanol) produced activation of both hTRPA1 and Δ1–688 hTRPA1 at −60 and +60 mV, whereas no activity was observed in the presence of activators on empty bilayers (Fig. 3*A* and Figs. S5, S6*B*, and S7). As shown for cinnamaldehyde, the effect was reversible (Fig. S3*B*). The activities of hTRPA1 and Δ1–688 hTRPA1 were blocked by HC030031 in a reversible manner (Fig. 3*B* and Fig. S3*C*): $P_o = 0.56 \pm 0.09$ and $P_o = 0.03 \pm 0.02$ as calculated for 1 min before and 1 min after the addition of HC030031, respectively, for hTRPA1 ($n = 4$). Whereas the G_s values for hTRPA1 and Δ1–688 hTRPA1 at −60 mV were similar in the presence for all electrophilic compounds, the G_s values at +60 mV differed between hTRPA1 and Δ1–688 hTRPA1 in the presence of AITC and NMM (Fig. 4*A* and Table S1). Comparison of P_o values revealed differences in ligand activation between hTRPA1 and Δ1–688 hTRPA1 at both positive and negative test potentials (Fig. 4*B* and Table S1). Additional calculations of the rectification index (+60/−60 mV) for G_s and P_o showed clear differences between hTRPA1 and Δ1–688 hTRPA1 when exposed to electrophiles (Fig. 4*C*), indicating that the N terminus modified hTRPA1 channel behavior in a voltage-dependent manner.

The ability of the hydrophilic thiol oxidant 2-((biotinoyl) amino)ethyl methanethiosulfonate-biotin (MTSEA-biotin; Fig. S4), which is active on TRPA1 from the intracellular side (23), to activate hTRPA1 ($G_s = 128 \pm 2$ pS and $P_o = 0.71 \pm 0.02$ at +60 mV; $n = 5$) only when applied in the bath solution (Fig. S4) indicates a uniform orientation of the protein in the lipid bilayer. Based on our findings that NMM activated the N-terminal ARD-deleted hTRPA1 and its ability to bind cysteine residues outside the N-terminal ARD (23, 26), we used a hydrophilic maleimide-biotin derivative (Fig. S4) for studies of Δ1–688 hTRPA1. Our data suggest a similar uniform orientation for Δ1–688 hTRPA1 in the lipid bilayer, because maleimide-biotin only activated this protein when applied to the bath solution (Fig. S4). The Gs and P_o values for maleimide-biotin ($G_s = 46 \pm 6$ pS and $P_o = 0.41 \pm 0.03$ at +60 mV, $n = 4$) are similar to those obtained with NMM at a test potential of +60 mV (Fig. 4 *A* and *B* Table S1).

Activation of hTRPA1 by Nonelectrophilic Compounds. In addition to being a chemosensor of thiol-reactive electrophiles and oxidants, TRPA1 is also activated by nonelectrophilic compounds, including Δ^9-THC, C16, menthol, carvacrol, clotrimazole, and dihydropyridines (7). A few heterologous expression studies using site-directed mutagenesis, chimeric channel constructs, or isolated

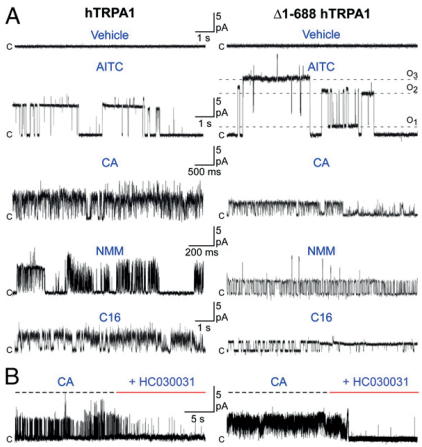

Fig. 3. Electrophilic and nonelectrophilic compounds activate purified hTRPA1 with and without the N-terminal ARD. (*A*) Representative traces show single-channel activity (upward deflection shows open-channel state, and c shows closed-channel state) for (*Left*) hTRPA1 and (*Right*) Δ1–688 hTRPA1 without the N-terminal ARD when inserted into planar lipid bilayers and exposed to the electrophilic compounds AITC (100 μM), cinnamaldehyde (CA; 100 μM), and NMM (100 μM) and the nonelectrophilic compound C16 (100 μM). Multiple distinct open-channel levels (dotted lines) were observed for AITC in Δ1–688 hTRPA1, of which the main level (O_3) was used for calculations of the G_s values presented in Fig. 4 and Table S1 (Fig. S5 presents responses at −60 mV). As shown by representative traces, the vehicle (ethanol at 1%) used for all test compounds evoked no activation of either hTRPA1 variant ($n = 3$). Amplitude histograms corresponding to each trace in *A* are shown in Fig. S7. (*B*) The TRPA1 antagonist HC030031 (100 μM) blocked CA-induced hTRPA1 ($n = 4$) and Δ1–688 hTRPA1 channel activity ($n = 2$). Channel currents were recorded with the patch-clamp technique in a symmetrical K^+ solution at a test potential of +60 mV.

inside-out patches suggest that nonelectrophilic compounds, including menthol and Δ^9-THC, directly interact with TRPA1 (35, 38). In this study using the purified channel, we provide final proof that Δ^9-THC, C16, and menthol directly activate hTRPA1 without the involvement of other cellular proteins or second messengers, including inositol triphosphate and Ca^{2+} (Figs. 3*A*, 4, and 5 and Figs. S1*E* and S5–S7). As with electrophilic compounds, menthol and C16 also activated hTRPA1 without the N-terminal ARD (Figs. 3*A*, 4, and 5 and Figs. S5 and S7). Importantly, the very lipophilic and potent cannabinoid receptor agonist CP55940, which in contrast to Δ^9-THC and C16, does not activate hTRPA1 expressed in HEK293 cells (29), did not trigger hTRPA1 channel activity, whereas Δ^9-THC produced activation when subsequently applied to the same bilayer (Fig. S6*A*); G_s for Δ^9-THC at +60 mV was 87 ± 7 pS ($n = 5$). This pharmacological profile together with our finding that electrophilic and nonelectrophilic TRPA1 activators are without effect on lipid bilayers in the absence of protein (Fig. S6*B*) support a specific interaction with hTRPA1.

Analysis of single-channel behavior revealed differences in the action of menthol and C16 on hTRPA1 and Δ1–688 hTRPA1 (Fig. 4 and Table S1). At +60 mV, G_s was larger and P_o was smaller for Δ1–688 hTRPA1 than hTRPA1 in the presence of menthol but not C16, whereas at −60 mV, P_o was larger for hTRPA1 than Δ1–688 hTRPA1 in the presence of C16 but not menthol (Fig. 4 *A* and *B* and Table S1). The rectification index (+60/−60 mV) for G_s and P_o showed clear differences in single-channel behavior between hTRPA1 and Δ1–688 hTRPA1 when exposed to nonelectrophilic compounds (Fig. 4*C*). Furthermore, C16 activated the menthol-insensitive chimera *Drosophila* transmembrane segment 5 (dTM5) -hTRPA1 between *D. melanogaster* (dTM5) and hTRPA1 (Fig. S8). Taken together, these findings are consistent with distinct binding sites for menthol and C16 and indicate that the N terminus modifies hTRPA1 channel responses to nonelectrophilic compounds in a voltage-dependent manner.

To further explore the influence of the N terminus on single-channel behavior, we used menthol as an hTRPA1 activator at room temperature. This ligand is assumed to bind to the transmembrane region of the channel protein and therefore, should not interfere with the integrity of the N terminus (35). As revealed by comparing single-channel currents and P_o between hTRPA1 and Δ1–688 hTRPA1 at different test potentials, the presence of the N-terminal ARD increased P_o at positive test potentials, while decreasing P_o at negative test potentials (Fig. 5). In contrast, the presence of the N-terminal ARD decreased G_s at positive test potentials, while leaving G_s unaffected at negative test potentials (Fig. 5).

Discussion

The ability to detect and avoid noxious temperatures is crucial for organism survival, but the underlying mechanisms of this beneficial property may also contribute to thermal allodynia or hypersensitivity, hallmarks of many chronic pain conditions in humans. Understanding the molecular mechanisms behind

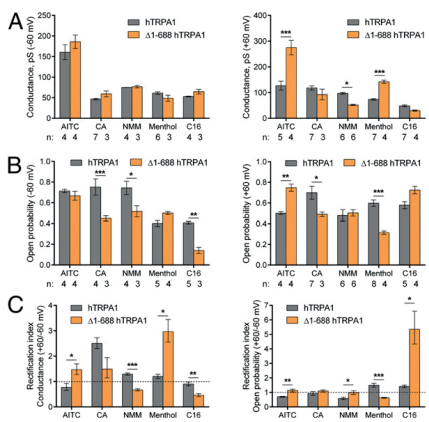

Fig. 4. The N-terminal ARD influences the channel behavior of the purified hTRPA1 when exposed to electrophilic and nonelectrophilic compounds. (*A* and *B*) Bar graphs summarize the mean G_s and P_o values for the TRPA1 activators AITC (100 μM), cinnamaldehyde (CA; 100 μM), NMM (100 μM), menthol (500 μM), and C16 (100 μM) at a test potential of either −60 or +60 mV. Multiple distinct open-channel levels were observed for AITC in Δ1–688 hTRPA1 (Fig. 3*A* and Fig. S5), of which the main levels (O_3 at +60 mV and O_1 at −60 mV) were used for calculations of G_s values. Single-channel currents of purified hTRPA1 and Δ1–688 hTRPA1 inserted into planar lipid bilayers were recorded with the patch-clamp technique in a symmetrical K^+ solution. (*C*) Analysis of the rectification index (+60/−60 mV) using the G_s and P_o data shown in *A* and *B* (Table S1). The dotted line indicates the level where no rectification would occur. Data are represented as means ± SEMs. $^*P < 0.05$, $^{**}P < 0.01$, and $^{***}P < 0.001$ indicate statistically significant differences between the hTRPA1 variants using (*A* and *B*) one-way ANOVA followed by Bonferroni's multiple comparison test or (*C*) a priori contrast analysis with adjustment for the degrees of freedom in the *F* test according to the Welch–Satterthwaite procedure.

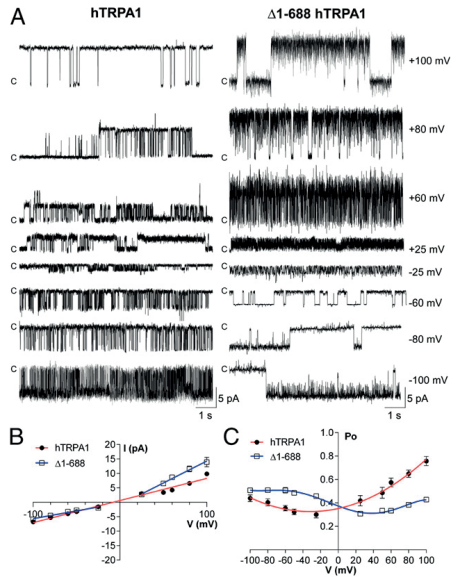

Fig. 5. The N-terminal ARD modifies hTRPA1 activity induced by menthol in a voltage-dependent manner. Purified hTRPA1 and Δ1–688 hTRPA1 were inserted into planar lipid bilayers. (*A*) As shown by representative traces, menthol (500 μM) evoked (*Left*) hTRPA1 and (*Right*) Δ1–688 hTRPA1 single-channel activity (upward deflection shows open-channel state at positive test potential, downward deflection shows open-channel state at negative test potential, and c shows closed-channel state). (*B*) Single-channel current–voltage (I–V) relationship and (*C*) single-channel P_o–voltage (P_o–V) relationship of the hTRPA1 and Δ1–688 hTRPA1 when activated by menthol (500 μM). The calculated mean slope G_s values were 77 ± 4 pS for hTRPA1 and 54 ± 6 pS (−100 to −25 mV) and 152 ± 7 pS (+25 to +100 mV) for Δ1–688 hTRPA1. These values are in good agreement with G_s values obtained at −60 and +60 mV in separate experiments (Fig. 4 and Table S1). Single-channel currents were recorded with the patch-clamp technique in a symmetrical K^+ solution at the various test potentials indicated on the right in *A*. Data are represented as means ± SEMs of four separate experiments. (*B*) $P < 0.01$ (+50 mV) and $P < 0.001$ (+60, +80, and +100 mV), and (*C*) $P < 0.05$ (+25 mV), $P < 0.01$ (−60 and +50 mV), and $P < 0.001$ (−50, −25, +60, +80, and +100 mV) indicate statistically significant differences at each test potential between the hTRPA1 channels using one-way ANOVA followed by Bonferroni's multiple comparison test.

thermosensation is, therefore, of importance from both biological and medical perspectives (1, 39). Several TRP channels have recently been proposed as thermosensors, of which the majority is involved in warm sensation (1–3, 39). However, to define a TRP channel as a thermosensor would require examination of the purified channel protein in a defined membrane environment, and to date, only rat TRPM8 and rat TRPV1 have been shown to be intrinsically thermosensitive proteins (4, 5). Here, we show for the first time, to our knowledge, that the purified hTRPA1 inserted into artificial lipid bilayers is an inherently cold-sensitive protein. Thus, the mammalian TRP channel family consists of an additional cold sensor—TRPA1—that, together with TRPM8, covers noxious to pleasant cold temperatures.

Mutational and chimeric strategies have been used to suggest specific thermosensitive regions and drug binding sites in TRP channels (8, 11, 13, 14, 16, 17, 19, 40). In this study, using the purified N-terminal ARD-deleted hTRPA1 to avoid potential artifacts in TRPA1 function caused by mutations or the creation of xenogeneic channels (7), we clearly show that the cold sensitivity and the binding site for HC030031, an inhibitor of rodent TRPA1 and hTRPA1 (7, 41), are located outside the N-terminal ARD. The search for a specific cold-sensitive region in mammalian TRPA1 channels should, thus, be directed toward the transmembrane and the C-terminal domains of TRPA1.

As shown for cold, electrophilic compounds also evoked robust hTRPA1 activity in the absence of the N-terminal ARD, providing a more complex picture of electrophile activation of hTRPA1 than generally believed. By comparing G_s and P_o values at +60 and −60 mV, we found voltage-dependent differences in channel behavior between the two hTRPA1 variants when exposed to electrophilic compounds. Interestingly, a triple cysteine mutation of the hTRPA1 N-terminal region (hTRPA1-3C) changed the voltage-dependent electrophilic activation of hTRPA1 by *p*-benzoquinone, an acetaminophen (paracetamol) metabolite (28, 29). Furthermore, the N-terminal region may suppress hTRPA1 channel gating, because the response to NMM was intact in the N-terminal ARD-deleted hTRPA1 (this study) but lost in the N-terminal triple cysteine mutant (22), having a greatly reduced capacity to form disulfide bonds (25). The response of hTRPA1 to the nonelectrophilic compounds menthol and C16 also did not require the presence of the N-terminal ARD, which however, modified hTRPA1 channel behavior in a voltage-dependent manner.

Although our data clearly show that electrophilic and nonelectrophilic compounds activate hTRPA1 outside the N-terminal ARD, random protein orientation in the artificial lipid bilayer and the existence of multiple levels of channel opening could complicate the analysis of the voltage-dependent channel behavior. A uniform protein insertion was not confirmed in each single experiment, but separate experiments showed the ability of the biotin derivatives of 2-((biotinoyl)amino)ethyl methanethiosulfonate and maleimide to activate hTRPA1 and the N-terminal ARD-deleted hTRPA1, respectively, only when applied to the bath solution, supporting a consistent asymmetric orientation of both proteins in the lipid bilayers. For comparison of G_s between the hTRPA1 variants at different voltages, we analyzed the current magnitude only for the main open-channel level. Because distinct multiple open-channel levels were frequently observed for AITC in the N-terminal ARD-deleted hTRPA1, G_s values and the rectification index obtained with AITC in hTRPA1 without the N terminus should be interpreted with caution. Interestingly, the hTRPA1 single-channel G_s values for electrophilic and nonelectrophilic compounds vary greatly, although within the wide range of values reported for mammalian TRPA1 (7). Whether this ligand-dependent variation in single-channel G_s is caused by pore dilation and modified by the N terminus warrant additional investigations. Based on our electrophysiological data, it is difficult to provide a simple biophysical fingerprint of hTRPA1, which may not be surprising considering the great variety of chemical interactions between ligands and TRPA1 (7). Nevertheless, our data raise the possibility that the N terminus modifies hTRPA1 channel behavior in a voltage-dependent manner.

The ability of TRPA1 to respond to nonelectrophilic compounds is intriguing but could indicate that endogenous TRPA1 modulators with similar chemical structures or properties exist (7). In this study, we show that menthol and the cannabinoids C16 and Δ^9-THC directly activate hTRPA1 without the need for cytoplasmic (e.g., Ca^{2+}) or cell membrane-associated factors. We found that the menthol-insensitive dTM5–hTRPA1 chimera (35) expressed in HEK293 cells was activated by C16, indicating that menthol and cannabinoids interact with distinct binding sites. Future studies identifying the binding sites for C16 and other cannabinoids may help us to understand nonelectrophilic regulation of TRPA1 and the potential of these binding sites as targets for

analgesics, including nontissue-damaging TRPA1 activators (29). Perhaps such TRPA1 activators can also be used to modulate aging in humans, because the TRPA1 activator AITC extended lifespan in transgenic *Caenorhabditis elegans* expressing hTRPA1 (42).

Although this study clearly shows that hTRPA1 is an inherently cold-activated ion channel, it does not resolve why studies of the expressed hTRPA1 have generated such conflicting findings regarding its cold sensitivity (8–15). However, we know that the regulation of TRPA1 is complex and that the channel sensitivity to ligands is dependent on the cellular context, including the redox state in the cell, the phosphoinositide composition of the cell membrane, and the intracellular activities of proline hydroxylase and protein kinase/phosphatase enzymes (7). Many of these factors are probably dependent on the cell expression system and the experimental conditions, and their future disclosure may pinpoint novel drug targets other than TRPA1 for treatment of clinical conditions characterized by TRPA1-dependent cold allodynia or hypersensitivity (7).

In conclusion, we show that hTRPA1 is an intrinsically cold-activated ion channel that constitutes a molecular thermosensor explaining TRPA1-dependent behavioral responses to noxious cold (7). The N-terminal ARD is not needed for activation of hTRPA1 by cold, electrophiles, and nonelectrophilic compounds or inhibition of hTRPA1 by HC030031. However, the N-terminal ARD may modify hTRPA1 channel behavior in a voltage-dependent manner. Targeting chemical interaction sites outside the TRPA1 N-terminal ARD may offer possibilities to fine tune TRPA1-based drug therapies [e.g., for treatment of pain associated with cold hypersensitivity (7) and cardiovascular disease (32)].

Materials and Methods

P. pastoris cell membranes, containing hTRPA1 or Δ1–688 hTRPA1, were collected and solubilized with fos-choline-14 detergent (Anatrace). Both proteins were purified using Ni-nitrilotriacetic acid affinity chromatography; Δ1–688 hTRPA1 was also subjected to size exclusion chromatography. Purified hTRPA1 (after Ni-nitrilotriacetic acid purification) and Δ1–688 hTRPA1 (tetrameric fraction from size exclusion chromatography) were reconstituted into preformed planar lipid bilayers or giant unilamellar vesicles. The vesicles were formed by electroformation using Vesicle Prep Pro Station (Nanion Technologies). Lipid stock was made by dissolving 10 mM 1,2-diphytanoyl-*sn*-glycero-3-phosphocholine:cholesterol (9:1) in trichloromethane. All lipid bilayer recordings were done on a Port-a-Patch planar patch-clamp system (Nanion Technologies) in a symmetrical K^+ solution at room temperature (22 °C) or below. Group data are expressed as means ± SEMs from *n* independent experiments (lipid bilayers or cell transfections). *SI Materials and Methods* has full details.

ACKNOWLEDGMENTS. We thank Brita Sundén-Andersson and Adine Karlsson for technical assistance and Dr. Ardem Patapoutian for providing us with the dTM5–hTRPA1 chimera. This work was supported by Swedish Research Council Grants 2010-5787 (to E.D.H. and P.M.Z.), 2010-3347 (to E.D.H. and P.M.Z.), 2007-6110 (to U.J.), and Formas 2007-718 (to P.K., E.D.H., U.J., and P.M.Z.), the Research School of Pharmaceutical Sciences at Lund University (U.J. and P.M.Z.), and the Medical Faculty at Lund University (E.D.H. and P.M.Z.).

1. Clapham DE, Miller C (2011) A thermodynamic framework for understanding temperature sensing by transient receptor potential (TRP) channels. *Proc Natl Acad Sci USA* 108(49):19492–19497.
2. Voets T, Talavera K, Owsianik G, Nilius B (2005) Sensing with TRP channels. *Nat Chem Biol* 1(2):85–92.
3. Panzano VC, Kang K, Garrity PA (2010) Infrared snake eyes: TRPA1 and the thermal sensitivity of the snake pit organ. *Sci Signal* 3(127):pe22.
4. Cao E, Cordero-Morales JF, Liu B, Qin F, Julius D (2013) TRPV1 channels are intrinsically heat sensitive and negatively regulated by phosphoinositide lipids. *Neuron* 77(4): 667–679.
5. Zakharian E, Cao C, Rohacs T (2010) Gating of transient receptor potential melastatin 8 (TRPM8) channels activated by cold and chemical agonists in planar lipid bilayers. *J Neurosci* 30(37):12526–12534.
6. Story GM, et al. (2003) ANKTM1, a TRP-like channel expressed in nociceptive neurons, is activated by cold temperatures. *Cell* 112(6):819–829.
7. Zygmunt PM, Högestätt ED (2014) TRPA1. *Handbook Exp Pharmacol* 222:583–630.
8. Kremeyer B, et al. (2010) A gain-of-function mutation in TRPA1 causes familial episodic pain syndrome. *Neuron* 66(5):671–680.
9. Bandell M, et al. (2004) Noxious cold ion channel TRPA1 is activated by pungent compounds and bradykinin. *Neuron* 41(6):849–857.
10. Jordt SE, et al. (2004) Mustard oils and cannabinoids excite sensory nerve fibres through the TRP channel ANKTM1. *Nature* 427(6971):260–265.
11. Wang H, Schupp M, Zurborg S, Heppenstall PA (2013) Residues in the pore region of Drosophila transient receptor potential A1 dictate sensitivity to thermal stimuli. *J Physiol* 591(Pt 1):185–201.
12. Zurborg S, Yurgionas B, Jira JA, Caspani O, Heppenstall PA (2007) Direct activation of the ion channel TRPA1 by Ca^{2+}. *Nat Neurosci* 10(3):277–279.
13. Chen J, et al. (2013) Species differences and molecular determinant of TRPA1 cold sensitivity. *Nat Commun* 4:2501.
14. Cordero-Morales JF, Gracheva EO, Julius D (2011) Cytoplasmic ankyrin repeats of transient receptor potential A1 (TRPA1) dictate sensitivity to thermal and chemical stimuli. *Proc Natl Acad Sci USA* 108(46):E1184–E1191.
15. May D, et al. (2012) Differential expression and functionality of TRPA1 protein genetic variants in conditions of thermal stimulation. *J Biol Chem* 287(32):27087–27094.
16. Gracheva EO, et al. (2010) Molecular basis of infrared detection by snakes. *Nature* 464(7291):1006–1011.
17. Kang K, et al. (2012) Modulation of TRPA1 thermal sensitivity enables sensory discrimination in Drosophila. *Nature* 481(7379):76–80.
18. Kang K, et al. (2010) Analysis of Drosophila TRPA1 reveals an ancient origin for human chemical nociception. *Nature* 464(7288):597–600.
19. Jabba S, et al. (2014) Directionality of temperature activation in mouse TRPA1 ion channel can be inverted by single-point mutations in ankyrin repeat six. *Neuron* 82(5): 1017–1031.
20. Bautista DM, et al. (2005) Pungent products from garlic activate the sensory ion channel TRPA1. *Proc Natl Acad Sci USA* 102(34):12248–12252.
21. Macpherson LJ, et al. (2005) The pungency of garlic: Activation of TRPA1 and TRPV1 in response to allicin. *Curr Biol* 15(10):929–934.
22. Hinman A, Chuang HH, Bautista DM, Julius D (2006) TRP channel activation by reversible covalent modification. *Proc Natl Acad Sci USA* 103(51):19564–19568.
23. Macpherson LJ, et al. (2007) Noxious compounds activate TRPA1 ion channels through covalent modification of cysteines. *Nature* 445(7127):541–545.
24. Cvetkov TL, Huynh KW, Cohen MR, Moiseenkova-Bell VY (2011) Molecular architecture and subunit organization of TRPA1 ion channel revealed by electron microscopy. *J Biol Chem* 286(44):38168–38176.
25. Eberhardt MJ, et al. (2012) Methylglyoxal activates nociceptors through transient receptor potential channel A1 (TRPA1): A possible mechanism of metabolic neuropathies. *J Biol Chem* 287(34):28291–28306.
26. Wang L, Cvetkov TL, Chance MR, Moiseenkova-Bell VY (2012) Identification of in vivo disulfide conformation of TRPA1 ion channel. *J Biol Chem* 287(9):6169–6176.
27. Escalera J, von Hehn CA, Bessac BF, Sivula M, Jordt SE (2008) TRPA1 mediates the noxious effects of natural sesquiterpene deterrents. *J Biol Chem* 283(35):24136–24144.
28. Ibarra Y, Blair NT (2013) Benzoquinone reveals a cysteine-dependent desensitization mechanism of TRPA1. *Mol Pharmacol* 83(5):1120–1132.
29. Andersson DA, et al. (2011) TRPA1 mediates spinal antinociception induced by acetaminophen and the cannabinoid Δ(9)-tetrahydrocannabiorcol. *Nat Commun* 2:551.
30. Weng Y, et al. (2012) Prostaglandin metabolite induces inhibition of TRPA1 and channel-dependent nociception. *Mol Pain* 8(1):75.
31. Nilius B, Prenen J, Owsianik G (2011) Irritating channels: The case of TRPA1. *J Physiol* 589(Pt 7):1543–1549.
32. Eberhardt M, et al. (2014) H_2S and NO cooperatively regulate vascular tone by activating a neuroendocrine HNO-TRPA1-CGRP signalling pathway. *Nat Commun* 5:4381.
33. Törnroth-Horsefield S, et al. (2006) Structural mechanism of plant aquaporin gating. *Nature* 439(7077):688–694.
34. Long SB, Tao X, Campbell EB, MacKinnon R (2007) Atomic structure of a voltage-dependent K^+ channel in a lipid membrane-like environment. *Nature* 450(7168): 376–382.
35. Xiao B, et al. (2008) Identification of transmembrane domain 5 as a critical molecular determinant of menthol sensitivity in mammalian TRPA1 channels. *J Neurosci* 28(39): 9640–9651.
36. Karashima Y, et al. (2009) TRPA1 acts as a cold sensor in vitro and in vivo. *Proc Natl Acad Sci USA* 106(4):1273–1278.
37. Sawada Y, Hosokawa H, Hori A, Matsumura K, Kobayashi S (2007) Cold sensitivity of recombinant TRPA1 channels. *Brain Res* 1160:39–46.
38. Kim D, Cavanaugh EJ, Simkin D (2008) Inhibition of transient receptor potential A1 channel by phosphatidylinositol-4,5-bisphosphate. *Am J Physiol Cell Physiol* 295(1): C92–C99.
39. Voets T (2012) Quantifying and modeling the temperature-dependent gating of TRP channels. *Rev Physiol Biochem Pharmacol* 162:91–119.
40. Brauchi S, Orta G, Salazar M, Rosenmann E, Latorre R (2006) A hot-sensing cold receptor: C-terminal domain determines thermosensation in transient receptor potential channels. *J Neurosci* 26(18):4835–4840.
41. Bianchi BR, et al. (2012) Species comparison and pharmacological characterization of human, monkey, rat, and mouse TRPA1 channels. *J Pharmacol Exp Ther* 341(2):360–368.
42. Xiao R, et al. (2013) A genetic program promotes C. elegans longevity at cold temperatures via a thermosensitive TRP channel. *Cell* 152(4):806–817.

Supporting Information

Moparthi et al. 10.1073/pnas.1412689111

SI Materials and Methods

Protein Expression and Purification. The full-length hTRPA1 and Δ1–688 hTRPA1 were heterologously expressed in *Pichia pastoris*. The cDNA coding for hTRPA1 was subcloned from pFROG3 (provided by Sven-Eric Jordt, Duke University, Durham, NC) (1) into a modified pPICZB vector and had an N-terminal decahistidine (deca-His) tag (provided by Andreas Kirscht, Lund University, Lund, Sweden). The following primers were used: 5′-GATTCGAACGGAATTCCGACCGAAAACCTGTATTTTCAGGGCAAGCGCAGCCTGAGGA-3′ (forward primer for hTRPA1), 5′-GACTTCGAACGGAATTCCGACCGAAAACCTGTATTTTCAGGGCATGGTACAAAATAAC-3′ (forward primer for Δ1–688 hTRPA1), and 5′- CAGGTCTCGAGCCTAGATTACTAAGGCTCAAGATGGTGTGTTTTTGCCTTGACTGCTC-3′ (reverse primer for both constructs). Restriction sites BstBI and XhoI were introduced in forward and reverse primers, respectively, and used in subcloning (enzymes from Fermentas). A tobacco etch virus protease cleavage site was created between the deca-His tag and the corresponding gene sequence. The plasmids were amplified in *Escherichia coli* XL1-Blue cells and sequenced to confirm the correct nucleotide sequence.

The constructs were linearized at the PmeI (Fermentas) restriction site and transformed into WT *Pichia* X-33 strain by electroporation according to the Easy Select *Pichia* Expression Kit Manual (Invitrogen). High gene copy number clones were selected with the Zeocin resistance marker, and the level of expression was investigated by Western blot using a tetra-His antibody (2). Selected high-expression clones were cultured by either baffled flasks or a 3-L bench-top fermenter (Belach Bioteknik).

The cells were resuspended in cold breaking buffer [50 mM NaH_2PO_4, 2 mM EDTA, 20% (vol/vol) glycerol, pH 7.4] containing the protease inhibitors phenylmethylsulfonyl fluoride (1 mM; MBL International Corporation), pepstatin (1 μg/mL; Sigma-Aldrich), and leupeptin (1 μg/mL; Sigma-Aldrich). The resuspended cells were transferred to a Bead Beater (BioSpec Products) container with cold glass beads (0.5 mm; BioSpec Products) and mechanically broken by 12 cycles of 30-s beatings with 30-s intervals in a cold room (8 °C). Cell debris and unbroken cells were removed by low-speed centrifugation at 1,380 × *g* for 30 min. Membranes were collected by ultracentrifugation (185,000 × *g* for 2 h) and washed with urea solution (4 M urea, 5 mM Tris·HCl, 2 mM EDTA, 2 mM EGTA, pH 9.5) to remove peripheral membrane proteins (3). After the urea wash, membranes were washed with buffer A containing 20 mM Hepes, 50 mM NaCl, 10% (vol/vol) glycerol, and 5 mM β-mercaptoethanol (pH 7.8).

The membranes were solubilized in buffer A and supplied with 2% (wt/vol) fos-choline-14 (FC-14; Anagrade; Anatrace) at room temperature for 3 h with mild agitation. Detergent-insoluble membranes were removed by ultracentrifugation at 100,000 × *g* for 30 min. The solubilized membranes were incubated with preequilibrated Ni-NTA agarose resin (Qiagen) for 2 h in a cold room (8 °C). For hTRPA1 purification, 10 mM imidazole was added to the solubilized membranes to prevent unspecific binding to the resin. The binding solution was transferred to a polyprep chromatography column (Bio-Rad), and the column was washed with buffer B containing 20 mM Hepes, 300 mM NaCl, and 10% (vol/vol) glycerol (pH 7.8) supplemented with 0.014% FC-14 and 50 mM imidazole. The protein was eluted with buffer B containing 0.014% FC-14 and 300 mM imidazole. After the Ni-NTA purification, hTRPA1 was desalted, and the buffer was changed to PBS (137 mM NaCl, pH 7.8) supplemented with 10% (vol/vol) glycerol and 0.014% FC-14 in a PD-10 column (GE Healthcare) and concentrated with Vivaspin 4 with a 50-kDa molecular mass cutoff (Sartorius Stedim Biotech). The concentrated hTRPA1 protein was used in functional assays. For purification of Δ1–688 hTRPA1, 20 mM (instead of 10 mM) imidazole was added to the solubilized membranes. The column was washed and eluted with the same buffers as mentioned for hTRPA1, except that 5 mM β-mercaptoethanol was included and the washing buffer contained 120 mM (instead of 50 mM) imidazole. To refine the homogeneity of the sample, the protein was loaded on a preequilibrated Superdex 200 column (GE Healthcare), and the protein was collected in PBS supplemented as described above. The tetramer-containing fraction of Δ1–688 hTRPA1 was used in additional structural and functional characterizations.

Expression of TRPA1 in HEK293 Cells. The gene coding for hTRPA1 with N-terminal deca-His tag was subcloned from pPICZB (described above) to the pcDNA3 vector. The sequences of the constructs were confirmed by nucleotide sequencing. HEK293 cells were transfected with pcDNA3 plasmid containing hTRPA1 with N-terminal deca-His tag and also pcDNA5/FRT plasmid containing dTM5–hTRPA1 chimera (plasmid provided by Ardem Patapoutian, Scripps Research Institute, La Jolla, CA) (4). The transiently transfected cells were used for ratiometric calcium imaging experiments as described below. In some transfections, the expression of hTRPA1 was confirmed by Western blot (see below).

SDS/PAGE and Western Blot Analysis. The purified proteins and lysed HEK293 cells using ProteoJET Mammalian Cell Lysis Reagent (Fermentas) according to the manufacturer's protocol were subjected to 12% SDS/PAGE gel (Bio-Rad), and electrophoresis was performed for 1 h at 180 V. After electrophoresis, the protein bands were visualized by Coomassie G-250 staining or transferred to polyvinylidene fluoride membranes for Western blot analysis. The tetra-His antibody (Qiagen), which binds to the N-terminal His tag, and the hTRPA1 antibody (Sigma-Aldrich), which binds to the C terminus of hTRPA1, were used to visualize the proteins in Western blot. The purity of the fractions was analyzed by Image Quant TL 7.0 Image analysis software (GE Healthcare).

Circular Dichroism Spectroscopy. Circular dichroism (CD) spectra were recorded with a Jasco 815 spectrometer (Jasco) at 20 °C using a 1-mm path-length quartz cuvette. Far UV spectra were collected between 190 and 260 nm, with a step size of 1 nm. PBS (100 mM NaCl) used in CD experiments was supplemented with 10% (vol/vol) glycerol and 0.014% FC-14. The same buffer was used to correct for the spectral background. Mean spectra were obtained from three replicate scans. The secondary structural content was estimated using Dicroweb software (5).

Reconstitution of Purified Proteins into Planar Lipid Bilayer or Giant Unilameller Vesicles. Giant unilameller vesicles (GUVs) were produced by electroformation using a Vesicle Prep Pro Station (Nanion Technologies) (6, 7). Approximately 20 μL lipid stock solution containing 1,2-diphytanoyl-*sn*-glycero-3-phosphocholine (9 mM) and cholesterol (1 mM) in trichloromethane was placed on the indium tin oxide glass surface of the Vesicle Prep Pro Station and allowed to dry. The dry lipid film was rehydrated with 250 μL 1 M sorbitol in water. The vesicles were formed by electroswelling under the influence of an alternating electrical field for

2 h at 36 °C. GUVs were collected and used for making either planar lipid bilayers or proteoliposomes (6, 7). For formation of a planar lipid bilayer, 5 μL GUV solution was pipetted onto the patch-clamp chip (aperture of 1–2 μm), and a negative pressure (from −10 to −40 mbar) was applied. After formation of planar lipid bilayers, 0.15–0.2 μL hTRPA1 (0.4–0.5 μg/mL) or Δ1–688 hTRPA1 (0.06–0.08 μg/mL) micellar solution was added for studying the chemical responsiveness of the ion channels.

For preparation of proteoliposomes, the proteins were added to the GUV solution (final protein concentration of 10 ng/mL to 5 μg/mL for hTRPA1 and from 10 ng/mL to 1 μg/mL for Δ1–688 hTRPA1), and the mixture was incubated for 60–120 min at room temperature. The detergent was removed with polystyrene Biobeads SM2 (Bio-Rad) using 40 mg beads per milliliter. After incubation overnight at 4 °C, the beads were removed by centrifugation. The proteoliposomes were then used to make planar lipid bilayers, as described above, for studying cold activation of the ion channels.

Electrophysiological Recordings. A symmetrical K^+ solution of the following composition was used in all lipid bilayer recordings: 50 mM KCl, 10 mM NaCl, 60 mM KF, 20 mM EGTA, and 10 mM Hepes (adjusted to pH 7.2 with KOH). Signals were acquired with an EPC 10 amplifier (HEKA) and the data acquisition software PatchMaster (HEKA) at a sampling rate of 50 kHz. The recorded data were digitally filtered at 3 kHz. The patch-clamp experiments were performed either at room temperature or below, for which the Port-a-Patch was equipped with an external perfusion system (Nanion Technologies) and an SC-20 dual in-line solution cooler connected to a temperature-controlled (CL-100) liquid cooling system (Warner Instruments).

Electrophysiological data were analyzed using Clampfit 9 (Molecular Devices), Igor Pro (Wave Metrics), and GraphPad Prism 6.0 software. Data were filtered at 1,000 and 500 Hz for analysis and traces, respectively, using a low-pass Gaussian filter. The mean G_s of single channels was obtained from Gaussian fit of all-points amplitude histograms. Time constant values for calculating P_o values were obtained from exponential standard fits of dwell time histograms. The current–voltage relationships (I–V curve) were obtained from the amplitudes of single-channel openings at different membrane potentials. The Q10 values for P_o were obtained from the slope of regression lines fitted to Arrhenius plots (8, 9).

Ratiometric $[Ca^{2+}]_i$ Measurements. Transfected HEK293 cells were plated in 96-well black-walled plates (Costar) or 8-well slides (Ibidi) coated with poly-D-lysine, and they were loaded with Fura 2-AM (1–2 μM; Invitrogen), probenecid (2 mM; Sigma-Aldrich), and pluronic acid (0.02%; Invitrogen) for 1 h at 37 °C. The cells were then washed with physiological buffer solution containing 140 mM NaCl, 5 mM KCl, 10 mM glucose, 10 mM Hepes, 2 mM $CaCl_2$, and 1 mM $MgCl_2$ (pH 7.4) and allowed to equilibrate for a period of 30 min in the dark before the start of the experiments. Changes in the intracellular calcium levels were determined at 25 °C in a Flexstation 3 (Molecular Devices) or with an Olympus IX70 microscope connected to a digital camera (Hamamatsu) controlled by the software program SimplePCI 6 (Hamamatsu). Basal emission (510 nm) ratios with excitation wavelengths of 340 and 380 nm were measured, and changes in dye emission ratio (Δratio) were determined at various times after compound addition.

Chemicals. All test compounds, except 2-((biotinoyl)amino)ethyl methanethiosulfonate (MTSEA-biotin) and maleimide-biotin, were dissolved in ethanol and diluted with a symmetrical K^+ solution (see above for composition). MTSEA-biotin and maleimide-biotin were dissolved in dimethyl sulfoxide and diluted with the symmetrical K^+ solution. AITC, cinnamaldehyde, NMM, (−)-menthol, CP55940, and HC030031 were obtained from Sigma-Aldrich, MTSEA-biotin was obtained from Santa Cruz Biotechnology, and maleimide-biotin was obtained from Pierce Biotechnology. C16 and Δ^9-THC were synthesized as previously described (10).

1. Jordt SE, et al. (2004) Mustard oils and cannabinoids excite sensory nerve fibres through the TRP channel ANKTM1. *Nature* 427(6971):260–265.
2. Nordén K, et al. (2011) Increasing gene dosage greatly enhances recombinant expression of aquaporins in Pichia pastoris. *BMC Biotechnol* 11:47.
3. Törnroth-Horsefield S, et al. (2006) Structural mechanism of plant aquaporin gating. *Nature* 439(7077):688–694.
4. Xiao B, et al. (2008) Identification of transmembrane domain 5 as a critical molecular determinant of menthol sensitivity in mammalian TRPA1 channels. *J Neurosci* 28(39): 9640–9651.
5. Compton LA, Johnson WC, Jr (1986) Analysis of protein circular dichroism spectra for secondary structure using a simple matrix multiplication. *Anal Biochem* 155(1):155–167.
6. Gassmann O, et al. (2009) The M34A mutant of Connexin26 reveals active conductance states in pore-suspending membranes. *J Struct Biol* 168(1):168–176.
7. Kreir M, Farre C, Beckler M, George M, Fertig N (2008) Rapid screening of membrane protein activity: Electrophysiological analysis of OmpF reconstituted in proteoliposomes. *Lab Chip* 8(4):587–595.
8. Vyklický L, et al. (1999) Temperature coefficient of membrane currents induced by noxious heat in sensory neurones in the rat. *J Physiol* 517(Pt 1):181–192.
9. Voets T (2012) Quantifying and modeling the temperature-dependent gating of TRP channels. *Rev Physiol Biochem Pharmacol* 162:91–119.
10. Andersson DA, et al. (2011) TRPA1 mediates spinal antinociception induced by acetaminophen and the cannabinoid Δ(9)-tetrahydrocannabiorcol. *Nat Commun* 2:551.

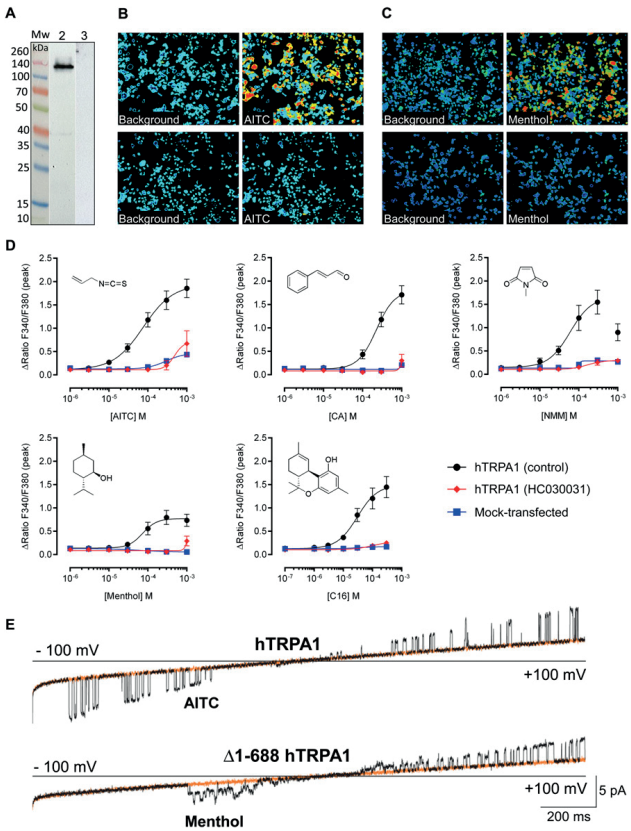

Fig. S1. The hTRPA1 with N-terminal decahistidine tag is functional in HEK293 cells. (*A*) hTRPA1 expression in HEK293 cells was visualized with TRPA1 antibody (lane 2) in Western blot. HEK293 cells transfected with empty plasmid (mock transfection) were used as negative controls (lane 3). (*B* and *C*) Pseudocolored images, representative of three separate experiments, show $[Ca^{2+}]_i$ in (*Upper*) hTRPA1-expressing HEK293 cells and (*Lower*) untransfected HEK293 cells before (background) and after exposure to (*B*) 100 μM AITC or (*C*) 500 μM menthol. (*D*) The TRPA1 agonists AITC, cinnamaldehyde (CA), NMM, menthol, and C16 all produced a concentration-dependent activation of hTRPA1 ($n = 8$) that was blocked by the TRPA1 antagonist HC030031 (100 μM; $n = 3$). The chemical structures of these TRPA1 activators are shown as *Insets*. HEK293 cells transfected with empty plasmid (mock transfection; $n = 3$–4) did not respond to the TRPA1 activators. Data are represented as means ± SEMs, and each experiment was performed in triplicate. (*E*) Purified hTRPA1 and Δ1–688 hTRPA1 are functional proteins (black traces) when inserted into planar lipid bilayers and exposed to the electrophilic activator AITC (100 μM) or the nonelectrophilic activator menthol (500 μM). Orange traces show baseline currents. Channel currents were recorded with the patch-clamp technique (2-s voltage ramps from −100 to +100 mV) in a symmetrical K^+ solution. Mw, molecular mass.

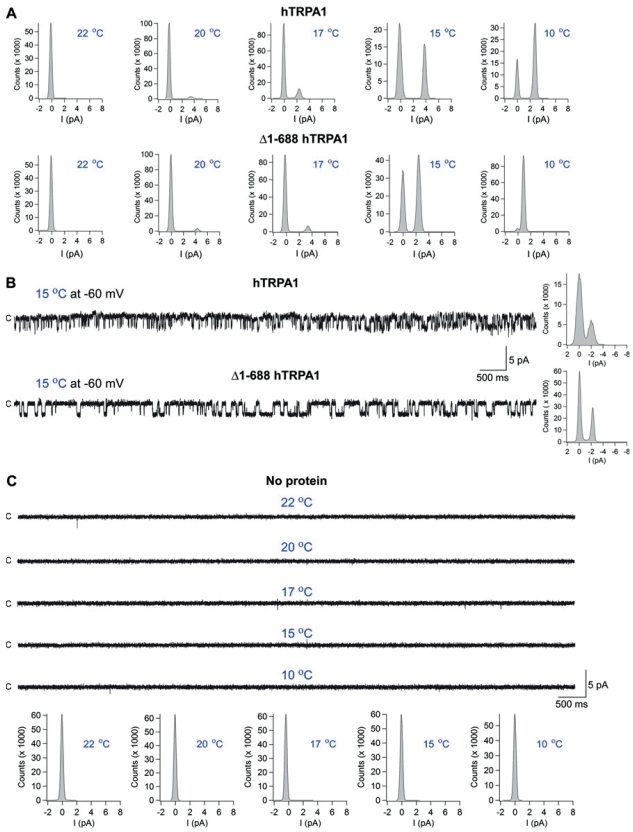

Fig. S2. (*A*) Amplitude histograms corresponding to representative traces in Fig. 2 showing activity of purified hTRPA1 and Δ1–688 hTRPA1 at various temperatures. (*B*) Traces and corresponding amplitude histograms for hTRPA1 and Δ1–688 hTRPA1 responding to cold at a test potential of –60 mV when inserted into planar lipid bilayers. (*C*) Lipid bilayers without hTRPA1 did not respond to cold at a test potential of +60 mV ($n = 6$). Single-channel currents were recorded with the patch-clamp technique in a symmetrical K^+ solution (downward deflection shows open-channel state, and c shows closed-channel state).

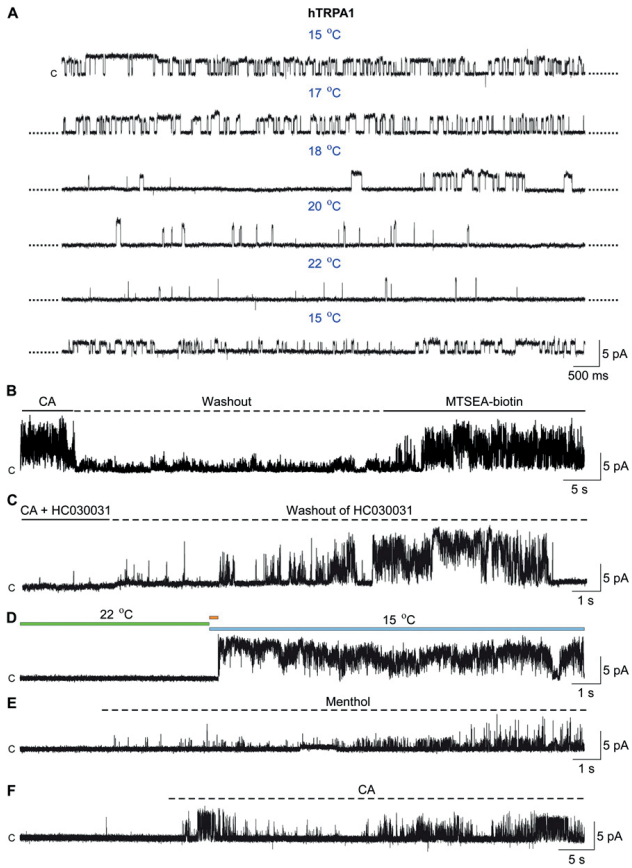

Fig. S3. Reversibility and onset of cold and ligand effects on hTRPA1. (*A*) hTRPA1 was continuously exposed to different temperatures, and its activity was reduced by increased temperatures but regained when returned to 15 °C (20 min total recording time). The G_u, but not P_o, decreased when hTRPA1 was repeatedly exposed to 15 °C. (*B* and *C*) The effect of the electrophilic TRPA1 activator cinnamaldehyde (CA; 100 μM) and the TRPA1 antagonist HC030031 (100 μM) was reversed on washout. Traces showing onset kinetics for the effects of (*B*) MTSEA-biotin (500 μM), (*D*) cold (blue bar indicates perfusion with a cold solution at 15 °C, and orange bar shows the 300-ms interval within which the temperature changed from 22 °C to 15 °C in the bath), (*E*) menthol (500 μM), and (*F*) CA (100 μM). (*E*) Open-channel sublevels were mainly observed at the early exposure to menthol. (*A*–*E*) Purified hTRPA1 and (*F*) hTRPA1 without the N-terminal ARD were inserted into planar lipid bilayers, and channel currents were recorded with the patch-clamp technique in a symmetrical K^+ solution at a test potential of +60 mV (upward deflection shows open-channel state, and c shows closed-channel state).

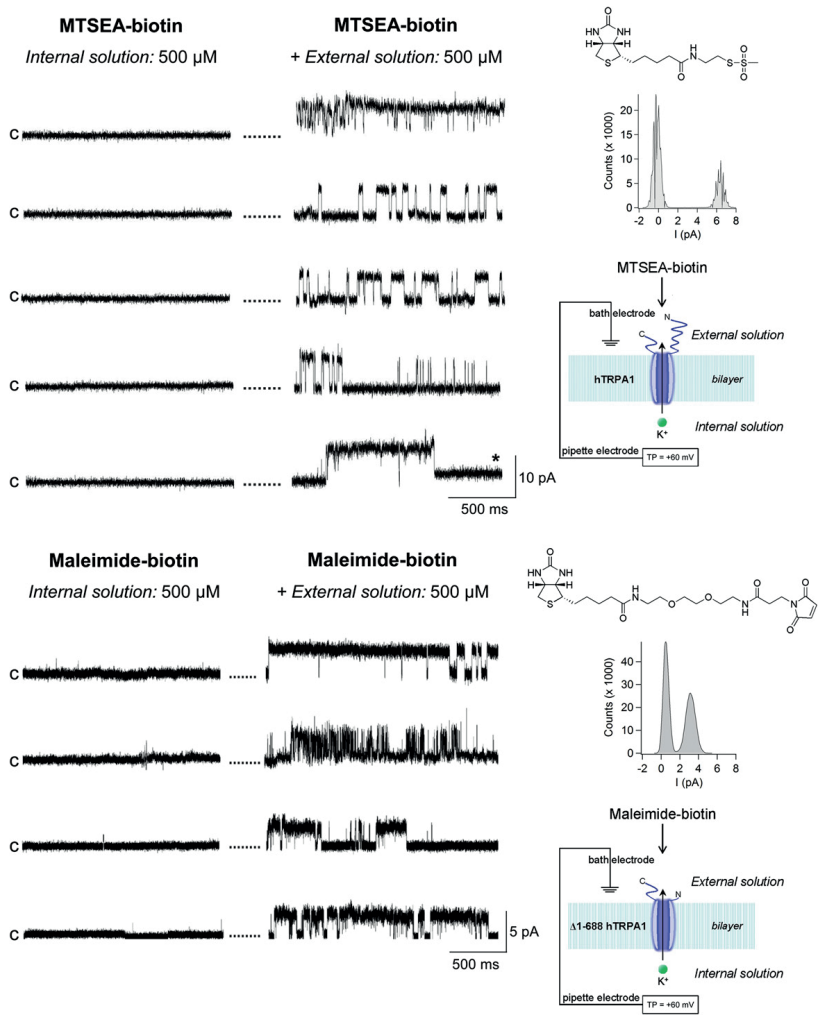

Fig. S4. hTRPA1 orientation in the lipid bilayer. The thiol oxidant MTSEA-biotin and the electrophilic biotinylated maleimide (maleimide-biotin) at 500 µM (0.1% dimethyl sulfoxide) activate hTRPA1 with and without (Δ1–688 hTRPA1) the N-terminal ARD, respectively, but only when applied in the external solution. Representative sequences of traces from individual experiments with internal (200 s) and consecutive external (400 s) exposure of the hydrophilic (bilayer-impermeable) thiol-reactive agents MTSEA-biotin and maleimide-biotin. The small single-channel current level (*) observed in the fifth MTSEA-biotin experiment disappeared within a few seconds. Shown are also representative histograms for each TRPA1 activator. Purified hTRPA1 proteins were inserted into planar lipid bilayers, and channel currents were recorded with the patch-clamp technique in a symmetrical K^+ solution at a test potential (TP) of +60 mV (upward deflection shows open-channel state, and c shows closed-channel state).

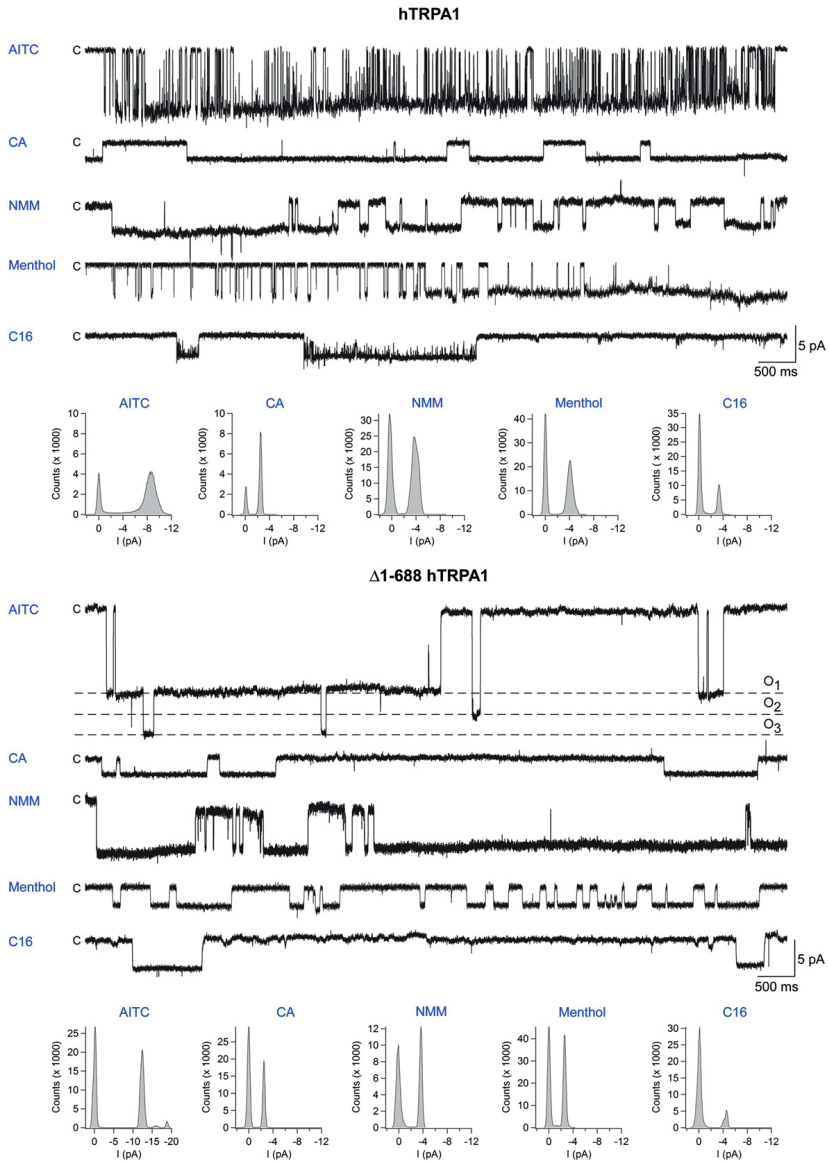

Fig. S5. Representative traces and corresponding histograms showing activity (downward deflection shows open-channel state, and c shows closed-channel state) of hTRPA1 and Δ1–688 hTRPA1 at a test potential of −60 mV when exposed to the electrophilic compounds AITC (100 μM), cinnamaldehyde (CA; 100 μM), and NMM (100 μM) and the nonelectrophilic compounds menthol (500 μM) and C16 (100 μM). Multiple distinct open-channel levels (dotted lines) were observed for AITC in Δ1–688 hTRPA1, of which the main level (O_1) was used for calculations of the G_s values presented in Fig. 4 and Table S1. Purified hTRPA1 and Δ1–688 hTRPA1 were inserted into planar lipid bilayers, and single-channel currents were recorded with the patch-clamp technique in a symmetrical K^+ solution.

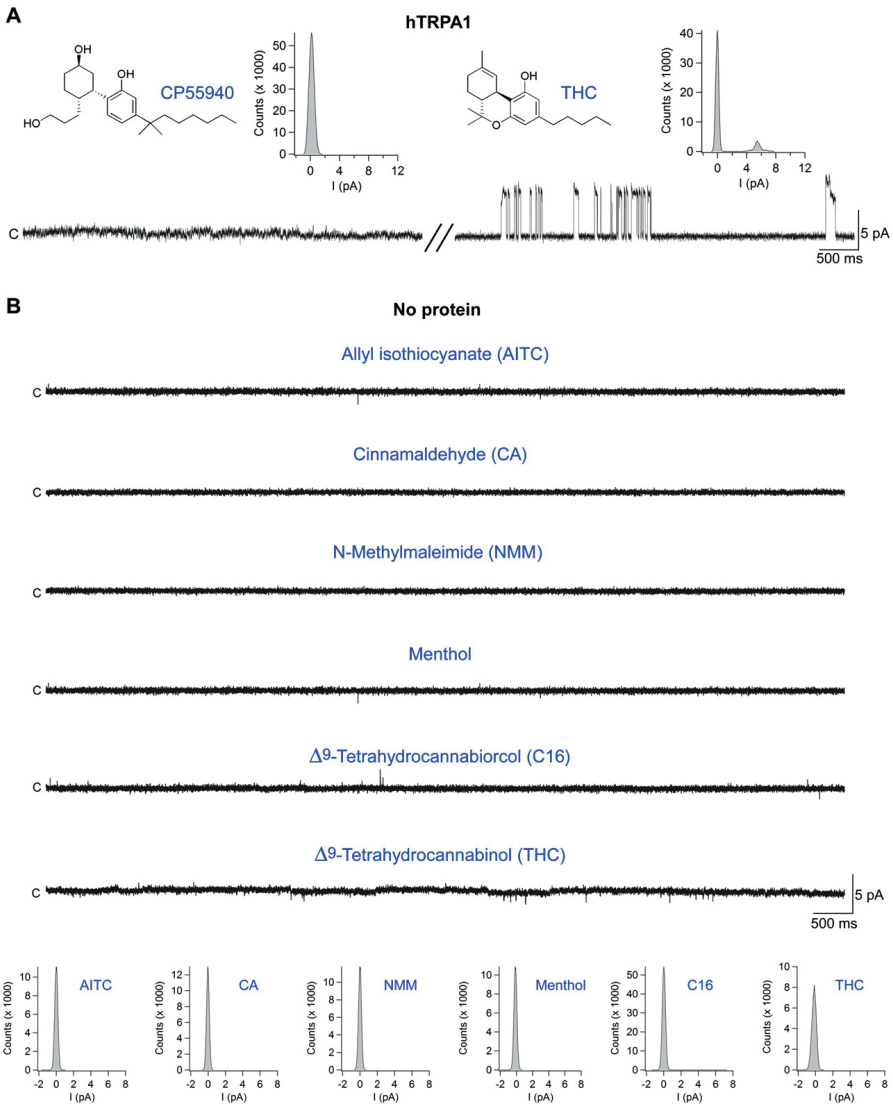

Fig. S6. (*A*) The lipophilic (log $P_{oct/water}$ = 6.16) and potent cannabinoid receptor agonist CP55940, which does not activate hTRPA1 when heterologously expressed in HEK293 cells (1), was without effect. The subsequent addition of the less lipophilic cannabinoid receptor agonist Δ^9-THC (log $P_{oct/water}$ = 5.53), an activator of TRPA1 (1–3), evoked hTRPA1 channel activity in the same bilayer preparation (n = 3). (*B*) Planar lipid bilayers without hTRPA1 did not respond to TRPA1 activators. Representative traces and corresponding amplitude histograms are shown (n = 3–5). Single-channel currents were recorded with the patch-clamp technique in a symmetrical K^+ solution at a test potential of +60 mV (upward deflection shows open-channel state, and c shows closed-channel state). CA, cinnamaldehyde.

1. Andersson DA, et al. (2011) TRPA1 mediates spinal antinociception induced by acetaminophen and the cannabinoid Δ(9)-tetrahydrocannabiorcol. *Nat Commun* 2:551.
2. Jordt SE, et al. (2004) Mustard oils and cannabinoids excite sensory nerve fibres through the TRP channel ANKTM1. *Nature* 427(6971):260–265.
3. Kim D, Cavanaugh EJ, Simkin D (2008) Inhibition of transient receptor potential A1 channel by phosphatidylinositol-4,5-bisphosphate. *Am J Physiol Cell Physiol* 295(1):C92–C99.

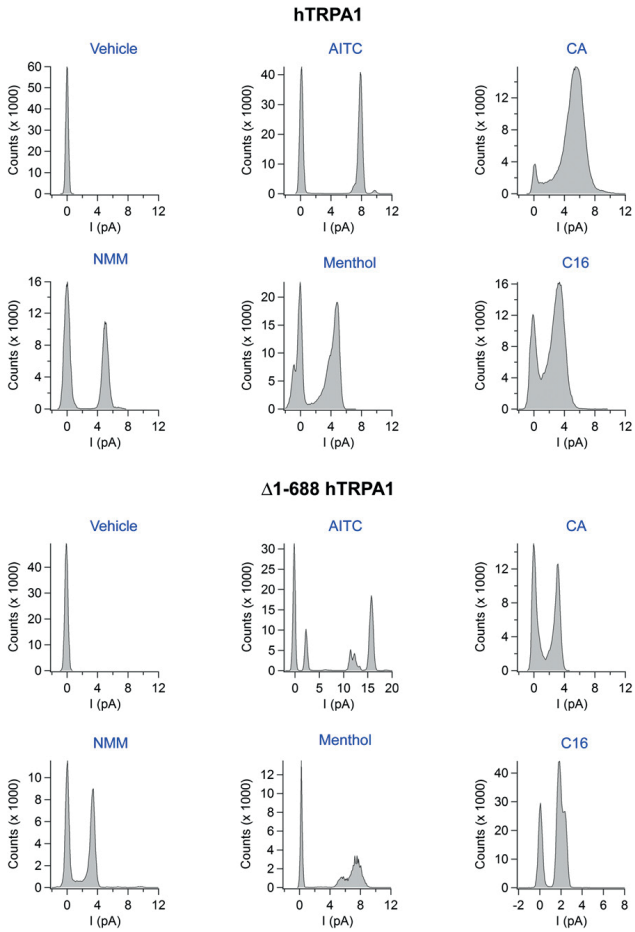

Fig. S7. Histograms corresponding to traces shown in Fig. 3*A* [vehicle, AITC, cinnamaldehyde (CA), NMM, and C16] and Fig. 5*A* (menthol) for hTRPA1 and Δ1–688 hTRPA1 at a test potential of +60 mV.

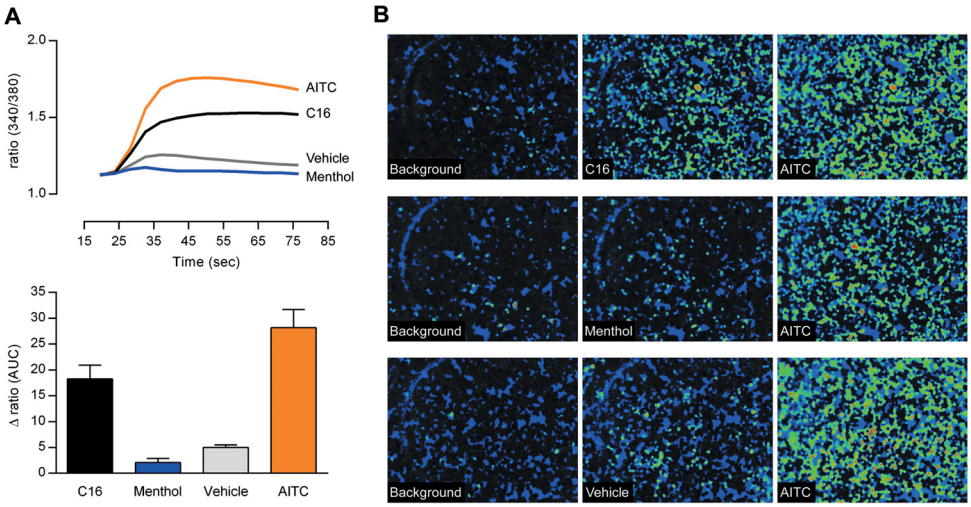

Fig. S8. C16 and menthol activate hTRPA1 at different binding sites. Both C16 and menthol are nonelectrophilic compounds. Specific residues (Ser-873 and Thr-874) in the transmembrane segment 5 are required for menthol sensitivity of hTRPA1 (1). Here, we tested C16 on dTM5–hTRPA1, a menthol-insensitive chimera between *Drosophila melanogaster* (dTM5) and hTRPA1 (1). Menthol was inactive, as previously shown (1), whereas C16 still activated the channel, indicating that menthol and C16 interact at different sites on hTRPA1. (*A*) Traces show average calcium responses to AITC (0.1 mM), C16 (0.1 mM), and menthol (1 mM) at concentrations that produce maximal activation of hTRPA1 (1, 2) and vehicle (ethanol at 0.1%). Bar graph shows responses given as area under the curve (AUC) for the recording time period displayed by traces ($n = 5$). Data are represented as means ± SEMs, and each experiment was performed in triplicates. (*B*) Pseudocolored images show $[Ca^{2+}]_i$ in hTRPA1–dTM5 expressing HEK293 cells before (background) and after exposure to C16, menthol, or vehicle. All cells were finally exposed to AITC.

1. Xiao B, et al. (2008) Identification of transmembrane domain 5 as a critical molecular determinant of menthol sensitivity in mammalian TRPA1 channels. *J Neurosci* 28(39):9640–9651.
2. Andersson DA, et al. (2011) TRPA1 mediates spinal antinociception induced by acetaminophen and the cannabinoid Δ(9)-tetrahydrocannabiorcol. *Nat Commun* 2:551.

Table S1. G_s and P_o values for hTRPA1 and Δ1–688 hTRPA1 activated by chemical compounds and cold

	hTRPA1		Δ1–688 hTRPA1		hTRPA1		Δ1–688 hTRPA1	
Stimuli and voltage (mV)	G_s (pS) mean ± SEM	*n*	G_s (pS) mean ± SEM	*n*	P_o mean ± SEM	*n*	P_o mean ± SEM	*n*
AITC								
+60	127 ± 17	5	275 ± 28	4	0.50 ± 0.01	4	0.75 ± 0.04	4
−60	161 ± 18	4	186 ± 7	4	0.71 ± 0.02	4	0.68 ± 0.04	4
Cinnamaldehyde								
+60	118 ± 8	7	92 ± 21	3	0.70 ± 0.06	7	0.49 ± 0.03	3
−60	47 ± 2	7	59 ± 7	3	0.75 ± 0.08	4	0.45 ± 0.03	3
NMM								
+60	97 ± 3	6	51 ± 4	6	0.48 ± 0.06	6	0.50 ± 0.03	6
−60	75 ± 0	4	77 ± 3	3	0.74 ± 0.06	4	0.52 ± 0.05	3
Menthol								
+60	74 ± 3	7	142 ± 6	4	0.60 ± 0.03	8	0.31 ± 0.02	4
−60	61 ± 3	6	49 ± 7	3	0.40 ± 0.03	5	0.50 ± 0.02	4
C16								
+60	48 ± 4	7	30 ± 2	4	0.58 ± 0.03	5	0.72 ± 0.04	4
−60	53 ± 1	4	65 ± 6	3	0.41 ± 0.01	5	0.14 ± 0.03	3
20 °C								
+60	46 ± 14	3	68 ± 17	3	0.01 ± 0.00	5	0.02 ± 0.02	3
17 °C								
+60	35 ± 10	4	54 ± 10	4	0.26 ± 0.03	4	0.22 ± 0.04	4
15 °C								
+60	65 ± 2	6	41 ± 6	11	0.30 ± 0.02	8	0.62 ± 0.04	10
10 °C								
+60	50 ± 4	4	15 ± 3	4	0.69 ± 0.07	4	0.93 ± 0.02	4

Paper II

Human TRPA1 is a heat sensor displaying intrinsic U-shaped thermosensitivity

Lavanya Moparthi[1], Tatjana I. Kichko[2], Mirjam Eberhardt[3], Per Kjellbom[1], Urban Johanson[1], Peter W. Reeh[2], Andreas Leffler[3], Milos R. Filipovic[4,5] and Peter M. Zygmunt[6]

[1]Department of Biochemistry and Structural Biology, Center for Molecular Protein Science, Lund University, SE-221 00 Lund, Sweden.

[2]Institute of Physiology and Pathophysiology, Friedrich-Alexander University Erlangen-Nürnberg, Universitätsstrasse 17, 91054 Erlangen, Germany.

[3]Department of Anesthesiology and Intensive Care, Hannover Medical School, Carl-Neuberg-Strasse 1, 30625 Hannover, Germany.

[4]Department of Chemistry and Pharmacy, Friedrich-Alexander University Erlangen-Nuremberg, Egerlandstrasse 1, 91058 Erlangen, Germany.

[5]IBGC, UMR 5095, Universite de Bordeaux, 1, rue Camille Saint Saëns, CS 61390, 33077 Bordeaux cedex, France.

[6]Clinical Chemistry and Pharmacology, Department of Laboratory Medicine, Lund University, SE-221 85 Lund, Sweden.

Correspondence: peter.zygmunt@med.lu.se

Abstract

Thermosensitive Transient Receptor Potential (TRP) channels respond to either cold or heat. In the case of TRP subtype A1 (TRPA1), it is believed that non-mammalian TRPA1 is heat-sensitive whereas mammalian TRPA1 is sensitive to cold. Here we show that redox modification and ligands affect human TRPA1 (hTRPA1) cold and heat sensing properties in lipid bilayer and whole-cell patch-clamp recordings as well as heat-evoked TRPA1-dependent calcitonin gene-related peptide (CGRP) release from mouse trachea. Studies of purified hTRPA1 intrinsic tryptophan fluorescence, in the absence of lipid bilayer, consolidate hTRPA1 as an intrinsic thermosensor that is modified by the redox state and ligands. The heat sensing property of TRPA1 is conserved in mammalians, in which TRPA1 may contribute to sensing warmth and uncomfortable heat in addition to noxious cold.

Introduction

The discovery of TRP ion channels as molecular thermosensors has opened up new avenues for understanding how organisms monitor and adapt to environmental temperature. In contrast to the role of TRPA1 as a heat sensor in non-mammalian species, the temperature-sensitivity of mammalian TRPA1 and its role in thermosensation has been debated ever since TRPA1 was proposed as a noxious cold sensor in the mouse sensory nervous system[1]. We have recently shown that the purified hTRPA1 is intrinsically sensitive to noxious cold when inserted into lipid bilayers and studied with the patch-clamp technique[2], adding direct evidence to the many studies suggesting that mammalian TRPA1 plays a role in noxious cold sensation[3]. There is, however, no evidence that TRPA1 itself is a heat sensor in mammalians, although it seems involved in TRPV1-dependent heat detection[4,5]. It has been speculated that thermosensitive TRP channels are capable of sensing both cold and heat, but experimental evidence is lacking to support such a U-shaped TRP channel thermosensitivity [6-9]. Here we show that TRPA1 heat sensitivity is conserved in mammalians and for the first time provide evidence of TRP channel inherent U-shaped thermosensitivity.

Results and discussion

The purified hTRPA1 inserted into lipid-bilayers responded with single-channel activity when exposed to increasing warm temperatures from 22 °C to 40 °C, and as previously reported[2] to noxious cold (**Fig. 1**, **Supplementary Fig. 1** and **Supplementary Table 1**). Based on the single-channel mean open probability (Po) (**Fig. 1b**), we calculated a Q10 value of 6 from the Arrhenius plot (25 °C to 35 °C), which is close to the Q10 value 7.5 of the heterologously expressed TRPM3, a recently identified heat detector present in capsaicin-sensitive primary afferents[10]. At 40 °C, there was still substantial channel activity although Po decreased, suggesting channel gating desensitization (**Fig. 1b**). The single-channel mean conductance (Gs) did not increase with increasing temperatures (**Supplementary Table 1**), suggesting that the TRPA1 channel pore is negatively affected by heat. As shown at 30 °C, hTRPA1 channel currents were observed at both positive and negative test potentials (**Fig. 1c** and **Supplementary Fig. 1**), and the non-selective TRP channel pore blocker ruthenium red and the selective TRPA1 antagonist HC030031 inhibited temperature responses (**Fig. 1d**) without affecting bilayers

(**Supplementary Fig. 2**). No currents were detected in bilayers without hTRPA1 when exposed to the same test temperatures (**Supplementary Fig. 3**).

Because TRPA1 with its many cysteines is highly sensitive to thiol reactive agents including oxidants[3], we asked if changes in redox state could affect the temperature sensitivity of hTRPA1, possibly explaining the many contradictory findings on mammalian TRPA1 and cold[3] as well as the lack of mammalian TRPA1 heat responses in heterologous expression systems[11-13]. As shown by the Cy3-dye disulphide labeling assay, which has been used to study TRPA1 disulphide bond formation[14], the purified hTRPA1 used for the bilayer patch-clamp recordings was partially oxidized, a condition that could be rectified by the thiol reducing agent dithiothreitol (DTT) and further oxidized by H_2O_2 (**Fig. 2a**). The consequences of changes in cysteine redox state for hTRPA1 channel activity are shown in **Fig. 2b-d**, where the reducing agents DTT and Tris (2-carboxy ethyl)phosphine (TCEP) inhibited cold and heat responses, and H_2O_2 evoked hTRPA1 channel activity at 22 °C that was blocked by TCEP. Furthermore, H_2O_2 decreased hTRPA1 channel activity triggered by 30 °C, and increased cold responses at 15 °C (**Fig. 2c** and **d**), also indicating different conformational states behind hTRPA1 heat and cold responses. Bilayers without hTRPA1 were unaffected by DTT, TCEP and H_2O_2 (**Supplementary Fig. 2**). As TRPA1 is a potential mechanosensor[15], possibly indirectly affected by mechanical forces within the lipid bilayer due to temperature changes, we used the tryptophan fluorescence assay to study lipid bilayer-independent conformational changes of hTRPA1 when exposed to cold and warm temperatures, and also when treated with either DTT or H_2O_2 (**Fig. 2e**). Both cold and warm temperatures evoked changes in tryptophan fluorescence, supporting that hTRPA1 is intrinsically cold- and heat-sensitive. The changes in tryptophan fluorescence were inhibited by reducing agents and enhanced by H_2O_2 pre-treatment. Notably, the hump on fluorescence traces at lower emission wavelengths for hTRPA1 when exposed to warm temperatures was less pronounced at cold temperatures (**Fig. 2e**), once again indicating that different hTRPA1 channel conformations are involved in its cold and heat sensation. Taken together, partial oxidation seems to favor both cold- and heat-evoked hTRPA1 channel activity.

In line with reports questioning hTRPA1 being a cold sensor[11,16-18], we could not observe cold-induced hTRPA1 currents in HEK293t cells, using external Ca^{2+}-free conditions to avoid rapid desensitization of hTRPA1, whereas the non-electrophilic TRPA1 activator carvacrol produced robust hTRPA1 currents at 25 °C, confirming that the channel was functionally expressed (**Supplementary Fig.**

4a). However, pre-exposure of hTRPA1 to H_2O_2 or acrolein at threshold concentrations triggered cold-evoked currents (**Fig. 3e** and **g,** and **Supplementary Fig. 4b**). Likewise, allyl isothiocyanate disclosed the cold-sensitivity of hTRPA1 (**Supplementary Fig. 4c**), which is in accordance with the finding that it potentiated rat TRPA1 cold responses[19]. A similar approach with carvacrol also sensitized hTRPA1 to cold, but only after having been exposed to heat (**Fig. 3f**), indicating that non-thiol reactive TRPA1 modulators can produce additional conformational changes of hTRPA1 allowing it to respond to changes in temperature. Indeed, the tryptophan fluorescence assay disclosed substantial hTRPA1 conformational changes to cold as well as heat when exposed to carvacrol (**Supplementary Fig.5**). In contrast to cold, heat alone evoked hTRPA1 currents, which were reduced at 40 °C (**Fig. 3a**-**c**, **g**). At 35 °C the heat-induced currents were not different from those at 25 °C in the presence of H_2O_2, but not acrolein and carvacrol (see **Supplementary Fig.6**), suggesting that heat responses were partially redox sensitive (**Fig. 3d** and **g**). Using the mouse trachea to study TRPA1 in its native environment, we observed a robust TRPA1 but not TRPV1-dependent CGRP release upon warming (to 36 °C) under oxidative stress, achieved by combining H_2O_2 and NaOCl to produce singlet oxygen[20] (**Fig. 4** and **Supplementary Fig. 7**). A small but significant TRPA1-mediated CGRP release was also detected in the absence of chemical oxidation. Thus, the mouse TRPA1 is not only sensitive to heat after single point mutations within its N-terminal ARD[13], but also in its native environment depending on the cellular redox state and without the influence of TRPV1. Increasing the temperature to 40 °C caused a smaller TRPA1/TRPV1-independent CGRP release (**Fig. 4a**) in line with the reduced hTRPA1 activity observed at 40 °C in the bilayer and whole-cell patch clamp recordings (**Figs. 1b** and **3c**).

Our findings show that the TRPA1 heat-sensitivity is conserved in mammalians and that its U-shaped thermosensitivity is influenced by redox state and ligands. Further studies of purified hTRPA1 may help to unravel the molecular mechanisms linking both cold and warm temperatures to channel gating in TRP and other ion channels.

Material and methods

Recording of hTRPA1 activity in planar lipid bilayers

The expression and purification of hTRPA1 was performed as described previously[2]. Detergent purified hTRPA1 were reconstituted either into preformed planar bilayers, or giant unilamellar vesicles (GUVs)[2]. Briefly, planar lipid bilayers were formed by pipetting 5 µl of either empty GUVs or protein reconstituted into GUVs on patch-clamp chips (1-2 µm, 3.5-5 MΩ resistance) which were mounted on a recording chamber. Following giga Ohm seal formation, single channel activity was recorded using the Port-a-Patch (Nanion Technologies) at both positive and negative test potentials in a symmetrical K^+ solution adjusted to pH 7.2 with KOH and containing (in mM): 50 KCl, 10 NaCl, 60 KF, 20 EGTA, and 10 HEPES. The patch-clamp experiments were performed at various temperatures, for which the Port-a-Patch was equipped with an external perfusion system (Nanion Technologies) and an SC-20 dual in-line solution cooler/heater connected to a temperature controlled (CL-100) liquid cooling system (Warner Instruments). Signals were acquired with an EPC 10 amplifier (HEKA) and the data acquisition software Patchmaster (HEKA) at a sampling rate of 50 kHz. The recorded data were digitally filtered at 3 kHz. Electrophysiological data were analysed using Clampfit 9 (Molecular Devices) and Igor Pro (Wave Metrics software). Data were filtered at 1,000 and 500 Hz low-pass Gaussian filter for analysis and traces, respectively. The single-channel mean conductance (Gs) was obtained from a Gaussian fit of all-points amplitude histograms. The single-channel mean open probability (Po) was calculated from time constant values, which were obtained from exponential standard fits of dwell time histograms. The Q10 values were obtained from the slope of regression line fitted to the Arrhenius plot[21,22].

Cy3 dye labelling of protein disulphides using modified biotin-switch

Purified hTRPA1 was treated with 0.1 mM H_2O_2 or 1 mM DTT for 30 min at 37 °C. Protein was precipitated with chloroform/methanol/water (1/4/4), dried under argon and re-suspended in PBS containing 1.5 % SDS. Free thiols were blocked with N-ethyl maleimide (1 mM, 1 h at 37 °C) and oxidized cysteines reduced with 10 mM DTT (1 h at 37 °C) in the following step. Protein was again precipitated using chloroform/methanol/water protocol and re-suspended in PBS

containing 1.5 % SDS and 0.1 mM Cy3-maleimide. Samples were incubated 1 h at 37 °C, resolved in 10 % SDS electrophoresis and visualized by ChemiDoc (BioRad) imaging system.

Intrinsic tryptophan fluorescence assay

Conformational changes in hTRPA1 were recorded on FP-8200 spectrofluorometer (Jasco, Germany) with thermostat unit. Protein was incubated at each desired temperature for 15 min and emission spectra recorded using excitation wavelength of 280 nm. For H2O2 treatments, in order to achieve the maximal thiol oxidation, the protein was mixed with H2O2 and left overnight and the spectra recorded the following day. Cold and heat experiments were done in separate experiments and for better presentation the spectra are always normalized to the starting spectrum at room temperature. DTT and carvacrol treatments were performed prior the measurements and samples incubated for 1 h to achieve stable modification.

Whole-cell patch clamp recordings

HEK293 were cultured in standard DMEM (D-MEM, Gibco, BRL Life Technologies, Karlsruhe Germany) with 10 % FBS (Biochrom, Berlin Germany), 100 U/ml penicillin and 100 µg/ml streptomycin (Gibco, Karlsruhe, Germany) and 2 mM Glutamax (Gibco, Karlsruhe Germany). They were transfected with plasmids of hTRPA1 and eGFP to visualize transfected cells using jetPEI transfection reagent according to the instructions of the manufacturer (Polyplus-Transfection, France). Cells were split into 35 mm dishes, cultured at 37 °C and 5 % CO_2 and patch clamped 24 to 48 h after transfection. For some experiments naïve HEK 293t cells were used as a control.

Voltage-clamp patch clamp experiments were carried out with a HEKA Electronics USB 10 amplifier and the Patchmaster Software (HEKA Electronics, Lambrecht, Germany) installed on a conventional PC. Borosilicate pipettes with a resistance of 1-2 MΩ were filled with a pipette solution containing [mM]: KCl 140, $MgCl_2$ 2, EGTA 5, HEPES 10 with pH adjusted to 7.4 by KOH. Standard calcium free extracellular solution contained in [mM]: NaCl 140, KCl 5, $MgCl_2$ 2, EGTA 5, HEPES 10 and glucose 10. pH 7.4 was adjusted by TMA-OH. For TRP channel mediated membrane currents, data were sampled at 10 kHz and filtered at 2 kHz. Cells were either constantly held at a membrane potential of -60 mV or 500 ms long voltage ramps from -100 to + 100 mV were applied repetitively.

All substances were applied by a gravity-driven perfusion system allowing a focal application of the test solution within a distance of < 100 µm from the cell. Temperature of the applied test solutions was controlled with a perfusion system incorporating a rapid-feedback temperature control allowing rapid heating or cooling[23]. The Patchmaster software (HEKA Elektronik) was used to pass current to an insulated copper wire coiled around the capillary tip of the outlet of the perfusion system. Test solutions were precooled by ice cold water, and for application of cold stimuli the continuous current necessary to warm solutions to room temperature was reduced. Heat stimuli were applied by increasing current to the coiled wire at the capillary tip. The temperature of the test solution was constantly measured using a miniature thermocouple fixed at the orifice of the capillary tip. The Patchmaster/Fitmaster software (HEKA Elektronik) was used for acquisition of temperature and current data and for off-line analysis.

Calcitonin gene-related peptide release

Animals: The experiments were carried out in accordance with the guidelines of the International Association for the Study of Pain[24]. Adult C57BL/6, TRPV1-/- and TRPA1-/- mice were used. Breeding pairs of heterozygous TRPV1 and TRPA1 mutants were obtained from Dr. John Davis[25] and Dr. David Corey[26] and continuously backcrossed to C57BL/6. The mice were housed in group cages in a temperature-controlled environment on a 12 h light/dark cycle and were supplied with water and food ad libitum. Mice of either sex (body weight 15 – 25 g) were sacrificed by exposure to a rising CO_2 concentration (approved by the Animal Protection Authority, District Government of Mittelfranken, Ansbach, Germany).

Trachea preparation and incubation: The trachea was excised together with the two main bronchi and hemisected along the sagittal midline. One half of the bronchotracheal preparation was used as control and the other half for experimental treatments (here oxidant pretreatment), taking advantage of the lesser intraindividual than interindividual variability of CGRP release. The preparations were first placed for 30 min at 37 °C in carbogen-gassed (95 % O_2, 5 % CO_2, obtaining pH 7.4) synthetic interstitial fluid (SIF) containing (in mM) 107.8 NaCl, 3.5 KCl, 1.53 $CaCl_2$, 0.69 $MgSO_4$, 26.2 $NaHCO_3$, 1.67 NaH_2PO_4, 9.64 sodium gluconate. After the initial rest period, the isolated trachea was consecutively incubated for 5 min in each of four test tubes containing 125 µl SIF and mounted in a shaking bath at 22 °C. The first incubation was to determine basal CGRP release, the second through fourth tube did or did not contain the two oxidants NaOCl and H_2O_2 (both 30 µM) diluted in SIF. However, the fourth

tube was placed in a shaking bath at either 36 ° or 40 °C to stimulate the tracheal nerve endings. The fifth incubation was again in SIF at 22 °C to determine the recovery from stimulation. To establish the concentration-response relationship of CGRP release evoked by NaOCl+H_2O_2, four incubations of trachea preparations were performed at constant 37 °C, the third one containing both oxidants at various equimolar concentrations or, for control, either NaOCl or H_2O_2 at 100 μM concentration.

To apply the oxidants, concentrated stock solutions of NaOCl and H_2O_2 were freshly prepared and minute volumes were synchronously pipetted into the incubation fluid as soon as the trachea preparation was immersed.

CGRP enzyme immunoassay (EIA): The CGRP content of the incubation fluid was measured using commercial enzyme immunoassay (EIA) kits with a detection threshold of 5 pg/ml (Bertin Pharma, Montigny-le-Bretonneux, France). For this purpose 100 μl sample fluid were stored on ice and mixed, immediately following the incubation, with 25 μl of fivefold-concentrated commercial CGRP-EIA buffer (Bertin) that contained a proprietary cocktail of peptidase inhibitors. The CGRP-EIA procedures were run after the end of the experiment; the antibody reactions took place overnight. The EIA plates were determined photometrically using a microplate reader (Dynatech, Channel Islands, UK). All results are processed as measured by the EIA in pg CGRP/ml SIF. Reducing interindividual variability and day-to-day baseline variability, the data were referred to the third (or second) individual baseline value (before stimulation). This value was subtracted from all five (or four) data points of a typical experiment so that only the absolute change in CGRP release (Δ pg/ml) is displayed in the figures.

Statistical analysis: Statistical comparisons were performed using Statistica 7 software (Statsoft, Tulsa, USA). All time series of experimental values were first analyzed for the effect of stimulation as compared to baseline using the nonparametric Wilcoxon matched pairs test. The baseline-corrected (i.e., Δ pg/ml) CGRP values were entered into a one-way analysis of variance (ANOVA) followed by Tukey least significant difference (HSD) test, focusing on the peak values of stimulated CGRP release. $P < 0.05$ was considered statistically significant. Data points represent means ± s.e.m. of the given number (n) of experiments.

References

1. Story, G.M.*, et al. Cell* **112**, 819-829 (2003).
2. Moparthi, L.*, et al. Proc Natl Acad Sci U S A* **111**, 16901-16906 (2014).
3. Zygmunt, P.M. & Högestätt, E.D. *Handb Exp Pharmacol* **222**, 583-630 (2014).
4. Bautista, D.M.*, et al. Cell* **124**, 1269-1282 (2006).
5. Hoffmann, T.*, et al. Eur J Pain* **17**, 1472-1482 (2013).
6. Baez, D., Raddatz, N., Ferreira, G., Gonzalez, C. & Latorre, R. *Curr Top Membr* **74**, 51-87 (2014).
7. Clapham, D.E. & Miller, C. *Proc Natl Acad Sci U S A* **108**, 19492-19497 (2011).
8. Laursen, W.J., Anderson, E.O., Hoffstaetter, L.J., Bagriantsev, S.N. & Gracheva, E.O. *Temperature* (2015).
9. Vriens, J., Nilius, B. & Voets, T. *Nat Rev Neurosci* **15**, 573-589 (2014).
10. Vriens, J.*, et al. Neuron* **70**, 482-494 (2011).
11. Cordero-Morales, J.F., Gracheva, E.O. & Julius, D. *Proc Natl Acad Sci U S A* **108**, E1184-1191 (2011).
12. Wang, S., Lee, J., Ro, J.Y. & Chung, M.K. *Mol Pain* **8**, 22 (2012).
13. Jabba, S.*, et al. Neuron* **82**, 1017-1031 (2014).
14. Eberhardt, M.*, et al. Nat Commun* **5**, 4381 (2014).
15. Ranade, S.S., Syeda, R. & Patapoutian, A. *Neuron* **87**, 1162-1179 (2015).
16. Chen, J.*, et al. Nat Commun* **4**, 2501 (2013).
17. Jordt, S.E.*, et al. Nature* **427**, 260-265 (2004).
18. Zurborg, S., Yurgionas, B., Jira, J.A., Caspani, O. & Heppenstall, P.A. *Nat Neurosci* **10**, 277-279 (2007).
19. del Camino, D.*, et al. J Neurosci* **30**, 15165-15174 (2010).
20. Greer, A. *Acc Chem Res* **39**, 797-804 (2006).
21. Voets, T. *Rev Physiol Biochem Pharmacol* **162**, 91-119 (2012).
22. Vyklicky, L.*, et al. J Physiol* **517 (Pt 1)**, 181-192 (1999).
23. Dittert, I.*, et al. J Neurosci Methods* **151**, 178-185 (2006).
24. Zimmermann, M. *Pain* **16**, 109-110 (1983).
25. Davis, J.B.*, et al. Nature* **405**, 183-187. (2000).
26. Kwan, K.Y.*, et al. Neuron* **50**, 277-289 (2006).

Acknowledgements

This work was supported by the Swedish Research Council (2014-3801), the Medical Faculty at Lund University and the Research School of Pharmaceutical Sciences (FLÄK) at Lund University. M.R.F., T.I.K. and P.W.R. were supported by intramural funds provided by the University of Erlangen within an Emerging Field Initiative (Medicinal Redox Inorganic Chemistry) and by the Sander-Stiftung (#2014.068.1). Susanne Haux-Oertel provided valuable technical assistance.

Author contributions

P.M.Z. developed the concept, designed and directed the study, analyzed data and wrote the paper. L.M. conducted and analyzed bilayer patch-clamp experiments, designed the study, analyzed data and wrote the paper. M.R.F. conducted and analyzed biochemical studies. M.E. and A.L. conducted and analyzed whole cell patch-clamp studies. T.I.K. and P.W.R. conducted and analyzed CGRP release studies. U.J. and P.K. contributed with financial support of L.M. and purification of hTRPA1. All authors discussed the results and commented on the manuscript.

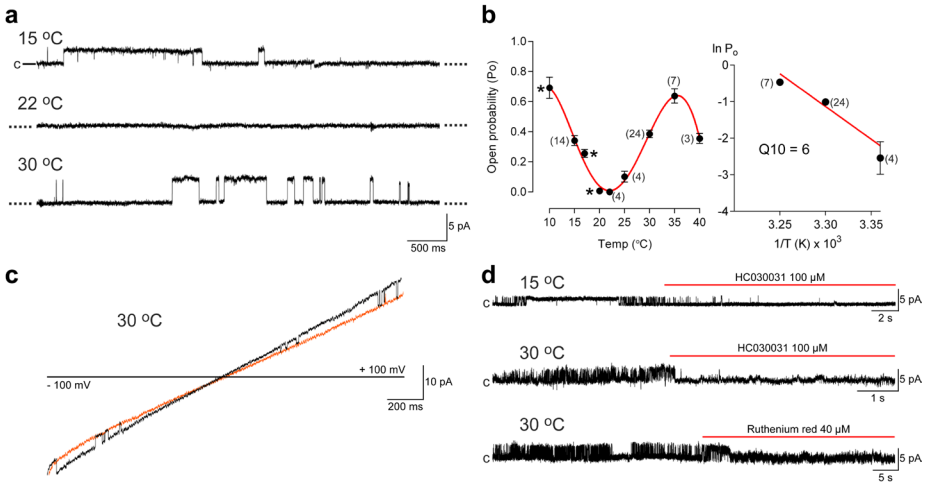

Figure 1 The purified hTRPA1 displays intrinsic U-shaped thermosensitivity. (**a**). Traces are part of a continuous recording (13 min) of hTRPA1 single channel currents at various temperatures at a test potential of +60 mV. (**b**) Left graph shows single-channel open probability values at different temperatures. Data points marked by asterisk were published previously[2]. Right graph shows Arrhenius plot for the heat responses (25, 30 and 35 °C). Data are represented as mean ± s.e.m. (numbers of experiments within parentheses). (**c**) Black trace shows hTRPA1 channel openings when separated from orange trace (baseline current) at both negative and positive test potentials (2-s voltage ramps from -100 to +100 mV). (**d**) The selective TRPA1 antagonist HC030031 and the non-selective TRP channel pore blocker ruthenium red inhibited cold and heat hTRPA1 responses at a test potential of +60 mV (n = 3). Purified hTRPA1 was inserted into planar lipid bilayers and channel currents were recorded with the patch-clamp technique in a symmetrical K^+ solution (c indicates the closed channel state).

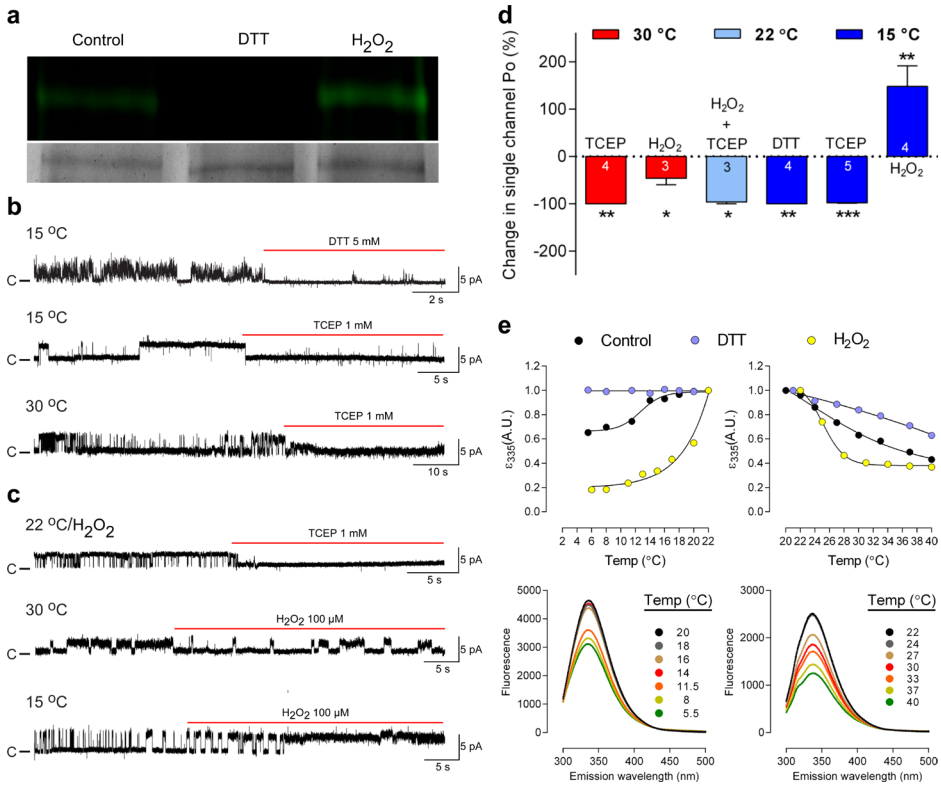

Figure 2 Redox modification influences the responsiveness of purified hTRPA1 to cold and heat. (**a**) The Cy3-dye disulphide labeling fluorescence assay (top gel) revealed that the purified hTRPA1 used for functional studies was partially oxidized (control) as the reducing (DTT) and oxidizing (H_2O_2) agents abolished and increased the disulphide bond formation, respectively. Coomassie blue staining (bottom gel) shows the amount of protein used for analysis of respective treatment. (**b**) Cold and heat responses of hTRPA1 were abolished by DTT and TCEP. (**c**) H_2O_2 activated hTRPA1 at 22 °C (see also **Supplementary Table 1**) and the activity was abolished with TCEP. Notably, H_2O_2 blocked heat and increased cold responses. Purified hTRPA1 was inserted into planar lipid bilayers and channel currents were recorded with the patch-clamp technique in a symmetrical K^+ solution (c indicates the closed channel state). (**d**) The effect of the reducing (DTT and TCEP) and oxidizing (H_2O_2) agents on hTRPA1 single channel open probability (Po) as examined at 30 °C, 22 °C and 15 °C at a test potential of +60 mV. Data are represented as mean ± s.e.m. of paired comparisons before and after treatment (numbers of experiments are shown within bars). *P<0.05, **P<0.01 and ***P<0.001 indicate statistically significant differences using the Student's paired t test. (**e**) As shown by analysis of Trp fluorescence, cold and heat produced lipid bilayer-independent conformational changes of hTRPA1 (control) that were potentiated and inhibited by H_2O_2 (100 µM) and DTT (500 µM), respectively (n = 3). Emission at 335 nm normalized to 22 °C. Data are represented as mean ± s.e.m. Spectra of control is shown below.

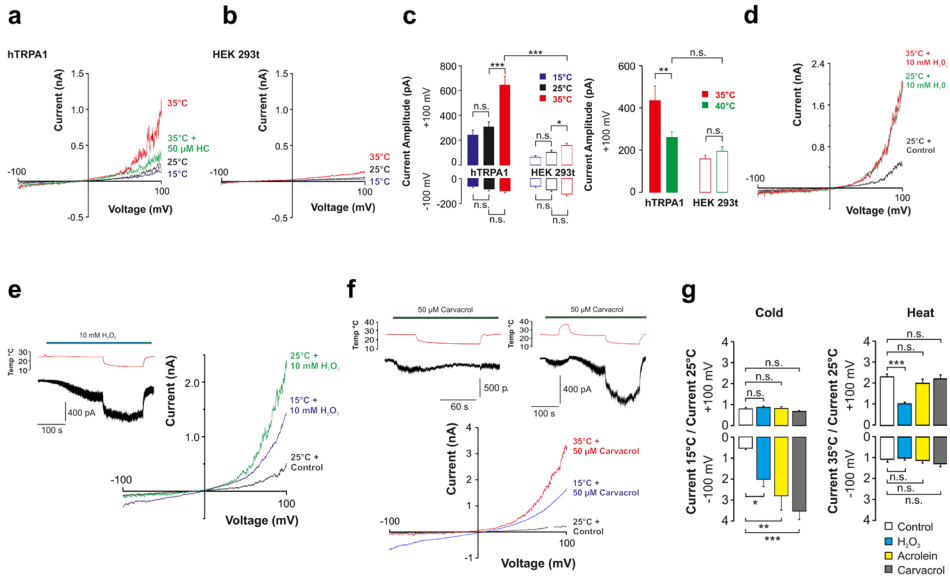

Figure 3 Human TRPA1 cold and heat sensitivity is influenced by redox state and ligands. (**a-c**) Increasing the temperature from 25 °C to 35 °C evoked outward hTRPA1 currents in HEK293t cells that were blocked by the selective TRPA1 antagonist HC030031 (91 ± 5 %, n = 5), whereas only minor currents were observed in non-transfected cells (n = 10-19). At 40 °C, outward currents were not different from those in non-transfected cells (n = 6-8). (**d**) H_2O_2, but not acrolein or carvacrol (see **Supplementary Fig. S5**), prevented a further rise in outward currents when increasing the temperature from 25 °C to 35 °C. (**e**) H_2O_2 triggered cold-evoked inward currents at -60 mV and in 500 ms voltage ramps (n=12). (**f**) Carvacrol also triggered hTRPA1 cold responses, but only in cells pre-exposed to heat (n = 5-8). (**g**) Bar graph summarizing the effect of cold and heat in the absence (control) and presence of the various treatments at either -100 or +100 mV (n = 5-7). Data are represented as mean ± s.e.m. *P<0.05, **P<0.01 and ***P<0.001 indicate statistically significant differences using ANOVA Tukey post-hoc test.

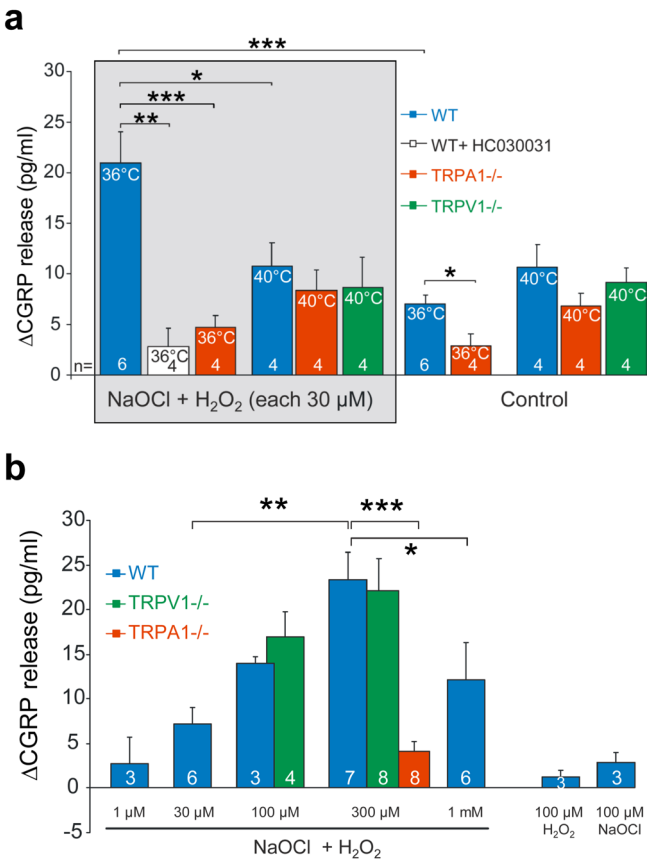

Figure 4 Mouse TRPA1 heat sensitivity is influenced by redox state. (**a**) Raising the temperature from 22 °C to 36 °C caused a small TRPA1-dependent calcitonin gene-related peptide (CGRP) release from mouse trachea. After pre-incubation of trachea with subliminal concentrations of H_2O_2+NaOCl, producing singlet oxygen, there was a substantial increase in CGRP release at 36 °C that was inhibited by the selective TRPA1 antagonist HC030031 (50 µM) and in TRPA1 knock-out mice. (**b**) At 37 °C, acute exposure to various concentrations of H_2O_2 and NaOCl combined caused a concentration-dependent release of CGRP that was dependent on TRPA1 but not TRPV1. Under these conditions, H_2O_2 and NaOCl (each at 100 µM) alone evoked minor CGRP release compared to their combination. Interestingly, the combination of H_2O_2 and NaOCl (each 1 mM) was less effective causing CGRP release indicating desensitization of TRPA1. This further supports our conclusion that partial oxidation favors TRPA1 activity. Data are represented as mean ± s.e.m. (numbers of experiments within bars). *P<0.05, **P<0.01 and ***P<0.001 indicate statistically significant differences using ANOVA Tukey post-hoc test.

Human TRPA1 is a heat sensor displaying intrinsic U-shaped thermosensitivity

Lavanya Moparthi, Tatjana I. Kichko, Mirjam Eberhardt, Per Kjellbom, Urban Johanson, Peter W. Reeh, Andreas Leffler, Milos R. Filipovic and Peter M. Zygmunt

Supplementary Information

Figures 1-7

Table 1

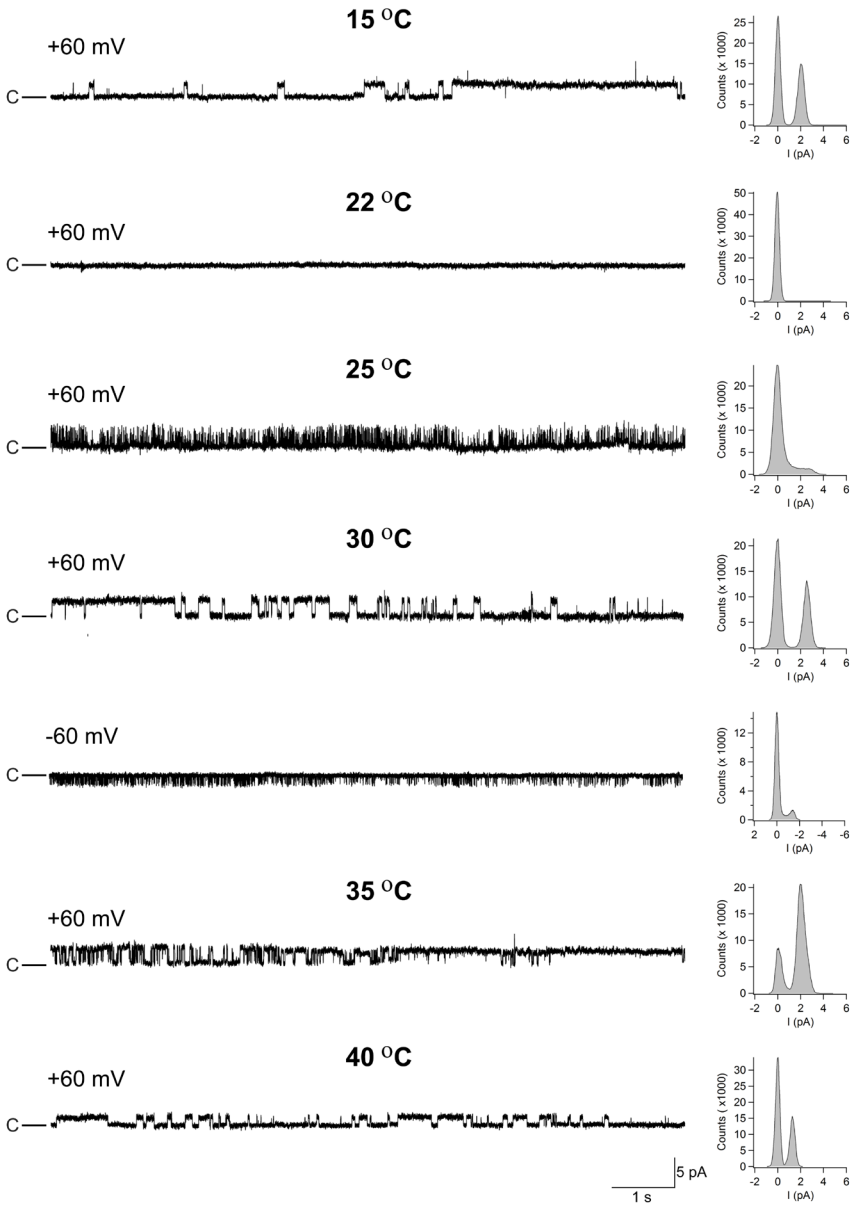

Supplementary Figure 1 Temperatures below and above 22 °C evoked steady state outward and inward hTRPA1 single channel currents at a test potential of +60 and -60 mV as shown by representative traces and the corresponding amplitude histograms. Purified hTRPA1 was inserted into planar lipid bilayers and channel currents were recorded with the patch-clamp technique in a symmetrical K^+ solution (c indicates the closed channel state).

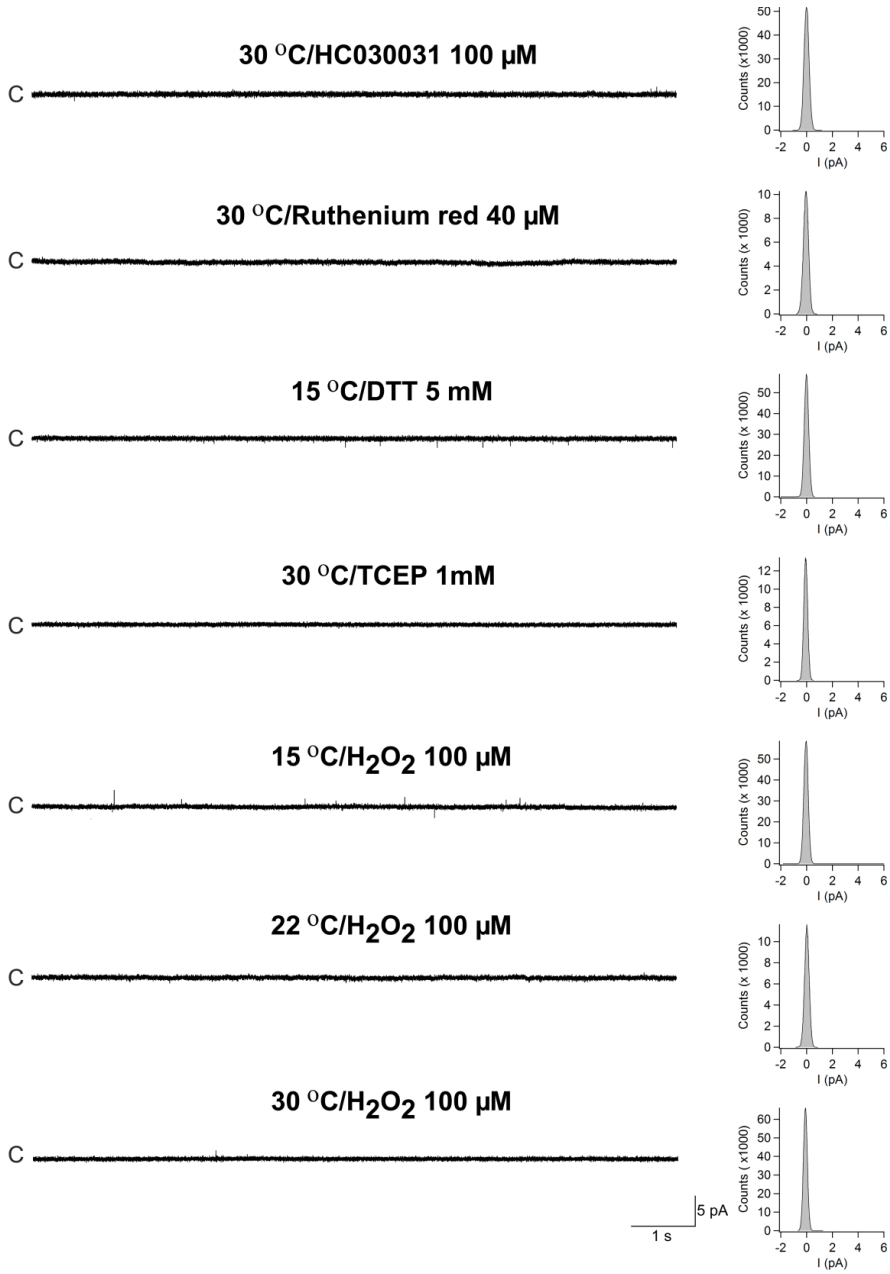

Supplementary Figure 2 Lipid bilayers without hTRPA1 did not respond to the TRPA1 antagonists HC030031 and ruthenium red as well as reducing (DTT and TCEP) and oxidizing (H_2O_2) agents at a test potential of +60 mV (n = 3-4). Representative traces and the corresponding amplitude histograms are shown; c indicates closed channel state. Single channel currents were recorded with the patch-clamp technique in a symmetrical K^+ solution.

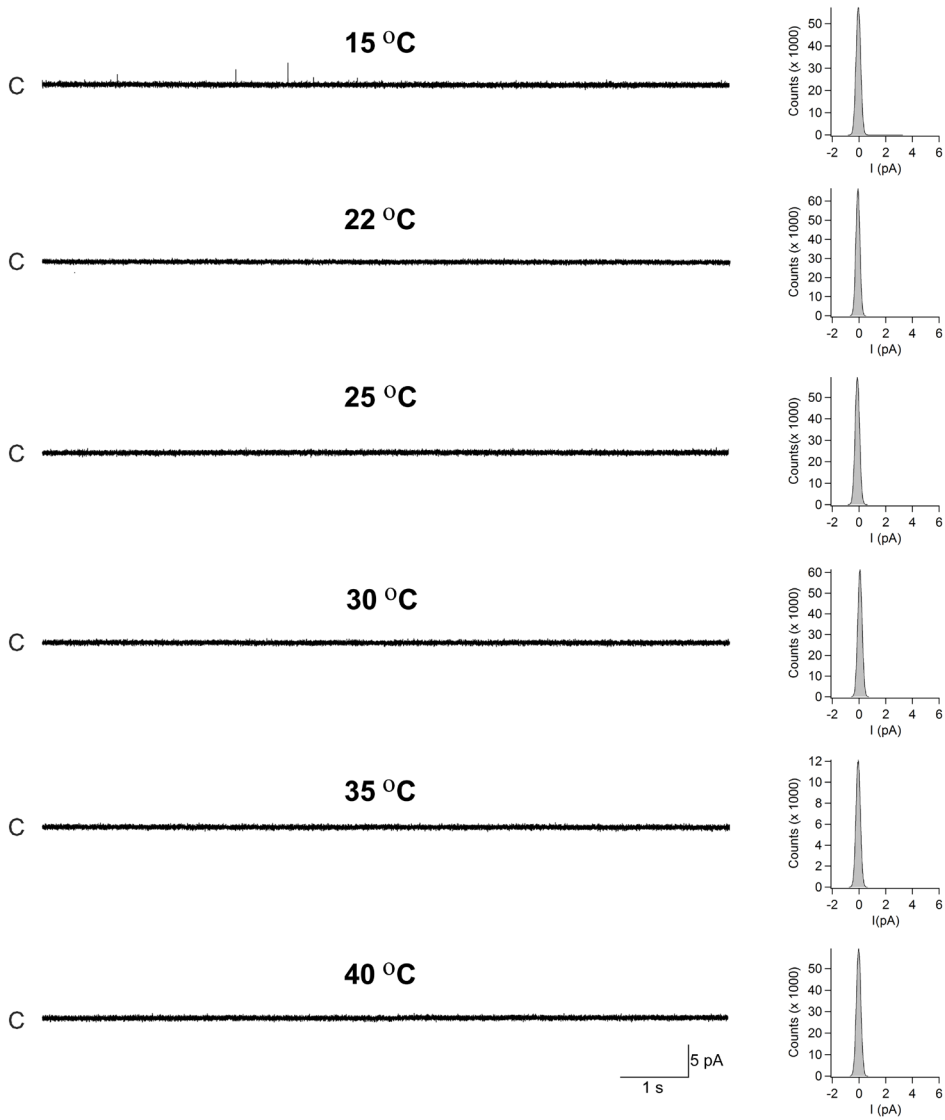

Supplementary Figure 3 Lipid bilayers without hTRPA1 did not respond to various temperatures at a test potential of +60 mV (n = 3). Representative traces and the corresponding amplitude histograms are shown; c indicates closed channel state. Single channel currents were recorded with the patch-clamp technique in a symmetrical K^+ solution.

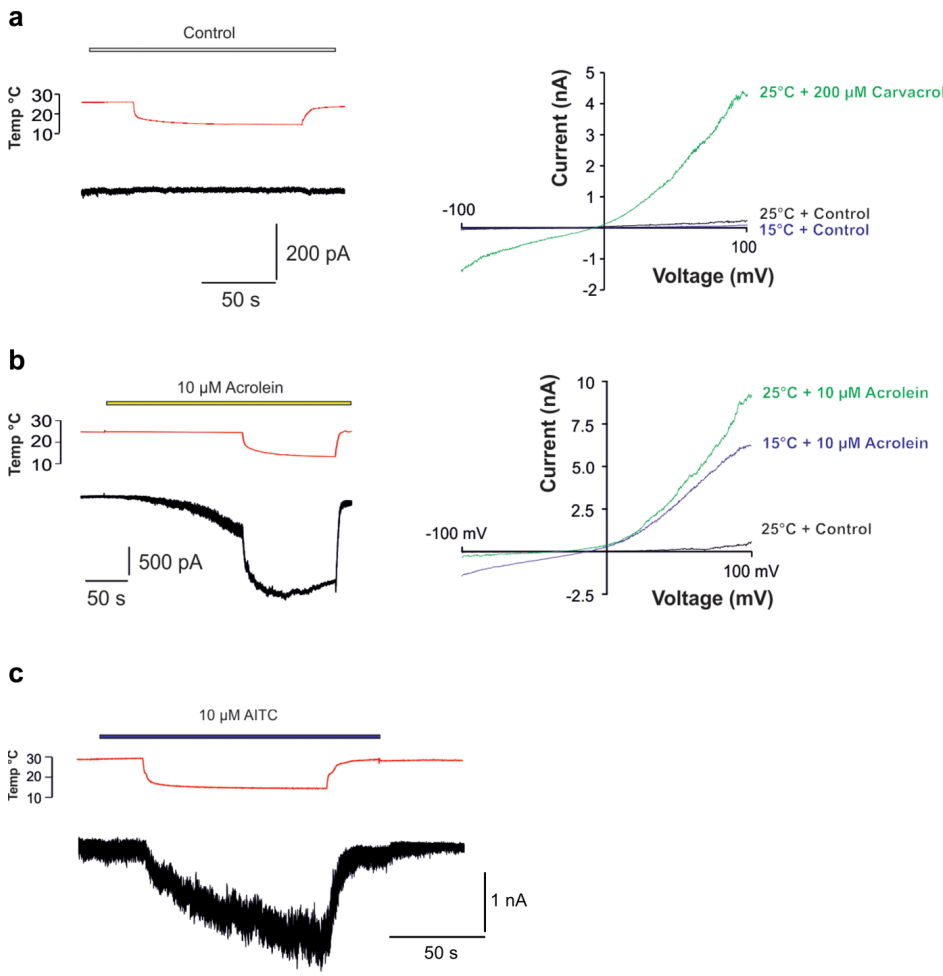

Supplementary Figure 4 Representative traces showing the effect of cold as well as electrophilic compounds on hTRPA1 cold responses in HEK293t cells expressing hTRPA1. (**a**) No inward currents were observed at 15 °C whereas the non-electrophilic compound carvacrol at a high concentration produced inward and outward currents confirming that hTRPA1 was functionally expressed. (**b** and **c**) The electrophilic compounds acrolein (n = 6-9) and allyl isothiocyanate (n = 4), at a concentration that produced no or minor hTRPA1 inward currents at 25 °C, triggered the cold-sensitivity of hTRPA1. Cells were either constantly held at a membrane potential of -60 mV (left panel traces) or subjected to 500 ms voltage ramps from -100 to + 100 mV (right panel traces).

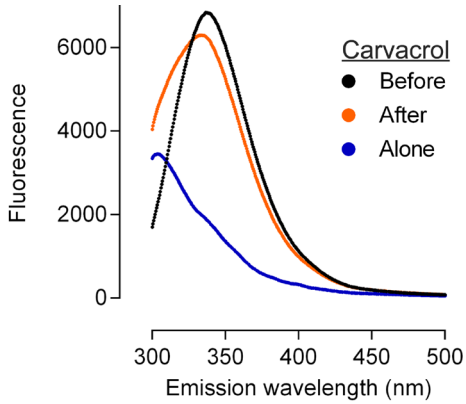

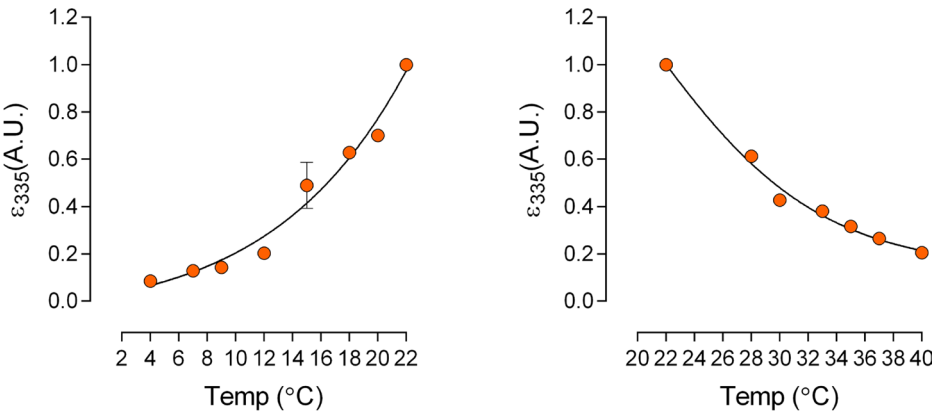

Supplementary Figure 5 Representative fluorescence spectra showing the effect of the non-electrophilic compound carvacrol (100 μM) on hTRPA1 cold and heat responses. At 22 °C, carvacrol itself emitted fluorescence that was subtracted when its effect on cold and heat was analyzed at the emission wavelength (ε) of 335 nm. Excitation was done at 280 nm and spectra were collected from 300 nm to 500 nm. Data are represented as mean ± s.e.m. of 3 separate experiments.

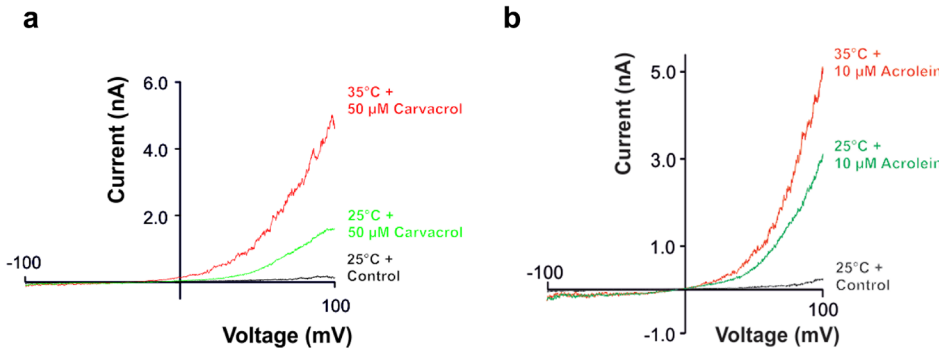

Supplementary Figure 6 Representative traces showing the effect of the non-electrophile carvacrol and the electrophilic compound acrolein on hTRPA1 heat responses in HEK293t cells expressing hTRPA1. Heat currents in the presence of (**a**) carvacrol (n = 7) and (**b**) acrolein (n = 6) in cells subjected to 500 ms voltage ramps from -100 to + 100 mV.

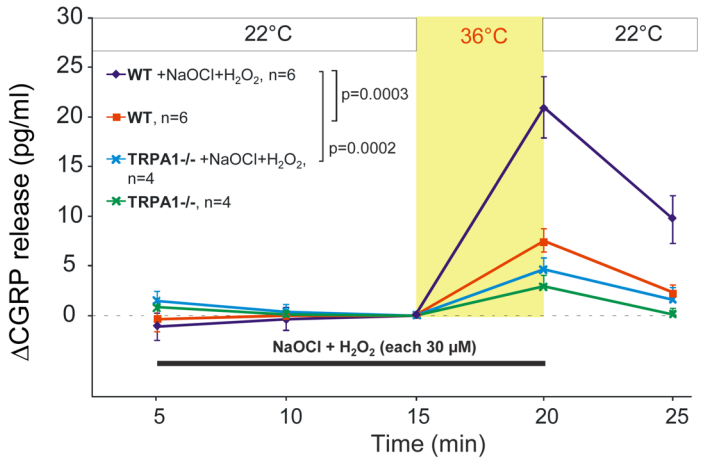

Supplementary Figure 7 Heat-induced TRPA1-dependent neuropeptide release from mouse trachea. Shown is the experimental design for studying the effect of heat under various conditions on the release of the neuropeptide calcitonin gene-related peptide (CGRP) from mouse trachea as presented in **Fig. 4a**. Importantly, the combination of H_2O_2 and NaOCl, used to oxidize the cellular TRPA1 environment, did not cause CGRP release at the pre-incubation temperature of 22 °C. The release of CGRP is calculated as increase of CGRP over baseline (ΔCGRP in pg/ml) and data are represented as mean ± s.e.m. of separate experiments (n) as indicated in the graph. P values below 0.05 indicate statistically significant differences using ANOVA Tukey post-hoc test.

Supplementary Table 1 Single channel open probability and conductance values for hTRPA1.

Stimuli	Voltage (mV)	Open probability (mean ± SEM)	n	Conductance (pS) (mean ± SEM)	n
40 °C	+60	0.35 ± 0.03	3	26 ± 2	3
35 °C	+60	0.64 ± 0.05	7	36 ± 5	6
30 °C	+60	0.38 ± 0.02	24	36 ± 3	22
	-60	0.13 ± 0.03	6	31 ± 5	6
25 °C	+60	0.10 ± 0.04	4	35 ± 4	3
22 °C	+60	0.00 ± 0.00	4	0 ± 0	4
$+H_2O_2$	+60	0.57 ± 0.06	7	63 ± 9	7
15 °C	+60	0.34 ± 0.03	10	43 ± 3	7

Paper III

The N-terminal ankyrin repeat domain is not required for activation of purified mosquito TRPA1 by heat or mustard oil

Sabeen Survery[a], Lavanya Moparthi[a], Per Kjellbom[a], Edward D. Högestätt[b], Peter M. Zygmunt[b,*] and Urban Johanson[a,*]

[a]Department of Biochemistry and Structural Biology, Center for Molecular Protein Science, Lund University, SE-221 00 Lund, Sweden
[b]Clinical Chemistry & Pharmacology, Department of Laboratory Medicine, Lund University, SE-221 85 Lund, Sweden

*Corresponding authors: P.M.Z. (peter.zygmunt@med.lu.se) and U.J. (urban.johanson@biochemistry.lu.se).

Highlights:

- TRPA1 from Malaria mosquito heterologously expressed and purified
- Single channel recordings demonstrate a functional thermo- and chemo-receptor
- N-terminal half of TRPA1 is not required for activation by heat or mustard oil
- Quenching of tryptophan fluorescence by activation reports structural changes

eTOC blurb:

Survery et al. demonstrate that Malaria mosquito TRPA1 is an intrinsic heat and chemoreceptor where heat-sensing properties reside outside the N-terminal Ankyrin repeat domain which has earlier been suggested to contain these functions. This finding will facilitate the localization and investigation of the nature of the intriguing thermo-sensor.

Keywords: heat sensing, repellents, pain, thermosensor, TRP channels, tryptophan fluorescence

Summary

Temperature sensors are crucial for animals to optimize living conditions. The temperature response of the ion channel transient receptor potential A1 (TRPA1) is intriguing, some orthologs have been reported to be activated by cold and others by heat, but the molecular mechanisms responsible for its activation remain elusive. Single-channel electrophysiological recordings of heterologously expressed and purified *Anopheles gambiae* TRPA1 (AgTRPA1), with and without the N-terminal ankyrin repeat domain, demonstrate that both proteins are functional as they responded to the electrophilic compound allyl isothiocyanate (AITC) and heat. The proteins similar intrinsic fluorescence properties and corresponding quenching when activated by AITC or heat, suggest lipid bilayer-independent conformational changes outside the N-terminal domain. The results show that AgTRPA1 is an inherent temperature- and chemoreceptor, and analogous to what has been reported for the human TRPA1 ortholog the N-terminal domain may tune the response but is not required for the activation by these stimuli.

Introduction

The discovery of **t**ransient **r**eceptor **p**otential (TRP) ion channels, such as the TRP subtype A1 (TRPA1), being involved in chemo- and thermosensation, has opened-up new avenues for understanding how organisms monitor the physicochemical environment (Holzer, 2011; Julius, 2013; Laursen et al., 2015; Nilius and Owsianik, 2011; Patapoutian et al., 2009). The identification by us and others of TRPA1 as a chemosensor activated by plant-derived electrophilic and thiol-reactive compounds (Bandell et al., 2004; Bautista et al., 2005; Jordt et al., 2004; Macpherson et al., 2005), including isothiocyanates and diallyl disulfide from mustard and garlic, together with findings from numerous subsequent studies have established TRPA1 as a unique detector of tissue damaging environmental chemicals and pro-inflammatory compounds in both invertebrates and vertebrates (Laursen et al., 2015; Panzano et al., 2010; Zygmunt and Högestätt, 2014).

Several TRPA1 homologues exist in the animal kingdom, and the ability of TRPA1 to sense potentially harmful electrophilic compounds has been conserved for ~500 millions of years, whereas the ancestral thermosensitive properties of TRPA1 are unclear and have diverged later (Kang et al., 2010b; Laursen et al., 2015; Panzano et al., 2010). A role for mammalian TRPA1, and especially the human TRPA1 (hTRPA1), as noxious cold sensors has been controversial ever since propose (Story et al., 2003), while the heat thermosensitive role of TRPA1 homologues in non-mammalians has been easily accepted (Laursen et al., 2015; Zygmunt and Högestätt, 2014). However, we have recently shown that hTRPA1 is indeed an intrinsically cold sensitive protein (Moparthi et al., 2014). If it is true that all TRPA1 are intrinsic thermo-gated ion channels, then it appears that human, rat and mouse TRPA1 respond to cold temperatures below 20°C whereas e.g., the rattlesnake, fruit fly and mosquito TRPA1 respond to warm temperatures above 25°C (Gracheva et al., 2010; Hamada et al., 2008; Kang et al., 2012; Karashima et al., 2009; Kremeyer et al., 2010; Sawada et al., 2007; Story et al., 2003; Wang et al., 2009; Wang et al., 2013; Viswanath et al., 2003; Xiao et al., 2008).

It has been suggested that the intracellular N-terminal ankyrin repeat domain (ARD) of TRPA1 in snakes contains the necessary thermosensitive modules for heat detection, whereas both the N-terminal ARD and the pore region of *Drosophila* (*melanogaster*) TRPA1 may contain heat-sensitive elements (Cordero-

Morales et al., 2011; Julius, 2013; Kang et al., 2012; Wang et al., 2013; Zhong et al., 2012). However, these and similar conclusions have to be regarded with some caution because the use of mutagenic and chimeric strategies results in artificial constructs, which makes it difficult to exclude indirect effects on a temperature sensor located elsewhere in the protein (Laursen et al., 2015; Zygmunt and Högestätt, 2014). Furthermore, each of three single point mutations of amino acids in the N-terminal ARD, not previously regarded critical like certain cysteine and lysine residues (Hinman et al., 2006; Macpherson et al., 2007), changed the mouse TRPA1 from being cold sensitive to being heat sensitive (Jabba et al., 2014). Importantly, the authors concluded that this could best be explained by an effect on the coupling of temperature to channel gating rather than altering the nature of the thermosensitive domain itself (Jabba et al., 2014). This reasoning is in line with our view that conformational changes of the N-terminal ARD indirectly affects thermo- and chemosensitive structures outside the N-terminal ARD of TRPA1 (Moparthi et al., 2014; Zygmunt and Högestätt, 2014). Studies of purified TRPA1 without its N-terminal ARD should therefore be a valuable contribution in the search of TRPA1 thermo- and chemosensory domains (Moparthi et al., 2014). Clearly, various methodological approaches are needed to identify the location of distinct temperature sensing domains, if at all existing (Baez et al., 2014; Clapham and Miller, 2011; Hilton et al., 2015; Voets, 2012).

The *Anopheles gambiae* TRPA1 (AgTRPA1), which exists as the two isoforms AgTRPA1(A) and AgTRPA1(B), is heat sensitive as well as activated by electrophilic compounds when expressed heterologously (Hamada et al., 2008; Kang et al., 2012; Kang et al., 2010a; Wang et al., 2009; Xiao et al., 2008). Depending on the anatomical location and isoform, AgTRPA1 is linked to avoidance or host seeking behaviors (Hamada et al., 2008; Kang et al., 2012; Liu and Zwiebel, 2013). In the present study, we have purified the AgTRPA1(A) with the aim to determine if this protein has inherent thermo- and chemosensitive properties, and if such properties are also located outside the N-terminal ARD. We show that AgTRPA1 irrespective of its N-terminal ARD undergoes conformational changes and is activated by the electrophilic mustard oil ingredient allyl isothiocyanate (AITC) as well as by temperatures above 25°C. Thus, our recent proposal that electrophiles modify TRPA1 channel activity by interacting with binding sites, such as cysteine and lysine residues, outside the N-terminal ARD (Moparthi et al., 2014) is not restricted to hTRPA1 but also valid for the heat-sensitive AgTRPA1. Most important is our conclusion that temperature-sensitive regions of AgTRPA1 should be searched for outside the N-terminal ARD as proposed for the cold sensitive hTRPA1 (Moparthi et al., 2014).

Results

Overexpression and purification of AgTRPA1

The methylotrophic yeast *Pichia pastoris* has been established as an excellent host for efficient expression of a number of heterologous eukaryotic membrane proteins (Horsefield et al., 2008; Moparthi et al., 2014; Tornroth-Horsefield et al., 2006). In this study we have used this system to express the full-length isoform A of TRPA1 from *Anopheles gambiae* (Hamada et al., 2008; Kang et al., 2012) (from here on referred to as AgTRPA1) as well as a truncated construct lacking the N-terminal ARD (Δ1-776 AgTRPA1; Fig. 1a). After cell lysis, peripheral proteins were removed from the *Pichia* membrane fraction by urea- and alkali washes, and TRPA1 proteins were extracted by the detergent fos-choline-12, which was identified as the best choice for protein stability and yield in screens performed with various detergents (data not shown). The proteins were further purified, by means of a hexa-His tag in the C-terminal extension by Nickel affinity chromatography followed by size exclusion chromatography (SEC). The highly expressed Δ1-776 AgTRPA1 was quite pure already after the affinity purification, whereas the full length construct suffered from both contaminating proteins and some degradation products after the corresponding step (Fig. 1b). In SEC Δ1-776 AgTRPA1 eluted mainly as a tetramer, while AgTRPA1 eluted as double peak corresponding to the tetramer and the dimer (Fig. 1c). After the two-step purification, the tetrameric Δ1-776 AgTRPA1 yield was estimated to be 1.3 mg from 20 g of *Pichia* cells. In comparison, the yield of the 2.5 times longer AgTRPA1 was found to be 0.7 mg from the same amount of cells. Only the tetrameric fractions were used for structural and functional characterization of TRPA1.

Synchrotron Radiation Circular Dichroism spectra and thermal denaturation of AgTRPA1

The tetrameric fractions of purified AgTRPA1 and Δ1-776 AgTRPA1 were subjected to syncrotron radiation circular dichroism (SRCD) spectroscopy to examine their overall fold and thermal unfolding (Fig. 2a). At low temperature the SRCD spectra of both constructs exhibited the expected characteristic α-helical protein signature with a maximum at 193 nm and two deep minima at 210 and 222 nm suggesting that the proteins retained their native fold after purification.

The SRCD spectra obtained at higher temperatures show that both proteins gradually lose their secondary structure to become almost completely unfolded around 80°C. The unfolding appears to be irreversible since lowering the temperature does not result in re-appearance of an α-helical spectrum (data not shown).

TRPA1 channels are believed to act as thermoreceptors, hence we performed more careful analysis of the thermal denaturation of AgTRPA1 and Δ1-776 AgTRPA1 to monitor temperature-induced changes in the purified proteins. From differential plots of the spectra obtained at 24.3°C and at 41.4°C the most prominent changes were found at 193 nm and at 222 nm (Fig. 2b). Therefore we chose these two wavelengths for construction of thermal transition curves (Fig. 2c, d). Although the complete transition of the truncated construct has a slightly lower mid-point (Table S1; around 54°C, both at 193 nm and 222 nm) than the full-length TRPA1 (55°C and 58°C at 193 nm and 222 nm, respectively) there appears to be additional early minor transitions at 30 and 45°C in the latter. A closer investigation of the thermal denaturation between 24 and 45°C in the truncated construct cannot conclusively support or exclude a similar early transition at 30°C due to the relatively large variability between samples but a distinct transition between 41 and 43°C is observed (Fig. 2d).

Intrinsic tryptophan fluorescence is quenched by an agonist and temperature

In contrast to CD spectrometry that monitors the secondary structure of a protein, tryptophan residues in a protein can be informative when it comes to detecting changes in tertiary structure caused by e.g. the binding of agonists. The intrinsic fluorescence of tryptophans residing in a non-polar environment may be quenched or shifted in wavelength by direct interaction with a ligand or due to induced conformational changes exposing the tryptophan to a different milieu(Lakowicz, 2002). In AgTRPA1 there are 13 tryptophan residues whereof eight are retained in Δ1-776 AgTRPA1 (Fig. 3a). An alignment with the sequence of the recently reported structure of hTRPA1 (Paulsen et al., 2015) reveals that five of the corresponding amino acid residues are resolved in the structure and that tryptophans 915, 926 and 1108 are likely to be located on the surface of the protein, interacting with detergent in the micelle or the aqueous phase (Fig. 3b). Two conserved tryptophans, corresponding to W779 and W950 in AgTRPA1, are

buried in the structure. A classification of these tryptophans in the structure of hTRPA1 using PFAST (Protein Fluorescence and Structure Toolkit (Shen et al., 2008)) suggests that the former is located in a fairly polar environment (class III P = 0.87), whereas the latter is packed into more hydrophobic milieu (class S P = 0.55, or class I P = 0.45). The conserved amino acid residues within 5 Å of the two tryptophan indole rings (Fig. S1) support a similar polar and hydrophobic setting in AgTRPA1 for W779 and W950, respectively. The expected emission maximum for a tryptophan of class III is between 346 and 350 nm, whereas the ranges for tryptophans belonging to classes S and I are blue shifted to 321-325 nm and 330-333 nm (Shen et al., 2008). Concentration-response experiments show that both constructs have intrinsic tryptophan fluorescence with a maximum at 337 nm, which can be totally quenched by the agonist allyl isothiocyanate (AITC) without any associated shift of the maximum in the spectra (Fig. 4a). Interestingly, similar absolute fluorescence intensities are obtained for the two constructs in the absence of AITC when the same molar concentration of protein is used. This suggests that the five N-terminal tryptophans that are missing in the truncated construct do not contribute much to the total fluorescence, and furthermore the emission maximum would exclude W779 and favor W950 as more likely to be responsible for most of the fluorescence emission. Although statistical analysis favor a model with different pEC50 values for AITC of the two constructs ($P < 0.005$), the corresponding EC50 values 256 and 444 μM, for AgTRPA1 and Δ1-776 AgTRPA1, respectively, differ less than 2-fold.

To investigate if the quenching of tryptophan fluorescence also occurs at thermal activation of the protein we monitored the tryptophan fluorescence as a function of temperature in the interval 25 to 48°C (Fig. 4b). There is indeed a thermal quenching with a mid-point at 38.7 ± 1.0°C and 41.1 ± 3.3 for AgTRPA1 and Δ1-776 AgTRPA1, respectively, and similar to the ligand induced quenching there is no associated shift of the wavelength for the maximal intensity. Notably, in contrast to AITC, the maximal quenching in the temperature range investigated does not totally abolish the fluorescence. Instead the intensity at the highest temperature corresponds to about half of the non-quenched signal.

Chemical and heat activation of AgTRPA1

Several studies have shown that heterologously expressed AgTRPA1 is activated by the electrophilic compounds AITC, cinnamaldehyde and N-methylmaleimide as

well as by heat (Hamada et al., 2008; Kang et al., 2012; Kang et al., 2010a; Wang et al., 2009; Xiao et al., 2008). In this study, we used AITC to study electrophile activation of purified AgTRPA1 with and without its N-terminal ARD. As shown in patch-clamp voltage-ramp recordings (-100 to +100 mV in 2 s), both AgTRPA1 and Δ1-776 AgTRPA1 when inserted into planar lipid bilayers were activated by AITC (100 μM) at negative and positive test potentials (Fig. 5). The vehicle of AITC (1% ethanol) had no effect on AgTRPA1 and Δ1-776 AgTRPA1 (Fig. 5), and AITC did not evoke currents in bilayers without protein (Fig. S2). At a steady state test potential of +60 mV, we observed mainly one single-channel current level, and occasionally a lower single-channel current level. Analysis of the main single-channel current level showed higher Gs and lower Po values for Δ1-776 AgTRPA1 as compared to AgTRPA1 (Table S2). For AgTRPA1, the AITC-induced activity was inhibited by the TRP channel pore blocker ruthenium red at the same concentration (40 μM, n = 4, data not shown) that inhibits both AITC and heat activation of heterologously expressed AgTRPA1 (Hamada et al., 2008; Kang et al., 2010a).

Heat responses of AgTRPA1 and Δ1-776 AgTRPA1 were observed in voltage-ramp recordings (-100 to +100 mV in 2 s), and studied in detail at a single-channel level at a steady state test potential of +60 mV (Figs. 6 and 7). Both TRPA1 channels displayed intense channel activity at 30°C and above (Figs. 6 and 7). No activity was shown in bilayers without AgTRPA1 and Δ1-776 AgTRPA1 (n = 4, Fig. S2). At 25°C, sporadic activity of AgTRPA1, but not of Δ1-776 AgTRPA1, was recorded (Figs. 6 and 7). Using a simplified approach (Latorre et al., 2007; Vriens et al., 2014), a Q10 value of 28 was calculated for AgTRPA1 using Po values at 25°C and 30°C from 3 separate bilayer recordings. The analysis of Gs and Po at a steady state test potential of +60 mV revealed differences between AgTRPA1 with and without its N-terminal ARD (Table S2). Thus, at 30°C the Gs for Δ1-776 AgTRPA1 was 39% of that for AgTRPA1 (Table S2). However, when the temperature was raised to 40°C, the Gs for Δ1-776 AgTRPA1 increased by 72% whereas the Gs for AgTRPA1 decreased by 46% (Table S2). Although not reaching statistical significance, raising the temperature from 30°C to 40°C increased the Po by 45% for Δ1-776 AgTRPA1 (Table S2). As shown by continuous recordings, the heat responses were temperature-dependent in a reversible manner (Fig. 7).

Discussion

Studies of isolated proteins are crucial for elucidation of the molecular mechanisms responsible for activation of thermo- and chemoreceptors. Here we report on the heterologous expression and purification of functional full-length AgTRPA1 as well as the truncated Δ1-776 AgTRPA1, lacking the N-terminal ARD. The truncated version not only produced a higher yield than the full length protein, but also form a more stable tetramer under the conditions applied, since most of the protein eluted in the tetrameric peak when size exclusion chromatography was applied. In contrast almost half of the full-length AgTRPA1 was lost in dimeric fractions. The tetrameric structures suggest that the isolated proteins are correctly folded. This was confirmed by SRCD measurements generating characteristic spectra for α-helical proteins. Although the quaternary structure of Δ1-776 AgTRPA1 appeared more stable there was more variability between samples at the lower temperatures of the thermal denaturation curve, as compared to the full-length construct. This might hint that the N-terminal ARD helps to stabilize the helical content at lower temperatures. However, overall the thermal stabilities of the two constructs were very similar, and there appears to be some minor transitions between 25 and 45°C in both constructs, although compelling evidence for common distinct transitions specifically coupled to the thermal activation of the channel is missing due to the variation between samples.

Tryptophan fluorescence might be quenched by a direct interaction with the ligand or may report on subtle conformation changes that are not detected by CD. Surprisingly both constructs had a similar molar intrinsic fluorescence. Although there are alternative explanations for this, the most simple would be that the five tryptophans in the N-terminal ARD do not contribute to the fluorescence of AgTRPA1. Likewise, the total quenching and EC50 values for AITC are in the same range for both constructs which suggest that any binding sites for AITC in the N-terminal ARD add little to the quenching.

The EC50 of fluorescence quenching is somewhat high compared to functional studies of activation of AgTRPA1 by AITC in CHO cells (70.7±12.4 μM (Xiao et al., 2008)). This may indicate that some low affinity binding sites that are required to bind AITC for complete quenching, are not necessary for the activation of the protein by this agonist, and that any conformational changes associated with activation of the channel are not sufficient to get a complete quenching. This is in line with the partial quenching obtained by temperature. The full-length AgTRPA1 and the truncated construct exhibit similar temperature quenching

curves, and it is interesting to note how well they follow each other between 40 to 46ºC with a common transition between 42 and 44ºC. Identification of tryptophans that contribute to the fluorescence may indicate where AITC binds and more important where structural changes take place. AITC is expected to bind to cysteines and lysines. In AgTRPA1 there are 65 lysines and 23 cysteines, but there are only 25 lysines and 4 cysteines in the truncated variant. Examination of the corresponding amino acid residues in the recently solved hTRPA1 structure (Paulsen et al., 2015) allows a crude evaluation of the environment where some of the tryptophans reside. From this structural analysis W950 appears as a promising candidate for the intrinsic fluorescence that is quenched by activation of the channel. It is situated in a hydrophobic pocket at the interface between S1 and S5 helices of neighboring subunits and may therefore report on conformational changes in the tetramer. This is supported by the fact that there are no lysines or cysteines in the close vicinity of W950 that could act as binding sites. The changes in conformation reflected by quenching of fluorescence may report on the activation state of the channel and can potentially be used to investigate the mechanisms behind activation in a membrane independent manner. We note that the complete integrated nexus as recognized in the structure of hTRPA1 is missing in our truncated construct (Paulsen et al., 2015). This would indicate that neither activation by temperature nor AITC mediated activation requires Helix-turn-helix 1 or 2 of this intricate structure.

Our patch-clamp studies provide evidence that the purified AgTRPA1 is a functional ion channel with and without its N-terminal ARD. We show for the first time, to our knowledge, that both heat- and chemo sensitivity of a non-mammalian TRPA1 are functionally relevant inherent channel properties. Using the purified AgTRPA1 without its N-terminal ARD allows us to conclude that TRPA1 polymodal sensory properties, which are strongly believed to be mediated by the N-terminal ARD domain (Julius, 2013), are also determined by channel structures outside the N-terminal ARD. A similar conclusion was reached regarding the intrinsically cold- and chemosensitive hTRPA1 (Moparthi et al., 2014). Although, it cannot be excluded that a truncation similar to mutagenesis and chimeragenesis may induce artificial properties (Laursen et al., 2015; Zygmunt and Högestätt, 2014), like exposure of new binding sites, studies of purified TRPA1 without its N-terminal ARD should be a valuable complementary strategy to identify the electrophile binding sites and temperature domains linked to TRPA1 channel gating.

The AgTRPA1 exists as A and B isoforms, of which AgTRPA1(B) is extremely heat sensitive (Kang et al., 2012). Corresponding isoform-dependent differences in heat properties have also been shown for *Drosophila* TRPA1, whereas the maximal response and sensitivity to the electrophilic compound N-methylmaleimide were not different (Kang et al., 2012), indicating that heat sensitivity may not always be evolutionary gained at the expense of electrophile sensitivity (Cordero-Morales et al., 2011; Laursen et al., 2015). Here, we have focused on AgTRPA1(A), since this isoform was originally reported as the heat sensitive TRPA1 in *Anopheles gambiae* (Hamada et al., 2008; Wang et al., 2009). In agreement with these studies, we observed heat responses within the same temperature interval starting at 25°C and reaching saturation at 30°C for both Gs and Po when compared to 40°C. Although this very steep temperature-response interval (25°C to 30°C) did not allow us to perform a detailed thermodynamic analysis of Q10 and the thermal threshold for AgTRPA1(A) activation, our data suggest a Q10 of 28 based on Po values obtained at 25°C and 30°C, and a thermal threshold close to 25°C, which is within the temperature activation range of this AgTRPA1 isoform when expressed in *Xenopus* oocytes (Hamada et al., 2008; Wang et al., 2009). However, a later study, also using the *Xenopus* oocyte expression system, determined a thermal threshold of 32°C and a Q10 of 4 for AgTRPA1(A) (Kang et al., 2012). This discrepancy may perhaps be due to the AgTRPA1(A) basal activity observed below thermal threshold even at 15°C (Kang et al., 2012). Furthermore, variation in channel expression levels and test potential are confounding factors in the thermodynamic analysis of TRP channels (Vriens et al., 2014). Compared to AgTRPA1(B), AgTRPA1(A) has additional amino acids at the distal end of the N-terminus reducing its heat sensitivity (Kang et al., 2012). However, without the N-terminal ARD both isoforms of AgTRPA1 are identical and thus have the same thermo- and chemosensitive properties as described for Δ1-776 AgTRPA1 in the present study. Whether the N-terminal ARD of AgTRPA1(B) renders AgTRPA1(B) more sensitive than AgTRPA1(A) to heat in our test system remains to be shown. Nevertheless, there is no doubt that the purified AgTRPA1(A) used in our study is a functional thermosensitive ion channel either intact or without its N-terminal ARD,

because we could only observe heat responses in bilayers containing AgTRPA1 or Δ1-776 AgTRPA1. It has been suggested that the sensitivity of TRPA1 to electrophiles is species-dependent (Julius, 2013; Laursen et al., 2015). Indeed, at a single-channel current level there are clear differences between the purified hTRPA1 and AgTRPA1 in such a way that we observed mainly one current level in AgTRPA1 whereas hTRPA1 displayed several current levels in response to AITC at 100 μM (Moparthi et al., 2014). The Gs, calculated for the main current level, was much lower for AgTRPA1 compared to hTRPA1 both in the presence and absence of the N-terminal ARD. Furthermore, without the N-terminal ARD the Po for AgTRPA1 was much smaller than that of hTRPA1 (Moparthi et al., 2014). Altogether this may be related to differences in the number of cysteine residues with hTRPA1 having 28 and AgTRPA1 23 cysteines, of which AgTRPA1 only has 4 cysteines compared to 9 for hTRPA1 outside the N-terminal ARD. Interestingly, the Gs and Po of AgTRPA1(A), when exposed to heat and AITC, were different in the presence and absence of the N-terminal ARD, indicating that the temperature and chemosensitivity of AgTRPA1 is modulated by the N-terminal ARD, as has also been proposed for the purified hTRPA1 (Moparthi et al., 2014).

In conclusion, our study on the purified AgTRPA1 together with that on purified hTRPA1 (Moparthi et al., 2014) provide the important information that heat and cold thermosensation as well as electrophile chemosensitivity of TRPA1 is also detected by channel structures and binding sites outside the N-terminal ARD. This TRPA1 thermo- and chemosensitive framework should help to identify the molecular mechanism behind temperature and ligand gating of TRPA1 as well as species selective fine tuning chemicals of TRPA1 that can be used as analgesics and repellents.

Experimental Procedures

AgTRPA1 overexpression and purification

The coding sequence for Transient Receptor Potential A1 from *Anopheles gambiae* (AgTRPA1 (Hamada et al., 2008), acc. number EU624401)

referred to as isoform A in (Kang et al., 2012), was inserted into the pPICZB vector in the SacII and NotI restriction sites, using forward primer TGCCGCGGCAAAATGTCTCCTACTCCGCTGTAC and reverse primer TTTTCCTTTTGCGGCCGCTTTGCCAATAGATTTGT (SacII and NotI sites underlined), resulting in a translational fusion with the plasmid encoded C-terminal hexa-histidine tag. An N-terminal truncated construct lacking the first 776 codons (*Δ1-776 AgTRPA1*) was also subcloned into pPICZB vector between EcoRI and NotI restriction sites, using forward primer GCGGAATTCAAAATGTCTAAGTGGAACTCCTACGGC (EcoRI site underlined) and the same reverse primer as was used for the full-length construct. Both forward primers introduced an extra serine residue after the initiation methionine to optimize the translational initiation in *Pichia pastoris.* The constructs were verified by DNA sequencing and plasmids encoding the His-tagged AgTRPA1 (here on referred to as AgTRPA1) or the His-tagged Δ1-776 AgTRPA1 (here on referred to as Δ1-776 AgTRPA1) were electroporated into the methylotrophic *Pichia pastoris* strain X-33 (*Pichia* Expression Kit manual, Invitrogen). High gene copy clones were selected on zeocin as described previously (Norden et al., 2011) and the integrity of constructs were confirmed by PCR and subsequent agarose gel electrophoresis. Crude lysates of induced cultures were screened to identify high expression clones, using an anti tetra-histidine antibody and western blot (Norden et al., 2011).

Large-scale expression of AgTRPA1 and Δ1-776 AgTRPA1 was conducted in a 3 l bench top fermenter (Belach bioteknik). The cells obtained after expression in fermenter were collected and crude membrane was prepared as described elsewhere (Karlsson et al., 2003). Briefly, the cells were resuspended in ice cold breaking buffer (50 mM NaH_2PO_4, 1 mM EDTA, 5% glycerol, 1 mM PMSF (MBL International Corporation), pH 7.4) and lysis was carried out using a bead beater (Biospec product). The cell lysate was centrifuged in cold at 7,000 g for 30 min to remove the cell debris and the supernatant was centrifuged again at 100,000 g for 2 h to pellet the crude membrane. The crude membranes were washed with urea and alkali to remove peripheral proteins (Karlsson et al., 2003).

The washed membranes were resuspended in buffer A (20 mM HEPES, 0.5 M NaCl, 10% glycerol, 2 mM β-mercapto ethanol (βME), 1 mM PMSF, 100 µM leupeptin (Sigma-Aldrich), 10 µM pepstatin (Sigma-Aldrich) and 1% fos-cholin-12 (FC-12; Anagrade, Anatrace) pH 7.8) at room temperature for 2 h to solubilize the AgTRPA1 and Δ1-776 AgTRPA1 protein. The soluble fraction was separated by ultracentrifugation at 100,000 g for 30 min. The supernatant was loaded onto equilibrated Ni-NTA resin and incubated overnight at 4°C with gentle agitation to allow binding of His-tagged proteins. The Ni-NTA resin was washed with buffer B (20 mM HEPES, 0.3 M NaCl, 10% glycerol, 2 mM βME, 1 mM PMSF, 100 µM leupeptin, 10 µM pepstatin and 0.15% FC-12, pH 7.8) supplemented 30 mM imidazole to remove loosely bound proteins and the His-tagged proteins were eluted with 300 mM imidazole in Buffer B. Eluted proteins were concentrated using a VIVASPIN concentrator with a 50 and a 100 kDa cutoff for Δ1-776 AgTRPA1 and AgTRPA1, respectively.

The proteins were further purified on a Hiload Superdex 200 16/60 gel filtration column (GE healthcare) equilibrated with PBS buffer (10 mM potassium phosphate, 150 mM NaCl, pH 7.5) supplemented with 10% glycerol and 0.15% FC-12. The purity of AgTRPA1 and Δ1-776 AgTRPA1 were assessed by SDS-PAGE and western blot. The protein concentration was determined by NanoDrop spectrophotometer using calculated extinction coefficients based on the amino acid composition http://web.expasy.org/protparam/. The extinction coefficients for AgTRPA1 and Δ1-776 AgTRPA1 in water measured at 280 nm were 121475 and 69580 M^{-1} cm^{-1}, respectively.

Synchrotron Radiation Circular Dichroism (SRCD)

Far UV Synchrotron Radiation Circular Dichroism (SRCD) spectra of purified AgTRPA1 and Δ1-776 AgTRPA1, at a concentration of 0.6 mg/ml and 1.3 mg/ml respectively in 10 mM potassium phosphate, 40 mM NaCl, 60 mM KF, 10% glycerol and 0.15% FC-12, pH 7.5, were collected at beamline CD1 of the ASTRID2 storage ring at University of

Aarhus, Denmark. To monitor the temperature dependent changes in secondary structure, spectra between 180 and 280 nm were collected at different temperature (25-80^{o}C), allowing 5 min of equilibration time at each temperature. All the measurements were performed in a quartz cell (0.0102 cm path length). The buffer without protein was also measured to subtract the baseline from SRCD spectra (Whitmore and Wallace, 2004). The subtracted SRCD (mdeg) signals were normalized to the maximal values and plotted against the temperature to generate transition curves (Lees et al., 2004). To obtain midpoints the data were fitted to a non-linear Boltzman sigmoidal equation using GraphPad Prism version 6.00 (GraphPad Software La Jolla California, USA).

Tryptophan fluorescence

Changes in emission of intrinsic tryptophan fluorescence upon binding of the electrophilic ligand, allyl isothiocyanate (AITC) was monitored at ambient temperature (22^{o}C) using a Perkin Elmer spectrofluorimeter. Briefly, the purified AgTRPA1 or Δ1-776 AgTRPA1 (0.6 μM) was pre-incubated with different concentrations of AITC (0 μM-4000 μM) for 15 min at room temperature. Excitation was done at 280 nm and emission spectra were collected from 310 nm to 400 nm. The spectra for different concentrations of AITC without protein were also recorded in similar manner to correct the baseline. The emission data at 337 nm were fitted to sigmoidal dose response equation using GraphPad Prism version 6.00 (GraphPad Software La Jolla California, USA) to estimate pEC50 values. The extra-sum-of-squares F-test within GraphPad Prism was used to evaluate the null hypothesis of a shared pEC50 value for AgTRPA1 and Δ1-776 AgTRPA1. Temperature dependent changes in fluorescence emission of AgTRPA1 were also examined from 25^{o}C to 48^{o}C.

A topology plot was generated with TeXtopo (Beitz, 2000) via the web application Protter (Omasits et al., 2014), based on manual alignments and the structure of hTRPA1 (PDB ID:3J9P). Structural pictures were rendered in PyMOL (Schrodinger, 2010).

Preparation of giant unilamellar vesicles

Giant unilameller vesicles (GUVs) were produced by the electroformation method, using a Vesicle Prep Pro Station (Nanion Technologies) (Gassmann et al., 2009; Kreir et al., 2008). Breifly, a lipid stock was prepared by mixing 10 mM 1,2-diphytanoyl-sn-glycero-3-phosphocholine (DPhPC) and 1 mM cholesterol in trichloromethane. Approximately 20 µl of this solution was placed on the indium tin oxide (ITO) coated glass slide and allowed to dry. After complete evaporation of trichloromethane, an O-ring was placed on the dry lipids. The ITO coated glass surface is electrically conductive and serves as an electrode. To prevent conduction between two glass slides 300 µl 1M sorbitol was added gently. The ITO coated glass slides were assembled on the Vescicle prep pro station (Nanion Technologies), orienting ITO coated conductive surfaces towards each other. Vesicles were formed by electro swelling under the influence of an alternating electrical field for 2 h at 36°C.

Reconstitution of purified proteins into planar lipid bilayer or giant unilamellar vesicles

Further, GUVs were used for making either planar lipid bilayers or proteoliposomes (Gassmann et al., 2009; Kreir et al., 2008). For formation of a planar lipid bilayer, 5 µl GUV solution was pipetted onto the patch-clamp chip (aperture of 1–2 µm), applying a negative pressure from –10 to –40 mbar to position vesicles over the aperture. The process of bilayer formation was controlled by Patch Control software (Nanion Technologies).

Approximately 0.2 µl of AgTRPA1 or Δ1–776 AgTRPA1 protein micelles solution of concentration 50–100 µg/ml was added to preformed planar lipid bilayers (final concentration of protein 0.15 –0.2 µg/ml) in studies of the AITC responsiveness of the ion channels.
For preparation of proteoliposomes, the purified proteins were added to the GUV solution (final protein concentration of 2.5–10 µg/ml for AgTRPA1 and Δ1–776 AgTRPA1), and the mixture was incubated for 2 h at room

temperature. Detergent was removed with polystyrene Biobeads SM2 (Bio-Rad), using 40 mg beads per ml. After an initial incubation at room temperature for 2 h, the incubation was continued overnight at 4°C and Biobeads were subsequently removed by centrifugation. The proteoliposomes were applied onto the patch-clamp chip to allow formation of planar lipid bilayers, as described above, and used in studies of heat activation of the ion channels.

Electrophysiological recordings

A symmetrical K^+ solution of the following composition was used in all lipid bilayer recordings: 50 mM KCl, 10 mM NaCl, 60 mM KF, 20 mM EGTA, and 10 mM HEPES (adjusted to pH 7.2 with KOH). Signals were acquired with an EPC 10 amplifier (HEKA) and the data acquisition software PatchMaster (HEKA) at a sampling rate of 50 kHz. The recorded data were digitally filtered at 3 kHz. The patch-clamp experiments were performed either at room temperature or the stated temperatures. The Port-a-Patch was equipped with an external perfusion system (Nanion Technologies) and an SC-20 dual in-line solution heater/cooler connected to a temperature controlled (CL-100) liquid cooling system (Warner Instruments) to control the temperature of the perfusion solution. Electrophysiological data were analyzed using Clampfit 9 (Molecular Devices), Igor Pro (Wave Metrics software). Data were filtered by a low-pass Gaussian filter at 1,000 and 500 Hz for analyses and traces, respectively. The single-channel mean conductance (Gs) was obtained from Gaussian fit of all-points amplitude histograms. The single-channel mean open probability (Po) was calculated from time constant values, which were obtained from exponential standard fits of dwell time histograms.

The Q10 for Po was obtained from the following equation (Latorre et al., 2007; Voets, 2012):

$$Q10 = \left(\frac{P_{o2}}{P_{o1}}\right)^{10/(T_2-T_1)}$$

Author contributions

E.D.H., P.M.Z. and U.J. conceived and designed the study. P.M.Z. and U.J. directed the study. S.S., P.K. and U.J. planned, performed and analyzed biochemical and biophysical experiments. L.M., E.D.H. and P.M.Z. planned, performed and analyzed electrophysiology experiments. S.S., P.M.Z. and U.J. drafted the manuscript. P.M.Z. and U.J. wrote the paper. All authors discussed the results and commented on the manuscript.

Acknowledgements

This work was supported by the Swedish Research Council 2014-3801, 2010-5787 (P.M.Z., E.D.H.), 2007-6110 (U.J.), Formas 2007-718 (P.M.Z., E.D.H., U.J., P.K.), the Research School of Pharmaceutical Sciences FLÄK (U.J., P.M.Z.) and the Medical Faculty at Lund University (P.M.Z., E.D.H.). We thank Brita Sundén-Andersson and Adine Karlsson for technical assistance, and Dr. Paul Garrity for providing a plasmid carrying the coding sequence for TRPA1(A) from *Anopheles gambiae*. SRCD spectra were collected at ASTRID2 and sponsored by the CALIPSO program. We thank Dr. Nykola Jones and Dr. Søren Vrønning Hoffmann for providing time and assistance at ASTRID2. The authors declare no competing financial interests.

References

Baez, D., Raddatz, N., Ferreira, G., Gonzalez, C., and Latorre, R. (2014). Gating of thermally activated channels. Curr Top Membr *74*, 51-87.

Bandell, M., Story, G.M., Hwang, S.W., Viswanath, V., Eid, S.R., Petrus, M.J., Earley, T.J., and Patapoutian, A. (2004). Noxious Cold Ion Channel TRPA1 Is Activated by Pungent Compounds and Bradykinin. Neuron *41*, 849-857.

Bautista, D.M., Movahed, P., Hinman, A., Axelsson, H.E., Sterner, O., Hogestatt, E.D., Julius, D., Jordt, S.E., and Zygmunt, P.M. (2005). Pungent products from garlic activate the sensory ion channel TRPA1. Proc Natl Acad Sci U S A *102*, 12248-12252.

Beitz, E. (2000). T(E)Xtopo: shaded membrane protein topology plots in LAT(E)X2epsilon. Bioinformatics *16*, 1050-1051.

Clapham, D.E., and Miller, C. (2011). A thermodynamic framework for understanding temperature sensing by transient receptor potential (TRP) channels. Proc Natl Acad Sci U S A *108*, 19492-19497.

Cordero-Morales, J.F., Gracheva, E.O., and Julius, D. (2011). Cytoplasmic ankyrin repeats of transient receptor potential A1 (TRPA1) dictate sensitivity to thermal and chemical stimuli. Proc Natl Acad Sci U S A *108*, E1184-1191.

Gassmann, O., Kreir, M., Ambrosi, C., Pranskevich, J., Oshima, A., Roling, C., Sosinsky, G., Fertig, N., and Steinem, C. (2009). The M34A mutant of Connexin26 reveals active conductance states in pore-suspending membranes. J Struct Biol *168*, 168-176.

Gracheva, E.O., Ingolia, N.T., Kelly, Y.M., Cordero-Morales, J.F., Hollopeter, G., Chesler, A.T., Sanchez, E.E., Perez, J.C., Weissman, J.S., and Julius, D. (2010). Molecular basis of infrared detection by snakes. Nature *464*, 1006-1011.

Hamada, F.N., Rosenzweig, M., Kang, K., Pulver, S.R., Ghezzi, A., Jegla, T.J., and Garrity, P.A. (2008). An internal thermal sensor controlling temperature preference in Drosophila. Nature *454*, 217-220.

Hilton, J.K., Rath, P., Helsell, C.V., Beckstein, O., and Van Horn, W.D. (2015). Understanding thermosensitive transient receptor potential channels as versatile polymodal cellular sensors. Biochemistry *54*, 2401-2413.

Hinman, A., Chuang, H.H., Bautista, D.M., and Julius, D. (2006). TRP channel activation by reversible covalent modification. Proc Natl Acad Sci U S A *103*, 19564-19568.

Holzer, P. (2011). Transient receptor potential (TRP) channels as drug targets for diseases of the digestive system. Pharmacol Ther *131*, 142-170.

Horsefield, R., Norden, K., Fellert, M., Backmark, A., Tornroth-Horsefield, S., Terwisscha van Scheltinga, A.C., Kvassman, J., Kjellbom, P., Johanson, U., and Neutze, R. (2008). High-resolution x-ray structure of human aquaporin 5. Proc Natl Acad Sci U S A *105*, 13327-13332.

Jabba, S., Goyal, R., Sosa-Pagan, J.O., Moldenhauer, H., Wu, J., Kalmeta, B., Bandell, M., Latorre, R., Patapoutian, A., and Grandl, J. (2014). Directionality of Temperature Activation in Mouse TRPA1 Ion Channel Can Be Inverted by Single-Point Mutations in Ankyrin Repeat Six. Neuron *82*, 1017-1031.

Jordt, S.E., Bautista, D.M., Chuang, H.H., McKemy, D.D., Zygmunt, P.M., Högestätt, E.D., Meng, I.D., and Julius, D. (2004). Mustard oils and cannabinoids excite sensory nerve fibres through the TRP channel ANKTM1. Nature *427*, 260-265.

Julius, D. (2013). TRP channels and pain. Annu Rev Cell Dev Biol *29*, 355-384.

Kang, K., Panzano, V.C., Chang, E.C., Ni, L., Dainis, A.M., Jenkins, A.M., Regna, K., Muskavitch, M.A., and Garrity, P.A. (2012). Modulation of TRPA1 thermal sensitivity enables sensory discrimination in Drosophila. Nature *481*, 76-80.

Kang, K., Pulver, S., Panzano, V., Chang, E., Griffith, L., Theobald, D., and Garrity, P. (2010a). Analysis of Drosophila TRPA1 reveals an ancient origin for human chemical nociception. Nature *464*, 597-600.

Kang, K., Pulver, S.R., Panzano, V.C., Chang, E.C., Griffith, L.C., Theobald, D.L., and Garrity, P.A. (2010b). Analysis of Drosophila TRPA1 reveals an ancient origin for human chemical nociception. Nature *464*, 597-600.

Karashima, Y., Talavera, K., Everaerts, W., Janssens, A., Kwan, K.Y., Vennekens, R., Nilius, B., and Voets, T. (2009). TRPA1 acts as a cold sensor in vitro and in vivo. Proc Natl Acad Sci U S A *106*, 1273-1278.

Karlsson, M., Fotiadis, D., Sjovall, S., Johansson, I., Hedfalk, K., Engel, A., and Kjellbom, P. (2003). Reconstitution of water channel function of an aquaporin overexpressed and purified from Pichia pastoris. FEBS Lett *537*, 68-72.

Kreir, M., Farre, C., Beckler, M., George, M., and Fertig, N. (2008). Rapid screening of membrane protein activity: electrophysiological analysis of OmpF reconstituted in proteoliposomes. Lab Chip *8*, 587-595.

Kremeyer, B., Lopera, F., Cox, J.J., Momin, A., Rugiero, F., Marsh, S., Woods, C.G., Jones, N.G., Paterson, K.J., Fricker, F.R., *et al.* (2010). A gain-of-function mutation in TRPA1 causes familial episodic pain syndrome. Neuron *66*, 671-680.

Lakowicz, J.R. (2002). Topics in fluorescence spectroscopy. In Protein fluorescence, J.R. Lakowicz, ed. (New York: Kluwer Academic Publisher).

Latorre, R., Vargas, G., Orta, G., and Brauchi, S. (2007). Voltage and Temperature Gating of ThermoTRP Channels. In TRP Ion Channel Function in Sensory Transduction and Cellular Signaling Cascades, W.B. Liedtke, and S. Heller, eds. (Boca Raton (FL)).

Laursen, W.J., Anderson, E.O., Hoffstaetter, L.J., Bagriantsev, S.N., and Gracheva, E.O. (2015). Species-specific temperature sensitivity of TRPA1. Temperature *2*, 214-226.

Lees, J.G., Smith, B.R., Wien, F., Miles, A.J., and Wallace, B.A. (2004). CDtool-an integrated software package for circular dichroism spectroscopic data processing, analysis, and archiving. Anal Biochem *332*, 285-289.

Liu, C., and Zwiebel, L.J. (2013). Molecular characterization of larval peripheral thermosensory responses of the malaria vector mosquito Anopheles gambiae. PLoS One *8*, e72595.

Macpherson, L.J., Dubin, A.E., Evans, M.J., Marr, F., Schultz, P.G., Cravatt, B.F., and Patapoutian, A. (2007). Noxious compounds activate TRPA1 ion channels through covalent modification of cysteines. Nature *445*, 541-545.

Macpherson, L.J., Geierstanger, B.H., Viswanath, V., Bandell, M., Eid, S.R., Hwang, S., and Patapoutian, A. (2005). The pungency of garlic: activation of TRPA1 and TRPV1 in response to allicin. Curr Biol *15*, 929-934.

Moparthi, L., Survery, S., Kreir, M., Simonsen, C., Kjellbom, P., Hogestatt, E.D., Johanson, U., and Zygmunt, P.M. (2014). Human TRPA1 is intrinsically cold- and chemosensitive with and without its N-terminal ankyrin repeat domain. Proc Natl Acad Sci U S A *111*, 16901-16906.

Nilius, B., and Owsianik, G. (2011). The transient receptor potential family of ion channels. Genome Biol *12*, 218.

Norden, K., Agemark, M., Danielson, J.A., Alexandersson, E., Kjellbom, P., and Johanson, U. (2011). Increasing gene dosage greatly enhances recombinant expression of aquaporins in Pichia pastoris. BMC Biotechnol *11*, 47.

Omasits, U., Ahrens, C.H., Muller, S., and Wollscheid, B. (2014). Protter: interactive protein feature visualization and integration with experimental proteomic data. Bioinformatics *30*, 884-886.

Panzano, V.C., Kang, K., and Garrity, P.A. (2010). Infrared snake eyes: TRPA1 and the thermal sensitivity of the snake pit organ. Sci Signal *3*, pe22.

Patapoutian, A., Tate, S., and Woolf, C.J. (2009). Transient receptor potential channels: targeting pain at the source. Nat Rev Drug Discov *8*, 55-68.

Paulsen, C.E., Armache, J.P., Gao, Y., Cheng, Y., and Julius, D. (2015). Structure of the TRPA1 ion channel suggests regulatory mechanisms. Nature *520*, 511-517.

Sawada, Y., Hosokawa, H., Hori, A., Matsumura, K., and Kobayashi, S. (2007). Cold sensitivity of recombinant TRPA1 channels. Brain Res *1160*, 39-46.

Schrodinger, LLC, The PyMOL Molecular Graphics System, Version 1.5.0.4 (2010).

Shen, C., Menon, R., Das, D., Bansal, N., Nahar, N., Guduru, N., Jaegle, S., Peckham, J., and Reshetnyak, Y.K. (2008). The protein fluorescence and structural toolkit: Database and programs for the analysis of protein fluorescence and structural data. Proteins *71*, 1744-1754.

Story, G.M., Peier, A.M., Reeve, A.J., Eid, S.R., Mosbacher, J., Hricik, T.R., Earley, T.J., Hergarden, A.C., Andersson, D.A., Hwang, S.W., *et al.* (2003). ANKTM1, a TRP-like channel expressed in nociceptive neurons, is activated by cold temperatures. Cell *112*, 819-829.

Tornroth-Horsefield, S., Wang, Y., Hedfalk, K., Johanson, U., Karlsson, M., Tajkhorshid, E., Neutze, R., and Kjellbom, P. (2006). Structural mechanism of plant aquaporin gating. Nature *439*, 688-694.

Wang, G., Qiu, Y.T., Lu, T., Kwon, H.W., Pitts, R.J., Van Loon, J.J., Takken, W., and Zwiebel, L.J. (2009). Anopheles gambiae TRPA1 is a heat-activated channel expressed in thermosensitive sensilla of female antennae. Eur J Neurosci *30*, 967-974.

Wang, H., Schupp, M., Zurborg, S., and Heppenstall, P.A. (2013). Residues in the pore region of Drosophila transient receptor potential A1 dictate sensitivity to thermal stimuli. J Physiol *591*, 185-201.

Whitmore, L., and Wallace, B.A. (2004). DICHROWEB, an online server for protein secondary structure analyses from circular dichroism spectroscopic data. Nucleic Acids Res *32*, W668-673.

Viswanath, V., Story, G.M., Peier, A.M., Petrus, M.J., Lee, V.M., Hwang, S.W., Patapoutian, A., and Jegla, T. (2003). Opposite thermosensor in fruitfly and mouse. Nature *423*, 822-823.

Voets, T. (2012). Quantifying and modeling the temperature-dependent gating of TRP channels. Rev Physiol Biochem Pharmacol *162*, 91-119.

Vriens, J., Nilius, B., and Voets, T. (2014). Peripheral thermosensation in mammals. Nat Rev Neurosci *15*, 573-589.

Xiao, B., Dubin, A.E., Bursulaya, B., Viswanath, V., Jegla, T.J., and Patapoutian, A. (2008). Identification of transmembrane domain 5 as a critical molecular determinant of menthol sensitivity in mammalian TRPA1 channels. J Neurosci *28*, 9640-9651.

Zhong, L., Bellemer, A., Yan, H., Ken, H., Jessica, R., Hwang, R.Y., Pitt, G.S., and Tracey, W.D. (2012). Thermosensory and nonthermosensory isoforms of Drosophila melanogaster TRPA1 reveal heat-sensor domains of a thermoTRP Channel. Cell Rep *1*, 43-55.

Zygmunt, P.M., and Högestätt, E.D. (2014). Trpa1. Handb Exp Pharmacol *222*, 583-630.

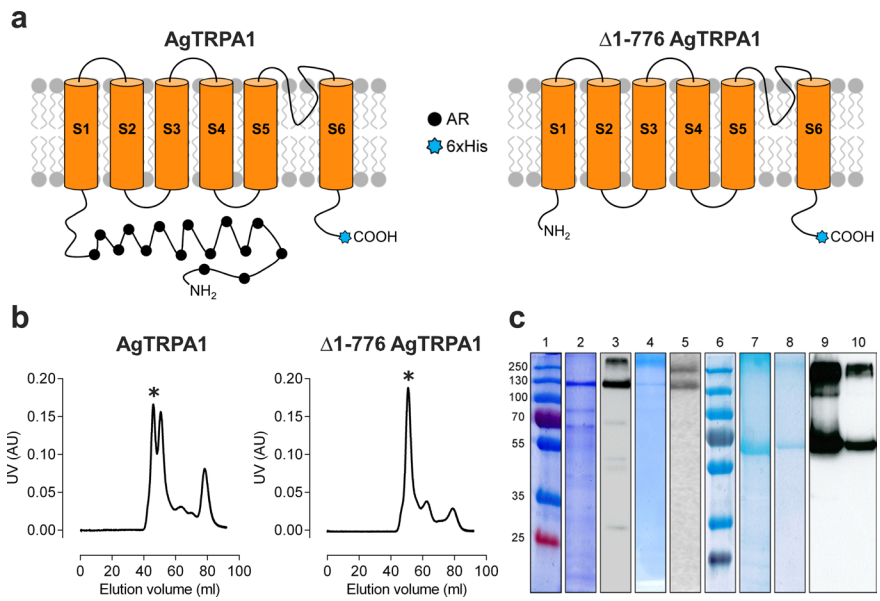

Figure 1. Purification of *Anopheles gambiae* TRPA1 full-length (AgTRPA1) and N-terminal truncated (Δ1-776 AgTRPA1) constructs. (**a**) Schematic representation of AgTRPA1 and Δ1-776 AgTRPA1 showing the N-terminal truncation, the six trans-membrane helices (S1-S6) with the pore region connecting last two helices (S5 and S6) and the N- and C-termini facing the cytoplasm. The N-terminal containing Ankyrin Repeats (AR; filled black circle) and C-terminal hexa His-tag (6xHis; blue star) are also indicated. (**b**) Purification profile of AgTRPA1 and Δ1-776 AgTRPA1 using Superdex 200 16/26 column with tetrameric fraction indicated by *. (**c**) SDS-PAGE and western blots of AgTRPA1 and Δ1-776 AgTRPA1. The panel is assembled from several gels and blots, thus two molecular weight markers are shown. Molecular weight markers (lane 1 and 6), AgTRPA1 after Ni-NTA affinity chromatography (lane 2 and 3), tetrameric fraction* after size exclusion chromatography (lane 4 and 5). Δ1-776 AgTRPA1 after Ni-NTA affinity chromatography (lane 7 and 9), and tetrameric fraction* after size exclusion chromatography (lane 8 and 10).

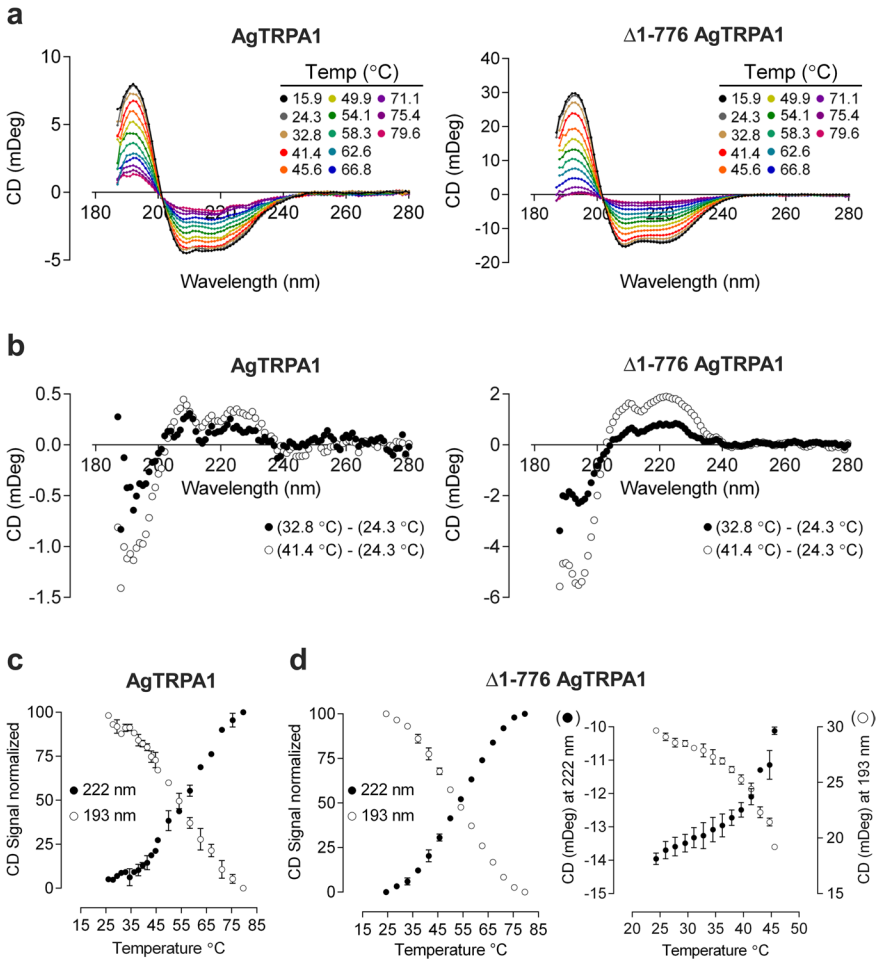

Figure 2. SRCD spectra and thermal transition curves. (**a**) SRCD spectra of AgTRPA1 and Δ1-776 AgTRPA1 obtained at higher temperatures show gradual loss of the maximum at 193 nm and the two minima at 210 and 222 nm that are characteristic for α-helical proteins. (**b**) Differential plot of spectra recorded at two different temperatures for AgTRPA1 and Δ1-776 AgTRPA1. Normalized transition curves at 193 nm and 222 nm as a function of temperature for (**c**) AgTRPA1 (n= 2) and (**d**) for Δ1-776 AgTRPA1 (n= 2). Additional data points collected between 24ºC and 45ºC for the latter construct (right) plotted without normalization of data (n=3). In c and d the average is plotted and error bars indicate SD.

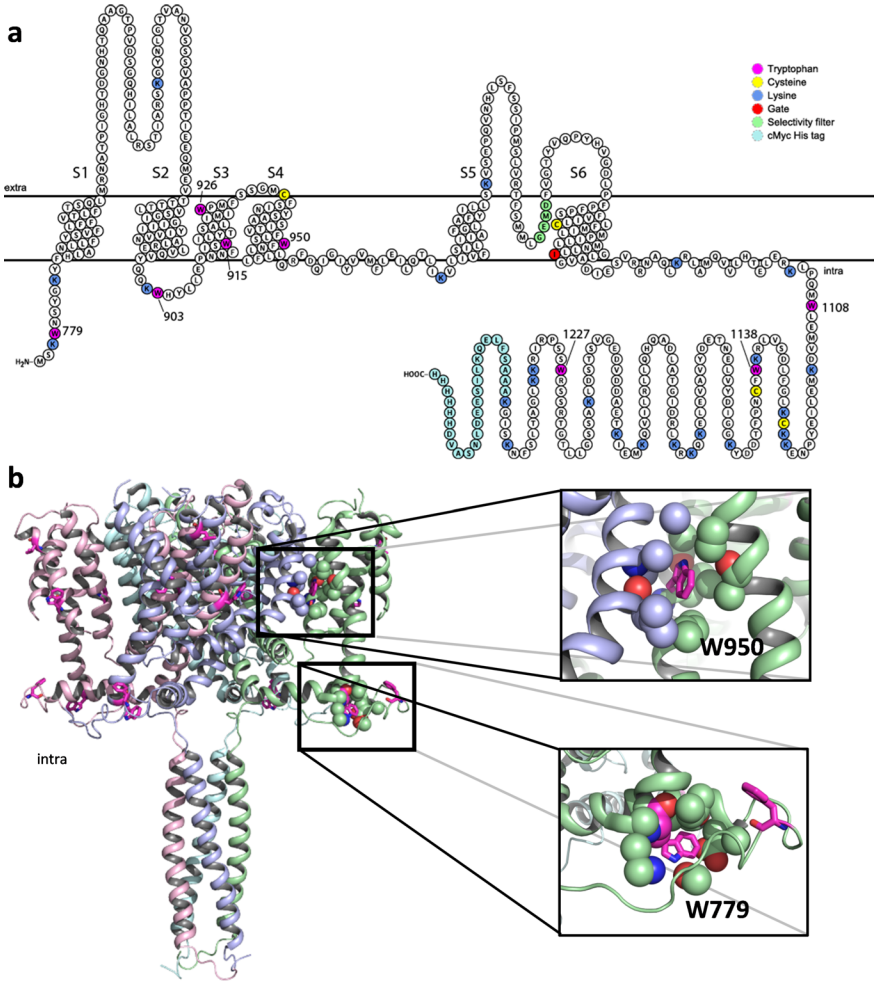

Figure 3. Tryptophan positions and potential AITC binding sites. (**a**) Topology plot of Δ1-776 AgTRPA1 highlighting all lysines and cysteines, which are potential binding sites for AITC, as well as the eight tryptophans. (**b**) Equivalent structure of tetrameric human TRPA1 (PDB ID 3J9P without the N-terminal ARD). The monomers are color coded and residues corresponding to tryptophans in Δ1-776 AgTRPA1 are indicated in magenta, omitting W903, W1138 and W1227 which are located in unresolved regions. Transmembrane domains are shown at the top and cytoplasmic regions in the lower half of the picture. Close-ups of two conserved tryptophan residues, corresponding to W779 and W950 in AgTRPA1. A similar setting of these residues in AgTRPA1 and hTRPA1 is supported by the alignment in Fig. S1. W950 in helix S4 is positioned in a hydrophobic pocket, sandwiched between helices S1 and S5 from a neighboring monomer whereas W779 resides in a more polar environment, likely to result in a lower quantum yield of fluorescence. All atoms within 5Å of the indole ring of the tryptophans are shown as spheres, oxygen and nitrogen atoms are colored red and dark blue, respectively.

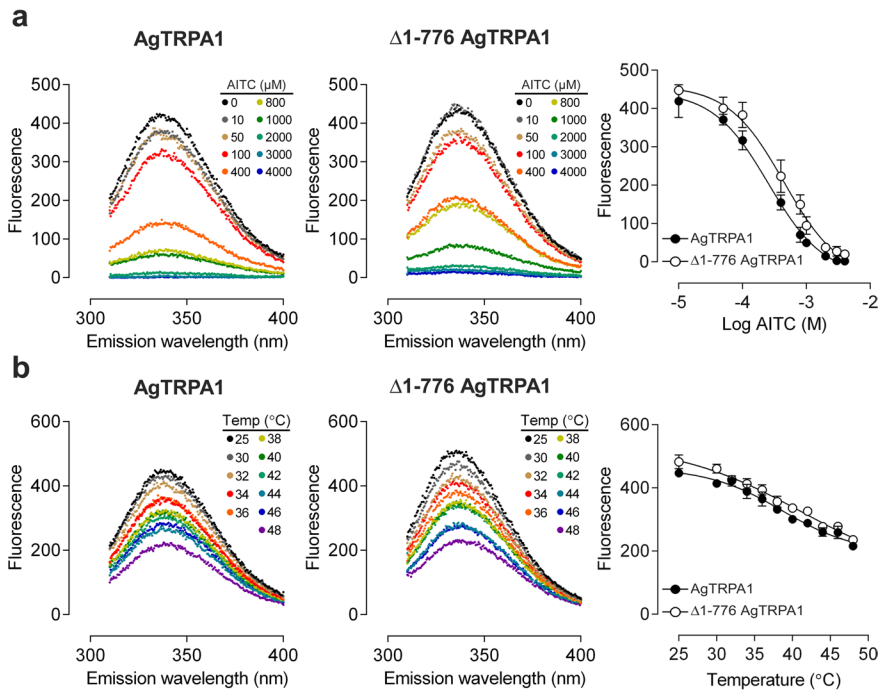

Figure 4. Quenching of intrinsic tryptophan fluorescence. (**a**) Binding of AITC quenches the tryptophan fluorescence emission intensity at 337 nm of AgTRPA1 and Δ1-776 AgTRPA1 in a concentration-dependent manner. The data was fitted to a sigmoidal concentration-response equation and the EC50 was estimated to be 256 μM and 444 μM (3.591 ± 0.046 and 3.352 ± 0.056; average pEC50 ± SEM; n = 4) for AgTRPA1 and Δ1-776 AgTRPA1, respectively. The null hypothesis with a common pEC50 value was rejected ($P < 0.005$). (**b**) Temperature-induced quenching of intrinsic tryptophan fluorescence of AgTRPA1 and Δ1-776 AgTRPA1. The midpoints are 38.7 ± 1.0°C and 41.1 ± 3.3°C (average ± SEM; n=3) for AgTRPA1 and Δ1-776 AgTRPA1, respectively. No shift is detected in the intrinsic fluorescence maximal intensity wavelength when AgTRPA1 or Δ1-776 AgTRPA1 is exposed to either AITC (**a**) or temperature (**b**).

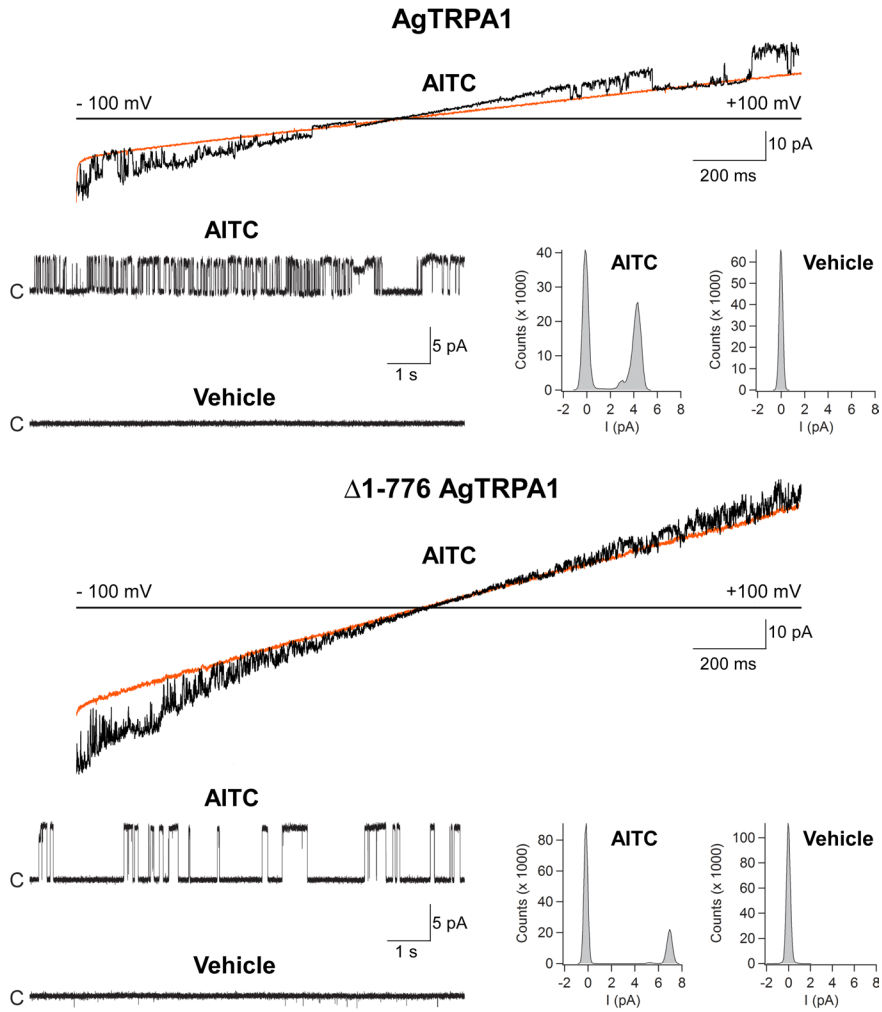

Figure 5. The electrophilic compound allyl isothiocyanate (AITC) activates purified AgTRPA1 with and without its N-terminal ARD. As shown in experiments measuring ramp currents (-100 to +100 mV in 2 s), AgTRPA1 and AgTRPA1 without its N-terminal ARD (Δ1-766 AgTRPA1) responded to AITC (100 μM) with channel currents at both negative and positive test potentials (black traces). Orange traces show baseline currents. At a steady state test potential of +60 mV, distinct single channel openings were observed. The vehicle of AITC (ethanol 1%) did not evoke activation of either AgTRPA1 variant. Shown are representative traces and corresponding amplitude histograms (see Table S2 for calculated single channel Gs and Po values). Purified AgTRPA1 and Δ1-766 AgTRPA1 were inserted into planar lipid bilayers and channel currents were recorded with the patch-clamp technique in a symmetrical K^+ solution (c = closed channel state; up-ward deflections = open channel state).

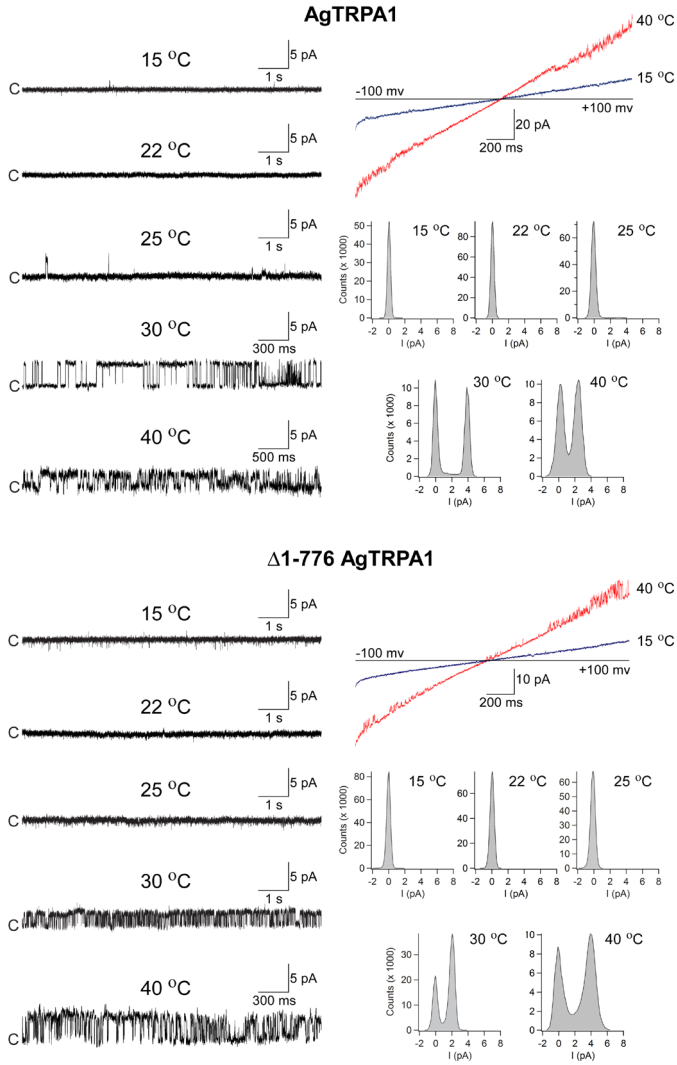

Figure 6. Heat activates purified AgTRPA1 with and without its N-terminal ARD. As shown in experiments measuring ramp currents (-100 to +100 mV in 2 s), AgTRPA1 and AgTRPA1 without its N-terminal ARD (Δ1-766 AgTRPA1) responded to increased temperatures with channel currents at both negative and positive test potentials. At a steady state test potential of +60 mV, distinct single channel openings were observed at 30°C and 40°C. Occasionally channel opening appeared already at 25°C for AgTRPA1, but never for Δ1-766 AgTRPA1. Shown are representative traces and corresponding amplitude histograms (see Table S2 for calculated single channel Gs and Po values). Purified AgTRPA1 and Δ1-766 AgTRPA1 were inserted into planar lipid bilayers and channel currents were recorded with the patch-clamp technique in a symmetrical K^+ solution (c = closed channel state; up-ward deflections = open channel state).

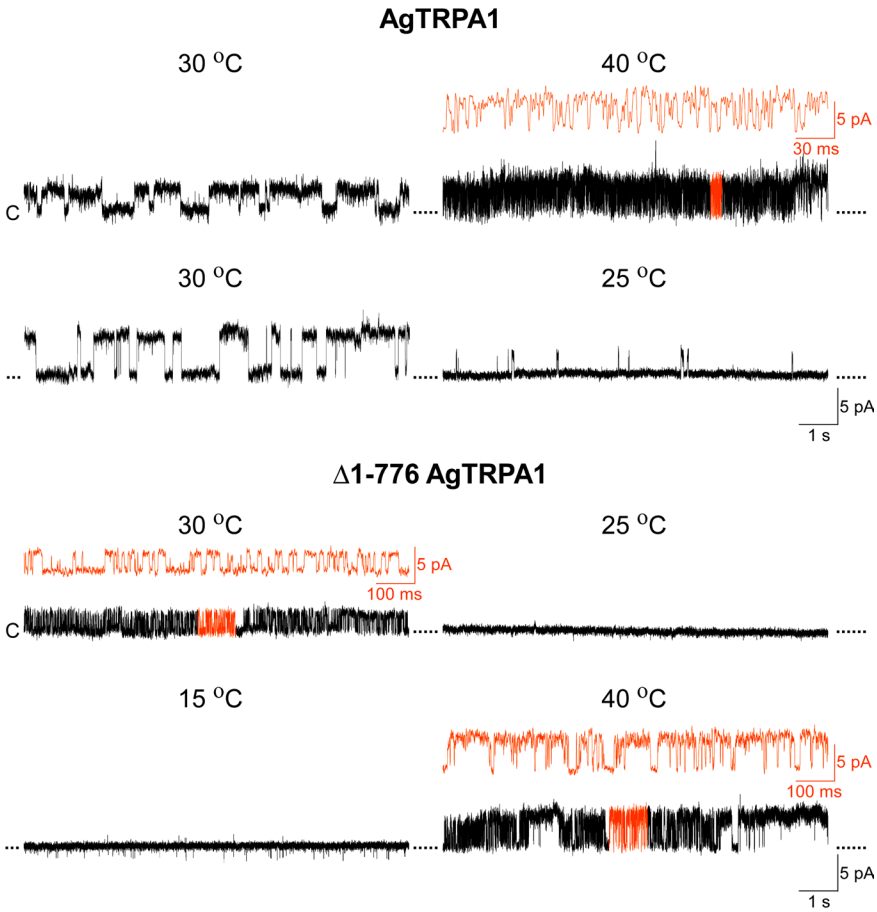

Figure 7. Reversibility of AgTRPA1 heat responses. The heat responses of AgTRPA1 with and without its N-terminal ARD (Δ1-766 AgTRPA1) were reversible when continuously exposed to different temperatures (30 to 35 min total recording time). Shown are representative recordings from 2 to 3 separate experiments. Black traces are shown at the same time scale (1 s) whereas orange traces show part of the recordings at a higher time resolution (30 and 100 ms). Purified AgTRPA1 (temperatures 30, 40, 30 and 25°C) and Δ1-766 AgTRPA1 (temperatures 30, 25, 15 and 40°C) were inserted into planar lipid bilayers and channel currents were recorded with the patch-clamp technique in a symmetrical K^+ solution at a test potential of +60 mV (c = closed channel state; upward deflections = open channel state).

Table S1. Related to Figure 2.

Midpoints for temperature transitions from SRCD AgTRPA1 and Δ1-776 AgTRPA1.

AgTRPA1			Δ 1-766 AgTRPA1		
Midpoint 193 nm (°C)	Midpoint 222 nm (°C)	n	Midpoint 193 nm (°C)	Midpoint 222 nm (°C)	n
55.3 ± 0.8	58.1 ± 0.8	2	53.6 ± 1.0	53.8 ± 1.1	2

The midpoint ± SD was obtained from fitted curve to two experiments.

Table S2. Related to Figure 5 and 6.

Single channel conductance and open probability values for AgTRPA1 and Δ1-776 AgTRPA1 activated by allyl isothiocyanate (AITC) and heat at a test potential of +60 mV.

	AgTRPA1		Δ1-766 AgTRPA1		AgTRPA1		Δ1-766 AgTRPA1	
Stimuli	Conductance (pS) mean ± SEM	n	Conductance (pS) mean ± SEM	n	Open probability mean ± SEM	n	Open probability mean ± SEM	n
AITC (100 μM)	56 ± 6[a]	6	87 ± 3[a]	6	0.53 ± 0.06[b]	5	0.28 ± 0.05[b]	6
30°C	74 ± 6[c,d]	3	29 ± 2[c,e]	4	0.45 ± 0.06	4	0.44 ± 0.04	5
40°C	40 ± 4[d]	4	50 ± 3[e]	3	0.53 ± 0.06	4	0.64 ± 0.04	3

[a] $P < 0.01$; unpaired t'test, two-tailed

[b] $P < 0.05$; unpaired t'test, two-tailed

[c,d,e] $P < 0.0001$, 1-way ANOVA, multiple comparisons

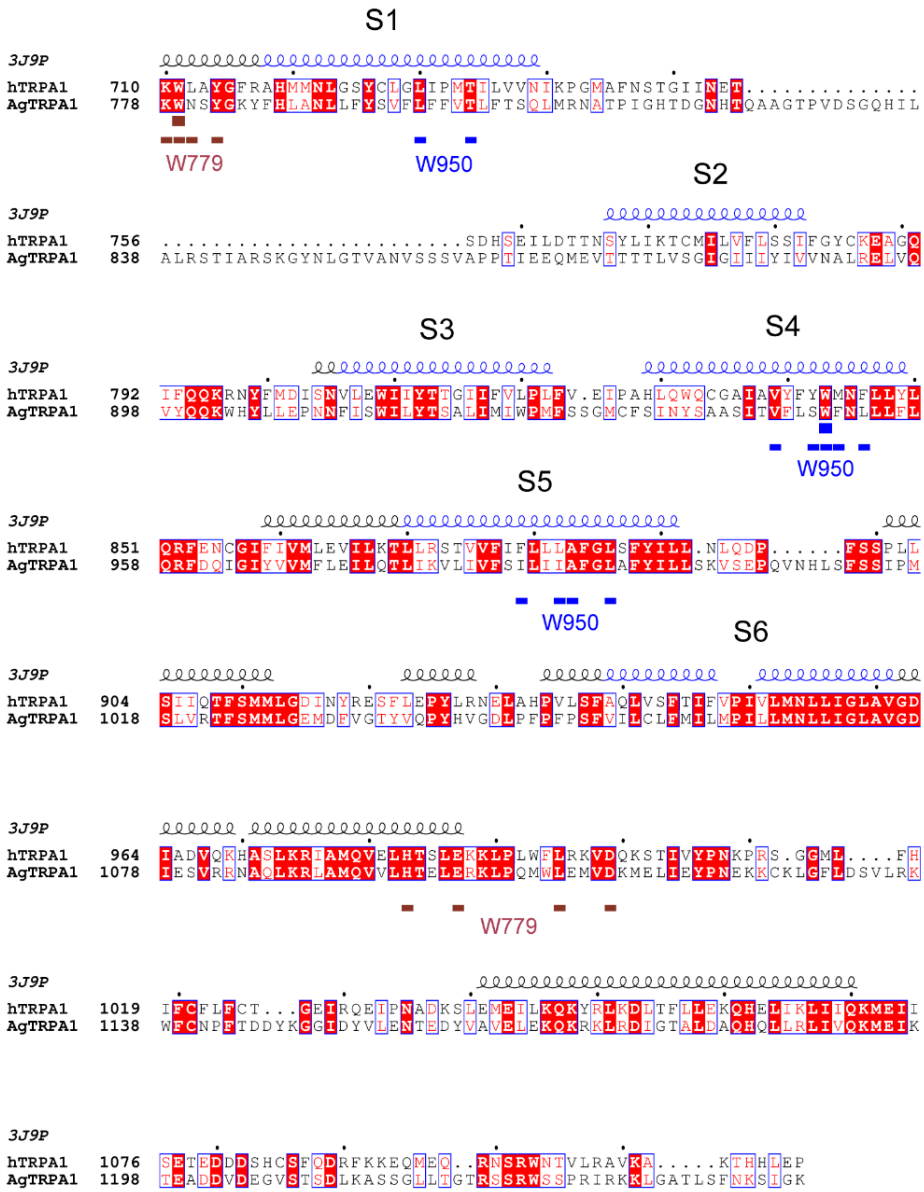

Figure S1. Related to Figure 3. Conservation of residues surrounding W779 and W950. Alignment of hTRPA1 and AgTRPA1 omitting the N-terminal ARD. The secondary structure of hTRPA1 extracted from PDB ID 3J9P is displayed at the top with transmembrane helices S1-S6 colored in blue. Residues within 5 Å of the indole rings of two tryptophans in 3J9P corresponding to W779 and W950 of AgTRPA1 are indicated in brown and blue, respectively, below the alignment.

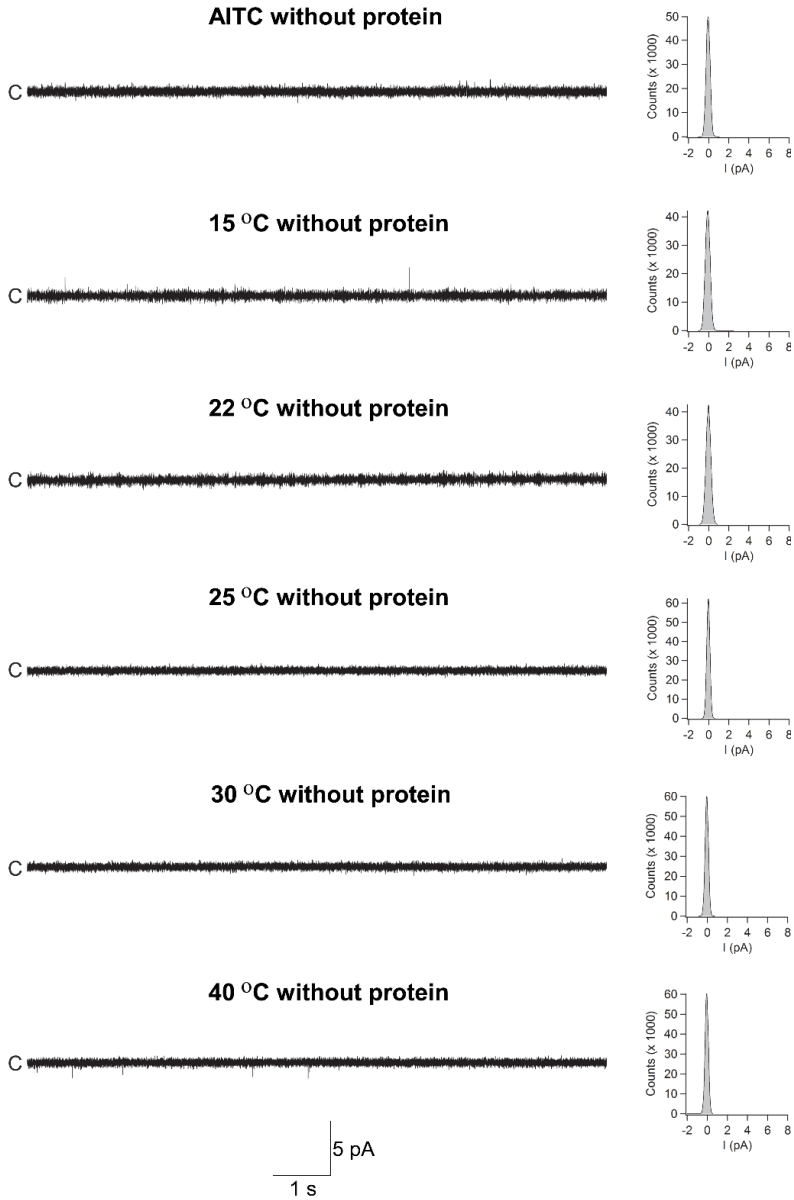

Figure S2. Related to Figure 5, 6 and 7. Control experiments without protein. Lipid bilayers without AgTRPA1 did not respond to the electrophilic compound AITC (100 µM) or various temperatures at a test potential of +60 mV (n = 4, c = closed channel state). Single channel currents were recorded with the patch-clamp technique in a symmetrical K^+ solution.

Paper IV

Agonist-induced conformational switch of the human TRPA1 ion channel detected by mass spectrometry

Lavanya Moparthi[a], Sven Kjellström[a], Edward D. Högestätt[b], Per Kjellbom[a], Milos R. Filipovic[c,d], Peter M. Zygmunt[b] and Urban Johanson[a,*]

[a]Department of Biochemistry and Structural Biology, Center for Molecular Protein Science, Lund University, SE-221 00 Lund, Sweden

[b]Clinical Chemistry & Pharmacology, Department of Laboratory Medicine, Lund University, SE-221 85 Lund, Sweden

[c]Department of Chemistry and Pharmacy, Friedrich-Alexander University Erlangen-Nuremberg, Egerlandstrasse 1, 91058 Erlangen, Germany.

[d]IBGC, UMR 5095, Universite de Bordeaux, 1, rue Camille Saint Saëns, CS 61390, 33077 Bordeaux cedex, France.

*Corresponding author: urban.johanson@biochemistry.lu.se

Abstract

The human Transient Receptor Potential A1 (hTRPA1) ion channel, also known as the wasabi receptor, act as a biosensor of various potentially harmful stimuli. It is activated by a wide range of chemicals, including the electrophilic compound N-methyl-maleimide (NMM), but the mechanism of activation is not fully understood. Here we used mass spectrometry to map and quantify the covalent labelling in hTRPA1 at three different concentrations of NMM. A functional truncated version of hTRPA1, lacking the large N-terminal ankyrin repeat domain (ARD), was also assessed in the same way.

In the full length hTRPA1 the labelling of different cysteines ranged from nil up to 95% already at the lowest concentration of NMM, suggesting large differences in reactivity of the thiols. Most important the labelling of some cysteine residues increase while others decrease with the concentration of NMM, both in the full length and the truncated protein. These findings indicate a conformational switch of the proteins, possibly associated with activation or desensitization of the ion channel. In addition, lysines in the transmembrane domain and the proximal N-terminal region were targeted by NMM, raising the possibility that this TRPA1 amino acid is also a key target for electrophilic activation of TRPA1.

Introduction

Animals have evolved a variety of biosensors to detect and avoid harmful conditions like detrimental chemicals and temperatures. Members of the transient receptor potential (TRP) ion channel family play an important role in the detection of such conditions. Among these ion channels, the sole mammalian member of the TRP ankyrin (TRPA) subfamily, TRPA1, has an important function in chemical nociception. This polymodal receptor is expressed in the peripheral sensory nerve endings that originate from the dorsal root, trigeminal and nodosa ganglia (Zygmunt and Högestätt, 2014). Similar to other TRPs, the functional unit of TRPA1 is a homotetramer, where each subunit has six transmembrane α-helices, whereof the last two and the intervening re-entrant pore loop contribute to the formation of the ion permeation pathway. Apart from the transmembrane domain, there are substantial cytosolic N- and C-terminal domains which constitute around 80% of the mass of the TRPA1 protein (Paulsen et al., 2015). The TRPA1 ion channel is activated by a large variety of chemicals, from exogenous plant derived chemicals and environmental toxic reagents to endogenous inflammatory mediators, such as isothiocyanates (mustard and wasabi), cinnamaldehyde (cinnamon), allicin and diallyl disulphide (garlic), acrolein (smoke and chemotherapeutic metabolite) and nitroxyl (Eberhardt et al., 2014). To this date, more than 100 compounds including non-electrophilic compounds have been identified as TRPA1 activators and the number is still growing (Zygmunt and Högestätt, 2014). Studies have shown that such chemicals interact with TRPA1 by different mechanisms, e.g. covalent interaction of electrophilic compounds with free thiols of cysteine residues, non-covalent interaction and oxidation of cysteines that eventually promote the formation of disulphide bonds (Eberhardt et al., 2014; Hinman et al., 2006; Jordt et al., 2004; Macpherson et al., 2007; Takahashi et al., 2011).

The human TRPA1 (hTRPA1) contains 28 cysteine, 76 lysine and 43 histidine residues, all of which are potential targets for an electrophilic attack. Studies have suggested that several conserved N-terminal cysteines in hTRPA1 (Cys421, Cys621, Cys641, and Cys665; hTRPA1 numbering will be used throughout this paper) are critical for the activation by thiol reactive electrophiles and oxidants (Hinman et al., 2006; Macpherson et al., 2007; Takahashi et al., 2008). In addition, a lysine (Lys710) has also been shown to contribute to activation of hTRPA1 by reaction with thiocyanates and ketoaldehydes (Eberhardt et al., 2012; Hinman et al., 2006). Several of these cysteines, as well as Lys710 are located in

the pre-S1 region between the N-terminal ankyrin repeat domain (ARD) and the transmembrane domain (Paulsen et al., 2015).

Recently our data from single channel recordings demonstrated that activation of hTRPA1 by electrophilic compounds occurs even in the absence of the first 688 amino acid residues (Moparthi et al., 2014). In line with our findings, other groups have shown that some electrophiles, including *p*-benzoquinone, polygodial, isovalleral and (E)-2 alkenals, robustly activated heterologously expressed TRPA1 lacking three of the N-terminal critical cysteines (Cys621, Cys641 and Cys665) (Blair et al., 2016; Escalera et al., 2008; Ibarra and Blair, 2013). Knowing the reactivity of each cysteine in hTRPA1 to electrophilic compounds is crucial for understanding their biological role and may facilitate the development of new therapeutics for relief of pain. Because of species-dependent differences in response of TRPA1 upon activation by different stimuli (Chen and Kym, 2009) we have chosen to exclusively focus on the hTRPA1 in our study. In this study, labelling at different concentrations of N-methyl-maleimide (NMM) is used to identify and grade accessible cysteines and lysines by mass spectrometry, which may also reveal agonist-induced structural changes in the human TRPA1 ion channel similar to what has been reported for mouse TRPA1 (Wang et al., 2012). In order to study the agonist binding sites outside the N-terminal ARD in a simplified system, the same approach was also employed on a truncated hTRPA1 protein lacking the N-terminal ARD (Δ1-688 hTRPA1) which has been shown to form functional tetramers (Moparthi et al., 2014). Here, we demonstrate that Cys651 appears to have highest reactivity for NMM but adducts are also formed with cysteines and lysines outside of the N-terminal region. These findings together with our reported functional data suggest that these residues located outside the N-terminal region may contribute to the detection and activation of TRPA1 by electrophiles. The reduced labelling of hTRPA1 and Δ1-688 hTRPA1 by NMM at higher concentrations indicates that conformational changes occur in the cytosolic pre-S1 region and the transmembrane S1-S4 domain. We speculate that these alterations in the reactivity may reflect structural rearrangements in an activation or a desensitization mechanism.

Methods

Protein purification and labelling with N-methylmaleimide

Two N-terminally His-tagged constructs of the human TRPA1 protein, a full length hTRPA1 and a truncated Δ1-688 hTRPA1 version, were overexpressed in the *Pichia pastoris* expression system. The expression and purification were done as described previously (Moparthi et al., 2014) except that the β-mercaptoethanol was omitted from the wash and elution buffers used in purification of Δ1-688 hTRPA1. The protein concentration was determined by measuring absorbance at 280 nm using Nano drop spectrophotometer. The extinction coefficients were estimated based on protein amino acid sequence using web tool (http://web.expasy.org/protparam/). At 280 nm the extinction coefficients for hTRPA1 and Δ1-688 hTRPA1 in water were 109670 $M^{-1}cm^{-1}$ and 56840 $M^{-1}cm^{-1}$, respectively. To allow labelling, the metal affinity chromatography purified and desalted TRPA1 proteins were each incubated at room temperature (22°C) for 10 min at three different molar ratios (0.1, 1 and 10) of N-methylmaleimide (NMM) in relation to cysteines present in TRPA1 proteins. In a final volume of 14 µl 0.23 nmol of full length hTRPA1 containing 28 cysteines was mixed with 0.64, 6.43 or 64.26 nmol of NMM, while the corresponding amounts for 0.56 nmol of Δ1-688 hTRPA1 which has 9 cysteines were 0.51, 5.06 and 50.58 nmol of NMM. 30 mM dithiothreitol (DTT) was used to stop the reaction of NMM by quenching. After addition of Laemmli sample buffer (4% SDS, 20% glycerol, 10% β-mercaptoethanol, 0.004% bromophenol blue and 125 mM Tris-HCl pH 6.8), the samples were loaded on 12% TGX gels (Bio-rad) and electrophoresis was performed.

In-gel digestions

To visualize the proteins, the SDS-polyacrylamide gels were stained with Coomassie Blue and destained with 25% methanol and 7% acetic acid in water to remove the background stain. Bands corresponding to the monomeric protein were excised and washed with distilled water and then with 50 mM ammonium bicarbonate (NH_4HCO_3) and 50% acetonitrile solution for 1-2 h to remove the stain from the protein. The gel pieces were dehydrated with 100% acetonitrile prior to reduction of the disulphide bonds using 10 mM DTT in 50 mM NH_4HCO_3 for 30 min at 37°C. After reduction, the gel pieces were dehydrated again with 100% acetonitrile prior to alkylation. The alkylation was performed to

prevent the reformation of disulphide bonds in the protein by incubating gel pieces with the alkylating agent 55 mM iodoacetamide (IA) in 50 mM NH_4HCO_3 for 30 min at room temperature in the dark. The gel pieces were washed (50 mM NH_4HCO_3 and 50% acetonitrile) and then again dehydrated (100% acetonitrile). After removal of acetonitrile, the gel pieces were allowed to dry completely. The enzymatic digestion was carried out separately for each enzyme by adding 50 µl of freshly prepared 20 ng/µl trypsin (Promega sequencing grade modified) and chymotrypsin (Roche Applied Science sequencing grade) in 50 mM NH_4HCO_3 in a 20:1 enzyme: protein ratio (w/w) to the samples. The samples were incubated at 37°C for overnight and the digestion was stopped by the addition of 0.5% trifluoroacetic acid.

Nano LC MS/MS

All experiments were performed in triplicates for each ratio of ligand to cysteines, employing an EasyLC nanoflow HPLC interfaced with a nanoEasy spray ion source (Proxeon Biosystems, Odense, Denmark) connected to a Fusion Orbitrap mass spectrometer (Thermo Fisher Scientific). The peptides were loaded on a PepMap column 2 cm (75 µm inner diameter, Packed with 3 µm resin) and the chromatographic separation was performed at 35°C on a 25 cm (75 µm inner diameter) EASY-Spray column packed with 2 µm of resin (Proxeon Biosystems). The nanoHPLC was operating at 300 nl/min flow rate with a gradient of 5-20% solvent B (0.1% (v/v) formic acid in acetonitrile) in solvent A (0.1% (v/v) formic acid in water) during 60 min and then 20-40% during 30 min, followed by an increase to 90% during 5 min.

A MS scan (400–1400 m/z) was recorded in the Orbitrap mass analyzer set at a resolution of 60,000 at 400 m/z, 1 × 10 automatic gain control target, and 500 ms maximum ion injection time. The MS was followed by top speed data-dependent collision-induced dissociation MS/MS scans on multiply charged ions. The general mass spectrometric conditions were as follows: spray voltage, 1.9 kV; no sheath or auxiliary gas flow; S-lens 60%; ion transfer tube temperature, 275°C. Collision induced dissociation was applied with 35% of energy and MS/MS spectra were recorded in the Orbitrap at a resolution of 15,000.

Database search

Raw data were processed by Mascot distiller searching the Swiss-Prot database with an in-house Mascot database. The search parameters for the Mascot searches were: Taxonomy: *Homo sapiens*; Enzymes; trypsin with one missed cleavage, chymotrypsin with five missed cleavages, Variable Modifications; IA (carbamidomethylation of Cys), NMM (Cys and Lys), and oxidation (Met), Precursor Tolerance, 5 ppm; MS/MS Fragment Tolerance, 0.1 Da. The modifications of detected peptides were identified by adding a mass of 111.0320 Da for NMM and 57.0516 Da for IA to the cysteines in the database search. The peaks corresponding IA and NMM modified peptides in MS mode were extracted and peak areas were calculated using the Xcalibur Software (Thermo Fisher Scientific).

Results

Two different constructs of the hTRPA1 protein, with and without the N-terminal ARD, were purified as described previously (Moparthi et al., 2014) with the modification that any reducing agent was completely avoided in all purification steps. In order to compare the labelling of cysteines and to probe for agonist-induced conformational changes of hTRPA1, the solubilized proteins were individually incubated with three different molar ratios of NMM in respect to the total cysteines of the protein (Fig. 1). Gel electrophoresis was performed for the purpose of removal of contaminants and bands corresponding to monomeric molecular weight were excised from the gel. These gel pieces were treated with DTT to reduce any disulphide bonds and subsequently alkylated with IA to prevent reformation of disulphide bonds. Trypsin and chymotrypsin were used for the in-gel digestion of the proteins and the resulting peptide samples were submitted to LC MS/MS analysis. Both enzymatic digestions gave good sequence coverage of the two hTRPA1 proteins which allowed identification of all cysteine containing peptides except Cys192, which was not detected in any enzymatic digestion (Supplementary Fig. 1). The reactivity of individual cysteines in TRPA1 was monitored in the form of relative labelling by NMM, using two different cysteine modifying agents, NMM at the folded state and IA at a subsequent reduced and denatured state. The NMM labelling was quantified by calculating the area of the NMM modified peptide and it was related to the sum of the areas of the NMM modified and the corresponding IA modified peptides (Figs. 2 and 3). The results from experiments in triplicates at each ratio with hTRPA1 and Δ1-

688 hTRPA1 are summarized in Figures 4 and 5, and numeric values are listed in supplementary Tables 1 and 2.

The full length hTRPA1

The hTRPA1 protein contains 28 cysteines, of which 20 are located in the N-terminal domain, 5 in the transmembrane domain and 3 in the C-terminal domain (Fig. 6A). In line with a previous mass spectrometric study of mouse TRPA1 (Wang et al., 2012), we identified NMM adducts to all of the cysteines in the covered peptides of hTRPA1 except for Cys621, and for Cys414/Cys421 and Cys1021/Cys1025, where it was not resolved which of the two cysteines in the peptide that carried the modification (Supplementary Table 1 and Fig. 4). In contrast, all of the peptides containing Cys462 were labelled by NMM, but none by IA which excluded a reliable assessment of labelling at this residue. To probe for reactivity and conformational changes in the protein, three different concentrations of NMM were used with a fixed reaction time. The lower concentrations with limiting amounts of NMM are anticipated to yield lower labelling and higher concentrations expected to increase the labelling of cysteines in the applied constant reaction time. A lower estimate of the average cysteine labelling at the 0.1 NMM:Cys ratio was 10.8 ± 0.2% (unquantified and undetected cysteines were counted as 0% labelled) which is slightly higher than a presumed maximal average labelling of 10%. At this ratio, the labelling at individual sites ranged from 0 to 95%, suggesting a huge variation in reactivity among the cysteines and specifying Cys651 as most readily labelled cysteine residue possibly with the exception of Cys462. Contrary to our expectations, a ten-fold or even a hundred-fold increase of the ratio did not increase the labelling of the majority of the cysteines much, suggesting that they are largely inaccessible in the structure or unreactive due to engagement in disulphide bridges. At 13 of these sites, 90% or more of the population of TRPA1 is unlabelled, indicating a relatively high degree of homogeneity among the subunits.

In contrast to the majority of cysteines that show saturation of labelling already at the lowest ratio of NMM:Cys, Cys308 and Cys540 show an increased labelling at the approximated equimolar ratio of NMM. This concentration is sufficient to reach their maximal binding of NMM, around 25 and 50%, corresponding to an average labelling of Cys308 and Cys540 in one and two subunits, respectively in the tetramer. Interestingly, the labelling at Cys651 shows a small but significant decrease at the highest concentration of NMM, and similarly, these higher ratios of NMM almost abolish the already poor labelling of Cys834.

The truncated hTRPA1 lacking the N-terminal ARD

The truncated Δ1-688 hTRPA1 construct provides a simplified model system of hTRPA1, since it contains only 9 of the 28 cysteines of hTRPA1 (Fig. 6) and still can be activated by NMM (Moparthi et al., 2014). NMM adducts were observed to all cysteines except that it was not resolved which of Cys1021 and Cys1025 that was modified in their common peptide. The average labelling was 5.7 ± 0.1% at the lowest ratio, ranging to 40.3 ± 1.1% at the highest ratio. The lowest concentration of NMM results in little or no labelling, but suggests that in the truncated construct Cys1085 has the highest reactivity at limiting amounts of NMM (Fig. 5 and supplementary Table 2). At an equimolar concentration of NMM an increased labelling of all cysteines was observed, and several cysteines other than Cys1085 are dominating, with Cys786 being most prominent in the labelling at this concentration. A further 10-fold increase in the NMM concentration resulted in a dramatic increase in labelling of Cys727 and a more modest but significant rise in labelling of Cys703 and Cys1085. Similar to the full length hTRPA1, the increased labelling of cysteines was accompanied by a decrease in labelling of Cys834.

NMM adducts to lysines

In addition to cysteines, NMM adducts to lysines were also observed in hTRPA1 but not quantified. The NMM modifications of Lys635, Lys704 and Lys787 in hTRPA1 were identified in reactions at all three concentrations of NMM. At higher concentrations of NMM, Lys649 was also modified. In line with this, Lys704 and Lys787 in Δ1-688 hTRPA1 were labelled by NMM at all concentrations (Supplementary Table 3).

Discussion

The labelling of individual cysteines of full length hTRPA1 and a truncated version lacking the large N-terminal ARD (Δ1-688 hTRPA1), were assessed by LC MS/MS after incubations with different concentrations of NMM in a fixed period of time. The NMM labelling demonstrated a concentration-dependent modification of certain cysteines in hTRPA1, Cys308 and Cys540 show an increase in labelling whereas Cys651 and Cys834 show decrease in labelling with higher concentrations of NMM. A similar pattern of bidirectional labelling in response to increasing ratios of NMM to cysteines was also seen in the truncated

Δ1-688 hTRPA1 protein. Although the three first responsive cysteines of the full length hTRPA1 are missing in this construct, other cysteines in particular Cys727, but also Cys703 and Cys1085 increase in labelling when Cys834 decrease in labelling. The decrease in labelling at Cys834 appear more convincing in the truncated protein due to the overall higher labelling, however, the relative change at the different ratios of NMM is in fact larger in the full length protein compared to the truncated version, corresponding to a 4-10 and a 2-fold decrease, respectively. The qualitatively similar response suggests that the structural changes in the two proteins are related.

These findings indicate that binding of NMM to hTRPA1 and Δ1-688 hTRPA1 triggers conformational changes that make some cysteines more reactive and turn some cysteines more unreactive to further binding of NMM at higher concentrations. The reactivity of different cysteines depend both on the binding affinity i.e. the on and off rates in formation of a non-covalent NMM:TRPA1 complex, and on the rate of the reaction resulting in the covalent labelling of the thiol. At a lower concentration of NMM the affinity is more important for the labelling whereas a higher initial concentration allows also binding at sites that are less accessible and have lower affinity. In addition to steric hindrance, also the chemical microenvironment of the cysteine in the native protein determine the reactivity of the thiol to reactive compounds (Paulsen and Carroll, 2013). Close proximity to positively charged amino acids will lower the p*K*a value of thiols and favour their ionization, resulting in higher reactivity of the cysteines (Lutolf et al., 2001). Thus changes in reactivity of the cysteines may be caused by rather small structural alterations at the binding sites.

Less labelling of the N-terminal region of hTRPA1

A previous study on the hTRPA1 ortholog from mouse reported similar observations of decreased and increased labelling in response to a higher concentration of NMM, however the changes do not occur at the corresponding cysteines in the two orthologs. Wang et al. observed that Cys213, Cys258 and Cys727 became more accessible while Cys31, Cys273 and Cys621 turned less accessible in the mouse TRPA1 at the higher concentration of NMM (hTRPA1 numbering of cysteines except Cys31), the authors suggested that the altered reactivity of cysteines is a result of NMM induced conformational changes, that can lead to either channel activation or desensitization (Wang et al., 2012). The majority of these cysteines are located in the distal N-terminal region which displayed relatively little labelling by NMM in hTRPA1. Species dependent

differences or differences in conformation due to performing the labelling at different temperatures (hTRPA1 22°C; mouse TRPA1 37°C) may explain this, but an even more likely explanation is that the purified hTRPA1 is in a more oxidized state making it difficult to monitor changes at these residues. The latter is supported by the fact that 300 μM DTT was used in the purification of mouse TRPA1 whereas no reducing agent was used in the preparation of hTRPA1. In fact in the absence of reducing agents Wang et al., reported that five cysteines located in the N-terminal region are involved in the formation of four disulphide bonds, which are Cys665-Cys621, Cys665-Cys462, Cys665-Cys192 and Cys621-Cys608. When exposed to oxidants, additional disulphide bonds may appear (Eberhardt et al., 2014). Nevertheless, Cys621 and Cys665 stand out as central in the formation of the TRPA1 N-terminal ARD disulphide network (Eberhardt et al., 2014; Wang et al., 2012). In our experiments, no NMM adducts were observed to Cys621 and relatively little NMM labelling was observed to Cys665, which is consistent with their central role in a disulphide network.

Comparisons of truncated versus full length hTRPA1

For some of the cysteines the labelling at the lowest ratio was higher in the full length protein compared to the truncated version, this was most evident for Cys786 but also seen for Cys703 and Cys856. This could be an indication of a higher affinity for NMM at these sites in the full length protein. Alternatively it may be explained by the effectively higher ratio of NMM to cysteines due to the many highly inaccessible cysteines and an overestimation of the added amount of full length hTRPA1 since its lower purity compared to Δ1-688 hTRPA1 was not taken into account. At the two higher ratios the relative labelling is higher at all sites in the truncated construct. An exposure of residues at the cytosolic N- and C-terminal regions of the truncated protein can be expected if they are protected by the ARD in the full length protein (Fig. 6 and 7). However, the increased labelling of the sites deep within the transmembrane domain is more difficult to rationalize since there is no direct contact to the deleted region. A possible interpretation is that the shortened construct is overall more dynamic and allow temporal structural changes whereas the conformation of the full length protein is tightly controlled by the ARD and therefore more static.

It is intriguing that labelling at some of the sites in the transmembrane domain like Cys786 and Cys856 reach an apparent saturation far from 100% already at a NMM ratio of 0.1:1 and 1:1 for the hTRPA1 and Δ1-688 hTRPA1, respectively. Although Cys856 has been proposed to be involved in disulphide bonds

(Takahashi et al., 2011), there is no support in the structure for any of these residues forming disulphide bonds within the protein which could have provided an explanation for the limited labelling. It cannot be excluded that the changed conformation limits the modification by NMM also at these sites.

It is tempting to speculate that it is the modifications of cysteines that show an increased labelling at higher ratios of NMM that trigger the conformational switch by stabilizing the new conformation. This would indicate that although the change of conformation is similar in the transmembrane domain of hTRPA1 and Δ1-688 hTRPA1 as judged from the common decreased labelling of Cys834 at the highest ratio, the sites that induce the change are different. Consistently, the conformational switch in the full length hTRPA1 appear to occur at a lower ratio than 10:1, which is the ratio observed to change conformation of Δ1-688 hTRPA1.

In addition to cysteines, mutations of lysines have been shown to affect the activation of TRPA1 by thiocyanates and ketoaldehydes (Eberhardt et al., 2012; Hinman et al., 2006). Thus modifications of lysines by NMM cannot be excluded to cause the change in conformation. In general, maleimides are specific for cysteines and only react with thiols at pH 7, but at more alkaline conditions they can also interact with amines (Giron et al., 2011). Here, we have identified that Lys649, Lys704, and Lys787 of hTRPA1 were modified by NMM at pH 7.8. Possibly a more basic pH would render also other lysines susceptible for modification by NMM. In this context it is interesting to note that alkalization has been suggested to activate TRPA1 (Fujita et al., 2008).

In conclusion, our data suggest that electrophiles induce conformational changes both in the N-terminal region and in the S1-S4 domain of hTRPA1. Our mass spectrometric analysis on Δ1-688 hTRPA1 together with functional studies (Moparthi et al., 2014), suggest that cysteines outside the N-terminal region are indeed involved in the detection and activation of TRPA1 by electrophiles, although this might vary depending on the chemical nature of the electrophile. Importantly, we have identified NMM reactive cysteines outside the N-terminal ARD, some of which may directly link channel gating by chemicals and temperature. Understanding the changes in the N-terminal disulphide-network and the identification of overall reactive cysteines and lysines in hTRPA1 might help to develop therapies for pain relief. To fully understand the electrophilic activation mechanism, high resolution structures of hTRPA1 in the presence of ligands are needed.

Acknowledgements

This work was supported by the Swedish Research Council 2014-3801, 2010-5787 (P.M.Z., E.D.H.), 2007-6110 (U.J.), Formas 2007-718 (P.M.Z., E.D.H., U.J., P.K.), the Research School of Pharmaceutical Sciences FLÄK (U.J., P.M.Z.) and the Medical Faculty at Lund University (P.M.Z., E.D.H.). We thank Adine Karlsson for technical assistance. The authors declare no competing financial interests.

References:

Blair NT, Philipson BI, Richards PM, Doerner JF, Segura A, Silver WL and Clapham DE (2016) Naturally Produced Defensive Alkenal Compounds Activate TRPA1. *Chem Senses*.

Chen J and Kym PR (2009) TRPA1: the species difference. *J Gen Physiol* **133**:623-625.

Eberhardt M, Dux M, Namer B, Miljkovic J, Cordasic N, Will C, Kichko TI, de la Roche J, Fischer M, Suarez SA, Bikiel D, Dorsch K, Leffler A, Babes A, Lampert A, Lennerz JK, Jacobi J, Marti MA, Doctorovich F, Hogestatt ED, Zygmunt PM, Ivanovic-Burmazovic I, Messlinger K, Reeh P and Filipovic MR (2014) H2S and NO cooperatively regulate vascular tone by activating a neuroendocrine HNO-TRPA1-CGRP signalling pathway. *Nat Commun* **5**:4381.

Eberhardt MJ, Filipovic MR, Leffler A, de la Roche J, Kistner K, Fischer MJ, Fleming T, Zimmermann K, Ivanovic-Burmazovic I, Nawroth PP, Bierhaus A, Reeh PW and Sauer SK (2012) Methylglyoxal activates nociceptors through transient receptor potential channel A1 (TRPA1): a possible mechanism of metabolic neuropathies. *J Biol Chem* **287**:28291-28306.

Escalera J, von Hehn CA, Bessac BF, Sivula M and Jordt SE (2008) TRPA1 mediates the noxious effects of natural sesquiterpene deterrents. *J Biol Chem* **283**:24136-24144.

Fujita F, Uchida K, Moriyama T, Shima A, Shibasaki K, Inada H, Sokabe T and Tominaga M (2008) Intracellular alkalization causes pain sensation through activation of TRPA1 in mice. *J Clin Invest* **118**:4049-4057.

Giron P, Dayon L and Sanchez JC (2011) Cysteine tagging for MS-based proteomics. *Mass Spectrom Rev* **30**:366-395.

Hinman A, Chuang HH, Bautista DM and Julius D (2006) TRP channel activation by reversible covalent modification. *Proc Natl Acad Sci U S A* **103**:19564-19568.

Ibarra Y and Blair NT (2013) Benzoquinone reveals a cysteine-dependent desensitization mechanism of TRPA1. *Molecular pharmacology* **83**:1120-1132.

Jordt SE, Bautista DM, Chuang HH, McKemy DD, Zygmunt PM, Högestätt ED, Meng ID and Julius D (2004) Mustard oils and cannabinoids excite sensory nerve fibres through the TRP channel ANKTM1. *Nature* **427**:260-265.

Lutolf MP, Tirelli N, Cerritelli S, Cavalli L and Hubbell JA (2001) Systematic modulation of Michael-type reactivity of thiols through the use of charged amino acids. *Bioconjug Chem* **12**:1051-1056.

Macpherson LJ, Dubin AE, Evans MJ, Marr F, Schultz PG, Cravatt BF and Patapoutian A (2007) Noxious compounds activate TRPA1 ion channels through covalent modification of cysteines. *Nature* **445**:541-545.

Moparthi L, Survery S, Kreir M, Simonsen C, Kjellbom P, Hogestatt ED, Johanson U and Zygmunt PM (2014) Human TRPA1 is intrinsically cold- and chemosensitive with and without its N-terminal ankyrin repeat domain. *Proc Natl Acad Sci U S A* **111**:16901-16906.

Paulsen CE, Armache JP, Gao Y, Cheng Y and Julius D (2015) Structure of the TRPA1 ion channel suggests regulatory mechanisms. *Nature* **520**:511-517.

Paulsen CE and Carroll KS (2013) Cysteine-mediated redox signaling: chemistry, biology, and tools for discovery. *Chem Rev* **113**:4633-4679.

Takahashi N, Kuwaki T, Kiyonaka S, Numata T, Kozai D, Mizuno Y, Yamamoto S, Naito S, Knevels E, Carmeliet P, Oga T, Kaneko S, Suga S, Nokami T, Yoshida J and Mori Y (2011) TRPA1 underlies a sensing mechanism for O2. *Nat Chem Biol* **7**:701-711.

Takahashi N, Mizuno Y, Kozai D, Yamamoto S, Kiyonaka S, Shibata T, Uchida K and Mori Y (2008) Molecular characterization of TRPA1 channel activation by cysteine-reactive inflammatory mediators. *Channels (Austin)* **2**:287-298.

Wang L, Cvetkov TL, Chance MR and Moiseenkova-Bell VY (2012) Identification of in vivo disulfide conformation of TRPA1 ion channel. *J Biol Chem* **287**:6169-6176.

Zygmunt PM and Högestätt ED (2014) Trpa1. *Handb Exp Pharmacol* **222**:583-630.

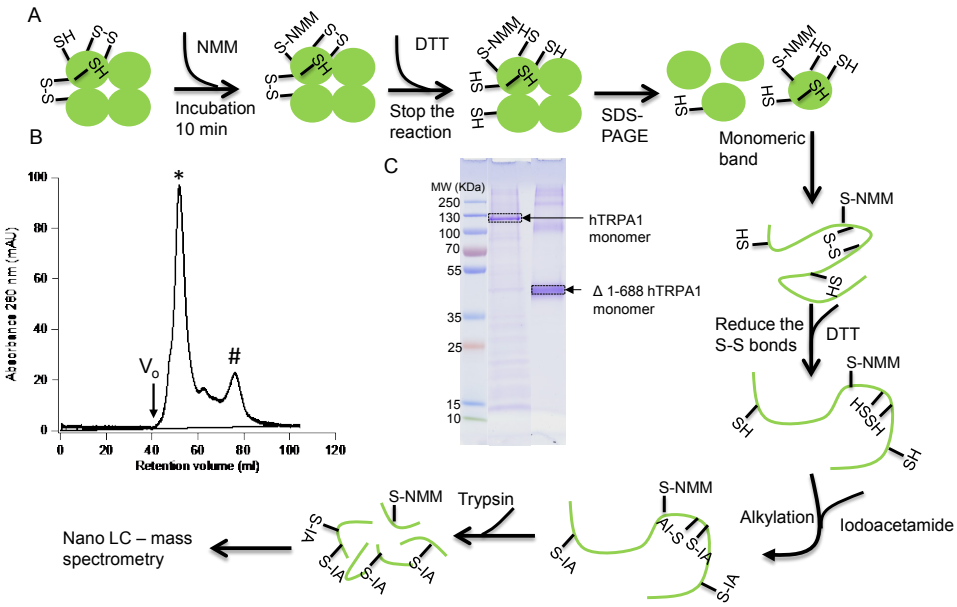

Figure 1. Schematic illustration of steps in the preparation of hTRPA1 proteins for the mass spectrometry analysis. A. The fate of different types of cysteine residues is shown, including modification of free thiols with N-methylmaleimide (NMM), denaturation, reduction of disulphide bonds with dithiothreitol (DTT), iodoacetamide alkylation of thiols not modified by NMM, and enzymatic digestion. B. Size exclusion chromatogram of the hTRPA1 sample used in the NMM labelling shows that it mainly eluted in a peak corresponding to the tetramer (*) and only a small fraction eluted as a monomer (#). V_o-indicate void volume. C. Coomassie stained SDS polyacrylamide gel of hTRPA1 and Δ1-688 hTRPA1. Marked bands are corresponding to monomers of hTRPA1 proteins and were excised from the gel for further reduction and labelling by IA.

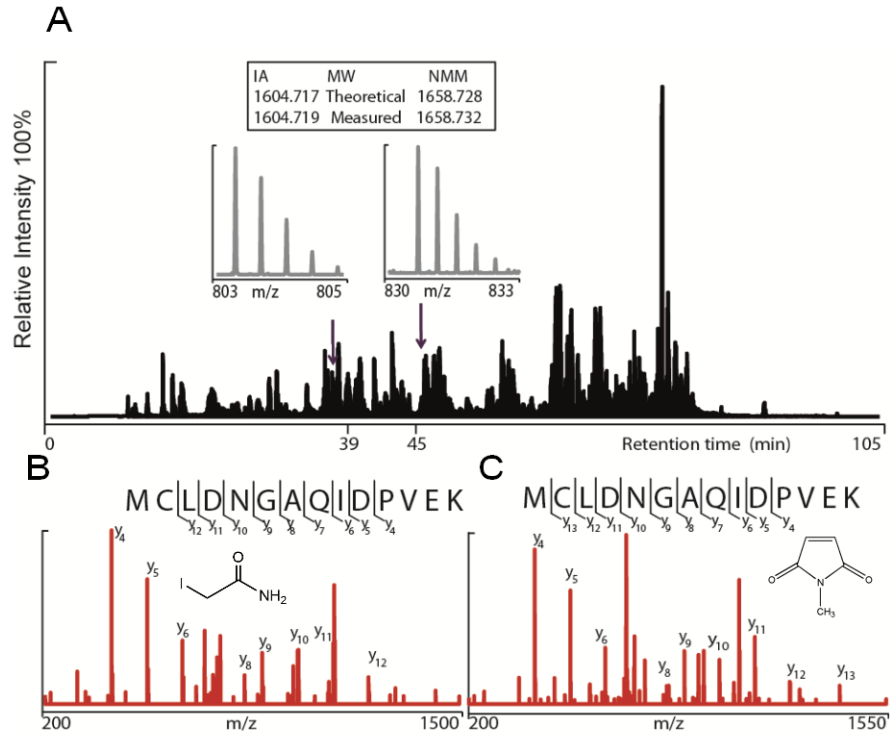

Figure 2. Annotation of iodo-acetamide (IA) modified and N-methyl maleimide (NMM) modified 257-270 hTRPA1 peptides (MCLDNGAQIDPVEK) using nanoHPLC and tandem mass spectrometry. A. Representative total ion chromatogram of trypsin digested hTRPA1 depicted in black. The IA and NMM modified peptides (257-270) for Cys258 were eluted at 39 min and 45 min respectively. The Orbitrap mass spectra of the double-charged Cys-258-IA peptide (m/z 803.3669) and the double-charged Cys-258-NMM peptide (m/z 830.3731) enabled accurate mass determination of both peptides (isotopic distribution depicted in grey). B. C. The assigned fragmentation pattern of IA (B) and NMM (C) modified peptides are given in red were denoted y-ions are depicted.

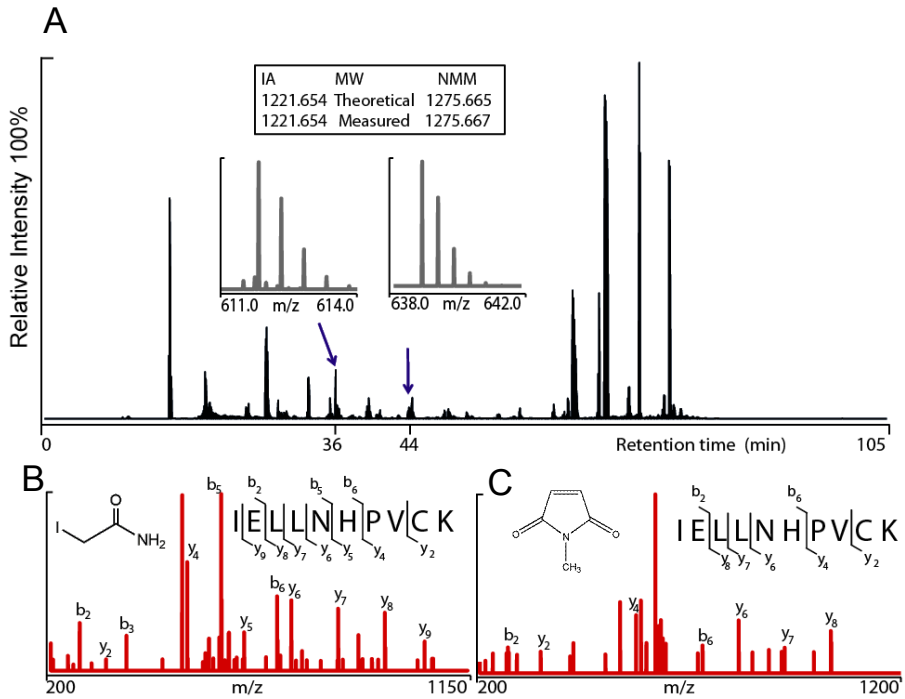

Figure 3. Annotation of iodo-acetamide (IA) modified and N-methyl maleimide (NMM) modified 695-704 Δ1-688 hTRPA1 peptides (IELLNHPVCK) using nanoHPLC and tandem mass spectrometry. A. Representative total ion chromatogram of trypsin digested Δ1-688 hTRPA1 depicted in black. The IA and NMM modified peptides (695-704) for Cys703 were eluted at 36 min and 44 min respectively. The Orbitrap mass spectra of the double-charged Cys-703-IA peptide (m/z 611.8342) and the double -charged Cys-703-NMM peptide (m/z 638.8406) enabled accurate mass determination of both peptides (isotopic distribution depicted in grey). B. C. The assigned fragmentation pattern of IA (B) and NMM (C) modified peptides are given in red were denoted y- and b-ions are depicted.

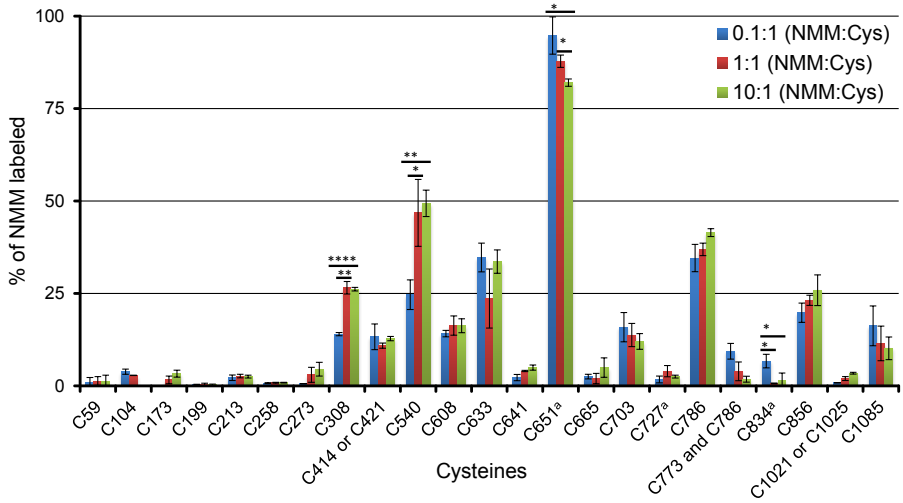

Figure 4. Mapping of binding sites for the electrophilic activator N-methylmaleimide (NMM) in the human TRPA1. The bar chart shows percent site labelling of NMM. The experiments were conducted in triplicates at each concentration of NMM under a fixed reaction time. The percentage of labelling are represented as means with standard deviation. * $P < 0.05$, ** $P < 0.01$, *** $P < 0.001$ and **** $P < 0.0001$ indicate that differences in labelling of cysteine at different concentrations of NMM are statistically significant using unpaired t test with Welch's correction. [a]data is retrieved from the chymotrypsin digestion.

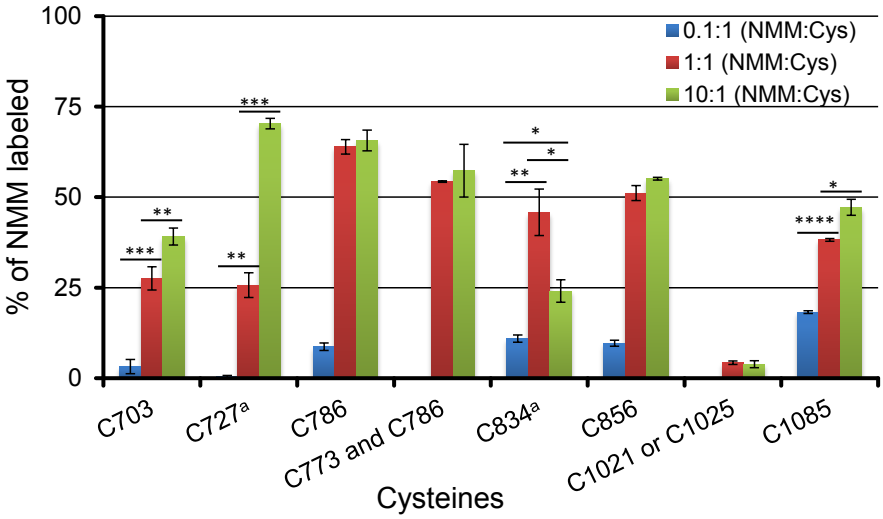

Figure 5. Mapping of binding sites for the electrophilic activator N-methylmaleimide in the truncated human TRPA1 lacking N-terminal ARD (Δ1-688 hTRPA1). The bar chart shows percent site labelling of NMM. The experiments were conducted in triplicates at each concentration of NMM under a fixed reaction time. The percentage of labelling are represented as means with standard deviation. * $P < 0.05$, ** $P < 0.01$, *** $P < 0.001$ and **** $P < 0.0001$ indicate that differences in labelling of cysteine at different concentrations of NMM are statistically significant using unpaired t test with Welch's correction. [a]data retrieved from the chymotrypsin digestion.

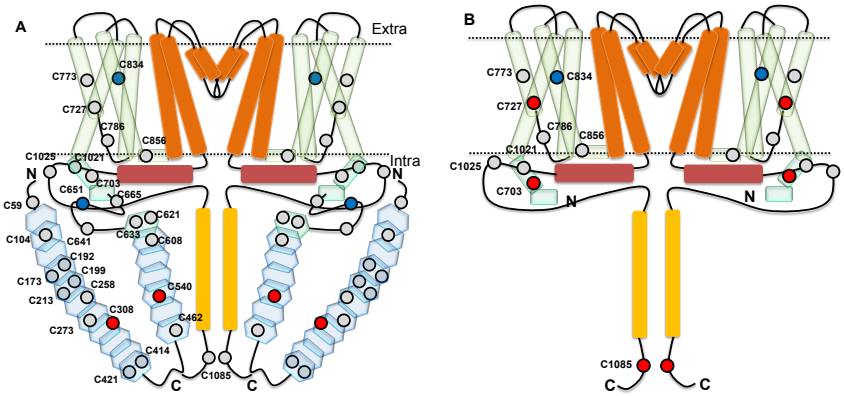

Figure 6. Schematic representation of structural elements in human TRPA1 and position of cysteine residues. The subunits in the TRPA1 are arranged into a tetramer surrounding a common ion permeation pathway. For clarity only two subunits of the tetramer are displayed. A. Each subunit of the full length human TRPA1 contains 28 cysteines highlighted by circles. The red and blue circles are representing increase and decrease in NMM labelling of the cysteines respectively, in response to higher concentrations. B. The N-terminal ARD deleted version of the human TRPA1 (Δ1-688 hTRPA1) has only 9 cysteines per monomer and a deviating pattern of NMM labelling. The domain organization of TRPA1 is represented in different colours, from N-terminus to C-terminus; Ankyrin repeat domain – blue (transparent), pre-S1 region – green (transparent), S1-S4 α-helices – light green (transparent), S5-S6 and pore helices – orange, TRP like domain – brick red, coiled-coil domain – yellow.

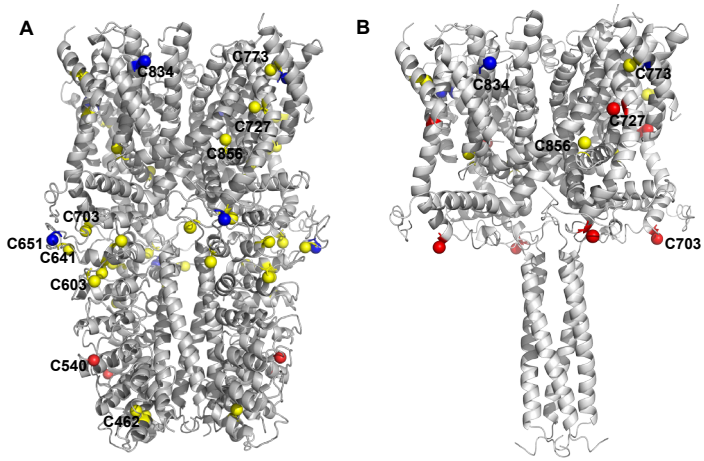

Figure 7. Single particle cryo-EM structure of human TRPA1 (PDB ID: 3J9P). A. Cartoon representation of human TRPA1 showing a side view of the resolved part of the tetrameric assembly with the transmembrane domain at the top. 12 of the 28 cysteines in the monomer are resolved in the structure and their sulphur atoms are shown as spheres. B. The same representation but with the N-terminal ARD completely removed displaying 5 of the 9 cysteines present in the truncated monomer of hTRPA1 (Δ1-688 hTRPA1). The red and blue coloured spheres represent cysteines exhibiting an increase and decrease, respectively in the NMM labelling at higher concentrations of NMM.

Supplementary Table 1: The percentage of NMM labelling for the each cysteine in the human TRPA1 was analysed from tryptic digested peptides. The NMM labelling was calculated for each cysteine by area of NMM modified peptide divided with total areas of NMM modified peptide and equivalent IA modified peptide. The mass spectrometry experiments were performed in triplicates for each concentration, and the quantified data presented in the mean value with standard deviation (SD).

Cysteine	**Peptide sequence**	**Range**	**0.1:1 NMM:Cys** % ± SD	**1:1 NMM:Cys** % ± SD	**10:1 NMM:Cys** % ± SD
C59	C_{NMM}DDMDTFFLHYAAAEGQIELMEK	59-81	0.98±1.30	1.34±1.19	1.09±1.83
C104	DSSLEVLHEM$_{ox}$DDYGNTPLHC_{NMM}AVEK	85-108	3.84±0.71	2.85±0.04	0.04±0.00
C173	TIDVNLEGENGNTAVIIAC_{NMM}TTNNSEALQ ILLK	155-186	0.05±0.07	1.65±1.05	3.32±0.92
C199	WGC_{NMM}FPIHQAAFSGSK	197-211	0.30±0.13	0.42±0.34	0.25±0.25
C213	EC_{NMM}M$_{ox}$EIILR	212-219	2.21±0.74	2.68±0.47	2.52±0.40
C258	M$_{ox}$C$_{NMM}$LDNGAQIDPVEK	257-270	0.76±0.12	0.87±0.10	0.87±0.10
C273	C_{NMM}TAIHFAATQGATEIVK	273-289	0.61±0.04	3.00±2.02	4.53±1.87
C308	LM$_{ox}$ISSYSGSVDIVNTTDGC_{NMM}HETMLHR	290-315	14.01±0.45	26.56±1.71	26.18±0.49
C414 or C421	ELVM$_{ox}$DEDNDGC_{IA}TPLHYAC_{NMM}R	404-422	13.28±3.47	10.88±0.71	12.80±0.57
C462[b]	INTC_{NMM}QR	459-464	all	all	all
C540	C_{NMM}TDRLDEDGNTALHFAAR	540-557	24.68±4.02	46.81±9.05	49.38±3.58
C608	WDEC_{NMM}LK	605-610	14.15±0.86	16.31±2.61	16.28±1.89
C633	C_{IA}PITEM$_{ox}$IEYLPEC_{NMM}M$_{ox}$K	621-635	34.73±3.88	23.65±7.99	33.62±3.17
C641	VLLDFC_{NMM}M$_{ox}$LHSTEDK	636-649	2.25±0.84	4.05±0.16	4.95±0.71
C651[a]	HSTEDKSC_{NMM}RDY	644-654	94.78±5.02	87.83±1.68	82.04±0.98
C665	YLQC_{NMM}PLEFTK	662-671	2.52±0.63	1.98±1.39	4.96±2.62
C703	IELLNHPVC$_{NMM}$K	695-704	15.90±3.96	13.76±3.13	12.04±2.11
C727[a]	C_{NMM}LGLIPM$_{ox}$TIL	727-736	1.76±0.94	3.99±1.52	2.52±0.40
C773 and C786	TC_{NMM}M$_{ox}$ILVFLSSIFGYC_{NMM}K	772-787	9.38±2.11	3.96±2.52	1.82±0.80
C786	TC_{IA}M$_{ox}$ILVFLSSIFGYC_{NMM}K	772-787	34.59±3.70	36.94±1.68	41.47±1.05
C834[a]	QWQC$_{NMM}$GAIAVY	831-840	6.73±1.83	0.66±0.12	1.53±1.97
C856	FENC_{NMM}GIFIVMLEVILK	853-868	19.81±2.62	23.16±1.40	25.89±4.16
C 1021 or C1025	SGGM$_{ox}$LFHIFC_{IA}FLFC_{NMM}TGEIR	1012-1030	0.87±0.03	1.99±0.53	3.44±0.24
C1085	M$_{ox}$EIISETEDDDSHC_{NMM}SFQDR	1072-1090	16.27±5.38	11.50±4.68	10.18±3.05
Average NMM labelling (lower estimate)			**10.84±0.19**	**11.27±0.43**	**11.79±0.38**

[a]data retrieved from chymotrypsin digestion, [b] all detected peptides by MS were modified by NMM.

In the calculation of average NMM labelling, all the NMM modified cysteines are taken into account and those are not modified by NMM or not identified in the sequence are counted as zero value.

Supplementary Table 2: The percentage of NMM labelling for the each cysteine in the Δ1-688 humanTRPA1 was analysed from tryptic digested peptides. The NMM labelling was calculated for each cysteine by area of NMM modified peptide divided with total areas of NMM modified peptide and equivalent IA modified peptide. The mass spectrometry experiments were performed in triplicates for each concentration, and the quantified data presented in the mean value with standard deviation (SD).

Cysteine	**Peptide sequence**	**Range**	**0.1:1 NMM:Cys** % ± SD	**1:1 NMM:Cys** % ± SD	**10:1 NMM:Cys** % ± SD
C703	IELLNHPVC$_{NMM}$K	695-704	3.21±1.96	27.53±3.21	39.14±2.36
C727[a]	C$_{NMM}$LGLIPM$_{ox}$TIL	727-736	0.37±0.40	25.70±3.14	70.30±1.44
C773 and C786	TC$_{NMM}$M$_{ox}$ILVFLSSIFGYC$_{NMM}$K	772-787	0	54.29±0.23	57.31±7.29
C786	TC$_{IA}$M$_{ox}$ILVFLSSIFGYC$_{NMM}$K	772-787	8.68±1.06	63.89±2.02	65.67±2.85
C834[a]	QWQC$_{NMM}$GAIAVYF	831-841	10.94±0.98	45.81±6.43	24.07±3.12
C856	FENC$_{NMM}$GIFIVMLEVILK	853-868	9.65±0.80	51.12±2.06	55.09±0.38
C1021 or C 1025	SGGM$_{ox}$LFHIFC$_{IA}$FLFC$_{NMM}$TGEIR	1012-1030	0	4.27±0.48	3.87±0.96
C1085	M$_{ox}$EIISETEDDDSHC$_{NMM}$SFQDR	1072-1090	18.22±0.38	38.19±0.40	47.19±2.22
Average NMM labelling (lower estimate)			**5.67±0.11**	**34.53±0.24**	**40.29±1.09**

[a]data retrieved from chymotrypsin digestion. In the calculation of average NMM labelling, all the NMM modified cysteines are taken into account and those are not modified by NMM are counted as zero value.

Supplementary Table 3: The observed NMM adducts to lysines in hTRPA1 and Δ1-688 humanTRPA1 from both trypsin and chymotrypsin digested peptides, when incubated protein at different concentrations of NMM.

Lysine	**0.1:1 (NMM:Cys)**	**1:1 (NMM:Cys)**	**10:1 (NMM:Cys)**
K635	●	●	●
K649	○	○	●
K704	●■	●■	●■
K787	●■	●■	●■

● Identified in hTRPA1

○ Not identified in hTRPA1

■ Identified in Δ1-688 hTRPA1

HumanTRPA1 sequence coverage of 76.2% by trypsin digestion

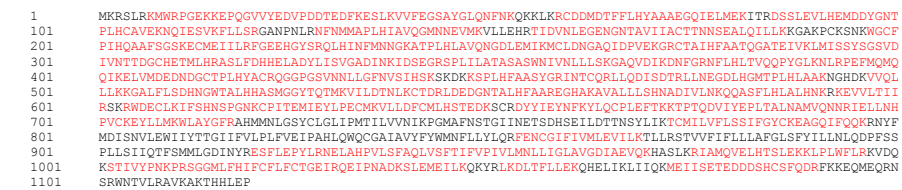

HumanTRPA1 sequence coverage of 87.8% by chymotrypsin digestion

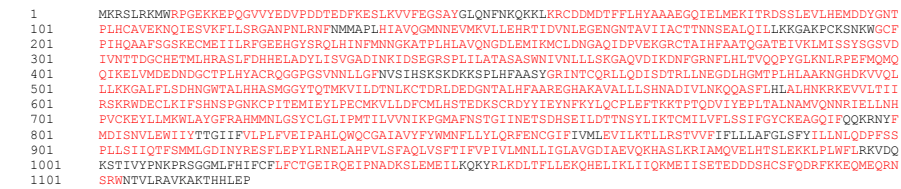

Δ1-688 humanTRPA1 sequence coverage of 52.9% by trypsin digestion

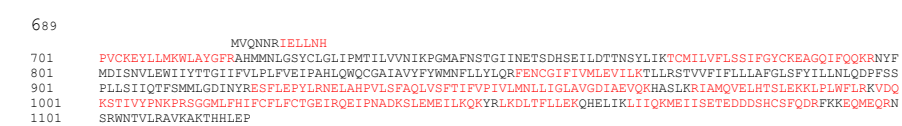

Δ1-688 humanTRPA1 sequence coverage of 87.5% by chymotrypsin digestion

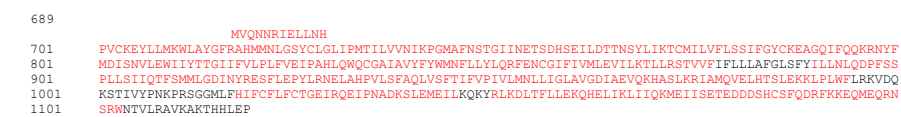

Supplementary Figure 1. The obtained sequence coverage of human TRPA1 and Δ1-688 humanTRPA1 was by mass spectrometry with trypsin and chymotrypsin digestion. The red coloured residues were detected in the digestion with treatment of specific enzyme. Black coloured residues were not detected in the corresponding enzyme treatment.

Printed by Media-Tryck, Lund University

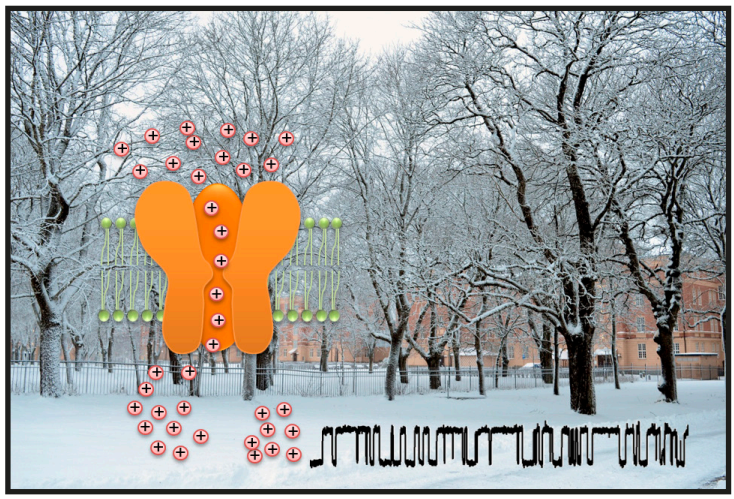

My interest in biological sciences directed me towards medical studies and to become a medical doctor, after which I decided to pursue a career in biomedical research. Along those lines, I performed master studies in protein science at Lund University, Sweden. Eventually, I completed my master studies and continued my research career with doctoral studies on the topic of "Structural and functional characterization of TRPA1". With my hot and spicy Indian background, it is fascinating to understand how temperature and spices can communicate to us via the sensory protein TRPA1. I cannot believe that being so sensitive to cold, I ended up in a cold country like Sweden and working on TRPA1 protein as a sensor of unpleasant cold.

My thesis shows that the human TRPA1 also responds to heat. It is indeed intriguing how a single protein such as TRPA1 can respond to and transduce so diverse harmful stimuli into electrical signals eventually reaching the brain and perceived as pain. My thesis shows for the first time that the purified TRPA1 itself responds to both cold and heat as well as to chemical irritants. This is important, because TRPA1 plays not only a role in protection of acute tissue damage, but also in chronic pain, which costs the society the most among all known diseases including Alzheimer, Parkinson, diabetes etc. It is my wish that the findings of this thesis will help to understand how the temperature sense is organised and facilitate the development of novel analgesics targeting the pain sensor TRPA1.

LUND UNIVERSITY

ISBN 978-91-7422-432-0

Biochemistry and Structural Biology,
Faculty of Science
Lund University